The immunopathogenic mechanism of severe cutaneous adverse reactions to first line anti-tuberculosis drugs

A dissertation presented

by

Phuti Sophia Choshi

to

The Department of Medicine

Division of Allergology and Clinical Immunology

for the degree of

Doctor of Philosophy in Medicine

UNIVERSITY OF CAPE TOWN

IYUNIVESITHI YASEKAPA • UNIVERSITEIT VAN KAAPSTAD

South Africa

2023

Declaration

I, Phuti Sophia Choshi, hereby declare that the work on which this thesis is based is my original work (except where acknowledgements indicate otherwise). It is being submitted for the degree of Doctor of Philosophy at the University of Cape Town. It has not been submitted for any degree in any other University.

_____

15 September 2023

Abstract

Background and hypothesis

In HIV-TB endemic settings like South Africa, first line anti-tuberculosis drugs (FLTD) are the commonest cause of severe immune mediated adverse drug reactions, including Stevens Johnson Syndrome (SJS), toxic epidermal necrolysis (TEN) and drug reaction with eosinophilia and systemic symptoms (DRESS). The mechanisms of these treatment-limiting, life-threatening reactions, particular in persons living with HIV (PLHV) is poorly understood, making diagnosis and treatment challenging in patients who can ill-afford suboptimal and prolonged anti-TB treatment interruptions. We hypothesize that polymorphisms in Human Leukocyte Antigen (HLA), Endoplasmic Reticulum Aminopeptidase (ERAP) and Killer Immunoglobulin Receptor (KIR) genes along with HIV-related immune dysregulation during drug exposure might confer susceptibility. In this thesis, we aimed to identify genetic markers in African populations for FLTD-induced SJS/TEN and DRESS, and using single-cell proteomic and transcriptomic analyses, we aimed to immunophenotype different stages of the reactions.

Methods

We selected three groups of participants from the IMARI in Africa registry: i) HIV+ FLTD SCAR cases, ii) HIV- FLTD SCAR cases and iii) HIV+/- FLTD tolerant controls (>8 weeks on treatment without any adverse events). We collected saliva and blood at baseline and in SCAR cases, we collected blood at different stages of the reaction including pre sequential drug challenge (SDC), on positive reaction to any FLTD (post SDC) and during recovery (at least three months from an acute reaction). We used RegiSCAR phenotype validation, Naranjo drug causality and ELISpot assay to identify offending drugs and precision phenotype cases. We isolated DNA from saliva for HLA, ERAP and KIR typing. In a well-defined subset of patients, we used an integrated single-cell approach involving: i) mass cytometry by time of flight (n=8), and ii) single cell RNA sequencing (scRNA-seq) (n=3) to characterise immune cells activated by drug.

Results

Forty-one RegiSCAR validated SCAR cases that reacted to one or more FLTD on rechallenge were included, Rifampicin-associated DRESS was commonest (n=18). IFN-gamma ELISpot, optimised for FLTDs, was most sensitive (75%) for Rifampicin-DRESS cases. Rifampicin-DRESS/SJS/TEN (with positive ELISpot) was associated with HLA-B*44:03 (OR:28.8; 95%CI: 5.6-107.7; P=<0.0001); with no single allele associations in KIR, and ERAP detected. No HLA, KIR, ERAP single allele association for other FLTD-SCAR combinations was found. Single-cell work was restricted to Rifampicin-DRESS HLAB*44:03 cases (n=4) and matched controls (n=4). HIV+ cases and controls

showed an expanded senescent (CD57+) and exhausted (PD-1+, TIGIT+) population of CD8+ T cells, due to chronic activation. However, a subpopulation of these CD8+ T cells in cases but not controls expressed co-stimulation (CD28+ CD27+) markers [Mean (range) of 1% (0.1 – 3.2%) in cases vs 0% (0 – 1%) in controls p=0.004)]. We confirmed with scRNA-seq (n=3), that these are KLRG1^{low}, CX3CR1^{high} CD8+ T cells with Rifampicin-specific proliferative and cytotoxic capabilities (IFNG^{hi}, TNF-α^{hi}, GNLY^{hi}, GZMB^{hi} and perforin^{hi}). We mapped the V-J junction and CDR3αβ pairings and found each case with unique TCR repertoire, with varying predominantly CD8+ oligoclonality. GLIPH2 algorithm analysis of TCRβ sequences found eight common T cell groups across the three cases. Differential gene expression identified the SQVP TCR motif as having Rifampicin-induced proliferative and cytotoxic profiles. Regulatory T cells (CD127^{low}, CD25^{hi}, CCR4^{hi}) were higher in drug-tolerant controls [Mean(range) of 5% (1.1 – 11.8%) in controls vs. 1% (0.4 – 3.2%) in cases] and produced more TGF-beta.

Conclusion

This study is the first detailed immunophenotyping work of Rifampicin-DRESS in PLHV; including precision phenotype with optimised ELISpot to identify drug-specific IFN-gamma T cells to FLTD. Strong association was found between HLA-B*44:03 and Rifampicin DRESS, with no other single risk allele in KIR or ERAP genes found. We propose that, despite expanded, exhausted CD8+ T-cell populations characteristic of HIV-related advanced immunosuppression, patients having Rifampicin-DRESS have drug-specific cytotoxic CD8+ T cells, potentially sharing low-frequency TCR-motifs like SQVP. Increased functional regulatory T cells may contribute to maintaining tolerance in HLAB*44:03 positive Rifampicin-tolerant controls. Future site-of-disease and in-vitro work is required to better define proposed pathogenic T-cell populations.

For my mom, Matshediso Agnes Choshi

Thank you for being my greatest teacher, for being a firm believer in my dreams and ability to achieve them.

Publications

Peter, Jonny, **Phuti Choshi**, and Rannakoe J. Lehloenya. 2019. 'Drug hypersensitivity in HIV infection', *Current opinion in allergy and clinical immunology*, 19: 272-82.

Copaescu, A, **P Choshi***, S Pedretti, E Mouhtouris, J Peter, and J. A. Trubiano. 2021. 'Dose Dependent Antimicrobial Cellular Cytotoxicity—Implications for ex vivo Diagnostics', *Frontiers in Pharmacology*, 12.

Porter, Mireille, **Phuti Choshi***, Sarah Pedretti, Tafadzwa Chimbetete, Rhodine Smith, Graeme Meintjes, Elizabeth Phillips, Rannakoe Lehloenya, and Jonny Peter. 2022. 'IFN-γ ELISpot in Severe Cutaneous Adverse Reactions to First-line Anti-tuberculosis Drugs in an HIV Endemic Setting', *Journal of Investigative Dermatology*.

Gibson, Andrew, Yueran Li, Michael Thorne, Ramesh Ram, Amy Palubinsky, **Phuti Choshi**, Mireille Porter, Jason Trubiano, Pooja Deshpande, and Abha Chopra. 2022. 'Single-cell multi-omic approaches define common molecular and cellular signals of dominant antigen-driven cells at the site of drug-induced Stevens Johnson Syndrome and Toxic Epidermal Necrolysis (SJS/TEN) tissue damage', *Journal of Allergy and Clinical Immunology*, 149: AB181.

Chimbetete, Tafadzwa, Chloe Buck, **Phuti Choshi**, Rose Selim, Sarah Pedretti, Sherrie Jill Divito, Elizabeth Jane Phillips, Rannakoe Lehloenya, and Jonny Peter. 2022. 'HIV-Associated Immune Dysregulation in the Skin: A Crucible for Exaggerated Inflammation and Hypersensitivity', *Journal of Investigative Dermatology*.

Chimbetete, Tafadzwa, **Phuti Choshi**, Sarah Pedretti, Mireille Porter, Riyaadh Roberts, Rannakoe Lehloenya, and Jonathan Peter. 2023. 'Skin infiltrating T-cell profile of drug reaction with eosinophilia and systemic symptoms (DRESS) reactions among HIV-infected patients', *Frontiers in Medicine*, 10: 1118527.

*First co-author

Acknowledgements

To my supervisors, Prof Jonny Peter: You believed in me when I was convinced, I couldn't do this. You challenged me, allowed me to fall apart and helped me get to the other side of fear and discouragement. I will forever be grateful for your patience, guidance, and teachings. Success and sustained interest in research are largely related to the learning environment. I made the right decision pursuing this PhD in your lab.

Prof Rannakoe Lehloenya: I always share with our team how one feels like a drug hypersensitivity expert after spending time with you and learning from you. Your passion for this work and the care you have for patients inspires me and it is a great reminder of why we are doing this research. Thank you for your support, encouraging feedback and guidance.

Prof Elizabeth Phillips: The time I spent in your lab at Vanderbilt University Medical Centre, will remain one of the best moments of my life and the greatest highlight of my career. Thank you for teaching me so much, pushing me and helping make this work better.

To my colleagues at the Division of Allergology and Clinical Immunology, Allergy and Immunology Unit, I have never met or worked with a more excellent and efficient team like you. Thank you so much for all your assistance and encouragement. I appreciate you and your brilliance.

To our collaborators at IIID Murdoch University, Vanderbilt University Medical Center, University of Cape Town South African Tuberculosis Vaccine Initiative, thank you so much for believing in this work as much as we do. Thank you for your assistance with experiments, data analysis, scientific input and more.

To the NIH Fogarty (award number D43 TW010559) UCT HATTP committee, this work wouldn't be possible without you. Thank you for the financial support, career development opportunities and for being a constant source of inspiration through all the seminars and talks with research experts. A special thanks to Kathryn Wood and Prof Graeme Meintjes, your dedication to making medical science research accessible to all students is admirable.

Additional thank you to the following institutions for financial support. South African Medical Research Council - the work reported herein was made possible through funding by the South African Medical Research Council through its Division of Research Capacity Development under the Bongani Mayosi National Health Scholars Programme from funding received from the Public Health Enhancement Fund/South African National Department of Health. National Research Foundation. EDCTP - The IMARI-Africa project is part of the EDCTP2 programme supported by the European Union (grant number TMA2017SF-1981). NIH Fogarty career development award number K43TW011178-04.

A huge thank you to all participants in the IMARI registry, doctors and nurses at Groote Schuur hospital, dermatology ward and the multidisciplinary drug allergy clinic. An additional thank you to Prof Graeme Meintjes's lab and Prof Rob Wilkinson's lab for the additional control participants used in this thesis.

To my friends all over the world, thank you so much for your love and for always reminding me I can do this.

To my family, God really did me solid with you. Thank you for providing soft landings and lifting me up when I needed it the most. I literally wouldn't have done this without you. Kea leboga Bakgalaka. Ke sepela ke tseba gore a ke Mmirwa ke le tee, Babirwa batshi ba tletse lehwiliri.

I thank God for the blessing of this opportunity. I am most grateful for the strength and wisdom to see it to finish. "*Ebe kganya le bogolo, le maatla le borena go Modimo wa lesedi."*

Table of Contents

List of Figures

List of Tables

Abbreviations

3TC - Lamivudine
ABC - Abacavir
ADME – Absorption, digestion, metabolism, and excretion
ADR – Adverse drug reactions
AGEP - Acute generalized exanthematous pustulosis
AHS - Abacavir hypersensitivity
ALDEN - Algorithm for drug causality in epidermal necrolysis
ALT - Alanine aminotransferase
ANA – Antinuclear antibody
APCs – Antigen presenting cells
AST - Aspartate aminotransferase
BDQ - Bedaquiline
BSA – Body surface area
CADR - cutaneous adverse drug reaction
CBZ - Carbamazepine
CDR – Complimentarity-determing region
CFZ - Clofazimine
CITE-seq - Cellular indexing of transcriptomes and epitopes by sequencing
CLIP - Class II associated invariant-chain peptide
CMV – Cytomegalovirus
CT - Computerized tomography
CTLs - Cytotoxic T lymphocytes
CyTOF – Mass cytometry by time of flight
DCs – Dendritic cells
DILI – Drug induced liver injury
DMSO - Dimethyl sulfoxide
DNA – Deoxyribonucleic acid
DRESS – drug reaction with eosinophilia and systemic symptoms
EBV - Epstein-Barr virus
EFV - Efavirenz
ELISpot – Enzyme linked immunospot assay
EMB - Ethambutol
ER - Endoplasmic reticulum
ERAP – Endoplasmic reticulum aminopeptidase
ESKOM - Electricity supply commission
ETH - Ethionamide
FBS - Foetal bovine serum
FDC - Fixed dose combination
FLTD – First line anti-tuberculosis drugs
GBFDE - Generalised bullous fixed drug eruption
GLIPH - Grouping of lymphocyte interactions by paratope hotspots
H&E - Haematoxylin and eosin
HAART - Highly active antiretroviral therapy
HHV - Human herpesvirus
HIV –Human immunodeficiency virus
HLA – Human leukocyte antigen
HSRs - Delayed hypersensitivity reactions
IHC - Immunohistochemistry
IIID - Institute for immunology and infectious diseases
IM-ADRs – Immune mediated adverse drug reactions
IMARI – Immune mediated adverse drug reactions in Africa
INF-γ - Interferon-gamma
INH - Isoniazid
IQR - Interquartile range
IRIS - Immune reconstitution inflammatory syndrome
ITIMs - Immunoreceptor tyrosine inhibitory motifs
KIR – Killer immunoglobulin receptor
LFX - Levofloxacin
LRC - Leukocyte receptor complex
LTT - Lymphocyte transformation test
LZD - Linezolid
MHC – Major histocompatibility complex
MOX - Moxifloxacin
MTB - Mycobacterium tuberculosis
NAD - Nicotinamide adenine dinucleotide
NK cell – Natural killer cell

NKC - NK gene complex
NPV - Negative predictive value
NRTIs – Nucleotide reverse transcriptase inhibitors
PBMCs – Peripheral blood mononuclear cells
PCR – Polymerase chain reaction
PLHV – Persons living with human immunodeficiency virus
PPV - Positive predictive value
PZA - Pyrazinamide
RHZE - Rifafour
RIF - Rifampicin
SAM - South African Mixed Ancestry
SCAR – Severe cutaneous adverse drug reactions
ScRNA-seq – Single cell ribonucleoside acid sequencing
SDC – Sequential drug challenge
SEB – Staphylococcal enterotoxin B
SFU - Spot forming units
SI- Stimulation index
SJS/TEN – Stevens Johnson syndrome and Toxic epidermal necrolysis
SLE - Systemic lupus erythematous
SNPs - Single nucleotide polymorphisms
TAP - Transporter associated with antigen processing
TB – Tuberculosis
TCR – T cell receptor
TGF-beta – Transforming growth factor-beta
Th - Helper T cells
TMP-SMX - Trimethoprim- sulfamethoxazole
TNF - Tumour necrosis factor
TZD - Terizidone
V-J junction – Variable – Joining junction
VUMC – Vanderbilt University Medical Center
t-SNE - t-distributed stochastic neighbour
UMAP – Uniform manifold approximation projection

Chapter 1 – General introduction

1.1. Adverse drug reactions classification and diagnosis

Adverse drug reactions (ADRs) are defined as any unwanted or harmful reaction following administration of a drug(s) at normal therapeutic dose (Blumenthal et al. 2019). ADRs are divided into two types: type A are on-target, predictable reactions from the known pharmacologic activity of the drug. They are dose dependent and comprise approximately 80% of all ADRs (Pavlos et al. 2015). Type B are off-target, unpredictable, normally immune-mediated ADRs (IM-ADRs) independent of the pharmacologic activity of the drug (figure 1-1). Not all ADRs fit into Type A and B categories and with advances in the mechanistic understanding of ADRs, further classification and additional categories have been proposed (Peter et al. 2017; White et al. 2015). Additional categories include Type C, D and E related to duration of drug use e.g., withdrawal effects; delayed effects e.g., teratogenicity; and drug interactions respectively (Schatz and Weber 2018). Further categorisation of Type B ADRs includes reactions that stem from off-target pharmacologic drug effects producing reaction with an immunological phenotype, without immunological memory - such as in patients with non-IgE mediated mast cell activation syndrome (McNeil et al. 2015). IM-ADRs are grouped according to the Gell-Coombs's classification based on duration of drug exposure and the primary immune cell involvement. They include B cells in antibody mediated (Gell-Coombs types I-III) and purely T cell mediated ADRs (Gell-Coombs Type IV, delayed) (Peter et al. 2017) (figure 1-1).

Immediate ADRs typically occur within one hour of drug exposure and can include dose independent IgE mediated mast cell activation reactions, in their severest form characterised by cardiovascular symptoms, angioedema and urticaria and dose related non-IgE mediated reactions with less cardiovascular involvement (Mertes et al. 2009). IgE and non-IgE reactions are not easily distinguishable on symptoms, but the recently well described mechanism for non-IgE reactions includes interaction with immune receptor MRGPRX2 for mast cell activation (McNeil et al. 2015). Delayed hypersensitivity reactions (HSRs) are mediated by T cells or antibodies other than IgE. While the commonest T-cell-mediated reactions such as maculopapular rash are mild, severe cutaneous adverse reaction (SCAR) phenotypes which includes drug reaction with eosinophilia and systemic symptoms (DRESS), Stevens-Johnson syndrome, toxic epidermal necrolysis, generalised bullous fixed drug eruption (GBFDE) and acute generalised exanthematous pustulosis, detailed below, can be life threatening. SCARs are considered purely T cell mediated reactions, thus classified in the Gell-Coombs Type IV group according to primary immune cell involvement (section 1.9). The most common phenotypes of SCARs seen in the South African setting are DRESS and SJS/TEN (Lehloenya and Dheda 2012) – the focus of this review.

1.1.1. Drug reaction with eosinophilia and systemic symptoms (DRESS)

Drug reaction with eosinophilia and systemic symptoms (DRESS) is a severe form of cutaneous adverse drug reaction (CADR) that involves a rash of varying severity, haematologic abnormalities such as eosinophilia and/or atypical lymphocytes, and internal organ involvement. It is a delayed HSR that usually occurs 2-6 weeks after the first exposure to the drug. As a multiorgan HSR, DRESS patients present with a combination of fever, pruritus, burning skin pain, a typical or suggestive rash, erythema, facial oedema and lymphadenopathy. Liver, kidney, lung, heart, spleen and pancreatic involvement have been noted in some patients because of specific eosinophil or lymphocyte tissue infiltration (Kardaun et al. 2013). Liver biological abnormalities manifest commonly as hepatic cytolysis, sometimes cholestasis. Kidney involvement is characterised by acute interstitial nephritis, a common cause of acute kidney injury, accompanied by interstitial inflammation, oedema and tubulitis. Patients with lung involvement present with dyspnoea, cough, eosinophilic pneumonitis, and in rare and severe cases, acute respiratory distress syndrome. The heart is affected in up to 27% of cases, characterised by myocarditis and pericarditis. Cardiac involvement with electrocardiogram, computerized tomography (CT) scan, or cardiac enzyme abnormalities, can be fatal (Cho, Yang, and Chu 2017a). Although relatively rare in comparison to others, pancreatic involvement most commonly manifests as type 1 diabetes mellitus and acute pancreatitis (Jevtic et al. 2021). Splenomegaly, particularly in children, and splenic thrombosis have also been described in association with DRESS(Bejia 2007; Ganeva et al. 2008; Jeong et al. 2019; LaHood and Sokol 2017; Metterle, Hatch, and Seminario-Vidal 2020; Michel et al. 2005).The variation in cutaneous signs and the number of organs involved makes the diagnosis of DRESS challenging. To reduce misdiagnosis, diagnostic criteria that require the presence and/or absence of certain clinical features and laboratory investigations during the acute stage. The most widely used are the Japanese and RegiSCAR validation criteria. Additional parameters considered include an eruption a minimum of 3 weeks after starting medication, persistence of symptoms despite withdrawal of the drug, and reactivation of single or multiple human herpesviruses (HHV) (Kardaun, Mockenhaupt, and Roujeau 2014; Shiohara and Mizukawa 2019)

The detection of a single or multiple HHVs reactivation has been proposed as a diagnostic marker for DRESS - with HHV6 as the most prevalent HHV to reactivate. HHV6 reactivation is usually detectable up to 2−3 weeks after the onset of DRESS. More recently, reactivation of other HHV including Epstein-Barr virus (EBV), HHV7, and cytomegalovirus (CMV) has been observed in up to 76% of DRESS patients with (Pavlos et al. 2014). HHV reactivation often wanes and flares in a sequential manner (Kano et al. 2006). This variable pattern of reactivation impacts clinical presentation, duration of disease as well as frequency and pattern of flare-ups, further complicating diagnosis, and management of DRESS (Ishida et al. 2014).

To standardise case definition, diagnosis and management and management of DRESS the RegiSCAR group developed a scoring system. This is an internationally validated algorithm for the definition of DRESS cases. Each case is accordingly graded as definite, probable, possible, or not a case of DRESS. (Kardaun et al. 2007; Kardaun, Mockenhaupt, and Roujeau 2014) RegiSCAR DRESS scores of <2 is defined as "not a case of DRESS", 2-3 define a "Possible case", 4-5 a "Probable case" and >5 a "Definite case". This is particularly important in mechanistic studies where precise case definition is required. Table 1-1 highlights included parameters and their weighting. Absence of certain parameters e.g., fever > 38°C and an incompatible rash attract negative points. Cases do not have to fulfil all criteria to be validated as definite (Chen et al. 2013).

Table 1-1 Scoring system for classifying DRESS cases as Definite, Probable, Possible, or No Case

SCORE	-1	0	1	2	min	max
Fever ≥ 38.5 ^{0}C	N/U	Y	-	-	-1	0
Lymphadenopathy	-	N/U	Y	-	0	1
Eosinophilia	-	N/U	-	-	0	2
Eosinophils	-	-	700-1499/µl	≥1500/µl	-	-
Eosinophils, if leukocytes <4000	-	-	10-19.9%	≥20%	-	-
Atypical lymphocytes	-	N/U	Y		0	1
Skin involvement	-	-	-	-	-2	2
Skin rash extent (% BSA)	-	N/U	>50%	-	-	-
Skin rash suggests DRESS	N	U	Y	-	-	-
Biopsy suggests DRESS	N	Y/U	-	-	-	-
Organ involvement *	-	-	-	-	0	2
Liver	-	N/U	Y	-	-	-
Kidney	-	N/U	Y	-	-	-
Lung	-	N/U	Y	-	-	-
Muscle/heart	-	N/U	Y	-	-	-
Pancreas	-	N/U	Y	-	-	-
Other organ(s)	-	N/U	Y	-	-	-
Resolution ≥ 15 days	N/U	Y	-	-	-1	0
Evaluation other potential causes:	-	-	-	-	0	1
ANA	-	-	-	-	-	-
Blood culture	-	-	-	-	-	-
Serology for HVA/ HVB/ HVC Chlamydia-/ Mycoplasma pneumoniae	-	-	-	-	-	-
Other serology/PCR	-	-				
If none positive and ≥ 3 of above negative						
TOTAL SCORE					-4	9

Abbreviations: U = unknown/unclassifiable; N = No; Y = Yes; ULN = upper limit of normal
* After exclusion of other explanations: 1 = 1 organ, 2 = ≥ 2 organs

Final Score:
<2: No case
2-3: Possible case
4-5: Probable case
>5: Definite case

1.1.2. Stevens Johnson syndrome and toxic epidermal necrolysis (SJS/TEN)

Stevens-Johnson syndrome and toxic epidermal necrolysis (SJS and TEN) form a spectrum of epidermal necrolysis (EN), differentiated by the extent of skin detachment and epidermal necrosis. In SJS, there is less than 10% of skin detachment, in TEN there is more than 30% and SJS/TEN overlap for anything in between. TEN, the more severe form, carry mortality rate of up to 50% (Sekula et al. 2013). A US study of administrative and survey data reported in-hospital mortality as high as 29.5% in cases where EN was made as a secondary diagnosis (Hsu et al. 2016). EN typically develop 4–28 days after drug exposure. General symptoms such as fever, stinging eyes, sore mouth, ear, nose, and throat involvement, and skin pain frequently precede dermatological signs. Although initial symptoms can be confused with upper respiratory tract infection, they are key in early diagnosis. Within 3 days, these signs, and symptoms progress to eruption on the face, upper trunk palms and soles (Auquier-Dunant et al. 2002; Sekula et al. 2013) and disease progression is limited to 7-10 days.

Initial lesions are characterised as erythematous, macules, blisters, and large epidermal detachment revealing areas of raw, red dermis seen in severe burns, and two or more erosive mucous membranes involved. Intact blisters have Nikolsky's sign, which involves dislodgment of the epidermis when lateral pressure is applied. Nose, mouth, eyes, genitalia, or anus are more mucous membranes affected by extensive erythema, blisters, or erosions in the early stages of the reaction. Eye involvement characterised by conjunctival lesions, which range from, hyperaemia, erosions, photophobia, and tearing. All affected mucous membranes can potentially sustain permanent damage (Catt et al. 2016). Severe ocular manifestations that could lead to permanent visual impairment include corneal ulceration, anterior uveitis, or purulent conjunctivitis. The lips develop haemorrhagic cheilitis that can result in angular adhesions and microstomia. The rest of gastrointestinal system involvement is supported by reports of EN affecting the oesophagus, stomach, small intestines, colon and the rectum supported by visualization on post-mortem and scopes, gut perforation, intussusception, strictures, stenosis, bleeding, diarrhoea, protein-losing enteropathy and hepatitis amongst others. Similarly, lung involvement is supported by evidence of chronic lung disease, bronchiolitis obliterans, interstitial lung disease, pulmonary air leak syndrome, laryngeal obstruction and obliterative bronchitis amongst others. Genitourinary involvement can manifest as acute kidney injury. Erosions can result in vaginal and introital adenosis, cervical/vaginal adhesions and stenosis, labial synechiae if neglected (Lehloenya 2022). The diagnosis of SJS/TEN mainly relies on identification of a broad range of clinical signs and symptoms and histological tests (Table 1-2). Differential diagnoses include erythema multiforme, bullous lupus erythematosus, GBFDE and linear IgA bullous dermatosis.

Table 1-2: SJS/TEN diagnosis and scoring

		PERCENTAGE	DATE
1. max. Involvement	Erythema		
	Blisters and erosions		
		Y/N/U	
2. Blisters and erosions of the Skin			
3. Epidermal detachment > 5 cm			
4. mucous membranes	red or stinging eyes		
	conjunctivitis or blepharitis		
	severe conjunctivitis or blepharitis diagnosed by an ophthalmologist		
	erosions of lips		
	oral erosions		
	genital erosions		
	erosions of other mucosa		
5a. Skin burning before			
5b. Skin pain before			
6. Nikolski's sign			
7. Erythema / large plaques without single spots			
8. Targets or spots			
9. Diagnosed by a dermatologist			
10. Photographs			
11. Biopsy			
	date of first blister / erosion of the skin or mucosa		
	ad 8. targets - spots, type:		
	1. spots		
	2. typical targets		
	3. atypical targets raised		
	4. atypical targets flat		
	5. type of targets unknown		
		Y/N/U	DATE
	ad 8. targets - spots, distribution:		
	1. limbs		
	2. widespread		
	3. other		
12. Erythema patches ≥ 5cm			
	brownish/violacous		
	well demarcated		
	number		
	different body parts		
13. Fever ≥ 38.5 °C within 3 days after admission			

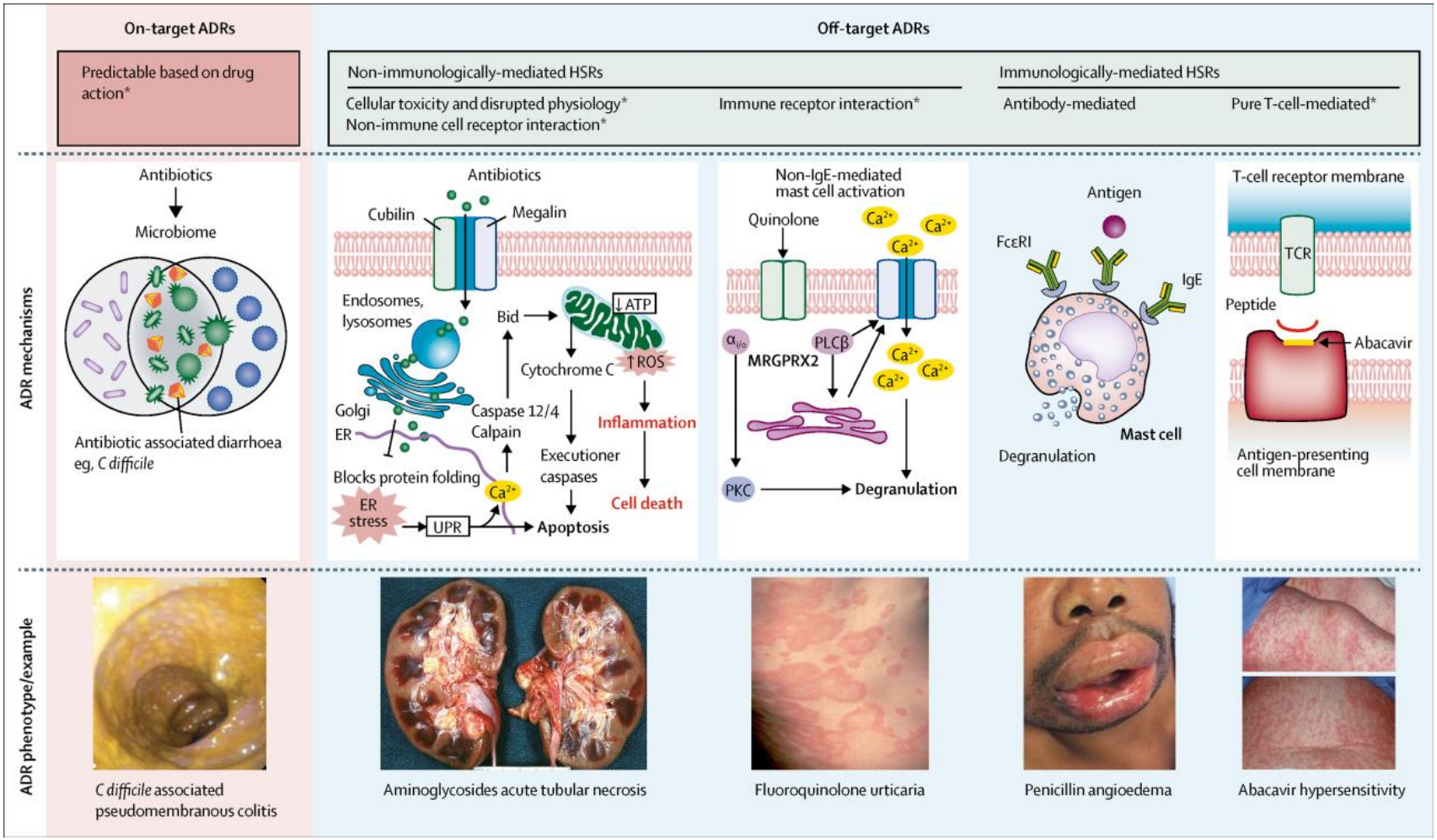

Figure 1-1: Schematic illustration of the classification of ADRs

Adapted from (Blumenthal et al. 2019)

1.2. Epidemiology of immune mediated adverse drug reactions (IM-ADRs)

The most common ADRs are CADRs such as maculopapular exanthema or morbilliform eruptions, fixed drug eruption, and urticaria which can be found listed among the side effects of almost all drugs. They are not life threatening, with the incidence estimated at 0.3 to 8%. Antibiotics and nonsteroidal anti-inflammatory drugs are the commonest causative agents (Bigby 2001; Svensson, Cowen, and Gaspari 2001; Mockenhaupt 2017). The estimated incidence, prevalence and mortality of the more severe life-threatening IM-ADR vary considerably between geographic regions. Factors that contribute to the variation across different regions include differences in ethnicity, the use of drugs that are high risk for SCARs, socioeconomic status limiting access to pre-screening methods and the lack or frequency of population based diagnostic biomarkers in some regions. Underlying diseases, particularly the severity of infectious diseases in the developing world not only increases the risk of SCARs, but also contributes to unacceptably high mortality rates and severe sequelae (Peter, Choshi, and Lehloenya 2019).

In a Korean study, annual incidence estimates were 3.96 to 5.03 in SJS and 0.94 to 1.45 in TEN per million, with in-hospital mortality of 5.75% for SJS and 15.1% TEN (Yang et al. 2016). Long term morbidity associated with SJS or TEN was ocular sequelae with the prevalence of 43.15% for SJS and 43.4% for TEN patients, followed by urethral sequelae occurring in 5.7% of SJS and 9.4% TEN patients (Yang et al. 2016). Previous East Asian study reported a higher prevalence of SCAR hospitalisations at 0.32/1000 people in Beijing (Li and Ma 2006). Among Caucasian/European regions, a prospective study on population based registry in Germany reported a SCAR incidence of 1.53–1.89 per million people (Mockenhaupt 2012; Naegele et al. 2020) and an incidence rate of 3.89 per 10 000 patients was observed in Spain (Ramírez et al. 2017). The incidence and prevalence vary even further when stratified by offending drug and SCAR combination. In another Korean study, DRESS was the most prevalent SCAR phenotype at 11.3% caused by allopurinol followed by 10.2% of cases classified as SJS/TEN (Kang et al. 2019). Generally, antibiotics and anticonvulsants are the most common reported offending drugs at the time of hospitalisation and in already hospitalized patients (Bigby et al. 1986; Loo et al. 2018).

Globally, SCAR incidence is estimated at 10 cases per million people annually – with SJS/TEN and DRESS as the 2 commonest SCAR phenotypes, with a prevalence of 1 to 7 cases per million and 1 to 4 cases per 10,000, respectively (Shiohara and Mizukawa 2019). SJS/TEN increases almost a 1000-fold to as high as 2 per 100 among persons living with HIV (Lehloenya and Dheda 2012). The incidence of DRESS is mainly driven by new users of anticonvulsants drugs (e.g., carbamazepine or phenytoin) with estimates at one per 1000 to one per 10 000 people (Seitz et al. 2006). Epidemiological data on AGEP are limited but prevalence is estimated at 0.35 to 5 cases per million.

Despite their low incidence, SCARs have a mortality rate of 14 to 70% depending on the severity of the reaction and concomitant infections (Lehloenya and Dheda 2012; Verma, Vasudevan, and Pragasam 2013; Yang et al. 2016)

1.2.1. Different epidemiology in HIV/TB settings driven by disease burdens and prescribing patterns.

This section and tables are modified from - Peter, Jonny, **Phuti Choshi**, and Rannakoe J. Lehloenya. 2019. 'Drug hypersensitivity in HIV infection', *Current opinion in allergy and clinical immunology*, 19: 272-82.

The continual development, optimization, and early initiation of highly active antiretroviral therapy (HAART) has made HIV infection a treatable chronic disease in many high-income countries; with the treatment frontier focused on drug-resistance and pre-exposure prophylaxis. Lower middle-income countries, particularly in Africa, that form the epicentre of the epidemic, are falling well below the 90:90:90 UNAIDS targets of HIV diagnosis and HAART initiation (Bain, Nkoke, and Noubiap 2017). In these countries, patients continue to present with advanced immunosuppression and multiple co-morbidities including opportunistic infections, particularly tuberculosis; malignancies, metabolic disorders; and end-organ damage (Coughlan and Cameron 2016). The wide disease spectrum and associated infections combined with country-specific markets and accessibility, determine a changing landscape of drug exposures and patterns of hypersensitivity.

There are more than 100 drugs that have been reported to cause IM-ADRs in HIV, most commonly CADRs. Table 1-3 lists the common offending drugs, dividing them into two broad groups – HAART and anti-infective agents used to treat comorbid infections. Wherever possible, the commonest individual offending agent in a particular drug class is listed, and prevalence data for specific hypersensitivity phenotypes are provided. IM-ADR to HAART is well recognized with the highest prevalence being CADRs to nonnucleoside occur in 15% of patients starting treatment, and a significant portion are SCARs, most commonly epidermal necrolysis and DRESS; as well as drug-induced liver injury (DILI) to nevirapine (Wu et al. 2017; Stewart et al. 2016; Sarfo et al. 2014). CADRs to NRTIs, such as tenofovir and emtricitabine are most recently described in large postexposure prophylaxis cohorts, when used in two-drug fixed dose combination (Bekker et al. 2018). In contrast, abacavir hypersensitivity reaction has been largely eliminated in populations where HLA-testing pre prescription has been implemented, but still occurs in African populations, but at a low frequency. The low prevalence of the allele in Africans makes testing not to be cost-effective (Stainsby et al. 2019). Increased use of integrase strand transfer inhibitors, and their availability in fixed dose combinations will mean increased exposure to this class of agents. IM-ADRs – mostly CADRs, drug hypersensitivity syndrome and case reports of drug-induced liver injury have been described with this class of drugs (Wang et al. 2018; Thomas et al. 2017). An interesting drug

hypersensitivity syndrome, associated with marked elevation in inflammatory cytokines and markers, developed in a small healthy volunteer study evaluating a combination of dolutegravir with isoniazid/rifapentine for anti-TB prophylaxis and associated with high isoniazid plasma concentrations (Brooks et al. 2018). Larger studies with dolutegravir report only a low incidence of IM-ADRs (Nyaku et al. 2019; Taiwo et al. 2018; Walmsley, Antela, Clumeck, Duiculescu, Eberhard, Gutierrez, Hocqueloux, Maggiolo, Sandkovsky, Granier, Pappa, Wynne, Min, Nichols, et al. 2013). High rates of injection site reactions, which may be immune mediated, have also recently been reported with the use of a suspension form of cabotegravir, given as an intramuscular depot preparation (Landovitz et al. 2018). There is an increased number and use of fixed dose combination HAART to improve adherence. Our clinic has several cases of CADRs, and even more severe DRESS, to fixed dose combination (FDC) preparations; where patients tolerate all individual drugs not as an FDC or an alternative FDC preparation, making excipients the likely offending agents (unpublished data). Two earlier reviews have discussed rare reactions to other HAART drug classes, such as protease inhibitors, for example, fosamprenavir, fusion inhibitors and the CCR5 inhibitor maraviroc (Yunihastuti, Widhani, and Karjadi 2014; Phillips and Mallal 2007).

Anti-infective agents used to treat comorbid infections are the other common offending drugs causing IM-ADRs in HIV-infected patients, with the overall prevalence reflecting drug use and disease burdens. IM-ADRs to the first line antituberculosis drugs (FLTDs) – rifampicin, isoniazid, pyrazinamide, and ethambutol, are the commonest given the high prevalence of comorbid TB in HIV endemic settings. A full spectrum of particularly delayed hypersensitivity reactions to FLTDs and second-line anti-TB drugs is listed in Table 1 and has recently been comprehensively reviewed. Isoniazid, rifampicin and pyrazinamide are the commonest offending agents for both SCAR and drug-induced liver injury (DILI) (Nagarajan and Whitaker 2018). A recent cohort of 307 Thai adults with HIV/TB co-infection reported CADRs as the commonest IM-ADRs, occurring at an incidence rate of 0.41 events/person-year (Boonyagars, Hirunwiwatkul, and Hurst 2017). Trimethoprim-sulfamethoxazole (TMP-SMX), used in large amounts for prophylaxis and treatment of Pneumocystis is a well-known cause of IM-ADR, with DRESS/drug hypersensitivity syndrome, SJS/ TEN, and fixed drug eruption often reported (Mockenhaupt et al. 2008; Hiransuthikul et al. 2016; Kouotou et al. 2017). In a recent Ethiopian study, 10% of patients discontinued therapy because of TMP-SMX allergy (Sisay et al. 2018). Our clinic has begun to see fewer cases of TMP-SMX IM-ADRs as the HIV treatment guidelines have changed, with initiation of HAART at diagnosis irrespective of CD4 cell count, and greater ART coverage resulting in a substantial drop in the usage of the drug (Murphy et al. 2007). Although infrequent, cross-reactivity has been reported between structurally related drugs including TMP-SMX and dapsone (Holtzer, Flaherty, and Coleman 1998); efavirenz and nevirapine (Soriano et al. 2000; Manosuthi et al. 2006); emtricitabine and lamivudine (Suarez-Lorenzo et al. 2016); and darunavir and TMP-SMX (Chung, Chang, et al. 2015).

Table 1-3: Epidemiology of ADRs induced by drugs used in HIV TB treatment

	Common Offending Drugs	Incidence	Types of reactions
Antiretrovirals	Abacavir	2.3 - 9 % (Borras-Blasco et al. 2008; Ma, Lee, and Kuo 2010), 4 - 8% (Sulkowski et al. 2002; Martin-Carbonero et al. 2003)	Abacavir hypersensitivity
	nevirapine	16 - 32% (Carr and Cooper 2000; Montessori et al. 2004; Phanuphak et al. 2007) 0.3 – 10% (Pollard, Robinson, and Dransfield 1998; Warren et al. 1998; Manosuthi et al. 2007)	Nevirapine-associated maculopapular rash SJS/TEN
	efavirenz	10–27% (Mehta and Maartens 2007) 0.1% (Colebunders et al. 2004; Sulkowski et al. 2002)	Mild to moderate rash Severe drug eruptions such as SJS/TEN and Erythema multiforme
	Fosamprenavir	19% (Chaponda and Pirmohamed 2011) 3 - 8% (Chaponda and Pirmohamed 2011; Borras-Blasco et al. 2008)	Skin rash Moderate to severe reactions.
	Tenofovir	5–7% (Woolley et al. 2004; Lockhart et al. 2007; Verma et al. 2012)	Maculopapular rash, photoallergic dermatitis, lichenoid eruption with eosinophilia
	Dolutegravir	1% (Walmsley, Antela, Clumeck, Duiculescu, Eberhard, Gutierrez, Hocqueloux, Maggiolo, Sandkovsky, Granier, Pappa, Wynne, Min, and Nichols 2013)	Hypersensitivity reactions and sometimes organ dysfunction, (i.e. liver injury)

Drugs used to treat HIV-associated infections				
	Common offending Drugs	Incidence		Type of reactions
		Without HIV	With HIV	
Antimicrobials	Trimethoprim sulfamethoxazole (TMP-SMX)	5% (3–5%) (Chaponda and Pirmohamed 2011; Khan and Solensky 2010)	>60% (30–80%) (Chaponda and Pirmohamed 2011; Khan and Solensky 2010)(Para et al. 2000)	Drug hypersensitivity, CADR
	Dapsone	Unknown, mainly case reports (Vinod, Arun, and Dutta 2013)	18% (El-Sadr et al. 1998; Sánchez-Borges et al. 2013)	Hypersensitivity reactions related to dapsone, DRESS

			3% (Beumont et al. 1996a)	
Antimycobacterial	Standard anti-TB treatment	1% (Nunn et al. 1991) 2% 10% (Matono et al. 2017)	20% Adults (Nunn et al. 1991) 21% Children (Chintu et al. 1993) 13% (Lehloenya and Dheda 2012) 23% (Lehloenya and Dheda 2012) 7.1% Elderly (Chang et al. 2014) 51% (Matono et al. 2017)	CADR Adverse events
	Rifampicin	1.3% (Girling 1977)	24% (Girling 1977)	Diverse types of hypersensitivity reactions (mild rash to severe reactions accompanied by systemic symptoms)(Martinez, Collazos, and Mayo 1999)
	Isoniazid	-	Unknown, mainly case reports (Bakkum, Waard-Van Der Spek, and Thio 2002)	Hepatoxicity, Maculopapular rash
	Pyrazinamide	-	2.8% (HIV status not clear) (Tan et al. 2007)	CADR
	Ethambutol	-	Unknown, mainly case reports (Surjapranata and Rahaju 1979; Pegram, Mountz, and O'Bar 1981; Wong et al. 1995; Sánchez-Borges et al. 2013; Bakkum, Waard-Van Der Spek, and Thio 2002)	Erythema multiforme, SJS/TEN, DRESS
	Fixed dose combinations (Rifafour)	-	Unknown, mainly case reports	
	Fluoroquinolones Ethionamide Kanamycin/Amikacin	-	~20% (Lehloenya, Wallace, et al. 2012)	SCAR

1.3. Drug causality tools

Assigning drug causality in SCARs is necessary for the management of patients. However, it is often made difficult by polypharmacy with multiple implicated drugs, the clinical heterogeneity and overlapping features of the different phenotypes, multifactorial pathophysiology, and a lack of reliable biomarkers. The two validated well-established methods or algorithms for assignment of drug causality following an adverse drug reaction are the Naranjo algorithm and algorithm for drug causality in epidermal necrolysis (ALDEN) scoring. Naranjo algorithm has a more general application while ALDEN is specific for EN. There are ten parameters that are assessed for the Naranjo algorithm that detail duration of exposure and chronology, dose, drug notoriety, index day (the day the first symptoms were noted), effect of drug withdrawal and outcomes of drug ere-exposure. The score must take into consideration information the clinical characteristics of each phenotype include latency period. It allocates a probability score for each drug assessed for causality and grades them as 'definite' (total score >9), 'probable' (total score of 5 to 8), 'possible' (total score of 1 to 4) or 'doubtful' (total score <0) that a drug administered in therapeutic doses caused an adverse reaction. It is frequently used, quick and simple tool that classifies > 90% of suspected adverse drug reactions as 'possible' (Naranjo et al. 1981).(appendix, section 1.1). However, the algorithm does not consider factors like drug–drug interactions.

ALDEN was developed by RegiSCAR and other drug allergy experts to evaluate the causality of suspected drugs in EN. Built into the algorithm is the ability to identify drugs that are safe to be administered again – making it appropriate for utilization when multiple drugs are implicated (appendix, section 1.2). The parameters evaluated in ALDEN include duration of drug exposure, drug present in the body on symptoms onset, rechallenge data and drug notoriety. Each drug is assigned a probability of being the offender, A score drug <0, very unlikely; 0–1, unlikely; 2–3, possible; 4–5, probable; ≥6, very probable (Sassolas et al. 2010). Their results strongly correlated with another case control study that quantified the risks associated with the use of specific drugs in SJS or TEN (Roujeau et al. 1995).

1.4. Offending drug testing methods – diagnostic accuracy and limitations

An important aspect of SCAR management is the determination and confirmation of the offending drug so as to avoid the drug in the future. ALDEN and Naranjo score have their limitations and their determinations often lack certainty. Additional confirmatory tests are critical, particularly in the setting of multiple potential offenders and limited therapeutic options. None of the current methods offers 100% sensitivity and specificity for all drugs at all times. Apart from not being standardised, having a low negative predictive value, insufficient sensitivity and specificity, they are still useful tests if multiple drugs are implicated. The best results are obtained with a combination of these

diagnostic tests. The majority of these tests' utility follows the occurrence of a SCAR, with the exception of human leucocyte antigen (HLA) (reviewed in section 1.6.1 of this thesis) screening.

Identification of specific HLA alleles associated with particular SCAR phenotypes, individual drugs or classes of drugs is currently the most important screening tool to avoid SCARs. However, its limitations include variable strength of association between suspected drug(s) and particular HLA alleles, the allele frequency in a specific population, and the combination of other host, drug and environmental factors that ultimately result in a SCAR (Duong et al. 2017). Particularly in HIV/TB endemic settings where patients are on multidrug regimens and optimal treatment exclusion or interruption is associated with drug resistance and causes major morbidity and mortality (Dheda, Barry, and Maartens 2016). The traditional culprit drug tests include, patch testing, intradermal testing, in vitro drug testing, oral drug rechallenge and have been reviewed extensively with recommendations (Phillips et al. 2019).

1.4.1. Patch testing

Patch testing is one of the routine diagnostic tools used in drug hypersensitivity reactions to determine offending agent. It involves taping the suspected drug in petroleum jelly onto the patients back for 48 h. The patch results are read after 48 h, follow up at 96 h and in some cases up to 7 days in comparison to unpatched skin. Patch tests have been demonstrated to be safe, with few reported recurrences or severe reactions. They are performed 4 to 6 weeks after first symptoms onset, with some studies recommending up to 6 months after recovery to avoid relapses. The patch test reaction timing, specificity and sensitivity vary according to the suspected drug and SCAR phenotype. The reaction may occur more quickly in abacavir hypersensitivity and fixed drug eruption; however, more sensitivity was observed in AGEP than SJS/TEN and DRESS. For drugs, highest sensitivity was reported with anticonvulsants and beta-lactam antibiotics and lowest for vancomycin, trimethoprim-sulfamethoxazole, allopurinol, macrolides and cephalosporins. However, the test is limited by lack of standardization, availability of commercial reagents and optimal testing concentrations without inducing systemic symptoms (Bakkum, Waard-Van Der Spek, and Thio 2002; Lehloenya, Todd, et al. 2016; Phillips et al. 2019; Trubiano et al. 2018; Lehloenya et al. 2020b).

1.4.2. Intradermal testing

Despite higher sensitivity than patch and prick testing, intradermal testing is not recommended because of the risk of relapse. In a study by Torres et al, sensitivity of delayed IDT for antimicrobials ranged from 6.6% to 36.3% for MPE and 64% to 100% for DRESS (Romano et al. 2004; Torres et al. 2003) . The use of intradermal testing has proven to be useful after a negative patch test, particularly for antibiotic associated CADRs. The existing recommended guidelines to avoid a relapse includes testing 6 months after the acute stage, using non-irritant concentrations of drugs and extra caution in

immunocompromised patients. Intradermal testing involves syringe injection of the drug in the forearm. A reaction is defined as erythema or swelling at injection site and immediate readings are taken within 20 minutes and delayed readings at 6, 24 and 48 hours. Intradermal testing is not easy to perform, requires commercially sterile drug preparation with limited availability in developing world and specialists' administration is recommended. Moreover, the use of non-irritant concentrations is associated with low sensitivity in mild reactions and delayed reactions which seem dose dependent (Lehloenya et al. 2020b).

1.4.3. Oral drugs rechallenge

In situations where drugs are needed urgently and the benefits outweighs the associated risks, oral challenge with culprit drug is considered as a diagnostic tool. The drug re-exposure testing has been performed in patients with ß-lactams, amikacin, and antituberculosis drugs induced DRESS. In SCAR induced by fixed drug combination or multiple single formulations of antituberculosis drugs, oral rechallenge is considered for the management of tuberculosis. In these patients, all drugs are stopped until normalization of skin and laboratory findings, and then drug re-exposure is performed sequentially. This method is well described in a cohort of South African patients with a history SCAR to anti-TB drugs. In a study by Lehloenya et al, 50% of patients sequentially rechallenged on rifampicin, isoniazid, pyrazinamide, and ethambutol experienced mild to moderate (75%) and severe reactions (26%). Rifampicin was the common offending drug (57%) followed by isoniazid, pyrazinamide, and ethambutol (Lehloenya et al. 2011). In subsequent studies from this group, high-dose steroids were implemented to reduce inflammation and stop the reaction (Lehloenya et al. 2021b) . In high TB settings, this has been the gold standard of testing shown to be an effective strategy that allows patients to continue optimal treatment with negative drugs. However, this method is limited by the need of collaborative specialists and the danger of severe reactions on drug re-exposure.

1.4.4. In vitro drug testing

Patch, intradermal testing, and oral drug rechallenge all carry the risk of severe reaction on drug re-exposure. For hypersensitivity reactions, two in vitro methods proposed to address this issue are the lymphocyte transformation test (LTT) and enzyme-linked immunospot assay (ELISpot). They are based on the activation drug-specific T cells upon stimulation with the culprit drug in patients with SCARs. LTT is a proliferation test, which measures ^{3}H-thymidine uptake of specific T cells that divide and expand after interaction with the culprit drug. A stimulation index (SI) is calculated as the ratio of ^{3}H incorporated by drug-stimulated cultures and baseline incorporation of ^{3}H by unstimulated cells - an SI $\geq$2 is considered positive. The highest sensitivity of 73% and 82% specificity have been reported in the recovery phase of DRESS. The sensitivity remained low for SJS/TEN even after

removal of regulatory T cells and their supposed suppression of drug specific responses. Additionally, positivity depends to a large extent on the drug with the highest confirmed for anticonvulsants, antituberculosis, and ß-lactams. LTT is currently not done routinely as it is labour intensive, requires skilled personnel, not standardized, uses radioactive material and lacks specificity as reported in patients with elevated PBMC proliferation to the drugs they have tolerated.

ELISpot is a widely used assay that quantifies drug specific interferon γ, tumour necrosis factor-α, interleukin 4, granulysin, or granzyme B release by PBMCs upon drug stimulation. PBMCs are stimulated with varying concentrations of culprit parent drug and/or metabolites and results are reported as spot forming units per million cells after the removal of unstimulated cell responses. In some studies, the threshold of positivity is defined by measuring the frequency of antigen specific INF-γ producing cells in drug tolerant controls (Rozieres, Hennino, et al. 2009), setting the positivity threshold at twice the average value of background spots (Wang et al. 2007) and based on the distribution of negative controls (Keane et al. 2014; Keane et al. 2012). Reported sensitivities are affected by drug, SCAR phenotype and variable positivity thresholds. A study by Polak et al (Polak et al. 2013) observed a combined IFN-γ and IL-4 ELISpot sensitivity of 82% compared to 50% for LTT. The amoxicillin induced maculopapular eruption study reported IFN-γ ELISpot sensitivity of was 91% with the positivity rate of more than 30 SFU/million cells.(Rozieres, Hennino, et al. 2009). A recent study by Copaescu et al (Copaescu, Mouhtouris, et al. 2021) reported 56% IFN-γ ELISpot sensitivity in DRESS patients – greater than skin testing. The same group previously reported sensitivity of 52% in patients with SCARs and specificity of 100%, confirming reproducibility (Trubiano et al. 2018). Although responses can be detected up to 20 years after SCAR onset, blood collected in the acute and early recovery stages of the reaction have shown greater sensitivity. This is advantageous particularly in HIV/TB patients as drugs that are safe can be administered again.

1.5. SCAR impact on clinical care – in the context of HIV TB infections

The clinical care and study of HIV-associated IM-ADRs is a major challenge. SCARs with Stevens-Johnson syndrome, toxic epidermal necrolysis, and DRESS syndrome as common entities, are not only life threatening, but carry a high risk of severe sequelae. Figure 1-2 outlines obstacles to treatment and prevention. The current management of IM-ADRs requires several drugs to be stopped. In a setting of TB and HIV co-infection, the advance of both infections means that these vulnerable patients can ill-afford these prolonged interruptions of optimal treatment. The many ways SCAR impacts the effectiveness of TB treatment includes high risk of developing drug resistance, defaulting treatment, and dying from TB. SCARs are also associated with high healthcare costs due to clinical investigations, increased and prolonged hospitalization, permanent disability, and mental illness (Zitha et al. 2014; Duong et al. 2017; Jin et al. 2021; Knight et al. 2019).

Some of the severe complications of SJS/TEN in the acute stage include renal failure, ocular-specific pulmonary lesions, or sepsis in already immune suppressed and vulnerable patients. Additionally, in patients with TB associated respiratory insufficiency, direct effects SCAR on involved organs exacerbates pulmonary infection with severe laryngeal lesions seen in SJS/TEN patients. In a study of pregnant women with SJS/TEN, 50% delivered by caesarean and there were two foetal deaths caused by SJS associated post-partum sepsis (Knight et al. 2015). The burden of SCARs management, effect on TB targeted curing rates and resultant negative public health consequences of inadequately treated or recurrent infection, makes research to identify appropriate prediction, prevention, and management strategies an urgent priority.

Figure 1-2: Obstacles to improved clinical care and research in HIV-related IM-ADRs

1.6. Genetic factors

1.6.1. Human leukocyte antigens (HLA) – key players in T cell mediated ADR.

The idea that we are genetically predisposed to either an increased or diminished risk of developing IM-ADRs stems from observations in genetic association studies in countries with a high prevalence of one specific allele and few ethnic groups. HLA genes are encoded on the short arm of chromosome 6, this part of the genome constitutes the MHC complex in humans. HLA genes encode closely linked cell surface glycoproteins that play a central role in immune system through antigen processing and presentation to T cells. The HLA gene complex is divided into three regions and ordered into loci (figure 1-3A). The class I region includes classical, highly polymorphic, and functional HLA-A, HLA-B, HLA-C genes and non-polymorphic, non-functional pseudogenes HLA-E, HLA-F and HLA-G. The class II region includes the HLA-DPA1, HLA-DPB1, HLA-DQA1, HLA-DQA2, HLA_DQB1, HLA-DQB2, HLA-DRA, HLA-DRB1, HLA-DRB2, HLADRB3, HLA-DRB4 and HLA-DRB5 genes. Class-II region also contain nonclassical genes (HLA-DM, -DO) involved in other immunological functions than direct peptide binding. Lastly, class III region contains genes which encode for inflammatory responses (e.g., tumour necrosis factor (TNF), leukocyte maturation and the complement cascade (C3, C4 and C5) (Dendrou et al. 2018).

The HLA loci are usually inherited together as haplotypes with one haplotype inherited from each parent. Each HLA locus has many variants or alleles of immune-relevant genes that can show extreme polymorphism. HLA polymorphism ensures that the HLA molecules from different haplotypes can bind a wide range of self and foreign peptide antigens necessary to mediate adaptive immunity. HLA-A, HLA-B, HLA-C can recognize different antigens because of differences in the amino acid sequence of HLA class I heavy (alpha) chains. Most differences are in the nucleotide substitutions in exon 2 (alpha 1) and exon 3 (alpha 2). The gene encoding the HLA class I light chain (B_2-microglobulin) and pairs with the alpha chain, is located on chromosome 15 and has no polymorphic variation. The class II molecules are also heterodimers with three classical loci, HLA-DP, HLA-DQ and HLA-DR, composed of homogenous alpha and beta chains. Genes for both the alpha and beta chains are in the HLA class II region and organized in pairs where one locus encodes the alpha chain and the other the beta chain for the same HLA molecule.

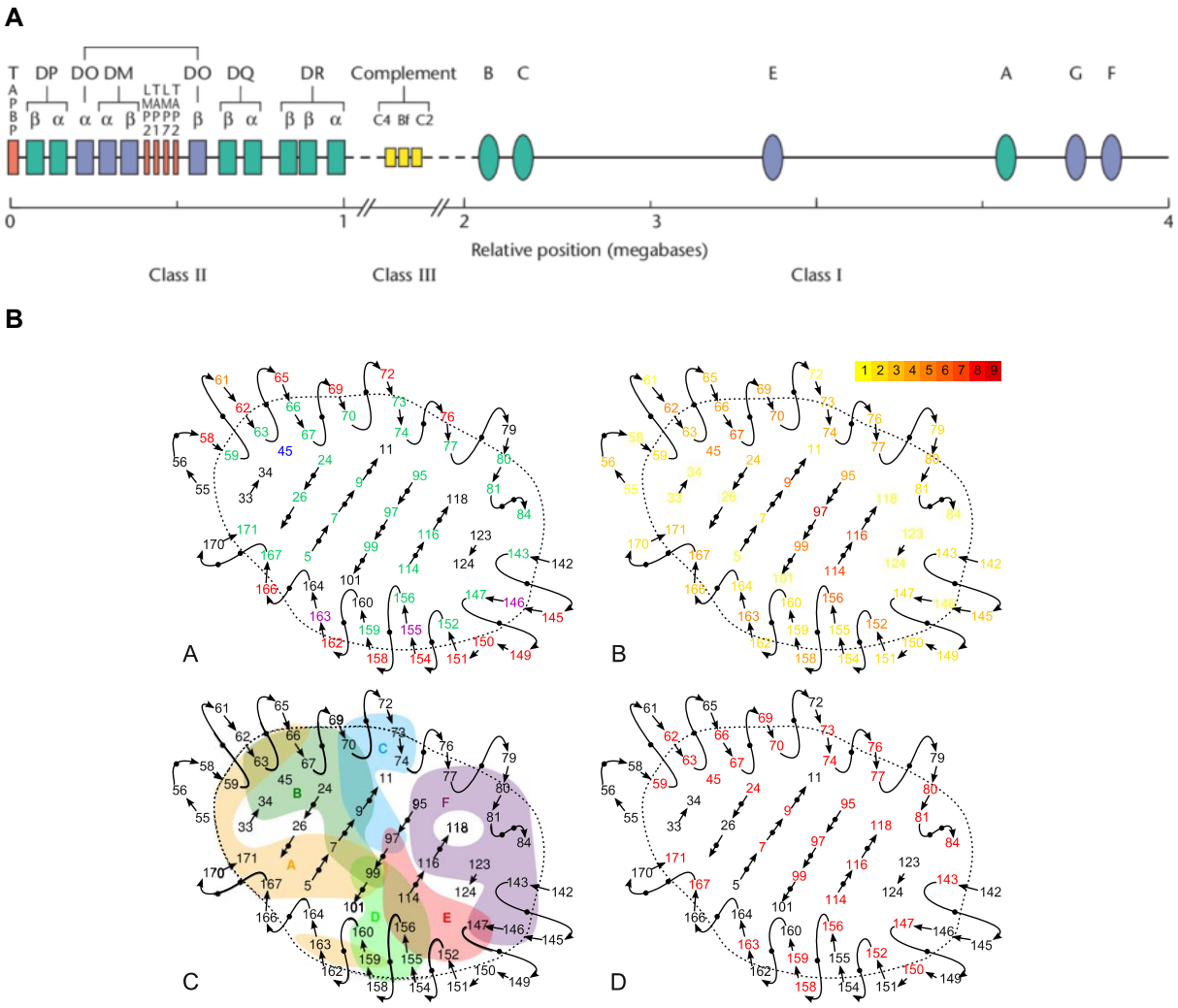

Fig. 1 A schematic overview of the binding groove (Adapted from Garrett et al 1989. Nature, Macmillan Publishers Ltd., copyright 1989). The *straight lines in the center* indicate the platform of β strands, the upper helix is the α1 helix, and the lower one is the α2 helix. Panel **a** shows which residues can influence peptide binding and T cell recognition according to Bjorkman et al. (1987). Residues pointing toward the peptide binding site and can interact with the peptide are colored in *green*. Those pointing up from the peptide binding site and can interact with the T cell receptor are colored in *red*. Residues 146, 155, and 163 are pointing both up and into the binding site (*purple*). Residue 61 points away from the binding site (*orange*), and residue 45 is located behind the α1 helix, pointing toward it (*blue*). The remaining residues are shown in *black*. Panel **b** shows the polymorphism of every position on the α1 and α2 domains. The number of different amino acids in our HLA subset (n=251; see "Materials and methods") found at a single position is indicated in the *colored bar*, numbers are colored accordingly. Panel **c** shows pockets *A*–*F* as defined in HLA-A2 (Saper et al. 1991). The positions in *red* in panel **d** are used as input for the in silico predictor NetMHCpan

Figure 1-3: Simplified map of the genetic organization of the HLA complex -

A) The principal class-I genes are represented by ovals and class-II genes by thick rectangles. The classical class-I and class-II HLA genes are indicated by green, whereas nonclassical ones by blue. The TAP and LMP genes, and tapasin encoding gene within the class-II region are shown by thin red rectangles. Within the class-III region only the genes encoding complement proteins are shown by short yellow rectangles**. B)** Schematic overview of the binding groove showing amino acids positions that make up each pocket. *Adapted from (Penn and Ilmonen 2005; van Deutekom and Keşmir 2015)*

HLA class I molecules are expressed on the surface of all nucleated cells and mostly present endogenous peptides to cytotoxic T cell receptors – this interaction has a crucial role in immune recognition of intracellular pathogens such as bacteria, viruses, and subsequent cytotoxic mediated killing of infected cells. HLA class II molecules are expressed on specific antigen presenting cells such as dendritic cells, macrophages, and present exogenous peptides to CD4 T cells. The activated helper T cells initiate defence against extracellular pathogens and parasites. T cells that recognize antigens presented by a particular class of HLA molecule restricted to that class.

The specificity of HLA–peptide–TCR interactions is essential in enabling the adaptive immune system to provide an efficient and effective response from infection and malignancy while maintaining self-tolerance and preventing T cell mediated autoimmunity. The specific recognition of HLA–peptide combinations is mediated by αβ T cell receptors (TCRs) on CD8+ T cells and on CD4+ T cells. Class I HLA molecules with the antigen binding cleft within the α-heavy chains typically favours 9–11 amino acids in length, with a small percentage of bound peptides a bit longer and protruding outside the class I binding cleft. Class I molecules' peptides are made on the ribosomes of rough endoplasmic reticulum (ER) and binds within the ER lumen. Most of the peptides are generated through the degradation of cytosolic protein by the proteasome. In the ER membrane is the transporter associated with antigen processing (TAP) which transports peptides from the cytosol into the ER lumen. Another antigen processing molecule within the ER lumen, tapasin delivers peptides from TAP move through the stacks of the Golgi apparatus to class I HLA molecules on the cell surface. A tight binding of peptides is established and HLA class I peptide assembly is presented to T cells for consequential cytotoxic attack. HLA class II α- and a β-chains assemble in the ER with a third protein called the invariant chain. This assembly is transported to endosomal compartment called MHC class II compartment. Within this compartment, the invariant chain is degraded by cathepsin proteases and a short part of it called class II associated invariant-chain peptide (CLIP peptide) remains bound to the peptide-binding site of the HLA class II molecule. The degradation of the invariant chain allows for transport of stable peptide MHC class II complexes to the cell surface. The polymorphic nature of the HLA locus enables HLA molecules to present a diverse array of peptide antigens, thus the peptide binding preferences largely depends on structural features of the binding cleft of each particular HLA allele. In addition to binding TCRs, HLA class I molecules also control functions of natural killer cells by receptor mediated interaction with killer cell immunoglobulin-like receptors (KIRs) and C-type lectin-like CD94/NKG2 family of receptors.

In recent years, important strides have been made in improving our understanding of the role of various genetic factors in the pathogenesis of SCAR. Several new loci and genetic variants have been identified that are associated with reactions in multiple populations. Gene variations in the HLA complex - enriched with immune genes are mainly associated with diseases with related immune

mechanisms. Due to their ability to interact with all nucleated cells, HLA class I molecules are thought to be responsible for most signals of disease associations in the MHC region.

The association between HLA-B*57:01 and abacavir hypersensitivity was one of the first best characterised examples of strong HLA association made to define the predisposition to IM-ADRs. These studies showed the development of abacavir hypersensitivity is mediated by the by an HLA-B*5701-restricted immune response to abacavir – although the presence of HLA-B*5701 allele was not the only predicting factor of abacavir hypersensitivity reaction (Keane et al. 2014; Hetherington et al. 2002; Mallal et al. 2002). In a randomized controlled trial, the HLA-B*5701 screening eliminated immunologically confirmed hypersensitivity reactions, with a negative predictive value of 100% and a positive predictive value of 47.9% (Mallal, Phillips, Carosi, Molina, Workman, Tomazic, Jägel-Guedes, et al. 2008).

In carbamazepine induced SJS/TEN, 100% of patients carried HLA B*15:02 compared to 3% of control patients. First identified in the Han Chinese population in Taiwan, carbamazepine SJS/TEN is firmly associated with HLA B*15:02 with an odd ratio of 2,504 (Chen et al. 2011; Chung et al. 2004). More studies in Japanese and European descents cohorts show HLA-A*31:01 and not HLA B*15:02 increases the risk of developing carbamazepine-induced SCARs (McCormack et al. 2011). Recently, association between HLA B*15:02 and anticonvulsant phenytoin induced SCARs was established in Malay population (Chang et al. 2017). These studies emphasise that influence of population specific HLA risk alleles is associated with the estimated prevalence of major SCAR phenotypes in different continents. This example illustrates the strong influence of ethnicity on HLA associations and the unique challenges that ethnicity presents when implementing HLA alleles as predictors of IM-ADRs.

Similarly, a strong 100% association has been identified between HLA-B*58:01 and allopurinol induced SJS/TEN or DRESS (Hung et al. 2005). This association has been observed in both Asian and European populations, and the severity and mortality of allopurinol-induced SCARs are influenced by clearance of oxypurinol, the primary metabolite of allopurinol. The negative predictive value (NPV) of HLA-B∗58:01 is 100% in Southeast Asians alone. HLA-B∗58:01 explains only 60% of allopurinol SCARs in other ethnicities (Tassaneeyakul et al. 2009). Other notable IM-ADRs associated with HLA alleles include dapsone hypersensitivity with the HLA-B*13:01 (Watanabe et al. 2017), HLA-B∗57:01 and DILI due to flucloxacillin, antithyroid-induced agranulocytosis and HLA-B∗27:05 and the HLA-B∗38:02-HLA-DRB1∗08:03 haplotype, C*04:01 and nevirapine induced SJS/TEN (Carr et al. 2013) and vancomycin DRESS strongly associated with HLA-A*32:01(Konvinse et al. 2019)

1.6.2. Endoplasmic reticulum aminopeptidases (ERAP)

Heavy and light chains of MHC class I complexes are composed in the endoplasmic reticulum but cannot exit the cell for expression on the surface without an 8-10 amino acid peptide. The MHC class I complex is restricted to the binding of mostly 9 amino acid peptides because the ends of the peptide binding groove interact with the N and C terminus of peptides. The N and C termini are anchor positions that determines affinity of bound peptides. Unlike MHC class II complexes that can extend on both side of the peptide binding groove accommodating longer 12 amino acids peptides. Longer peptides generated through proteasomal degradation and cytosolic aminopeptidase processing are further trimmed by ER aminopeptidases (ERAP) to properly fit the MHC class I complexes. ERAPs mainly trim peptides with extended N terminus in order to generate the correct length antigenic peptides for loading onto MHC class I molecules. The specificity of these peptidases can affect antigenic peptide selection. Humans have two genes that encode ERAPs (ERAP1 and ERAP2) associated with antigen processing. Encoded on the long arm of chromosome 5, region 15, ERAP1 gene is 47,379 base pairs long and consists of 20 exons; ERAP2 gene is 41,438 base pairs long and consists of 19 exons (figure 1-4D) (Cifaldi et al. 2012). ERAPs belong to the M1 family of zinc metallopeptidase enzymes characterized by GAMEN and HExxHx18E binding motifs.

The structure for the four protein domains of ERAP1 have been determined by crystallization. Domain I (residues 1-254) comprises of a β-sheet of eight saddle shaped strands which provide binding sites for the N terminus of a substrate peptide on one end of the strand close to the catalytic domain. Domain II (residue 255-529) is the catalytic domain that carries the zinc binding motif, GAMEN and HExxHx18E. It is one of the domains composed of alpha helixes that link the GAMEN motif and HExxHx18E which bind the N terminus end of the substrate. Domain III (residues 530-614) composed of two β-sheets that create an β-sandwich, is a small domain that connects domain II to domain IV. Domain IV (residues 615-940) is the second domain made of alpha helixes arranged like a bowl (figure 1-4A). In the open conformation of ERAP1, a large cavity exits between domain II and IV and in the closed form, domain IV connects with the catalytic domain and closes off the active site.

As mentioned above, ERAP1 exist in open form to allow substrate access to the active site and assumes a closed form once the substrate peptide is bound (figure 1-4B-C). Domain III pulls domain IV from the active site to make it accessible to substrates. The closed state is facilitated by the strong binding of preferably 9-16 long residues anchored in the S1 specificity pocket. In one the studies that described the crystal structure of ERAP1, active sites residues Met319, Glu183 form the N-terminal anchor for any peptide substrate and Gln181 which when mutated to glutamate increases the affinity of ERAP1 for basic N-terminal residues. Residues Arg430 and Glu865 form the end of the S1

specificity pocket. Shorter peptides with less than 8 residues in length do not extend from catalytic sites to the hydrophobic pocket, resulting most likely in reduced binding affinities for such substrates. Thus, the length preference and substrate specificity of ERAP1 influences which peptides are trimmed before HLA class I presentation and affects immune function (Falk and Rötzschke 2002; Saulle et al. 2020; Serwold, Gaw, and Shastri 2001).

ERAPs are highly polymorphic with many single nucleotide polymorphisms (SNPs) (figure 1-4D). They are present on the cell surface of all nucleated cells as well as ER in humans and the expression is regulated by interferon-γ (IFN-γ). In their peptide presentation role, ERAPs are linked to several diseases including ankylosing spondylitis (Evans et al. 2011), cervical cancer (Li et al. 2020), diabetes (Fung et al. 2009), hypertension (Yamamoto et al. 2002), psoriasis, Crohn's disease (Franke et al. 2010), pre-eclampsia (Ferreira et al. 2021), haemolytic uremic syndrome (Taranta et al. 2009), and osteoporosis (Yamada, Ando, and Shimokata 2007). Majority of in vitro and in vivo disease models investigating ERAP SNPs have shown that aberrant trimming of peptides or presentation by ERAP1 and HLA alleles are involved in the pathogenesis. The disease associated SNPs are positioned near the catalytic site within the binding groove, or near locations that can influence the conformational rearrangements and other SNPs are also present in interdomain areas or in domain IV, a regulatory region responsible for C-terminal residue peptide binding.

ERAP which trims polypeptides in the endoplasmic reticulum to epitopes of various lengths before presentation on HLA class I molecules is increasingly becoming a key element in cell mediated immunity. Recent genome wide association studies show the interaction of HLA-B27 and ERAP as a determining factor in the genetic predisposition to ankylosing spondylitis, HLA-A*29:02 and ERAP in birdshot retinopathy and HLA-B*51:01 and ERAP interaction in Bechet's disease. Relevant to IM-ADRs, a recent study showed abacavir tolerant subjects tend to have hypoactive trimming ERAP1 allotypes. Abacavir is shown to bind within the F pocket of the peptide-binding groove of HLA-B*57:01, and thus altering the repertoire of self-peptides presented to T cells. The potential for ERAP1 to influence the repertoire of peptides available to be presented to T cells in the presence of ABC is in keeping with the primary hypothesis of the altered peptide model by which ABC causes hypersensitivity. These preliminary studies show the importance of antigen processing and presentation and provide a strong motivation to investigate the influence and interaction of ERAP with HLA class I alleles in disease development.

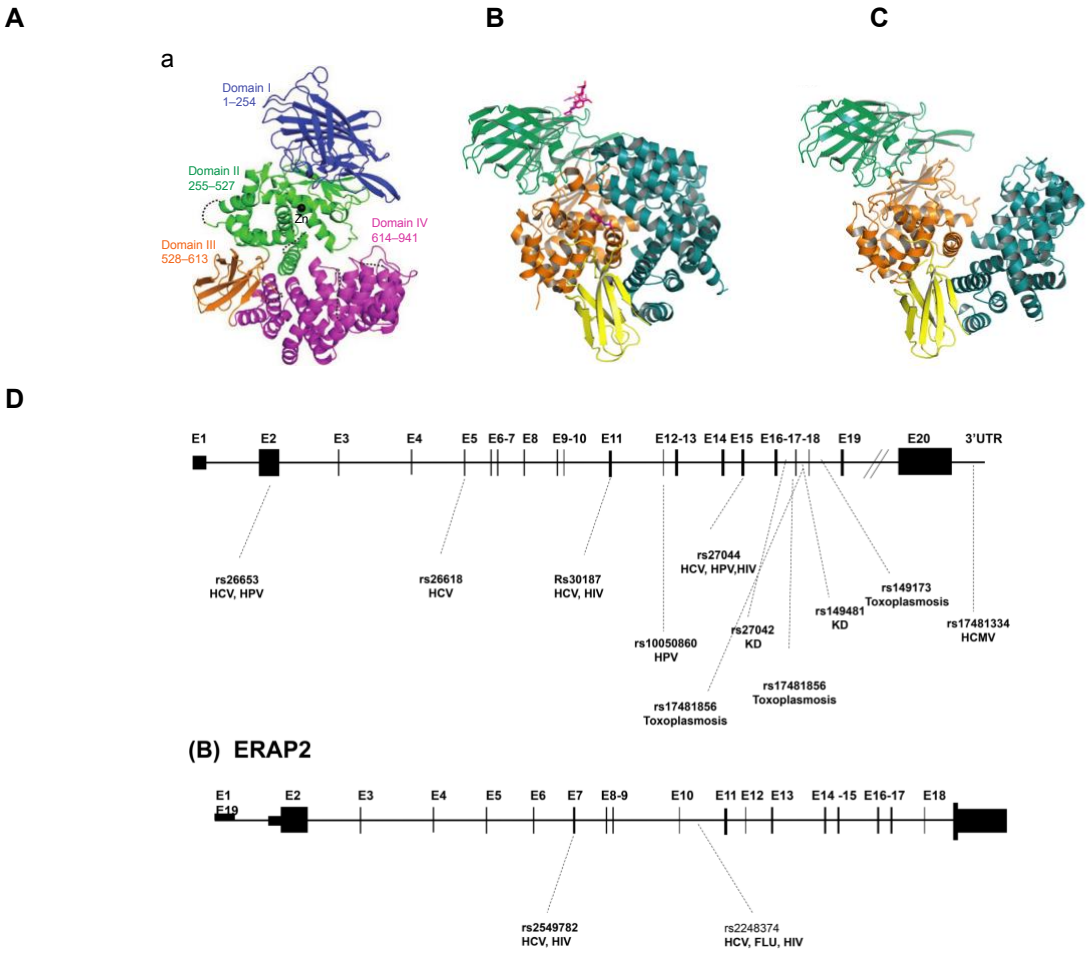

Figure 1. Genomic structure of the human ERAP1 (**A**) and ERAP2 (**B**) genes. Exons are numbered and depicted as boxes. Outlines indicate the sites of exonic or intronic polymorphisms described in the text as rs and related infections.

Figure 1-4: ERAP structure

A) ERAP1 consists of four different domains (I-IV) made up of alpha helices and beta sheets as indicated and colour coded. The residue numbers corresponding to different domains are indicated. **B**) The closed conformation of ERAP with bound substrate indicated. **C**) ERAP1 open conformation to allow substrate access to the active site. *Adapted from (Nguyen et al. 2011)*. **D**) ERAP1 an ERAP2 genes with SNPs and associated diseases. *Adapted from (Saulle et al. 2020)*

1.6.3. Killer immunoglobulin receptors (KIR)

Natural killer (NK) cells are innate immune cells, among the first to enter inflammation site and mediate a cytotoxic response to tumours and invading pathogens. NK cell responses are regulated by interaction between their polymorphic receptors and specific HLA class I ligands. NK cell receptors are categorised into inhibitory and activating receptors that regulate the protection of healthy cells and the killing of target cells. The absence of HLA class I molecules or expression compromised by infection renders the cell susceptible for NK cell lysis while they are prevented form lysing healthy cells by recognition of HLA class I molecules. In humans, these receptors include CD94/NKG2 and killer-cell immunoglobulin-like receptors (KIRs) (the focus of this review). The CD94/NKG2 molecules and KIRs are encoded by NK gene complex (NKC) and leukocyte receptor complex (LRC) respectively. NK cells can express more than one receptor and the varied combination defines a person's NK cell receptor repertoire. The NKC is on the short arm of chromosome 12 and while CD94 is a single copy gene, NKG2 region includes NKG2A, C, D and E. CD94 forms heterodimers with NKG2A to serve as inhibitory receptors and NKG2C to deliver activating signals through specific interaction with HLA-E.

The second genetic region known as leukocyte receptor complex is located on the long arm of human chromosome 19, region 13. It encodes the family of NK cell receptors with extracellular immunoglobulin (Ig) like domains. – the killer-cell immunoglobulin-like receptors that recognise HLA class I ligands. In the LRC, the KIR loci consist of 12 genes, organized by lineages (I, II, III, V), identified by the number of the Ig domains in the extracellular region (KIR2D – two Ig domains, KIR3D – three Ig domains) (figure 1-5A) and specificity of HLA class I molecules (figure 1-5B). KIR lineage I consist of 2DL4, 2DLS5A and 2DL5B which recognise HLA-G. KIR lineage II includes KIR3DL1/S1, 3DL2 and they recognise antigens on HLA-A (A3/11) and HLA-B allotypes. The lineage III of KIRs consist of KIR2DS1/2/3/4/5, 2DL1/2/3, 2DP1 and 3DP1 that interact with C1 and C2 epitopes of HLA-C and HLA-B allotypes with epitopes similar to C1. Despite the diversity of human KIR genes, they are only grouped into two haplotypes. Haplotype A and B (Boudreau and Hsu 2018). The A haplotypes are composed of Cen-A and Tel-A and include inhibitory KIRs, KIR2DL1, KIR2DL3, KIR3DL1, KIR3DL2, KIR2DL4 and one activating KIR2DS4. The B haplotype is composed of Cen-A/Tel-B, Cen-B/Tel-A and Cen-B/Tel-B characterised by the presence of KIR2DL2, KIR2DL5B, KIR2DL5A, KIR2DS3, KIRDS1, KIR2DS2, KIR2DS5 and KIR2DS1 (Pende et al. 2019) (figure 1-5B).

The HLA class I ligands for lineage II KIRs contain the Bw4 motif at amino acid position 80 of the HLA-B heavy chain and the HLA-C and HLA-B ligands for KIR lineage III are sorted into C1 and C2 groups based on the polymorphisms at this position. HLA-C1 allotypes, which are characterised by an

asparagine at position 80 are the preferred ligands for KIR2DL2 and KIR2DL3 whereas HLA-C2 allotypes with a lysine at position 80 are recognised by KIR2DL1. KIR3DL1 has a higher affinity for isoleucine80 (Bw4-80I) than threonine80 (Bw4-80T) – their interaction with Bw4-*80T results in inhibition of NK cells responses.

In the KIR genes nomenclature, the S indicates activating receptors whereas L represents inhibitory receptors. Their difference lies in the cytoplasmic tails of Ig domains (figure 1-5A). Inhibitory receptors have immunoreceptor tyrosine inhibitory motifs (ITIMs) that recruits and activates SH2-domain-containing protein tyrosine phosphatase 1 or 2 (SHP1 or SHP2). Their engagement terminates stimulatory receptor signals and delivers an inhibitory signal on the surface of NK cells after ligand binding. Activating receptors mediate their effects through immunoreceptor tyrosine-based activation motifs (ITAMs) which contains molecules, known as killer activating receptor associated proteins. After ligand binding, ITAM becomes phosphorylated and induces cytotoxic responses and cytokine production.

A

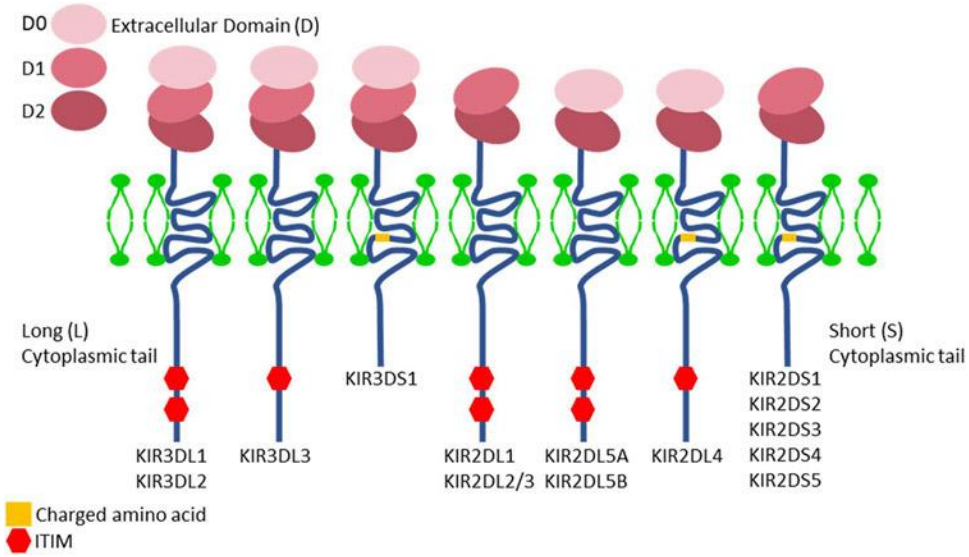

B

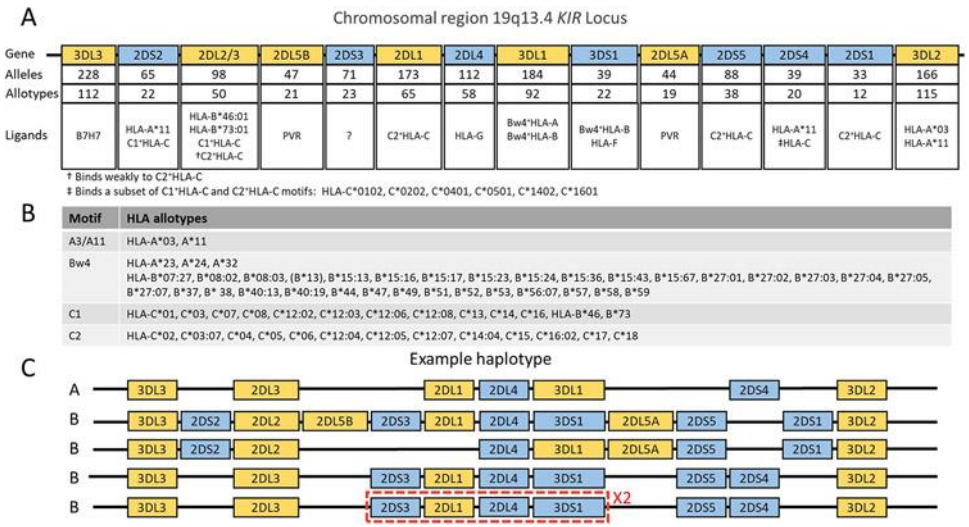

Figure 1-5: NK cell receptors, their nomenclature and function, genomic arrangement, and cognate ligands

Adapted from (Pollock, Harrison, and Norman 2022)

1.6.4. T cell receptor (TCR)

Majority of T cell express the alpha (α)-beta (β) receptor pair whereas the gamma (γ) delta (δ) receptor pair is expressed on 1-5% of T cells in peripheral blood. The αβ TCRs on CD8+ T cells recognise and bind antigens presented by MHC class I molecules and CD4+ T cells recognises and binds to MHC class II peptide complex. The α- and β-chains of TCR heterodimers arise when different variable (V), diversity (D) and joining (J) gene segments come together through somatic, convergent recombination in the thymus to give rise to a single type of functional TCRαβ complex expressed by each T cell. The V and J regions from the variable domain of the α chain whereas the V, D and J segments form the β-chain. The somatic recombination and additional variation due to the deletion and insertion of nucleotides results in highly variable complementarity-determining regions (CDRs): CDR1, CDR2 and CDR3 (Rossjohn et al. 2015).

In the interaction with peptide-MHC complex, TCR binds in a conserved diagonal orientation that positions the germline encoded CDR1 and CDR2 loops mainly over the MHC and the non-germline encoded CDR3 over peptide. The CDR3 of each of the two receptor chains defines the clonal specificity. Although, the CDR1 and CDR2 show no rearrangement, they have been shown essential in the MHC biding followed by CDR3 contact with the peptide (van der Merwe and Dushek 2011; Shah et al. 2021). T cell activation is triggered on the formation of stable interactions (figure 1-7). To mount a specific immune response, naïve T cells undergo antigen stimulation in secondary lymphoid tissues to either mediate a helper T cell or cytotoxic response to eliminate the foreign pathogen or abnormal cells. In the thymus, T cells subsequently undergo positive and negative selection to generate T cells expressing a diverse and MHC restricted repertoire and to ensure specificity for foreign but not self-peptides – minimizing the possibility of autoreactive T cells (Bradley and Thomas 2019).

The proposed mechanistic models to explain the recognition of drugs by T cells involves interaction with highly variable T cell receptor (TCR). In carbamazepine induced SCAR a public TCR clonotype present in SJS/TEN patients and not tolerant controls showed a bias for HLA-B*15:02 carried by patients and controls (Ko et al. 2011; Pan et al. 2019). Similarly, in allopurinol induced SCAR, along with HLA-B*5801 risk allele, a specific TCR clonotype recognised its metabolite oxypurinol (Chung, Pan, et al. 2015). However, public TCRs in SCARs remain elusive due to patient specific repertoire and lack of molecular and functional signatures to identify drug specific clonotypes.

1.6.5. Structural and biochemical basis of how drugs induce an immune response.

There is now considerable evidence that a variety of individual drugs can cause multiple types of ADRs, and a specific type of ADR can be due to any drug in susceptible individuals. For a drug to elicit an IM-ADR, it must be both immunogenic (able to sensitize the immune system) and antigenic (able to evoke an immune response from the sensitized immune system). The mechanisms small drug molecules, typically in the size range of 1-3 amino acids and their metabolites, stimulate T cells and the ability of T cells to promote an immune response and associated tissue injury remain poorly understood. Several studies have reported on three proposed models explaining the recognition of drugs by the immune system. These include the hapten/pro-hapten, pharmacological interaction (p-i concept) and altered peptide repertoire models (figure 1-6). Once drugs enter cells such as hepatocytes, drug metabolizing enzymes detoxifies and make them water soluble. The phase I metabolic cytochrome P450 enzymes commonly mediate activation of drugs – this is the general mechanism through which reactive metabolites are generated and can bind covalently to host MHC molecules. However, in rare cases, a deficit in phase II metabolizing enzymes – which involve conjugation by coupling drugs or metabolites to other molecules, can render non-immunogenic parent drugs, immunogenic.

In the hapten/pro-hapten model, there is formation of covalent bonds between drug molecules and proteins or peptides, leading to a drug-specific cellular immune response. Haptens are chemically reactive small molecules that are able to bind covalently to larger proteins or peptides, initiating an immune response and pro-haptens are molecules that require enzymatic conversion to become chemically reactive (Gerber and Pichler 2004; White et al. 2015; Usui and Naisbitt 2017; Roujeau 2006; Pichler, Naisbitt, and Park 2011; Padovan et al. 1996). An example of a hapten model where a drug directly reacts with host MHC molecules is penicillin. In penicillin hypersensitivity, penicillin as the parent drug binds to serum albumin that undergoes intracellular processing to generate peptides. This forms a hapten-peptide conjugates associated with MHC molecules and transported on the surface of APCs, such as follicular dendritic cells, Langerhans cells in the skin, B cells and macrophages. Hapten–peptide conjugates on the surface of APCs interact with immature T cells through T cell receptors - this interaction governed by the antigen binding specificity of T cell receptors and influenced by binding specificity of MHC molecules, elicits an immune reaction.

The p-i concept involves pharmacological interaction of drugs with immunological receptors where the parent drug or metabolite binds directly and non-covalently to T cell receptors, or to specific HLA molecules without a specific peptide ligand (Pichler, Naisbitt, and Park 2011; Pichler et al. 2015; Porebski et al. 2013). The antigenic peptide processing by antigen presenting cells is not necessary in this model. This concept stems from the ability of certain drugs to bind selectively and reversibly to

certain protein pockets of receptors and enzymes. It is termed pharmacophore – which defined as the molecular framework that includes drug features responsible for its interactions with a specific biological target and to block its biological response. From this definition, Picher et al deduced, pharmacological interactions of drugs with highly variable TCR and MHC molecules induces an immune response. For example, in carbamazepine induced SJS/TEN, carbamazepine binds directly to the protein encoded by HLA-B*15:02 - without the involvement of intracellular carbamazepine metabolism or processing, endogenous peptide loaded HLA-B*15:02 presents the drug to cytotoxic T cells. In this study, other HLA-B75 family members could also present CBZ to activate cytotoxic responses. The peptide binding groove of HLA-B*1502 was suited to accommodate three residues (Asn63, Ile95, and Leu156) involved in carbamazepine presentation and cytotoxic T cell activation (Wei et al. 2012).

Unlike carbamazepine T cell activation, abacavir specific T cells are not activated by APCs expressing HLA-B*57:01 closely related HLA alleles HLA-B*57:03, HLA-B*57:02 and HLA-B*58:01 which differ by 2- 4 amino acids. Amino acids differences between these alleles locates abacavir binding to the C-terminal end of the peptide binding groove - suggesting that abacavir-HLA-B*57:01 specificity is particularly sensitive to the F-pocket (Illing et al. 2012). Abacavir binds non-covalently within the binding pocket of HLA-B*57:01 and interacts with two residues Asp114 and Ser116 which differentiates HLA-B*57:01 from naturally related HLA allotypes (figure 1-3B). This binding leads to alteration of both the chemistry of F pocket in the binding cleft and the self-peptide repertoire. This drug MHC molecule interaction is termed the altered peptide repertoire model.

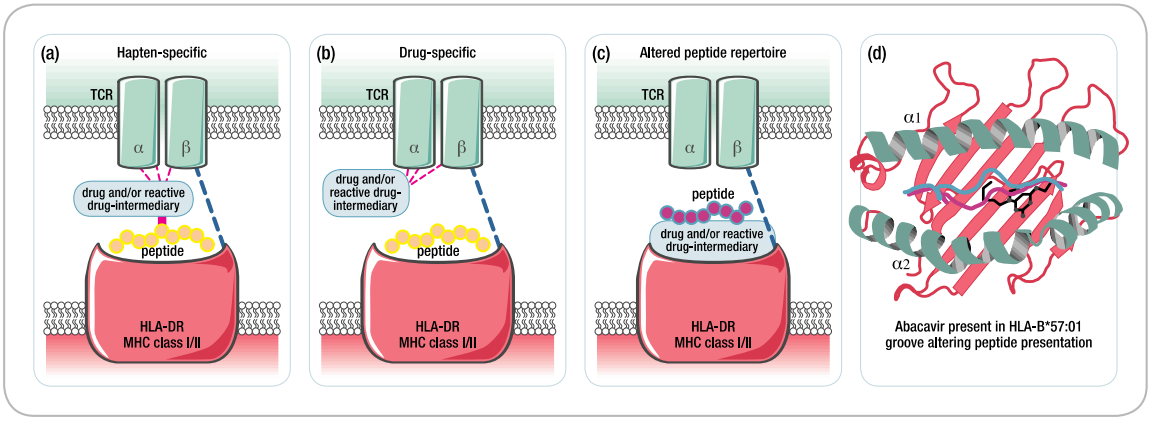

Figure 1-6: Schematic diagram showing proposed mechanisms of T cell activation in the development of SCARs.

(a) In the Hapten/prohapten model drugs form covalent bonds with endogenous proteins/peptides. These drug-modified peptides are then processed by antigen presenting cells and presented on the MHC resulting in a T-cell response. (b) The drug-specific Pharmacological-Interaction (P-I) model proposed that drug binds directly to immune receptors such as the T-cell Receptor (TCR) or HLA forming non-covalent bonds without the need for peptide processing. Dashed lines represent non-covalent bonds. (c) The Altered peptide repertoire model the drug forms non-covalent bonds within the binding pocket(s) of the MHC to alter the chemistry of the binding cleft and repertoire of self-peptides able to bind to the HLA molecule in question. Some of these newly presented self-peptides have not been previously tolerized and their presentation results in a T-cell response. (d) The interaction between abacavir and HLA-B*57:01 as occurs in abacavir hypersensitivity syndrome exemplifies the altered peptide repertoire model**.** *Adapted from (Peter et al. 2017)*

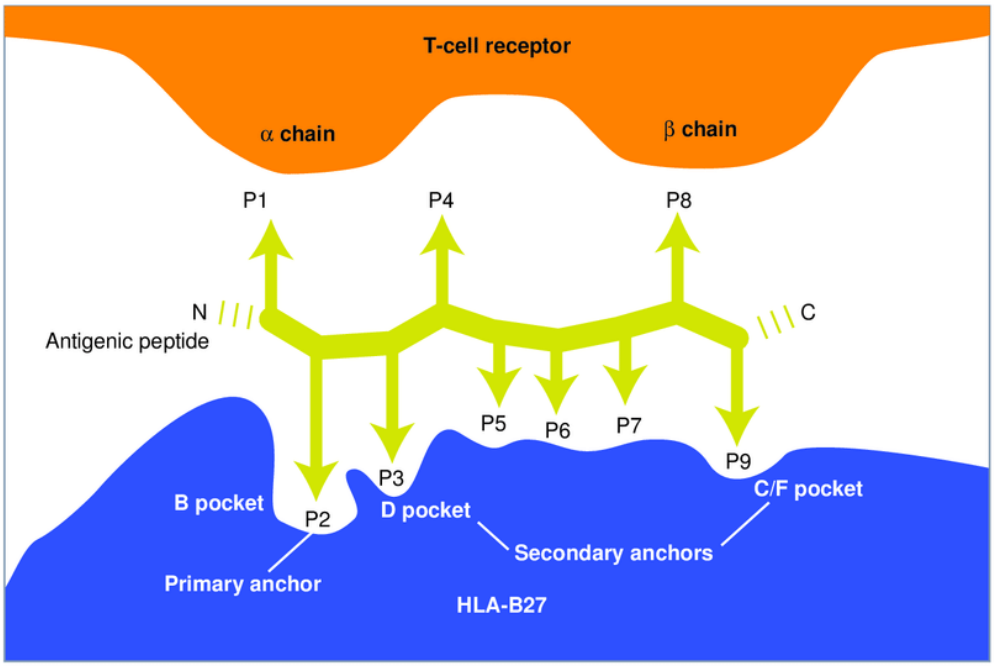

Figure 1-7: Schematic diagram showing binding of antigenic peptides to HLA-B27 and recognition by the T-cell receptor.

The sidechains of peptide 'anchor' residues P2, P3 and P9 (C-terminal) are bound in pockets. The sidechains of P1, P4 and P8, which extend out of the peptide-binding groove, are critical for T-cell recognition. *Adapted from (Zaccai, Bird, and Jones 1999).*

1.7. Pharmacology of FLTD

1.7.1. Details of tuberculosis treatment

First line drugs used for the treatment of tuberculosis are Isoniazid (INH), Rifampicin (RIF), Pyrazinamide (PZA), Ethambutol (EMB). The WHO currently recommends the use of fixed dose combination (FDC) for the treatment of drug sensitive tuberculosis. In South Africa, Rifafour (RHZE) e-275 tablets containing rifampicin 150 mg, isoniazid 75 mg, pyrazinamide 400 mg and ethambutol hydrochloride 275 mg are used for drug sensitive tuberculosis treatment. The effectiveness of TB treatment using FDC compared to separate drug formulations is still unclear. A new case of tuberculosis is recommended a highly effective regimen of 1-2 months on RHZE and 3-6 months on separate formulations of isoniazid and rifampicin. Guidelines for treatment with separate drug formulations recommends INH, RIF for 6 months, together with EMB, PZA for the first 2 months. First line anti-tuberculosis drugs (FLTD) are also administered as preventive therapy for people at high risk of tuberculosis. In high burden countries, preventative therapy is targeted at people with HIV – where it has been shown to be highly beneficial and children aged less than 5years with household contacts. In low burden countries, preventative therapy is recommended for individuals with latent mycobacterium tuberculosis infection to prevent progression to active TB disease. The standard TB preventative therapy regimen is INH for 6-12 months, although other one or more FLTD can be administered.

1.7.2. FLTD mode of action

Tuberculosis is caused by an intracellular bacterium, Mycobacterium tuberculosis (MTB), and is transmitted when the organism is aerosolised by the cough of an infected patient and inhaled into the alveoli of a new host (Alland et al., 1994). The introduction of MTB bacilli into the lungs can cause respiratory infection characterised pathologically by necrotic granulomas, termed pulmonary TB which can later disseminate to other organs resulting in extra-pulmonary TB (Rieder et al., 1990, Solovic et al., 2013). In the lung, after aerosol inhalation, bacteria are taken up by resident macrophages and a series of complex interactions with the host take place, more macrophages are recruited to the site, specific T cells begin to accumulate, and a granuloma is formed (Ramakrishnan, 2012). To achieve sterilization of infection, FLTD advantages their bactericidal and bacteriostatic properties against growing tubercule bacilli. Treatment for tuberculosis is lengthy and requires multiple drug regimen, in part because tubercule bacilli respond slowly to treatment and some Mycobacterium infected cells take longer to be killed by antibiotics. Identifying the pathways of actions is limited by the broad reaching metabolic effects of drug treatment. The two most potent sterilizing drugs are pyrazinamide and rifampicin - either of these drugs is most effective when administered with isoniazid.

Pyrazinamide is an effective sterilising drug in tuberculosis, but its mode of action is unclear. It works in the opposite of other three FLTD as it has no or little activity against growing tubercle bacilli and is primarily active against semi-dormant subpopulations of MTB persisters. Zhang et al model of PZA action describes it as a pro drug converted to its active derivative pyrazinoic acid by nicotinamidase in the bacterial cytoplasm. Due to the inefficient bacterial pump, pyrazinoic acid is excreted slowly through the cell wall and its accumulation leads to toxicity to the cell membrane. EMB as a bacteriostatic drug specifically interferes with the biosynthesis of arabinogalactan in the cell wall, halting multiplying bacilli (Palomino and Martin 2014). Isoniazid is only active against metabolically active replicating bacilli. Isoniazid as a pro-drug requires activation by the peroxidase enzyme KatG to exert its effect. It inhibits the enoyl reductase from MTB by forming a covalent toxic chemical adduct with the nicotinamide adenine dinucleotide (NAD) cofactor. Rifampicin forms the core of drug susceptible antituberculosis regimen by halting bacterial DNA-dependent RNA synthesis. It binds to the β-subunit of the RNA polymerase, inhibiting the elongation of messenger RNA (Blanchard 1996).

1.7.3. Immunogenicity of FLTD

An example on how anti-TB drugs could initiate ADRs, is a study on INH induced hepatoxicity (Sharma et al. 2002). INH metabolism is associated with INH-induced liver injury, with the major metabolites – Acetyl hydrazine, hydrazine, and acetyl isoniazid, shown to cause hepatic necrosis in this study, parent drug INH at a higher dose did not cause toxicity. Though other studies also found INH itself and not metabolites can bind to liver proteins and cause immune-mediated hepatotoxicity. These contrasting results show how accumulation of an anti-TB drug, or its reactive metabolite can activate T cells and stimulate a specific response. Various HLA alleles are associated with a drug-specific clinical phenotype, and recently they have been implicated in anti-TB ADRs. The presence of HLA-DQB1*0201 allele is associated with mild to serious INH-induced liver injury in patients of Indian ancestry. Previously, mechanism of INH DILI was thought to not involve an immune response and mainly due to the bioactivation of AcHz metabolite. The immune modulated severe phenotype of INH-induced DILI is associated with the production of antibodies against CYP2E1, CYP3A4 and CYP2C9 (Sharma et al. 2002) (Bothamley 2002).

1.7.4. Cross reactivity with drugs commonly used in in HIV TB coinfection treatment.

Structurally related drugs can cause cross-reactions with SCARs. Cross-reactivity occurs when an individual previously exposed and reacted to a drug, is exposed to a structurally similar drug, and the immune system recognises the shared structural similarities resulting in another reaction. Cross-reactivity is commonly reported in immediate rather than delayed hypersensitivity and associated with penicillin and related antibiotics (Blumenthal et al. 2019), corticosteroids (Coopman, Degreef, and Dooms-Goossens 1989), and aromatic antiepileptic drugs (Alvestad, Lydersen, and Brodtkorb 2008;

Hirsch et al. 2008). Recently a study confirmed the potential immunologic cross-reactivity between vancomycin, teicoplanin, and newer glycopeptide antibiotics in HLA-A*3201 positive patients with vancomycin-induced DRESS (Nakkam et al. 2021).

In HIV TB patients, possible interactions have been reported between dapsone and trimethoprim/ sulfamethoxazole (Carr, Penny, and Cooper 1993; Beumont et al. 1996b; Holtzer, Flaherty, and Coleman 1998). In our setting, the absence of cross-reactivity between drugs in the rifamycin class (rifampicin and rifabutin) has been reported (Lehloenya, Dlamini, et al. 2016). However, as the collection of ADR data expands, we have noted an increment in patients reacting to both rifampicin and rifabutin on oral sequential drug challenge (IMARI registry unpublished data). Rigorous data analysis ids required to confirm the likelihood of cross-reactivity between rifamycin.

1.8. Immune mechanisms

SCARs are type IV delayed hypersensitivity reactions mediated by T cells which initiate and perpetuate inflammation characterized by skin immune cell infiltration and the activation of different effector or regulatory cells secreting cytotoxic mediators and inflammatory cytokines (Duong et al. 2017). In support of this assumption the largest group of genes associated with SCAR susceptibility are involved in antigen presentation to T cells or in T cell signalling pathways (Peter et al. 2017). The variability of SCAR clinical entities has led to a further subclassification of type IV reactions, according to different cytokine production patterns by T cell subsets and to the contribution of certain subpopulations of immune cells to the inflammation and tissue damage. In this classification, type IVa reactions include Th1 immune responses with the release of large quantities of IFN-γ and the participation of monocytes. Type IVb reactions correspond to Th2 responses with production of IL-4, IL-13, and IL-5, that leads to the eosinophilia characteristic in some drug allergies. In type IVc reactions cytotoxic T lymphocytes are the main effectors of tissue injury. Finally, in Type IVd reactions T cells promote the recruitment of neutrophils to affected tissue through the secretion of IL-8/CXCL8 (Pichler 2003).

Classically, DRESS is considered as a type IV a and b Th1 and Th2-driven reactions; SJS/TEN as a type IVc cytotoxic reaction, and AGEP is classified as a type IVd reaction. Although this classification provides a useful understanding of the pathogenesis, their contribution to the mechanism of a given clinical entity is not mutually exclusive. For example, high IFN-y levels (typical of type IVa) have been identified in serum and blister fluid of SJS/TEN patients, and drug specific CD8+ cytotoxic T cells (typical of type IVc) may also be involved in DRESS and AGEP. On the other hand, any of these reactions may occur in response to any drug, meaning that similar immune mechanisms are triggered in response to different chemical compounds (Pichler 2003).

1.8.1. Innate immune cells in SCAR pathogenesis

Innate immune cells are white blood cells that serves as the front line against foreign agents and include basophils, dendritic cells, eosinophils, Langerhans cells, mast cells, monocytes and macrophages, neutrophils, and natural killer (NK) cells. T cell responses to antigens are directed by at least two signals. The first signal through the T cell receptor (TCR), removes T cells from a naïve state to proliferation and differentiation. The second co-stimulatory signal to acquire effector functions is provided by antigen presenting cells (APCs) such as DCs, macrophages and monocytes (Banchereau and Steinman 1998). The capacity of drugs and reactive drug metabolites to act as danger signals and induce DC maturation, activate monocytes and macrophages to increase T cell proliferation has been demonstrated (Lavergne et al. 2009). Not only drugs or drug-protein conjugates can induce DC maturation, but signals can also come from other cells such as keratinocytes, natural killer cells and B cells. Moreover, interaction of DCs and drugs might create an inflammatory microenvironment that triggers a degree of of bystander activation and proliferation of memory T cells without the continuous antigenic stimulation through the TCR (Rodriguez-Pena et al. 2006).

Proinflammatory cytokines released by CD14+ CD16+ monocytes in the epidermis in SJS/TEN skin lesions, have been suggested to contribute to the stimulation cytotoxic T cells (Tohyama et al. 2012). Another study by Araujo et al. (de Araujo et al. 2011) demonstrated CD1a+ CD14+ non-lymphoid dendritic cells in blister fluid not only produce proinflammatory cytokines such as TNF-α at higher concentrations in SJS/TEN patients than others, also the death ligands TWEAK and TRAIL capable of inducing keratinocyte death in an HLA class-I independent manner (Bellón 2019). In acute DRESS, a population of proinflammatory CD14+CD16+ monocytes were severely reduced and recovered after resolution. Neutrophils and the neutrophil chemotactic factor IL-8/CXCL8 have been observed as key players in dermal cytotoxicity in AGEP. In addition, the presence of tissue infiltrating neutrophils is a hallmark of T cell stimulated keratinocyte secretion of IL-8/CXCL8 which may also contribute to the activation and recruitment of neutrophils from the bone marrow to peripheral blood, causing increased circulating T cells and neutrophilia (Kabashima et al. 2011). A novel DRESS mechanism involving innate type 2 lymphoid cells expressing the IL-33 receptor ST2 in the skin and blood of patients during the acute phase, together with high serum concentrations of soluble ST2 and IL-33 was recently reported (Tsai et al. 2019).

1.8.2. NK cells like cytotoxic responses in SCAR

Two mechanisms involving NK cells in the development of SCAR have been suggested. First, particularly in SJS/TEN, drugs trigger the activation of NK cells and CD8 T cells to secrete granulysin, shown to play a pivotal role as a cytotoxic mediator inducing keratinocyte necrosis without direct cell contact. Second, perforin/granzyme B released by NK and T cells are also

considered mediators of drug-induced cytotoxicity through interaction with target cells. These pathways are not mutually exclusive and involve both the innate and adaptive mechanisms. Patients with active SCAR to drugs present activated CD56dim or CD56bright NK subpopulations and increased secretion of cytotoxic markers perforin and granzyme B and proinflammatory cytokines correlating with CD56 expression. A population of CD56dim cells has an increased cytotoxic pattern while CD56bright cells increased Th1 cytokine production such as IFN-γ (Chaves et al. 2010). The CD56+ NK and NKT cells characterised by expression of CD3, CD56 were present in SJS/TEN blister cells and were among the prominent sources of perforin, granzyme B and granulysin, a key cytotoxic molecule responsible for keratinocyte death (Chung et al. 2004).

1.8.3. Adaptive immune responses in SCAR

T lymphocytes are central to most immune responses, and severe immunosuppression occurs in individuals or animals deficient in T cells. They form part of adaptive immune system that is specific. Recognition of specific antigens is necessary for T cells to undergo proliferation, differentiation, acquisition of effector functions and also to provide 'help' to other cell subsets that participate in adaptive immunity, such as B cells and natural killer cells. After HLA restricted drug stimulation or inflammatory microenvironment, multiple subsets of T cells (CD4+, CD8+) from SCAR patients are aberrantly activated, mediate inflammatory responses, have similar proliferative gene signatures in peripheral blood and skin and their skin and blisters infiltration correlates with the severity of tissue damage (Kim et al. 2020; Duong et al. 2017).

1.8.4. CD4+ T cells

SCAR CD4+ T cells display helper T cells (Th1) chemokine CXCR3, skin homing chemokine receptors CLA, CCR10, CCR6, profound production of Th1 proinflammatory cytokines, cytotoxic molecules and their regulatory capacities are compromised. In AGEP, drug specific CD4+ T cells produce IL-8/ CXCL8 and IL-8/ CXCL8-specific receptor CXCR1, which could explain their recruitment to the skin and in the skin, production of IL-8 increases neutrophil and T cell recruitment to the epidermis. In T helper 17 subset (Th17), increased expression and serum levels of IL-17 and IL-22 mark the increased inflammatory responses (Kabashima et al. 2011). Indeed, chemokine CCR6, a distinctive marker of Th17 cells has been found in skin infiltrating lymphocytes (Keller et al. 2005). Altogether, these findings suggest increased circulating, Il-22 producing Th17 cells stimulate keratinocyte secretion of interleukin 8 for neutrophil recruitment thus contributing to skin disease in AGEP (Duong et al. 2017; Bellón 2019). In DRESS, Th2 cells, another subset of CD4+ T cells expressing increased levels of IL-5 are associated with the development of eosinophilia (Choquet-Kastylevsky et al. 1998). In the active stage of DRESS, circulating CD4+ T cells producing IL-4 and IL-13 are significantly increased. The secretion of IL-4 which drives the differentiation of naïve T

cells to Th2, confirms the major role of these cell subset in DRESS (Teraki and Fukuda 2017). In addition, CCL17 which is also regarded as a Th2 chemokine expressed by dermal macrophages in skin biopsies, has been associated with the recruitment of CCR4 + Th2 lymphocytes to the skin. Moreover, the frequencies of Th2 lymphocytes positively correlated with serum CCL17 levels in patients with DRESS (Bellón 2019; Ogawa et al. 2014).

1.8.5. CD8+ T cells

SCAR studies in CD8+ T cells are extensive, several reports demonstrate the cytotoxic capacity of CD8+ T cells in SCAR that leads to the cell death, severe tissue damage characteristic of SJS/TEN. For instance, CD8+ cytotoxic T lymphocytes (CTLs) and CD56+ and NKT cells have been found in SJS/TEN blister cells and showed cytotoxicity against target cells such as keratinocytes. In addition, the increased expression of granulysin (Chung et al. 2004), granzyme B, perforin and FasL in CD8+ T cells from SJS/Ten patients have been implicated as key molecules in the disseminated keratinocyte death (Viard-Leveugle et al. 2013). In addition, CD8+ T cells were found to be prominent sources of secretory granulysin and its in vitro induction along with perforin granzyme mediated cytotoxicity was in a drug specific, HLA class I manner in drug induced SJS/TEN patients (Schlapbach et al. 2011; Nassif et al. 2002). Although granzyme B and perforin have a lesser effect on SJS/Ten associated tissue damage than previously thought, the role of Fas-Fas ligand interaction in keratinocyte death and as effector molecules is debatable as previous findings have not always been reproduced (Chung et al. 2004; Cho et al. 2014). In DRESS, a flow cytometry analysis of circulating cells revealed predominance of CCR4+ CCR10+ CD8+ T cells with proliferative gene signatures (Kim et al. 2020). Furthermore, keratinocyte-specific chemokine CCL27 known to recruits CCR10+ lymphocytes, is increased in SJS/TEN affected skin, along with increased gene expression of CCR10 in skin infiltrates and in blister fluid cells. This strongly suggests that CCL27 may be involved in the recruitment of CCR10+ lymphocytes to the epidermis. In the acute phase of SJS/TEN, higher frequencies of circulating CCR10+ lymphocytes were found (Bellón 2019; Tapia et al. 2004).

The proliferative and inflammatory responses of circulatory and skin infiltrating CD8+ T cells are well documented in a T cell mediated clinical entity similar to SCARs called abacavir hypersensitivity syndrome. In patients with active AHS, there is an elevated induction TNF- α and IFN- γ in whole blood and PBMCs exposed to abacavir in vitro (Martin et al. 2007), nonspecific production of these cytokines were also noted in the recovery phase of AHS (King et al. 2005). In SJS/TEN, early studies reported increased serum and blister fluid concentrations of TNF-α, IFN-γ, IL-6 and IL-10, likely produced tissue resident cells (Nassif et al. 2004; Paquet and Piérard 1998; Correia et al. 2002). Another cytokine (IL-15) related to the severity of SJS/TEN was identified in a recent study (Su et al. 2017). The study was particularly relevant, as IL-15 is generally regarded as one of the main factors

supporting the differentiation and acquisition of effector functions by CTLs and NK cells (Castillo and Schluns 2012). In particular, CTLs and NK cells expression of granulysin has previously been shown to be highly dependent on IL-15 (Clayberger and Krensky 2003). Overall, studies of T cells in immunologically mediated hypersensitivity reactions have demonstrated the central functional role of these cells in SCAR pathogenesis and, furthermore, the elucidation of various molecules produced in these cells could not only be a diagnostic and prognostic marker but also a therapeutic target in SJS/TEN.

1.8.6. Viral reactivation in the immunopathogenesis of SCARs

There is an existing hypothesis that postulates pre-existing memory T cells are responsible for the development of IM-ADRs. A study by Picard et al (Picard et al. 2010) found Epstein-Barr virus (EBV), human herpes virus 6 (HHV-6), or HHV-7 reactivation in 76% of patients at the onset of DRESS. This study provides a better understanding of DRESS pathogenesis and confirm previous reports that linked reactivation of viruses of the herpes group (HHV-6, HHV-7, EBV, and CMV) with DRESS (Descamps et al. 2001; Shiohara, Inaoka, and Kano 2006; Kano et al. 2006). In this proposed mechanistic model, IM-ADRs occur as a result of cross reactivity between pre-existing effector memory T cells generated during a human herpesvirus infection and maintained by latency or re-exposure to viral epitopes and drug-modified antigens – a phenomenon similar to heterologous immunity has been demonstrated for CMV and EBV, and is mostly beneficial, mediating protective immunity but in this instance, results are severe immunopathology (Adler et al. 2017). As HHVs appear to be integral components of DRESS development responsible for the systemic symptoms observed, there is minimal evidence for this association in SJS/TEN (Teraki, Murota, and Izaki 2008), while some studies found association between CMV and development of AGEP (Haro-Gabaldón et al. 1996).

In the blood, skin (and other associated organs) of DRESS patients, expanded populations of CD8+ T cells recognized one of several EBV epitopes and share the same TCR repertoire (Picard et al. 2010; Cho, Yang, and Chu 2017a; Shiohara, Inaoka, and Kano 2006; Hashizume et al. 2013). This confirms drug-specific T cells are pathogen-specific effector memory T cells previously primed by viral exposure through cross reaction or molecular mimicry mechanism and become activated after drugs exposure in susceptible individuals causing disease. In the same Picard et al study discussed above, patients with DRESS syndrome had circulating CD8+ T cells secreting TNF-α and interferon γ and nearly half of the activated circulating CD8+ T cells recognised HHV, whereas circulating or skin infiltrated CD8+ T-cell mainly recognised EBV (Picard et al. 2010). In another study by Kim et al (Kim et al. 2020), they sorted memory T cell subsets and found that DNA from HHV6b was highly enriched in circulating central memory CD4+ T cells.

HIV is a known risk factor of SCARs (Peter, Choshi, and Lehloenya 2019). In abacavir hypersensitivity (AHS), the expansion of abacavir-specific CD8+ T cells from HIV-1-infected patients with was comparable to the expansion observed for EBV-specific memory T cells or allogeneic stimulator cells (Mifsud et al. 2008), suggesting proliferation of a memory T cell population. This was confirmed by an ELISpot assay on blood from patients with AHS in which abacavir-specific, IFN-γ producing T cells were detected with frequencies of up to 700 spots per million PBMCs. In contrast to the presence of memory T cells in the circulation of AHS patients, abacavir-specific IFN-γ producing T cells were not detected in an ELISpot using PBMCs from abacavir-naive HLA-B*5701-positive blood participants (Chessman et al. 2008). Immune reconstitution inflammatory syndrome (IRIS) that occurs soon after the initiation of highly active antiretroviral therapy in patients with HIV and is associated with an increase in CD4+ cell count and/or decrease in HIV viral load has been shown to mimic drug hypersensitivity reactions, presenting a diagnosis dilemma (Gupta, Mittal, and Nischal 2019). However, this should not be confused with DRESS observed in the setting of IRIS where IRIS occurs as a result of immune recovery and results in the host recognizing pre-existing or latent infections (Kano et al. 2014). And the unregulated immune activation against reactivated herpesviruses triggers DRESS (Almudimeegh et al. 2014).

1.8.7. Immune cell imbalances – lack of cytotoxic responses regulation

Regulatory T cells (Tregs) play a critical role in maintaining self-tolerance and immune homeostasis. They are $CD127^{low}$ CD4+ T cells characterized by the high cell surface expression of CD25 and induced expression of the nuclear transcription factor FoxP3. It has been proposed that the lack of Treg function during acute SCAR could lead to excessive activation of effector T cells. One study using mouse models to study the role of Tregs in pathogenesis of SJS/TEN found when CD4+ regulatory T cells are deficient, anti-OVA cytotoxic T cells killed OVA-expressing keratinocytes. The functional defects of T regs we also seen in patients (Rozieres, Vocanson, et al. 2009; Azukizawa et al. 2003). The frequencies of FoxP3 Tregs returned to normal numbers but functionally deficient after resolution of DRESS whereas they were in normal range and their functional defect was restored in SJS/TEN resolution (Hanafusa et al. 2012). These findings suggest that functional impairment in the acute stage of TEN may be related to severe epidermal damage, while a gradual loss of function after DRESS resolution may increase the risk of subsequently developing autoimmune disease.

In contrast, a study by Takahashi et al (Takahashi et al. 2009) was the first to report circulatory expansion of Foxp3+ regulatory T cells and skin infiltration during acute DRESS. Additional studies in animal models proposed, although Tregs are increased in the blood during the acute stage of DRESS, their capacity to migrate into the skin and to suppress the activation of effector T cells is profoundly impaired, thereby allowing drug-specific T cells to function in an uncontrolled manner

(Azukizawa et al. 2003; Azukizawa et al. 2005; Azukizawa and Itami 2007). Another study made this proposal unlikely, because they showed Treg subset expanded in the acute stage of DRESS is further characterized by an increase in expression of ESL and CCR4, well-known markers associated with skin-homing T cells (Takahashi et al. 2003; Hirahara et al. 2006; Campbell et al. 1999; Takahashi et al. 2009).

Immune characterisation of inflammatory infiltrates in TEN found a decrease in the number of skin-directed CD4+ T cells and an increase in the ratio of CD8+ to CD4+ T cells in HIV-infected patients compared to noninfected individuals. This particular study concluded, the loss of skin protective CD4+CD25+ regulatory T cells in HIV infected patients increases risk of developing drug reactions (Yang et al. 2014). HIV associated abnormalities in the number of CD4+ T cells and function of regulatory T cells, and resistance of cytotoxic effector CD8+ T cells to suppression, support the idea that aberrant T cell activity contributes to IM-ADRs. Another transgenic mouse model study of abacavir induced hypersensitivity reported that CD4+T cells which contain a subset of Tregs, are key players in the regulation of immune responses to new antigens induced by abacavir (Cardone et al. 2018).

1.9. AIMS

This study is structured around understanding the interactions between anti-TB drugs, the immune system and HIV TB co-infection in SCAR patients. Neither immune responses characterizing these reactions, nor the genetic underpinnings associated are known in populations of African descent, especially those with co-morbid HIV. From the reaction site and peripheral blood, we can learn about the type of reaction it is and the underlying pathomechanism by defining the nature of immune responses. We want to understand and define mechanism by which non-reactive drugs are rendered immunogenic and offer more plausible explanations on how immune dysregulation associated with HIV promotes hypersensitive reactions to medication. Thus, with the aim to characterize immunological events that underpin SCAR induced by first line anti-tuberculosis, we sought to:

In peripheral blood

1. Detect drug-specific T cells secreting analytes of interest at acute and recovery phases of the reaction
2. Asses proliferative response of drug-specific T cells
3. Determine the phenotype and function of drug specific T cells.
4. Identify HLA risk alleles and associated KIR and ERAP genes linked to specific drug-SCAR combination

At the site of disease (skin, blister fluid)

5. Determine the immune phenotype and function of activated T cells infiltrates and the TCR repertoire/clonotype
6. Identify the transcriptional profile of activated T cells

Chapter 2 – Precision phenotyping of SCAR cases and detecting drug specific T cells

This chapter and figures included are an expansion of our published work - Porter, Mireille, **Phuti Choshi***, Sarah Pedretti, Tafadzwa Chimbetete, Rhodine Smith, Graeme Meintjes, Elizabeth Phillips, Rannakoe Lehloenya, and Jonny Peter. 2022. 'IFN-γ ELISpot in Severe Cutaneous Adverse Reactions to First-line Anti-tuberculosis Drugs in an HIV Endemic Setting', *Journal of Investigative Dermatology*. * First co-author

2.1. Introduction

FLTD-associated SCAR is a diagnostic challenge, with the simultaneous use of multiple drugs; and often associated hepatic and/or renal failure.(Nalitye Haitembu et al. 2021). HIV co-infection increases complexity with the common use of sulfa antibiotics (for opportunistic infection prophylaxis or treatment) and anti-retroviral therapy (ART), themselves known to cause SCAR and often initiated simultaneously or in close proximity. (Kakande and Lehloenya 2015; Meintjes et al. 2019). FLTD are preferred agents for drug-sensitive TB due to higher efficacy, better accessibility, lower side-effect profiles and shorter treatment duration compared to non-FLTD treatment options. (Grobbelaar et al. 2019; Hoosen et al. 2019; Corbett et al. 2003; Councils 1980; East African-British Medical Research Councils 1974; Joint Tuberculosis Commitee of the British Thoracic Society 1998; Schaberg, Rebhan, and Lode 1996). Thus, when managing FLTD-associated SCAR, rapid low-risk methods to identify the offending drug, and allow expeditious and safe reintroduction of non-offending drugs, is critical. (Lehloenya and Dheda 2012)

Our team has pioneered the use of additive sequential drug challenge (SDC) as a form of oral drug provocation testing with FLTD, demonstrating that full-dose challenge is safe and effective at both identifying offending drugs, and allowing safe and rapid reintroduction of effective drugs. (Lehloenya et al. 2021a; Lehloenya et al. 2011; Lehloenya et al. 2020b). However, although benefits outweigh risk, SDC can result in moderate or severe adverse events requiring specialised care and considerable cost. (Lehloenya et al. 2011; Knight et al. 2019; Lehloenya, Todd, et al. 2012). As such, ex vivo/in vitro testing has the potential to add considerably in both the identification of the culprit drug and to inform risk stratification for SDC.

Given the role of T cells in cell mediated drug hypersensitivity reactions, ex vivo assays explored for their diagnostic value in IM-ADRs to-date include enzyme linked immunospot assay (ELISpot) and lymphocyte transformation testing (LTT). These assays are well known adjunctive diagnostic tools successfully used to risk-stratify SCAR patients for future drug safety by identifying offending agents in delayed drug hypersensitivity. (Lehloenya et al. 2020a; Copaescu, Choshi, et al. 2021; Copaescu, Mouhtouris, et al. 2021; Lehloenya et al. 2020b). Although dependent on the specific SCAR phenotype and the specific drug, g-INF ELISpot assay has shown to be more sensitive (82%) in the

early stage after SCAR onset and specific in comparison to lymphocyte transformation test (LTT) (50% sensitivity) (Polak et al. 2013) and flow cytometric-based assays testing various immunological parameters in cell mediated hypersensitivity reactions (Pavlos et al. 2014; Maecker et al. 2008). Many reports lack reproducibility and rigor and are contradictory and drug specific. In some studies LTT demonstrated a higher sensitivity in other types of anticonvulsant hypersensitivity (70–90%) (Elzagallaai et al. 2009). ELISpot assay is a highly sensitive method for ex vivo quantification of cytokine or antibody secreting cells after stimulation with an appropriate stimulus. The standard colorimetric ELISpot assay is based on the recognition and measurement of cytokine secreting cells by quantifying spot forming cells. This method was selected for its specificity in monitoring immune responses, detecting drug specific T cells and epitope discovery. It has also been shown to be less complex, does not involve use of radioactive isotopes and is less likely to be associated with false positives compared to traditional *in vitro* methods such as LTT. (Pavlos et al. 2014; Maecker et al. 2008; Polak et al. 2013).

However, IFN-γ ELISpot assays have not been optimised nor are they available for high TB burden, resource poor settings. (Kakande and Lehloenya 2015; Lehloenya and Dheda 2012) There is currently no defined protocol for FLTD IFN-γ ELISpot assay without the use of T cell clones and T cell co-stimulation (Ye et al. 2017). Due to the lack of standardised strategy for these drug tests and variability based on incubation times, co-stimulation factors and analyte of interest measured (e.g., granulysin, IFN-γ, TNF-a), the aim of this study was to optimise IFN-γ ELISpot for FLTD-associated SCAR in an HIV TB endemic setting. We needed to better characterise FLTD SCAR cases and to ideally translate anti-TB drugs IFN-γ ELISpot assay into a diagnostic test that could improve anti-TB drug safety and ensure optimal therapy, we explored its sensitivity and specificity.

2.2. Materials and Methods

2.2.1. Patients and controls participants recruitment and enrolment

This study was conducted as part of IMARI biorepository established at Groote Schuur Hospital. Participants who fit the criteria of drug induced adverse reactions were recruited into the IMARI registry since November 2018. The IMARI registry (HREC REF R031/2018) and this sub-study (HREC REF 500/2018) were approved by the UCT human research ethics committee (HREC). Informed consent was obtained from all participants. Reporting in this sub-study includes participants recruited between November 2018 and October 2021. All patients were assessed by dermatologists at Groote Schuur hospital dermatology ward or at the multidisciplinary drug allergy clinic. Patients recruited prospectively were followed up for 2 years at time of reporting. In all enrolled cases with suggested FLTD SCAR, FLTD were regarded as the offending drugs if the SCAR symptoms occurred on re-exposure and by drug exclusion when the symptoms resolved upon withdrawal of FLTD. Patients with tolerance on re-exposure to FLTD and patients with transient, milder reactions that did not meet the criteria of SCAR were excluded.

Included FLTD SCAR patients met the following inclusion criteria:

1. Age ≥ 18-year-old
2. Able to provide written informed consent
3. Clinical and laboratory phenotype consistent with IM-ADR
4. Drug(s) treatment stopped/interrupted due to clinical/laboratory abnormalities
5. Histological evidence supports immune-mediated pathology, where applicable e.g., skin, liver or kidney
6. Drug probability scores e.g., Naranjo and ALDEN suggest “possible”, “probable” or “definite” for a specific drug-ADR combination

Drug tolerant controls defined as participants who tolerated FLTD for more than 8 weeks and 12 weeks for participants taking TMP-SMX without any adverse events were recruited in the IMARI registry. Included drug tolerant controls met the following inclusion criteria:

1. Age ≥ 18-year-old
2. Able to provide written informed consent
3. Drug tolerant for at least 8 – 12 (for participants on TMP-SMX) weeks of treatment.

2.2.2. Blood collection and PBMCs isolation

Blood was collected in EDTA tubes (BD Biosciences) and peripheral blood mononuclear cells (PBMCs) were isolated by density gradient centrifugation. Blood was diluted with room temperature RPMI 1640 media (Gibco) or 1X PBS (life technologies) and gently layered on the Leucosep tube (greiner bio-one) top barrier containing ficoll histopaque (sigma Aldrich) under the barrier, centrifuged at 1000g for 10 minutes with brakes off. The buffy coat containing PBMCs was collected

into new falcon tube and washed with RPMI or 1X PBS three times. First centrifuge at 300g and the last two at 400g for 10 minutes. PBMCs were either cryopreserved at -80°C in 80% foetal bovine serum (FBS) – heat inactivated (life technologies) and 20% dimethyl sulfoxide (DMSO) (sigma Aldrich) or used fresh.

2.2.3. PBMCs thawing, resting and culture

Before use, cryopreserved cells were thawed in the 37°C water bath by swirling the tube until a small button of ice remained in the sample. Cells were transferred into 10ml into R10 media containing 10% FBS, 1% HEPES, L-glutamine, Pen/Strep (life technologies) and 10ug/ml DNAse (sigma Aldrich) in RPMI. Cells were washed twice and rested in a 6 well plate containing 5ml/well R10 media without DNAse for 6+ hours at 37°C, 5% CO2.

2.2.4. Drug preparation and stimulation

Cells were stimulated with rifampicin (R3501, sigma Aldrich), pyrazinamide (P7136, sigma Aldrich), ethambutol (E4630, sigma Aldrich), isoniazid (I3377, sigma Aldrich) and trimethoprim/ sulfamethoxazole (intravenous preparation, Groote Schuur pharmacy) for participants taking TMP-SMX at the time of major reaction. The FLTD stock solution was prepared by dissolving the drugs in relevant diluents (Table 2-1) and stored at -80°C for the stability tested period. The stock solution was serially diluted with R10 media to obtain working solutions concentrations (appendix, section 2.1).

Table 2-1: ELISpot stimulants preparation

Drug	Diluent	Soluble concentration	Concentrations tested (ug/ml)	Stability at -80C (days)
Rifampicin	methanol	50mg/ml	2.5, 25, 2500	626
Pyrazinamide	DMSO	50mg/ml	50, 500, 5000	274
Ethambutol	water	50mg/ml	50, 500, 5000	550
Isoniazid	water	50mg/ml	50, 500, 5000	83
Trimethoprim-Sulfamethoxazole (TMP-SMX)	pre-diluted	16/80mg/ml	50/250	room temperature
Positive controls				
Anti-CD3	R10 media	1mg/ml	1	-
SEB	R10 media	5mg/ml	0.05, 0.1, 0.5	-

2.2.5. ELISpot assay

On day one of the ELISpot assay, 96 well ELISpot plates (MAIPS4510 Millipore) were coated with 2ug/ml coating antibody (1-D1K) from the interferon gamma ELISpot assay kit (Mabtech), 100ul/well was added, covered with foil and incubated at 4°C overnight. On day two, ELISpot plates

were washed by hand 6 times with 200µl of 1XPBS. The ELISpot plate was incubated for 1.5 hours with 200µl/well R10 media to block no specific protein binding. After resting, cells were washed once with R10 media and viable cell number was determined using trypan blue viability staining. Cells were diluted with R10 media to 2 million/ml so that 100µl/well contains 200 000 cells. Drug stimulants and positive controls were prepared as per section 2.2.4, Table 2-1. First, 100µl of cells and stimulants were added into each well on a 96 well round bottom culture plate for a total volume of 200µl and incubated for 45 minutes at 37°C, 5% CO2, before transfer into an ELISpot coated plate (appendix, section 2.2, plate layout). The ELISpot plate was incubated at 37°C, 5% CO2 for 18 hours. Day three of the assay, the plate was washed 6 times with 1X PBS, then 100ul of 1ug/ml detection antibody prepared in 0.5% FBS and 1XPBS was added into each well and incubated for 2 hours at room temperature. The plate was washed 6 times after incubation with 1XPBS, then 100ul of 1ug/ml detection antibody prepared in 0.5% FBS and 1XPBS was added into each well and incubated for 1 hour at room temperature. Plate was washed 6 times with 1XPBS and filtered TMB substrate (Mabtech) was added at 100ul/well, incubated at room temperature for 15 minutes in the dark. The reaction was terminated by rinsing the plate under tap water. The plate was left to dry overnight in the dark before spot counting (figure 2-1).

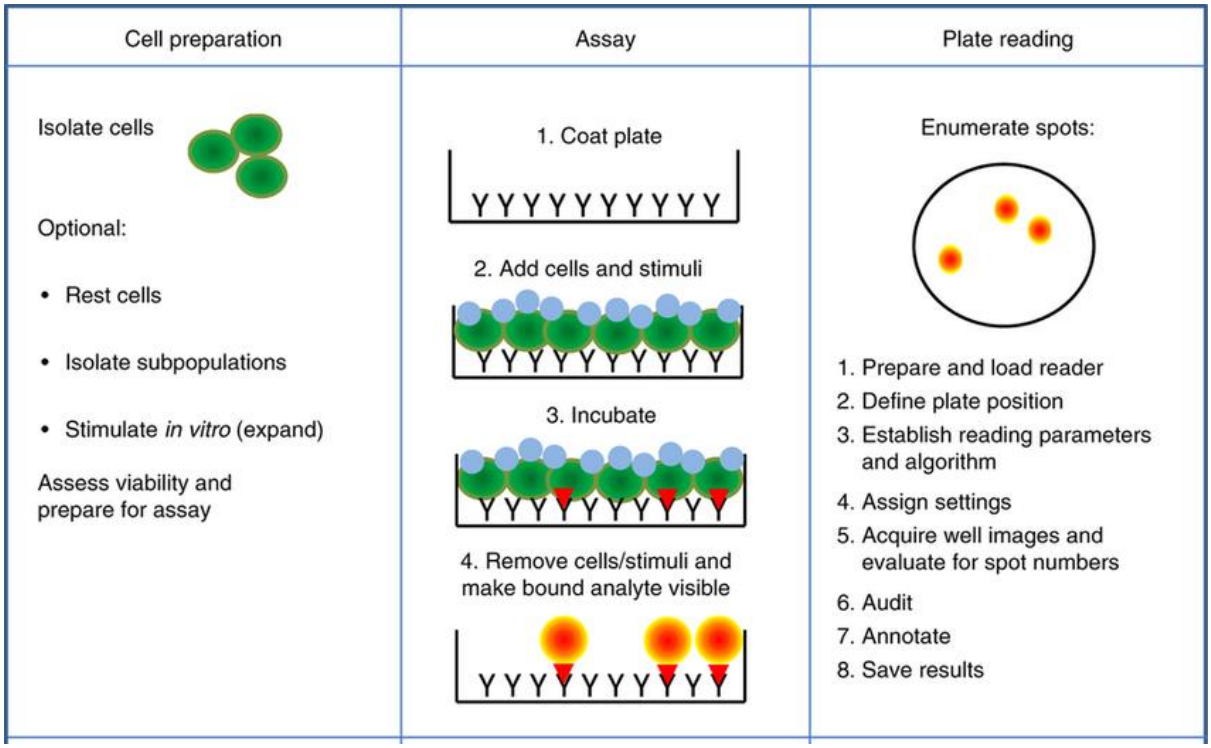

Figure 2-1 Automated ELISpot Assay over three days

Schematic diagram showing the three stages of an ELISpot assay - cell preparation, cell stimulation and plate reading. First is the isolation of cells and for cryopreserved cells, additional steps such resting are added to expand the number of cells and interest and ensure the integrity and high quality of viable cells. Isolation of subpopulation for assays on T cell lines and clones, invitro cell stimulation and cell viability are also assessed at this stage. *Adapted from (Janetzki et al. 2015)*

2.2.6. Spot counting

Generated spots were quantified and captured using an ELISpot AID automated reader (AID diagnostika, software version 7) and results are presented as number of spot-forming units (SFU) per million cells in response to stimuli after removal of background.

2.2.7. Flow cytometry staining and acquisition

To confirm optimal drug stimulation concentration without cytotoxicity we used flow cytometry to measure cell viability. Cells were cultured and stimulated as per ELISpot assay protocol in section 2.2.5. After 18 hours incubation with drugs, cells were transferred into FACS tubes and washed two times with FACS buffer (0.1% BSA (Sigma Aldrich), 0.01% NaN3 (Sigma Aldrich), in 1X PBS (life technologies), pH 7.4) at room temperature, 500g for 5 minutes. Cells were stained with 1µl (1µl to $<10^6$ cells) 7AAD, PE-Cy5.5 (BD Pharmingen), washed once, resuspended in 200µl FACS buffer and acquired on LSRII flow cytometer. FCS files were analysed using FlowJo (appendix, section 2.3, gating strategy).

2.3. Results

2.3.1. IFN-γ release ELISpot assay optimisation

To ensure we were using optimal drug concentrations and maintaining a good percentage of viable cells without inducing drug cytotoxicity - we have studied the highest non-cytotoxic rifampicin (25, 250, 2500ug/ml), isoniazid.(Copaescu, Choshi, et al. 2021), pyrazinamide, ethambutol (50, 500, 5000ug/ml) concentrations for *in vitro* 18-hour drug stimulation. Results showed that rifampicin induces cytotoxicity in a dose dependent manner, whereas ethambutol, isoniazid and pyrazinamide had no effect with exception of pyrazinamide at 100-fold concentration against DRESS patient cells (figure 2-2A-B). For optimal interaction between cells and drug antigens, high cell density is required, and as higher numbers of cells will lead to piling up of cells and linearity between cell input and detected spot frequency is lost. We evaluated the use of two higher numbers of cells per ELIPOT well (300 000 and 400 000 versus 200 000), and no notable improvement in spot forming units (SFU) per million cells was noted (figure 2-2C).

As with many cell-based assays, ELISpot performance and sensitivity depend on the integrity and high quality of viable cells. We compared ELISpot performance using fresh versus longer cryopreserved cells (0 days-18 months storage in the -80°C freezer). In 3 DRESS or SJS/TEN cases induced by rifampicin and isoniazid, we noted 2-4 times higher SFUs/million cells when using freshly isolated versus cryopreserved cells; in 2/3 cryopreserved cells samples, SFUs were lower than the set positivity threshold (figure 2-2D). In certain cases, it was not possible to use freshly isolate cells; and thus, where necessary we still used cryopreserved cells, as long as cell viability was ≥70%. We measured IFN-γ responses from different points of the reactions to test which phase displays greater sensitivity. Comparison of SFU/million cells by sampling time-point was possible due to multiple time-point sampling at acute stage of the reaction, before SDC, on positive reaction to any of the FLTD, 3-, 6-, 12-, 24-months and up to 10 years post SCAR onset. For analyses, patients were divided into two groups ≤12 weeks from onset of symptoms (*n=30)* (acute bloods and early recovery) and >12 weeks *(n=22)* (recovery phase bloods). Blood samples collected in the 1-12 weeks after SCAR onset showed higher SFU/million cells after rifampicin stimulation (P value = 0.0121) compared to bloods collected >12 weeks after SCAR onset No differences were noted after stimulation with isoniazid, pyrazinamide, and ethambutol (figure 2-2 E-F).

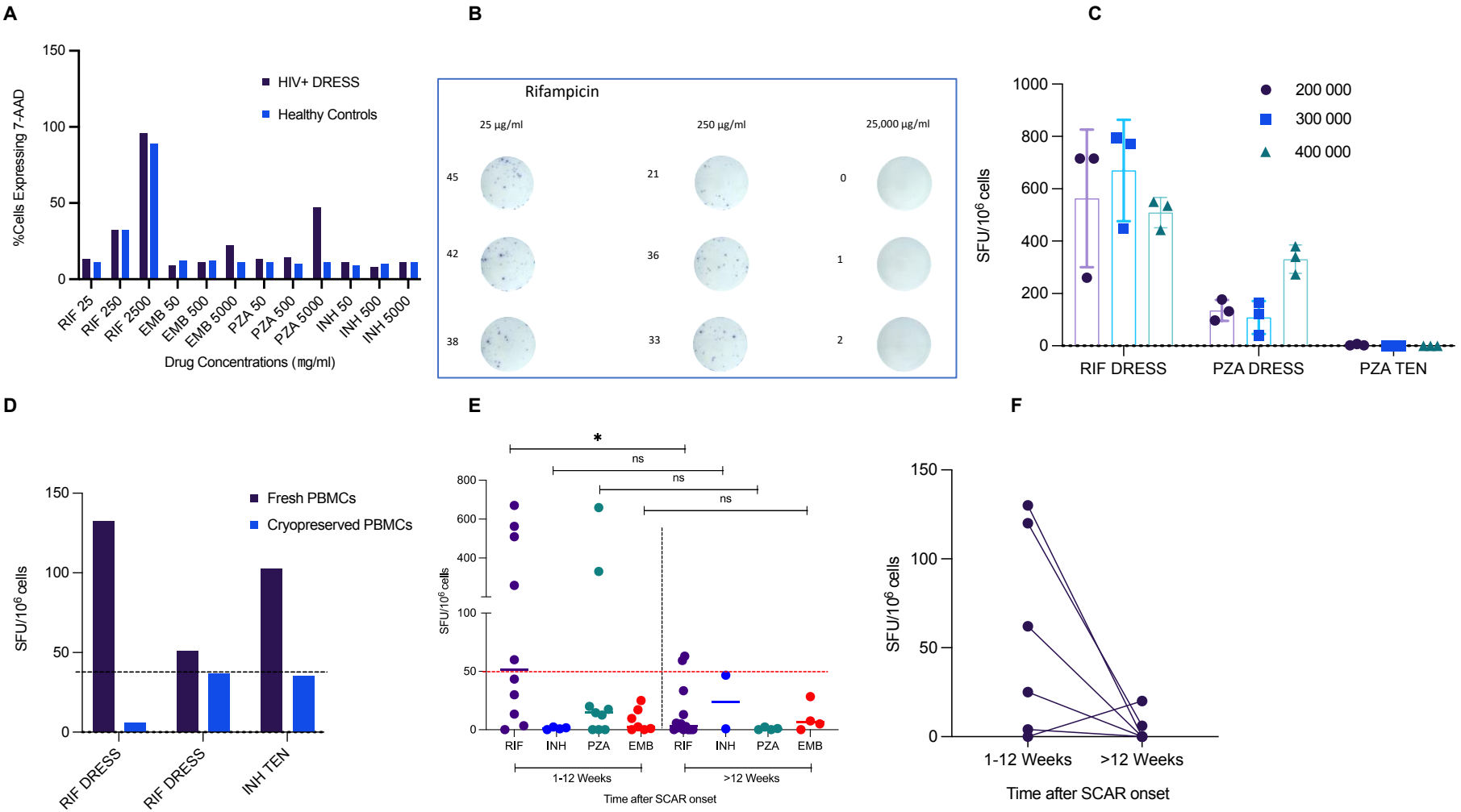

Figure 2-2 FLTD IFN-γ ELISpot optimisation

A-B) Non-cytotoxic drug concentration for 18-hour in-vitro drug stimulation. **C**) Number of cells per well. **D**) Fresh vs cryopreserved PBMCs. **E**) Bloods sampling timepoint by FLTD and **F**) Blood sampling time point comparison of rifampicin response in 6 cases. RIF - rifampicin, INH – isoniazid, PZA – pyrazinamide, EMB – ethambutol, SFU – spot forming units, DRESS – drug reaction with eosinophilia and systemic symptoms, TEN – toxic epidermal necrolysis, SCAR – severe cutaneous adverse reactions. *Adapted from (Porter et al. 2022).*

2.3.2. Characteristics of SCAR cases

Thus far, a total of 164 cases of CADRs have been enrolled in the IMARI registry. This includes *n=132* prospective and *n=32* retrospective cases. Of all CADR cases, 86 (52%) had FLTD as the suspected primary offending drug and after detailed review and clinical characterisation which included sequential drug challenge (SDC) outcomes, 53 (32%) cases were classified as FLTD SCAR (figure 2-3). SDC to one or more FLTB drugs was performed for 43 SCAR cases. This included *n=37* DRESS cases (15 definite (RegiSCAR score >5), 11 probable (RegiSCAR score 4-5) and 11 possible (RegiSCAR score 2-3) and *n=6* SJS/TEN cases (3 definite and 3 probable). SDC did not occur (*n=10*) due to death (*n=4*), un-confirmed TB diagnosis (*n=2*), and modified regimen use due to contraindication to challenge such as severe liver disease (*n=4*). SDC included isoniazid in 40 patients however only 34 included rifampicin, 31 pyrazinamide and 38 ethambutol (figure 2-3).

Table 2-2 shows the demographic and clinical characteristics of the 43 FLTD induced SCAR cases who underwent SDC to one or more FLTD. Most patients were female (65%). At the time of SCAR event 81% were HIV infected with a median CD4 cell count (closest to time of SCAR) of 103 cells/mm^3; 54% were on ART and 51% were on trimethoprim-sulfamethoxazole (TMP-SMX). Naranjo score where TMP-SMX was suspected (*n=16*) was 11 (Possible) and 5 (Probable). Disseminated TB was seen in 42% of patients and 9% had a history of previous TB prior to the index event and self-reported tolerance to anti-TB treatment on previous exposure.

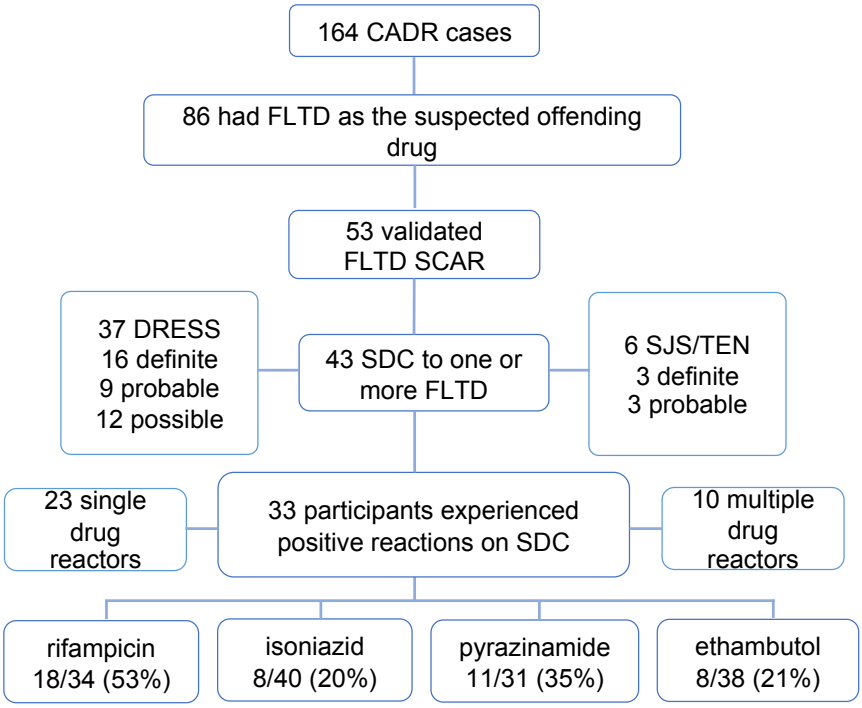

Figure 2-3 Enrolment and participants characteristics

CADR - cutaneous adverse drug reaction, FLTD - First line anti-tuberculosis drugs, SCAR: severe cutaneous adverse reaction, DRESS - drug reaction with eosinophilia and systemic symptoms, SDC - sequential drug challenge, SJS/TEN - Stevens-Johnson syndrome/ toxic epidermal necrolysis

Table 2-2: Demographic variables of 43 FLTD SCAR patients who underwent SDC to one or more FLTD

Female	28 (65)
HIV positive n (%)	35 (81)
CD4 count median (IQR) cells/mm^3	103 (42–228)
On ART at time of SCAR n (%)	19/35 (54)
On TMP-SMX at time of SCAR n (%)	18/35 (51)
Previous TB n (%)	4 (9)
Disseminated TB n (%)	18 (42)
Positive drug reactors n (%)	33 (77)
Single drug reactors n (%)	24/33 (73)
Multiple drug reactors n (%)	9/33 (27)
Positive ELISpot to any FLTD n (%)	24 (56)
Positive ELISpot to TMP-SMX and/or major metabolite n (%)	9 (21)

IQR - interquartile range, ART - anti-retroviral therapy, SCAR - severe cutaneous adverse reaction, TB - tuberculosis, FLTD - first-line anti-tuberculosis drugs

2.3.3. Oral drug provocation testing outcomes

Thirty-three (73%) of the 43 patients experienced one or more positive reaction to FLTD during SDC. The clinical phenotypes and timing of SDC reactions were varied and are detailed in Table 2-3. Reactions included immediate type reactions (<6 hours) and delayed reactions, and ranged from flushing and hypotension to worsening rash, eosinophilia, and liver functions. Rifampicin was the most common offending drug on SDC with 18/34 (53%) positive reactions (*n=16* DRESS, *n=2* SJS/TEN). Pyrazinamide was the next most common offending drug with 11/31 (35%) positive reactions (*n=7* DRESS, *n=4* SJS/TEN). Isoniazid and ethambutol were positive in 8/40 (20%) (*n=6* DRESS, *n=2* SJS/TEN) and 8/38 (21%) (*n=7* DRESS, *n=1* SJS/TEN) SDCs respectively (figure 2-3). Twenty-three of the 33 (70%) patients experiencing a positive SDC reactions showed a positive reaction to only one drug on SDC (single reactors) - twelve cases were positive for rifampicin, four for isoniazid, six for pyrazinamide, and one for ethambutol. Ten patients experienced a positive SDC to more than one FLTB drug, with the commonest combination being reactions to rifampicin and isoniazid (*n=5*) (Table 2-3). One patient (case ID 28, Probable SJS/TEN) experienced positive SDC reactions to each of the four FLTD and one patient (case ID 49, Probable DRESS) to each of rifampicin, isoniazid, and ethambutol (pyrazinamide SDC not done). Both of these latter two patients also exhibited intolerance to second-line anti-TB drugs including moxifloxacin, linezolid, clofazimine and bedaquiline.

In eight cases, rifampicin was not challenged as it was identified as the likely offending agent due to clinical history including a positive rifampicin patch test for one. In these cases, rifampicin causation was diagnosed based on exclusion with the successful challenge of the other FLTD. Similarly, five pyrazinamide, two ethambutol and one isoniazid causation were diagnosed based on exclusion with the successful challenge of the other FLTD. Two additional cases were not fully challenged, one was initiated on continuation phase (rifampicin and isoniazid) and the other for whom rifampicin and pyrazinamide were excluded due to severe renal and hepatic impairments (Table 2-3).

Table 2-3: Characteristics of oral drug provocation testing to FLTD

Case ID	Age/Sex	Drugs	Single or Multiple	Positive Reactors	Reaction Characteristics	ELISpot Results	ART	CD4	TMP/ SMX	Validated Phenotype
1	35/M	rifampicin, isoniazid, ethambutol, Rifabutin	Single	rifampicin	24 hours: facial oedema, rash (erythema)	RIF: 175 SFU	No	101	No	Probable DRESS
2	28/M	rifampicin, isoniazid, pyrazinamide, ethambutol	Single	isoniazid	unknown	INH: 0 SFU		5	Yes	Probable DRESS
3	45/M	rifampicin, isoniazid, ethambutol	Single	isoniazid	9 days: facial oedema, rash (erythema), eosinophilia	INH: 103 SFU	Yes	90	Yes	Probable SJS/TEN
4	24/F	rifampicin, isoniazid, pyrazinamide, ethambutol, Rifabutin	Single	pyrazinamide	20 minutes: Itching burning, sore throat, visual disturbances, visible rash (exanthema)	PZA: 46 SFU	Yes	63	Yes	Definite TEN
5	33/M	rifampicin, isoniazid, pyrazinamide, ethambutol, Rifabutin	Single	rifampicin	24 hours: visible rash	RIF: 45 SFU, EMB: 45 SFU	HIV negative	n/a	n/a	Probable DRESS
6	40/F	rifampicin, isoniazid, pyrazinamide, ethambutol	Single	rifampicin	2-3 hours: vomiting, fever	RIF: 261 SFU	No	117	No	Probable SJS/TEN
7	30/F	rifampicin, isoniazid, pyrazinamide, ethambutol, Rifabutin	Multiple	rifampicin	Within minutes: itching, burning, photophobia, rash (erythema), facial oedema.	RIF: 33 SFU	HIV negative	n/a	n/a	Probable SJS/TEN
				isoniazid	Within 24 hours: itching, facial oedema.	INH: 47 SFU				
				Rifabutin†	d19: burning, facial oedema, jaundice.	Rifabutin - not done				
				pyrazinamide†	d12: burning, facial oedema, jaundice, later tolerated	PZA: 45 SFU				
				ethambutol†	d10: burning, facial oedema, jaundice.	EMB: 28 SFU				
				BDQ/ CFZ/ MOX/ ethambutol/ ETH	d1: fever, headache, vomiting	-				
8	48/F	rifampicin, isoniazid, pyrazinamide, ethambutol	Multiple	isoniazid	48 hours: Visible rash (erythema)	PZA: 652 SFU	HIV negative	n/a	n/a	Definite TEN
				pyrazinamide	18 hours: headache, painful mouth and eyes	INH: 0 SFU				

9	38/F	rifampicin, isoniazid, pyrazinamide, ethambutol,	Single	rifampicin	Within minutes: burning, visible rash, facial oedema, erythema.	RIF:8 SFU	No	457	Yes	Definite DRESS
10	50/F	rifampicin, isoniazid, pyrazinamide	Single	pyrazinamide	10 days: itching, visible rash (exanthema)	PZA: 0 SFU	No	337	No	Definite SJS
11	45/M	rifampicin, isoniazid, pyrazinamide, ethambutol	Single	pyrazinamide	Within 24 hours: itching, visible rash (erythema), fever	PZA: 13 SFU, INH: 40 SFU	Yes	39	No	Definite DRESS
12	35/M	rifampicin, isoniazid, pyrazinamide, ethambutol	Single	isoniazid	4 days: itching, fever, elevated liver enzymes	INH: 0 SFU	No	58	Yes	Definite DRESS
13	29/F	rifampicin, isoniazid, pyrazinamide, ethambutol, Rifabutin	Single	ethambutol	1 day: itching, visible rash (erythema)	EMB: 8 SFU	No	112	Yes	Probable DRESS
14	56/F	rifampicin, isoniazid, ethambutol, Rifabutin	Multiple	rifampicin	d11: increased ALT, AST.	RIF: 0 SFU	HIV negative	n/a	n/a	Probable DRESS
				isoniazid	d9: increased ALT, AST only	INH: not done				
				Rifabutin	d1: increased ALT AST.	Rifabutin - not done				
				MOX/ TZD/ ethambutol	d3: itching, visible rash (exanthema)	-				
15	26/F	rifampicin, isoniazid, pyrazinamide, ethambutol, Rifabutin	Multiple	pyrazinamide	24 hours: itching, fever, facial oedema	PZA: 15 SFU	Yes	5	Yes	Definite DRESS
				ethambutol	24 hours: itching, visible rash (erythema)	EMB: 16 SFU, INH: 37 SFU				
16	23/F	rifampicin, isoniazid, pyrazinamide, ethambutol	Single	rifampicin	Within minutes: Itching, visible rash-erythema	RIF: 0 SFU	HIV negative	n/a	n/a	Probable DRESS
17	26/F	rifampicin, isoniazid, pyrazinamide, ethambutol	Single	pyrazinamide	48 hours: itching, visible rash (induration, erythema)	PZA: 0 SFU	No	330	No	Definite DRESS
18	41/F	rifampicin, isoniazid, pyrazinamide, ethambutol, Rifabutin	Single	rifampicin	5 days: itching, burning, visible rash (exanthema, erythema)	RIF: 60 SFU	No	39	No	Definite DRESS
19	37/F	rifampicin, isoniazid, pyrazinamide, ethambutol, Rifabutin	Single	rifampicin	24 hours: Fever, raised ALT	RIF: 563 SFU	No	121	No	Possible DRESS
20	31/F	isoniazid, pyrazinamide, ethambutol, Rifabutin	Single	isoniazid	72 hours: itching, burning, joint pain, nausea, fever, visible rash (erythema)	INH: 0 SFU	Yes	137	Yes	Possible DRESS

21	47/F	rifampicin, isoniazid, pyrazinamide, ethambutol	Single	pyrazinamide	24 hours: abdominal pain, ALT and AST increase, visible rash (erythema)	PZA: 0 SFU	No	576	No	Definite DRESS
22	36/M	rifampicin, isoniazid	Multiple	rifampicin/ isoniazid	Unclear timing >7 days: discharged and represented with erythema, induration, fever oedema	RIF: 0 SFU, INH:0 SFU	Yes	142	No	Definite DRESS
23	39/F	rifampicin, isoniazid, ethambutol	Multiple	rifampicin/ isoniazid	7 days: Visible rash (erythema)	RIF: 0 SFU, INH: 0 SFU	Yes	360	No	Possible DRESS
24	55/F	rifampicin, isoniazid, pyrazinamide, ethambutol	Single	pyrazinamide	7 days: itching, visible rash (erythema)	PZA: 0 SFU	No	41	Yes	Possible DRESS
25	30/M	rifampicin, isoniazid, pyrazinamide, ethambutol, Rifabutin	Multiple	rifampicin	2 days: rash, oral sores, eosinophilia, fever	RIF: 40 SFU	No	170	No	Definite DRESS
				ethambutol	2 days: burning skin, palmar desquamation	EMB: not done				
26	15/F	rifampicin, isoniazid, ethambutol	Multiple	rifampicin	8.5 hours: itching, sore throat, fever, burning eyes, palmar erythema, morbilliform rash, increased AST and ALT	RIF: 520 SFU	HIV negative	n/a	n/a	Probable DRESS
				isoniazid	14 hours: itching, fever, visible rash, purpurae, erythema	INH: 33 SFU				
				ethambutol	36 hours: itching, burning, visible rash, weakness in limbs, fever	EMB: 17 SFU				
27	37/F	rifampicin, isoniazid, ethambutol, Rifabutin	Multiple	ethambutol	unknown	EMB: 0 SFU	Yes	21	Yes	Definite DRESS
				rifabutin		Rifabutin - not done				
28	41/M	rifampicin, ethambutol	Multiple	rifampicin	visible rash and liver derangement	RIF: 0 SFU	Yes	162	No	Probable DRESS
				ethambutol		EMB: 0 SFU				
29	34/F	rifampicin, isoniazid, pyrazinamide, ethambutol, Rifabutin	Single	rifampicin	2 hours: fever, increased heart rate	RIF: 576 SFU	HIV negative	n/a	n/a	Definite DRESS
30	52/M	rifampicin, isoniazid, pyrazinamide, ethambutol	Single	rifampicin	high dose rifampicin	RIF: 3 SFU	No	23	No	Possible DRESS
31	51/F	rifampicin, isoniazid, pyrazinamide, ethambutol, Rifabutin	Single	rifampicin	14 hours: itching, fever, facial oedema	RIF: 0 SFU	Yes	111	Yes	Probable DRESS

32		rifampicin, isoniazid, pyrazinamide, ethambutol	Single	rifampicin	Within minutes: itching, fever, oedema	RIF: 188 SFU	No	93	Yes	Possible DRESS
33		rifampicin, isoniazid, pyrazinamide, ethambutol	Single	rifampicin	Within minutes: itching, burning, pins and needles, visible rash	RIF: 2400 SFU	No	142	Yes	Possible DRESS

34		isoniazid, pyrazinamide, ethambutol	Single	rifampicin‡	-	RIF: 65 SFU	No	26	No	Possible DRESS
35	37/M	isoniazid, ethambutol	Multiple	rifampicin‡ pyrazinamide‡	-	RIF: 245 SFU PZA: 0 SFU	Yes	72	No	Possible DRESS
36	39/M	isoniazid, pyrazinamide, ethambutol	Single	rifampicin‡	-	RIF:2 SFU	No	223	Yes	Definite DRESS
37	59/M	isoniazid, pyrazinamide, ethambutol, Rifabutin	Single	rifampicin‡	-	RIF 59 SFU	HIV negative	n/a	n/a	Definite DRESS
38	39/F	isoniazid, pyrazinamide, ethambutol, Rifabutin	Single	rifampicin‡	-	RIF:28 SFU	No	87	No	Probable DRESS
39	42/F	rifampicin, isoniazid	Multiple	pyrazinamide‡ ethambutol‡	-	PZA: 20 SFU EMB: not done	No	177	Yes	Definite DRESS
40	46/M	isoniazid, ethambutol, Rifabutin	Multiple	isoniazid ethambutol rifabutin rifampicin‡ pyrazinamide‡	10 days: visible rash, blisters, fever, peeling -	INH: 0 SFU EMB: 0 SFU Rifabutin - not done RIF: 0 SFU PZA: 0 SFU	Yes	141	Yes	Definite DRESS
41	53/F	rifampicin, isoniazid	Multiple	pyrazinamide‡ ethambutol‡	-	PZA: not done EMB: 0 SFU	Yes	82	Yes	Probable DRESS
42	33/F	isoniazid, pyrazinamide, ethambutol	Single	rifampicin‡	-	RIF: 0 SFU	Yes	19	Yes	Possible DRESS
43	43/M	ethambutol	Multiple	rifampicin‡ isoniazid‡ pyrazinamide‡	-	RIF: 0 SFU INH: 2 SFU PZA: 0 SFU	No	90	No	Possible DRESS
44	21/F	no rechallenge	-	-	-	RIF: 0 SFU INH: 0 SFU	Yes	384		Definite DRESS

						PZA: 0 SFU EMB: 0 SFU				
45	59/F	no rechallenge - RIP	-	-	-			118	Yes	Definite TEN
46	36/M	unknown outcome	-	-	-	RIF: 8 SFU INH: 20 SFU PZA: 0 SFU EMB: 8 SFU	No	22	No	Probable SJS
47	45/F	no rechallenge - RIP	-	-	-	RIF: not done INH: not done PZA: not done EMB: 25 SFU	Yes	66	Yes	Probable DRESS
48	43/M	no rechallenge - dose modified	-	-	-	RIF: not done INH: not done PZA: not done EMB: 5 SFU	Yes	169	Yes	Probable DRESS
49	41/F	no rechallenge	-	-	-	RIF: 0 SFU INH: 0 SFU PZA: 0 SFU EMB: 0 SFU	HIV negative	n/a	n/a	Definite DRESS
50	35/M	no rechallenge - RIP	-	-	-		Yes	113	Yes	Definite TEN
51	53/F	no rechallenge - TB misdiagnosis	-	-	-	RIF: 8 SFU INH: 0 SFU PZA: 0 SFU EMB: 11 SFU	HIV negative	n/a	n/a	Possible TEN
52	40/F	no rechhallenge - TB misdiagnosis	-	-	-	RIF: 0 SFU INH: 0 SFU PZA: 0 SFU EMB: 0 SFU	No	349	No	Probable DRESS
53	48/M	no rechallenge - RIP	-	-	-	RIF: 0 SFU INH: 0 SFU PZA: 0 SFU EMB: 1 SFU	No	205	Yes	Definite DRESS

† Individually initiated but reaction occurred during exposure to all, ‡ drug not challenged due to high clinical suspicion – regarded as the causative drug based on clinical review – offending drug by exclusion. FLTD - first-line anti-tuberculosis drugs, RIF - rifampicin, INH - isoniazid, PZA - pyrazinamide, EMB - ethambutol, RH - fixed drug combination rifampicin with isoniazid, MOX - moxifloxacin, TZD - terizidone, LZD - linezolid, LFX - levofloxacin, CFZ - clofazimine, BDQ - bedaquiline, ETH - ethionamide, ALT - alanine aminotransferase, AST **-** aspartate aminotransferase, d - time in days, SFU - spot forming units, ART - anti-retroviral therapy.

2.3.4. Diagnostic accuracy – ELISpot as a diagnostic tool for identifying culprit FLTD

To assess the diagnostic utility of IFN-γ ELISpot assay for the four FLTDs, its outcomes were compared to those of the gold standard of oral full dose SDC. This required both SDC and IFN-γ ELISpot assay to have been completed for each drug in question resulting in rifampicin comparison for 34 patients, isoniazid for 40, pyrazinamide for 31, and ethambutol for 38. The negative predictive value (NPV) ELISpot was 62% for rifampicin, 77% for isoniazid, 80% for pyrazinamide and 79% ethambutol respectively and positive predictive values (PPV) 100% for rifampicin, isoniazid, and pyrazinamide (figure 2-4). Due to lower numbers of SJS/TEN cases, no stratification was done based on SCAR phenotype. No difference was seen in NPV and PPV of IFN-γ ELISpot assay for each of the four FLTD when DRESS phenotype was stratified into RegiSCAR groups of possible, probable, or definite. It is acknowledged however that with our smaller samples sizes we are currently underpowered to detect this and also that RegiSCAR is a cross-sectional measurement tool to phenotype DRESS and is not validated or useful for causality or severity assessment.

Acute sampling and lower cut-point to improve sensitivity of rifampicin IFN-γ ELISPOT assay

If the threshold for positive IFN-γ ELISpot is reduced to SFU ≥20, the NPV for rifampicin increased to 70%, 86% isoniazid, 86% pyrazinamide and 83% ethambutol (DRESS and SJS/TEN combined) for any time of sampling with PPV maintained at 100% (figure 2-4). The average value of SFUs in background control wells was 0-7 for the cases with <50 to ≥20 SFU/million cells. Eight patients (Six DRESS and two SJS/TEN) of the 18 patients who experienced positive reactions to rifampicin on SDC had rifampicin ELISpot results ≥50 SFU/million cells (figure 2-4). Seven of these patients were single reactors, HIV-infected, not on ART or TMP-SMX at the time of SCAR and with low median CD4 cell count of 101 cells/mm3. Of the ten patients with positive SDC to rifampicin but negative rifampicin ELISpot ≥50 SFU/million cells, three had SFU/million cells of greater than 20, five were single reactors and five multiple reactors. In contrast to the six patients with rifampicin ELISpot results ≥50 SFU, half of this group were HIV positive with median CD4 count of 170 cells/mm3. The NPV of rifampicin ELISpot increased to 67% when only samples acquired during the first 12 weeks from SCAR onset were included (figure 2-4). Positive predictive value for these samples was maintained at 100%.

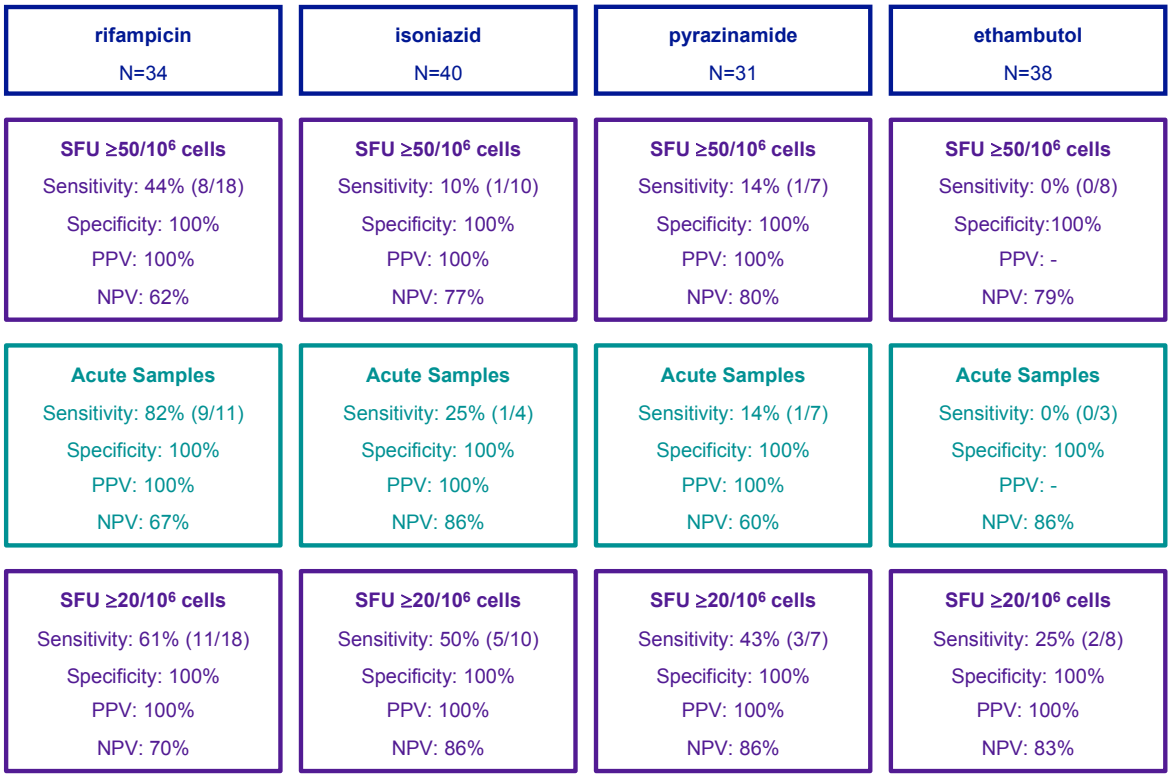

Figure 2-4: FLTD sensitivity and specificity compared to gold standard SDC.
Acute samples - ≤12 weeks from SCAR onset. PPV - positive predictive value, NPV - negative predictive value, SFU - spot forming unit, N – number of samples

2.4. Discussion

A high burden of life-threatening SCAR leading to treatment interruptions occurs amongst vulnerable persons living with HIV. In HIV/TB endemic settings, FLTD are common offending agents (Lehloenya et al. 2021a; Lehloenya et al. 2020a; Lehloenya et al. 2020b). Rapidly identifying the offending drug and reintroducing effective anti-TB therapy, as well as other important drugs such as TMP-SMX and ART can be lifesaving in advanced immunosuppression. This is the largest study to examine the utility and optimisation of *in vitro* IFN-γ ELISpot assay to aid the identification of the offending drug and characterisation of FLTD-associated SCAR. The major findings of our study were that several strategies could improve the NPV of IFN-γ ELISpot for FLTD, including: i) the use of fresh rather than -80°C freezer cryopreserved PBMCs, ii) acute sampling (≤12 weeks post-acute SCAR admission) and iii) a lowered SFU cut-point for assay positive to SFU≥20/million cells for rifampicin. Even when applying optimisation strategies such as use of acute samples, IFN-γ ELISpot NPV was less than 100% for SCAR to FLTD. Both DRESS and SJS/TEN phenotypes were included in this study, with a predominance of DRESS cases (86%). The small number of SJS/TEN cases in this cohort limits meaningful comparison between phenotypes. Unlike in other published studies where there is an increased sensitivity of IFN-γ ELISpot seen in DRESS with other drugs, these differences could not be investigated in our cohort (Polak et al. 2013).

We optimised the highest non-cytotoxic drug concentrations for stimulation in our rifampicin, isoniazid (Copaescu, Choshi, et al. 2021), pyrazinamide and ethambutol ELISpot assays, and we also showed that use of fresh rather than -80°C freezer cryopreserved samples improved drug-specific IFN-γ producing cells with rifampicin and isoniazid stimulation. Our findings are consistent with other studies that reported ELISpot sensitivity increases with use of acute samples in the early stage after DRESS onset (Polak et al. 2013). The reduced ELISpot positivity using cryopreserved cells may relate to cell viability after storage in -80°C freezers versus liquid nitrogen. The comparison between fresh and liquid nitrogen cryopreserved samples may be less significant, however -80°C freezer capacity is more widely available than liquid nitrogen facilities in LMICs (Mendy et al. 2014; De Oliveira et al. 2018). Use of an increased number of cells, which we hypothesised may be required in the context of HIV and CD4 T cell depletion, increases non-antigen specific responses and did not improve assay positivity. In contrast, adjustment of the threshold of SFUs (to ≥20 SFU/million cells) for a positive assay significantly improved NPV in the rifampicin INF-γ ELISpot, without compromising PPV. In some studies, the threshold of positivity is defined by measuring the frequency of antigen specific INF-γ producing cells in drug tolerant controls (Rozieres, Hennino, et al. 2009), setting the positivity threshold at twice the average value of background spots (Wang et al. 2007) and based on the distribution of negative controls (Keane et al. 2014; Keane et al. 2012). In our results, the mean of the background wells ranged from 0–7 SFU/million cells. With an optimised number of cells

to stimulate and incubation period, non-antigen specific responses are limited and a lower limit threshold of 20 drug specific IFN-γ producing cells, an ELISpot for rifampicin can be considered positive (Streeck, Frahm, and Walker 2009). Diagnostic accuracy was also not compromised in patients with reactions to multiple FLTD or second-line anti-TB drugs, which is reassuring. In one patient with reactions to all FLTD, IFN-γ ELISpot was borderline positive for all FLTD, while in the other rifampicin IFN-γ ELISpot was 0 SFU/million cells; the significance of these results on underlying mechanism of these reactions – whether "flare-ups" or multiple drug hypersensitivity remains under further investigations.

Rifampicin is a cornerstone potent and important first-line treatment for drug-susceptible TB. Rifampicin containing regimens are superior to those not containing rifampicin with sterilising activity allowing 6 months treatment duration (Grobbelaar et al. 2019; Hoosen et al. 2019). Immune-mediated adverse drug reactions, including SCAR, drug-induced liver injury and acute interstitial nephritis are major treatment-limiting side effects of rifampicin (Tan et al. 2007; Jin et al. 2021). In this and other South African cohorts of SCAR, rifampicin is the commonest of the four FLTD to cause SCAR (Lehloenya et al. 2011; Lehloenya and Dheda 2012). Strategies, such as optimised rifampicin IFN-γ ELISpot, could be an important adjunctive tool that adds to a clinical risk assessment that negates a need for SDC, and allowing the fast-tracked reintroduction of the other three FLTD, offers major clinical utility. The large number of FLTD-associated SCAR cases examined in our study compared to previous literature has enabled us to present the optimised NPV, sensitivity and excellent specificity and PPV, further supporting the use of rifampicin IFN-γ ELISpot (Copaescu, Choshi, et al. 2021). Further studies are now required to confirm these findings in other high HIV TB burden settings and increase the NPV to 100% where this assay can be used as a sole diagnostic test.

Limitations include the low number of SJS/TEN phenotype cases thus preventing comparison of the diagnostic use of IFN-γ ELISpot across SCAR phenotypes. The time points of sampling were limited due to the inclusion of retrospective cases as well as prospective sampling. The ability to achieve consistent sequential sampling at all key time points would have strengthened this study, but the complex clinical management makes this difficult to achieve. Furthermore, follow-up data, particularly regarding the role of ART initiation on IFN-γ ELISpot assay findings would have been a valuable addition.

The high HIV prevalence and concomitant use of ART and prophylactic TMP-SMX seen in this study highlights the complexity of FLTD-associated SCAR in an HIV endemic setting. We have also described a considerable occurrence of multiple-drug reactions (over 25% of FLTD drug SDC reactors and majority DRESS 70%). Multiple drug reactivity is a complex phenomenon and its

pathophysiology ill-understood (Lehloenya, Wallace, et al. 2012). This complicated environment limits the utility of the current gold standard of SDC, with particular reference to the variation in reaction phenotypes seen on SDC in multiple drugs reacting patients and the likelihood of non-specific and transient immune response that could be safely treated through. The frequent lack of drug specific IFN-γ producing T cells to FLTD in many of these cases may support this approach, although other factors may influence ELISpot performance and further laboratory optimisation is required.

Chapter 3 – Investigating genetic risk factors associated with FLTD-SCAR

3.1. Introduction

The distinct role of genetic factors pivotal to the mechanisms of SCAR have been discussed in the general introduction of this study (chapter 1). The current proposed mechanistic models to explain the recognition of drugs by T cells and the ability of T cells to initiate an immune response, include HLA-molecules (Peter et al. 2017). Most identified polymorphisms and strongest associations have been found within the class I region with an excess of 8000 variants (Kennedy, Ozbek, and Dorak 2017). The binding specificity of each HLA-I molecule depends on the components of the antigen processing pathway and peptide amino acid anchor residues favoured by particular HLA alleles. The binding affinity for these anchor residues is dictated by pockets A,B,C,D,E and F within the peptide binding groove of HLA class I molecules (figure 3-1) (van Deutekom and Keşmir 2015).

There are now several HLA class I associations with specific drug-SCAR pairings. HLA alleles and haplotypes vary in prevalence amongst different populations, based on the evolutionary pressures of infectious diseases and human migrations. Thus, there is a pressing need to study different Africa populations, each of which have distinct patterns of evolutionary influences that have driven the diversity of HLA alleles represented. This is relevant to HLA risk alleles for specific relevant drug-SCAR combinations. To-date there have been very few of these studies in African populations. Furthermore, discoveries of HLA risk have varied substantially in their scientific and translational impact, because of variable positive and negative predictive values (PPV, NPV) and the background prevalence of specific HLA risk alleles in different populations. In HIV-infected patients, the only clear implementation success story has been the association between HLA-B*57:01 and abacavir hypersensitivity (AHS) (Mallal, Phillips, Carosi, Molina, Workman, Tomazic, Jagel-Guedes, et al. 2008; Manson, Swen, and Guchelaar 2020) which has led to guideline-based universal pre-prescription screening for HLA-B*57:01 before abacavir use in the developed world.

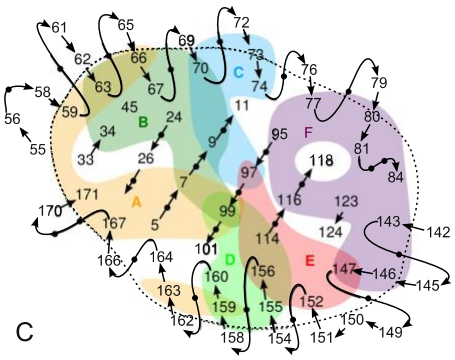

Figure 3-1: Schematic overview of the peptide binding groove.

Schematic overview of the binding groove showing amino acids positions that make up each pocket. As defined in HLA-A2. *Adapted from (van Deutekom and Keşmir 2015).*

For drugs prevalently used in the treatment of TB and HIV and its complications, such as rifampin and other first-line anti-TB drugs, there have been no studies defining HLA associations in SCAR. An association between nevirapine SJS/TEN and HLA-C*04:01 has been identified in a Malawian population and confirmed by our group in a South African population (Carr et al. 2013; Pavlos et al. 2017) Konvinse et al, Peter et al (unpublished). The NPV for HLA-C*04:01 and nevirapine SJS/TEN appears to be close to 100% in South African populations and to-date HLA-C*04:01 has not been associated with another IM-ADR outside of NVP SCAR (Pavlos et al. 2017). However, the PPV is only 2.5%, meaning this HLA allele appears necessary but not sufficient for developing SJS/TEN. This is similar to most other IM-ADR (Watanabe et al. 2017; Mallal, Phillips, Carosi, Molina, Workman, Tomazic, Jägel-Guedes, et al. 2008). This suggests that other genetic and ecologic factors must be important in the development of IM-ADRs.

Factors outside of HLA have also been found to be associated with SJS/TEN in heterogenous populations. For instance, a study including both Southeast Asian and East Asian participants, found that a poor metabolizing genotype CYP2C9*3 had the strongest association with phenytoin associated SJS/TEN, DRESS and maculopapular eruption.(Chung et al. 2014). A study by Pavlos et al looking at the new genetic predictors for abacavir tolerance in HLA-B*57:01 positive individuals predicted abacavir tolerant individuals tend to have hypoactive trimming ERAP1 allotypes and proposed ERAP1 may influence the repertoire of peptides available for presentation to T cells in the presence of abacavir (Pavlos et al. 2020). The importance of KIR in the development of IM-ADRs has not been well-defined. However, the increased expression of KIR2DL2 and KIR2DL3 subtypes on circulating T cells in SJS/TEN and the interaction of cognate HLA ligand with causative drugs which may potentially affect interactions with KIR warrants further investigation with case-control association studies – as KIRs are highly important in the regulation of cytotoxic NK and T cells responses implicated in the development of SCAR (Duong et al. 2017). Discovery of new HLA associations and non-HLA genetic associations could provide effective strategies for the prevention, diagnosis and mechanistic understanding of factors that are necessary for the development of IM-ADRs in HIV-infected African populations.

3.2. Materials and Methods

3.2.1. Patient and control participants matching, recruitment and enrolment.

For HLA association studies, 41 FLTD SCAR patients who were SDC and reacted to one or more FLTD and/or if the offending drug was identified by exclusion (successful rechallenge to all other drugs) were included. A total of 142 matched drug tolerant controls who consented to genetic testing were selected from three cohorts - IMARI registry (*n=6*), PredART cohort (*n=72*) (Meintjes et al. 2018) and TB drug resistance study (*n=64*) (Rockwood et al. 2017). All drug tolerant controls were sampled one time with all clinical data collected at baseline. The second control group consisted of 192 healthy participants in HLA studies from the electricity supply commission (ESKOM) cohort, in which 142 Black Africans (Loubser et al. 2020) and 50 South African Mixed Ancestry (Loubser, Paximadis, and Tiemessen 2017) were recruited. There was representation of participants of black Africans and South African Mixed Ancestry (SAM) background among the SCAR patients, drug tolerant controls, and referenced general healthy participants studies residing in South Africa. Black Africans form the largest ethnic group in South Africa, making up 80.2% of the population. Fourteen (34%) FLTD SCAR cases were of SAM, which account for 8.8% of the South African population. Drug tolerant controls were matched with cases on an average of 2:1 based on sex, age +/-5 years and CD4 count for HIV infected patients (0-100, 100-200 and >200 cells/mm^3).

3.2.2. Saliva collection, Oragene DNA kits

Saliva was collected into Oragene DNA OG-500 kit (DNAgenotek) according to manufacturer user instructions. Saliva samples were stored at room temperature until DNA extraction.

3.2.3. DNA isolation

DNA was extracted from saliva using the prepIT.L2P protocol developed by Oragene DNA kits manufacturer. DNA was extracted from blood for PredART cohort (*n=72*) (Meintjes et al. 2018) and TB drug resistance study (*n=64*) (Rockwood et al. 2017) using the QIAamp DNA blood mini and midi kits (Qiagen), following the manufacturer's protocols. The NanoDrop 2000 spectrophotometer (Thermo Scientific) or BioDrop were used to measure DNA concentrations and purity. TE buffer was used as the reference sample (blank). Samples were stored at -20°C until HLA high resolution genotyping and other sequencing.

3.2.4. HLA Genotyping

DNA extracted and purified from saliva and blood samples was sent to the institute for immunology and infectious diseases (IIID) at Murdoch University for HLA typing. HLA testing at IIID has been accredited by the American Society for Histocompatibility and Immunogenetics (ASHI) and the National Association of Testing Authorities (NATA). Specific HLA loci on the extracted DNA were

PCR amplified using sample specific molecular indexed primers (MID- tagged) that amplify polymorphic exons from Class I (A, B, C Exons 2 and 3) and Class II (DQ, Exons 2 and 3; DRB and DPB1, Exon 1) HLA genes. MID tagged primers have been optimised to minimize allele dropouts and primer bias. Amplified DNA products from unique MID tagged products were pooled in equimolar ratios and subjected to library preparation. Post QC and quantitation the normalised libraries were then sequenced on the Illumina MiSeq platform using the MiSeq V3 600-cycle kit (2X300bp reads). Sequences were separated by MID tags and alleles called using an in-house accredited HLA allele caller software pipeline that minimises the influence of sequencing errors. Alleles were called using the latest IMGT HLA allele database as the allele reference library. Sample to report integrity was tracked and checked using proprietary and accredited Laboratory Information and Management System (LIMS) and HLA analyse reporting software that performs comprehensive allele balance and contamination checks on the final dataset

3.2.5. Full allelic KIR genotyping

Uniquely indexed primers were designed to target KIR exons 3, 4 and 5, (D0, D1 and D2 Domain). Primer mixes were prepared containing 2-4 primers per amplicon to cover all KIR genes in a multiplexed assay with an amplicon size ~400 bp. The primers chosen have been adapted and refined from published literature (Lebedeva et al. 2007). Five separate PCR reactions were setup for each sample to cover all target exons. In a 96 well plate, there was 12.5µl volume with GoTaq DNA Polymerase (Promega) and the associated buffer system. As each sample was uniquely indexed during the PCR reactions, all amplicons from the PCR reactions were pooled using volumes appropriate to obtain balanced read coverage for each KIR exon. Each pool was then ligated with unique Illumina indexes and sequencing adapters ready for Illumina sequencing. The products were sequenced on the Miseq using 600V3 chemistry. Post sequencing, quality filtered paired reads were demultiplexed based on unique molecular sequence for each sample and each set of overlapping paired reads were merged based on the Q30 scores leading to a single read with a median read length of up to 500bps spanning the full amplicon. Since these amplicons span across the full exon, the SNPs within the exon are phased. These reads were then aligned to a reference sequence containing all KIR genes using CLCbio genomics workbench. Following alignment, using an inhouse developed application All Class the reads were moved to the correct gene by comparing each mapped read to the reference gene dataset generated from IMGTKIR database; reads that didn't map to any reference sequence data and reads mapping below the defined minimum cut off were discarded. Multi mapped reads were extracted and reassigned based on set defined rules based on KIR haplotypes and heterozygosity and final assignments were reported as igroups http://www.iiid.com.au/s/iiid_KIR_iGroups_v2100.xlsx. This entire workflow has been validated for precision, accuracy and specificity using the reference IWHG cell lines with known KIR alleles.

3.2.6. ERAP sequencing

DNA from multiple samples were processed using massively parallel sequence-based typing where, 10 PCR primers pairs were utilised to amplify targeted regions which contain 17 SNPs for ERAP1 and 2 SNPs for ERAP2. Amplified DNA products from unique MID (molecular sample index) tagged products were pooled in equimolar ratios and subjected to library preparation. Post QC and quantitation the normalised libraries were then sequenced on the Illumina MiSeq platform using the MiSeq V3 600-cycle kit (2X300bp reads). Post sequencing, sequences were separated by unique MID tags and aligned using CLCbio genomics workbench. Sequence visualising and analysis tool VGAS was then used for identification and reporting of the specific SNP variants and haplotypes.

3.2.7. Statistical analysis

Categorical variables were compared between cases and control participants using the Fisher's exact tests (suitable for small sample size) or chi-squared test, and continuous data (reported as median, with interquartile ranges given in parentheses) were compared with use of t tests or Mann Whitney tests depending on normalcy. A *P* value of <0.05 was considered statistically significant. For abacavir hypersensitivity, HLA-B*57:01 and carbamazepine SJS/TEN HLA-B*15:02, respectively, odds ratios of >500 meant that less than 10 cases would have been needed to show a highly statistically significant association. For this reason and from our experience with ERAP and nevirapine we expected to be able to detect highly significant associations for each of our target drugs in African ancestry. We had the benefit of matching at least 2:1 drug tolerant controls to cases to account for high samples sizes needed when the HLA allele is highly represented in a population for a moderate effect size (figure 3-2). Specific HLA allele frequencies for patients with FLTD induced SCAR were compared with FLTD tolerant controls and the general population using a multivariate logistic regression model to ascertain independent associations and examine differential effects on FLTD SCAR risk of HLA class I alleles and allele clusters based on HLA supertypes (Sidney et al. 2008; Lund et al. 2004), binding pocket structure and peptide binding groups assigned from MHCcluster binding specificities (Rasmussen et al. 2014; Thomsen et al. 2013). Although we performed multiple comparison correction using Bonferroni methods, due to the small numbers in this study, our analysis and discussion took both P values into consideration. The strength of association was estimated by calculating the odds ratio and 95% confidence interval (CI). Odds ratios were calculated with Haldane's modification, which adds 0.5 to all cells to accommodate possible zero counts (Haldane 1956). Odds ratios represent the estimated odds of SCAR development amongst cases carrying the identified risk allele/cluster relative to tolerant controls. Analysis of class I peptide binding pockets (A-F) were identified as in Sidney et al. (Sidney et al. 2008). Minor allele frequencies for genes outside of the MHC (MAF) were taken from national library of medicine SNP database (https://www.ncbi.nlm.nih.gov/snp/) or allele frequency net (http://www.allelefrequencies.net).

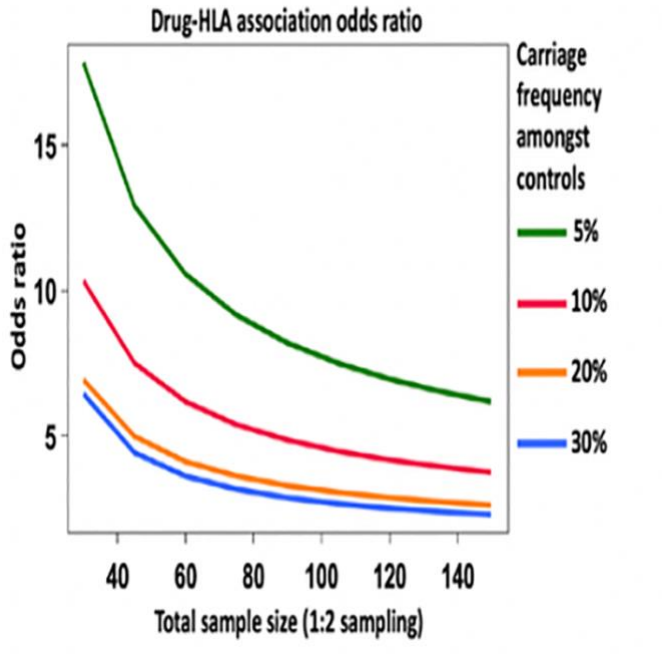

Figure 3-2: Sample size calculations for HLA analyses

Sample size needed is dependent on the carriage frequency of the HLA allele in the population and the effect size (odds ratio) of the association.

3.3. Results

3.3.1. Characteristics of patients and drug tolerant controls

The demographics, clinical characteristics, and HLA class I alleles of the 41 HLA-typed cases with FLTD SCAR are summarized in Table 3-1. A total of 142 TB patients who had been on FLTD for at least 8 weeks and 12 weeks for patients receiving FLTD along with TMP-SMX with no adverse events were used as the drug-tolerant controls. Of the enrolled patients with FLTD SCAR, 29 (76%) were Black Africans and 9 (24%) were of South African Mixed ancestry group. The median (IQR) age was 38 years (30-46 years), and majority of the patients (63%) were female. The onset of symptoms for all patients was within 29 days (12-42 days) of FLTD exposure. Thirty-one patients (76%) were HIV TB co-infected at the time of major reaction with a median CD4 count of 117 (50-160 cells/μL). A total of 24 patients (59%) were on multiple drug regimen including FLTD, ART (*n=17*) and TMP-SMX (*n=18*). Eleven patients were on both ART and TMP-SMX. TMP-SMX use was more prevalent amongst drug-tolerant controls than SCAR cases (73% versus 44%, P=0.0004). The difference can be explained by the fact that controls were selected from prospective cohort studies amongst advanced HIV-infected patients where TMP-SMX prescription was protocol specified in comparison to cases where routine practices may have varied. All patients received FLTD for TB treatment and 5 (10%) cases had a previous TB episode – and did not report any adverse events on previous exposure to FLTD (Table 3-2). Chronic diseases including hypertension, systemic lupus erythematous (SLE), diabetes, asthma, epilepsy, and additional opportunistic infections were absent or present at very low frequencies in the two groups (Table 3-3).

SCAR cases were from the prospective IMARI registry, and decision about SDC and omission of inclusion of specific FLTD post SCAR was dependent on the clinic management team. All HLA-typed cases were SDC, and 33 patients had a reaction to one (66%) or multiple (34%) FLTD on SDC. Due to high clinical suspicion of the culprit agent, 8 cases were not SDC on all FLTD and had a single (38%) or multiple (62%) FLTD excluded based on clinical review. Overall, 27 of 41 (66%) were single drug reactors and 14 of 41 (34%) were multiple drug reactors. Rifampicin accounted for more than half (59%) of all single drug reactions, followed by pyrazinamide (22%) and the common multiple drug combination was rifampicin and pyrazinamide in 3 of 14 (21%) multiple reactors. RegiSCAR scores for DRESS patients (*n=35*) were 4 to 7 in 25/35 (43% definite and 29% probable) and <4 in 10/34 (29% possible DRESS). Patients with SJS/TEN (*n=6*) were also scored and 50% were probable SJS/TEN, 17% definite SJS and 33% definite TEN. Excluding TMP-SMX exposure, there were no significant differences in demographic or laboratory parameters between the FLTD SCAR cases and the FLTD tolerant controls (Table 3-2).

Table 3-1: Characteristics of patients with FLTD induced SCAR and Class I HLA

Case ID	Age (yr)	Sex at Birth	CD4 Count	Phenotype	Latency	Highest Naranjo Scoring Drugs	HLA-A Allele 1	HLA-A Allele 2	HLA-B Allele 1	HLA-B Allele 2	HLA-C Allele 1	HLA-C Allele 2
Group 1 rifampicin was identified as the single offending drug by SDC or exclusion, patients were back on other three FLTD and had rifampicin ELISpot ≥20 SFU/million cells												
10001	35	Male	101	Probable DRESS	28	rifampicin	03:01:01	32:01:01	44:03:01	81:01:01	02:10:01	04:01:01
10020	33	Male	-	Probable DRESS	15	rifampicin	24:10:01	29:02:01	18:02	44:04	07:04:01	16:01:01
10024	40	Female	117	Probable SJS/TEN	52	rifampicin	23:01:01	34:02:01	44:03:01	58:02:01	04:01:01	06:02:01
10037	59	Male	-	Definite DRESS	47	rifampicin	03:01:01	32:01:01	15:01:01	18:01:01	02:02:02	03:03:01
10085	42	Female	-	Definite DRESS	39	rifampicin/ rifabutin	02:01:01	68:02:01	15:10:01	44:03:02	03:04:02	07:01:01
10092	38	Male	121	Possible DRESS	13	rifampicin	02:01:01	34:02:01	44:03:01	45:01:01	04:01:01	16:01:01
10188	34	Female	-	Definite DRESS	24	rifampicin	03:01:01	32:01:01	15:01:01	15:03:01	02:10:01	04:01:01
10225	54	Female	93	Possible DRESS	24	rifampicin	29:02:01	29:02:01	15:03:01	44:03:02	02:10:01	07:01:01
10278	30	Female	142	Possible DRESS	46	rifampicin	02:01:01	43:01:01	15:16:01	44:03:01	02:10:01	16:01:01
10322	26	Female	26	Possible DRESS	10	rifampicin	02:14:01	30:01:01	15:03:01	44:03:01	02:10:01	04:01:01
Group 2 patients reacting to rifampicin and other FLTD, rifampicin was amongst the highest Naranjo scoring drugs and rifampicin ELISpot ≥20 SFU/million cells												
10002	37	Male	72	Possible DRESS	71	rifampicin/ pyrazinamide/ ABC/ 3TC/EFV	34:02:01	43:01	15:10:01	44:03:01	04:01:01	04:01:01
10028	30	Female	-	Probable SJS/TEN	13	rifampicin/ isoniazid/ pyrazinamide/ ethambutol	30:02:01	74:01:01	42:02:01	45:01:01	16:01:01	17:01:01
10128	31	Female	170	Definite DRESS	59	rifampicin/ ethambutol	34:02:01	43:01:01	15:03:01	44:03:01	04:01:01	18:01:01
10145	15	Female	-	Probable DRESS	32	rifampicin/ isoniazid/ ethambutol	25:01:01	32:01:01	07:02:01	15:01:01	02:10:01	03:03:01
Group 3 includes all SCAR patients with reactions to rifampicin and additional FLTD, rifampicin was among the highest Naranjo scoring drugs irrespective of ELISpot result												
10032	38	Female	457	Definite DRESS	14	rifampicin	02:05:01	30:02:01	45:01:01	58:01:01	07:01:01	16:01:01
10034	39	Male	223	Definite DRESS	27	TMP-SMX/ rifampicin/ pyrazinamide	03:01:01	23:01:01	07:02:01	58:02:01	02:10:01	06:02:01
10049	56	Female	-	Probable DRESS	44	rifampicin/ isoniazid/ ethambutol	01:01:01	11:01:01	15:05:01	57:01:01	03:03:01	06:02:01
10068	23	Female	-	Probable DRESS	25	rifampicin	30:01:01	74:01:01	42:02:01	53:01:01	04:01:01	17:01:01
10105	36	Female	142	Definite DRESS	176	rifampicin/isoniazid	30:02:01	36:01:01	53:01:01	53:01:01	04:01:01	04:01:01
10137	46	Male	141	Definite DRESS	35	isoniazid/ ethambutol/ Rifamycin	29:02:01	68:02:01	44:03:02	53:01:01	04:01:01	07:01:01
10167	41	Male	162	Probable DRESS	34	pyrazinamide, isoniazid	03:01:01	29:02:01	08:01:01	15:03:01	02:10:01	07:02:01
10182	33	Female	19	Possible DRESS	48	Rifampicin/ TMP-SMX	30:01:01	34:02:01	42:01:01	44:03:01	04:01:01	17:01:01
10191	52	Male	23	Possible DRESS	31	levofloxacin/ linezolid/ rifampicin	01:01:01	68:02:01	14:01:01	81:01:01	08:02:01	18:01:01

10197	51	Female	-	Probable DRESS	30	rifampicin	01:03:01	33:01:01			17:01:01	17:01:01
10198	43	Male	111	Possible DRESS	6	rifampicin/ isoniazid/ pyrazinamide	02:05:01	66:01:01	15:10:01	58:02:01	06:02:01	08:04:01
Other FLTD SCAR cases												
10011	28	Male	5	Probable DRESS	40	isoniazid	02:05:01	29:01:01	07:05:01	58:01:01	07:01:01	07:02:01
10014	45	Male	90	Probable SJS/TEN	49	isoniazid	03:01:02	30:01:01	42:01:01	44:03:01	14:03:01	17:01:01
10018	24	Female	63	Definite TEN	15	pyrazinamide	30:02:01	68:02:01	07:02:01	07:02:01	07:02:01	07:02:01
10030	48	Female	-	Definite TEN, SLE	13	isoniazid/ pyrazinamide	02:05:01	43:01	27:05:02	44:03:01	02:10:06	07:01:01
10036	50	Female	388	Definite SJS	9	pyrazinamide	02:01:01	23:01:01	13:02:01	45:01:01	06:02:01	16:01:01
10041	45	Male	39	Definite DRESS	18	pyrazinamide	24:02:01	34:02:01	07:02:01	08:01:01	07:01:01	07:02:01
10042	35	Male	58	Definite DRESS	15	isoniazid	30:02:01	33:01:01	42:01:01	45:01:01	16:01:01	17:01:01
10044	29	Female	112	Probable DRESS	18	ethambutol	02:01:01	68:02:01	15:03:01	35:01:01	02:10:01	04:01:01
10051	26	Female	5	Definite DRESS	26	pyrazinamide/ ethambutol	30:01:01	30:02:01	08:01:01	42:02:01	07:01:01	17:01:01
10071	26	Female	158	Definite DRESS	28	pyrazinamide	32:01:01	68:01:01	58:01:01	58:02:01	06:02:01	06:02:01
10100	30	Female	137	Possible DRESS	25	isoniazid	01:01:01	68:02:01	57:02:01	58:01:01	07:01:01	07:01:01
10104	47	Female	576	Definite DRESS	12	pyrazinamide	01:03:01	74:01:01	15:03:01	15:03:01	02:10:01	04:01:01
10119	42	Male	177	Definite DRESS	84	pyrazinamide/ ethambutol	30:01:01	33:03:01	42:01:01	53:01:01	04:01:01	17:01:01
10121	55	Female	41	Possible DRESS	16	pyrazinamide	03:01:01	30:04:01	35:02:01	81:01:01	04:01:01	08:04:01
10162	37	Female	21	Definite DRESS	109	ethambutol/ rifabutin	29:02:01	74:01:01	15:03:01	58:01:01	02:10:01	03:02:01
10165	53	Female	82	Probable DRESS	48	pyrazinamide/ ethambutol/ TMP-SMX	11:01:01	34:02:01	35:01:01	44:03:01	04:01:01	04:01:01

DRESS – drug reaction with eosinophilia and systemic symptoms, SJS/TEN – Stevens Johnson syndrome and toxic epidermal necrolysis, ETH – ethionamide, TMP-SMX – trimethoprim-sulfamethoxazole, LNZ – linezolid, Moxi- moxifloxacin, RHZE – Rifafour (fixed drug combination), EFV – efavirenz, 3TC - lamivudine, ABC – abacavir

Table 3-2: Demographic variables, drug exposure details of FLTD SCAR patients and tolerant controls

Characteristic	FLTD SCAR *(n=41)*	Drug tolerant controls *(n=142)*	*P value*
Sex, n (%)			
Female	26 (63)	84 (61)	1.0000
Male	15 (37)	54 (39)	
Age, median (range), yrs.	38 (30-46)	38 (32-45)	0.8122
Drug exposure, median (range), days			
FLTD Duration	29 (12-42) days	≥8-12 weeks	-
Additional medication history, n (%)			
HIV+	31 (76)	118 (86)	0.0791
CD4 count, median (range)	117 (50-160)	90 (49-170)	0.8500
ART at major reaction/ sampling	17 (41)	83 (60)	0.0993
TMP-SMX at major reaction/ sampling	18 (44)	101 (73)	0.0004
TB	41 (100)	138 (100)	-
Previous TB episode	5 (12)	7/68 (10)*	0.5965
Additional bacterial and fungal infections	4 (10)	4/68 (10)*	0.8546

*Information not available for PredART controls

FLTD – first line anti-tuberculosis drugs, SCAR – severe cutaneous adverse reactions, ART – anti-retroviral therapy, TB – tuberculosis, n – number of participants

Numbers in parenthesis indicate percentage

Table 3-3: Summary of FLTD SCAR patients' clinical characteristics

Non-TB/HIV co-morbidities, n (%)	
SLE	1 (2)
Hypertension	1 (2)
Diabetes	1 (2)
Asthma	1 (2)
Epilepsy	2 (5)
Drug reaction, n (%)	
DRESS	35 (85)
Definite DRESS	15 (43)
Probable DRESS	10 (29)
Possible DRESS	10 (29)
SJS/TEN	6 (15)
Probable SJS/TEN	3 (50)
Definite SJS	1 (17)
Definite TEN	2 (33)
Offending drugs, n (%)	
Single drug reactors	27 (66)
rifampicin	16 (59)
isoniazid	4 (15)
pyrazinamide	5 (19)
ethambutol	1 (4)
Multiple drug	14 (34)
Rifampicin + pyrazinamide	3 (21)

SLE – systemic lupus erythematous, DRESS – drug reaction with eosinophilia and systemic symptoms, SJS/TEN – Stevens Johnson syndrome/toxic epidermal necrolysis, n – number of participants

Numbers in parenthesis indicate percentage

3.3.2. HLA associations with rifampicin-induced SCAR

SCAR cases were grouped and analysed by offending drug, and whether they reacted to one or multiple FLTD. In addition, rifampicin-associated SCAR cases were further divided based on a positive or negative ELISpot that demonstrated *in vitro* evidence of drug-specific T cells, making potential HLA-associations more likely (see chapter 2 for details of ELISpot optimisation and results for all FLTD) (Porter et al. 2022) . Cases in rifampicin-SCAR HLA studies were divided into three groups. In **group 1** rifampicin was identified as the single offending drug by SDC or exclusion, patients were back on other three FLTD and had rifampicin ELISpot ≥20 SFU/million cells. In **group 2** patients reacting to rifampicin and other FLTD, rifampicin was amongst the highest Naranjo scoring drugs and rifampicin ELISpot (≥20 SFU/million cells were added to patients in group 1. **Group 3** includes all SCAR patients with reactions to rifampicin and additional FLTD, rifampicin was among the highest Naranjo scoring drugs irrespective of ELISpot result. As shown in Table 3-4, HLA-B*44:03 was present in 7 of 10 (70%) patients compared to 5 of 41 (12%) group 1 matched tolerant controls (odds ratio: 16.8; 95% CI: 3.2-87, P=0.0008) and 19 of 192 (10%) of the general healthy population (odds ratio: 21.2; 95% CI: 5.1-89.1; P<0.0001). In group 2, HLA-B*44:03 was present in 9 of 14 (64%) patients but only 5 of 54 (9%) tolerant controls (odds ratio: 17.6; 95% CI: 4.2-73.6, P=0.0001) and 10% of the general population controls (odds ratio: 16.4; 95% CI: 6.5-54; P<0.0001). The odds decreased when patients (*n=11*) with a negative rifampicin ELISpot (≤20 SFU/million cells) were added (Table 3-4). After adjusting for HLA-B*44:03 carriage, HLA-B*15:01was the second significant allele carried by 3 cases with rifampicin positive ELISpot and zero controls (P= 0.0005) (figure 3-3). Notably, all three cases were HIV negative (Table 3-1). Table 3-4 shows odds ratio for HLA-B*15:01 in group 1(odds ratio: 24.4; 95% CI: 1.1-555.5, P=0.0451 and general healthy population (odds ratio: 7.8; 95% CI: 1.3-44.6; P=0.0218); group 2, (odds ratio: 33.2; 95% CI: 1.6-687.1, P=0.0235) and the general population controls (odds ratio: 8.5; 95% CI: 1.9-34.4; P=0.0057).

Guided by four patients with ³20 SFU/million cells and non-carriage of HLA-B*44:03 in group 2, we used MHCcluster (which groups HLA molecules into supertypes according to their peptide-binding specificity) to examine similarities between their identified alleles (HLA-B*15:01, -*15:03, -*18:01, -*18:02 -*42:02, -*44:04 and -*45:01) and HLA-B*44:03. We found two HLA-B supertypes associated with the development of rifampicin-SCAR (figure 3-4). HLA-B*44:03 was grouped together with HLA-B*18:01 and -*45:01 as part of the HLA-B44 superfamily. HLA-B44 alleles occurred at significantly increased frequencies in rifampicin SCAR patients (90% group 1 and 86% group 2) compared to 37% in tolerant controls (group 1 odds ratio: 15.6; 95% CI: 1.8-135.48; P=0.0127 and group 2 odds ratio: 10.2; 95% CI: 2.1-50.3; P=0.0043) (Table 3-4). However, the effect significantly decreased when ELISpot negative rifampicin SCAR cases and matched tolerant controls were added (group 3 odds ratio: 3.3; 95% CI: 1.3-8.1; P=0.0112). HLA-B 44 supertype was

influenced by the presence of HLA-B*44:03 (*n=12 alleles*) followed by HLA-B*45:01 (*n=3 alleles*) irrespective of groups (Table 3-3). HLA-B62 supertype was identified as the second significantly increased supertype present in 11% of cases compared to 0% in matched tolerant controls (figure 3-3). And the HLA-B62 association was significantly influenced by HLA-B*15:01 (*n=3 alleles*). We analysed the allele distribution of the combined HLA loci to define the haplotypes using in house software, Coby Gram. The HLA-A*34:02, -*44:03, C*04:01 haplotype was present in 4 of 14 (29%) patients with ELISpot positive rifampicin–SCAR and 1 of 54 (2%) tolerant controls (odds ratio: 21.2; 95% CI: 2.1-210.0; P=0.0090). This significant association was confirmed with linear regression in Coby Gram (figure 3-5). Although we had a small sample size to further divide rifampicin SCAR cases, there was no significant differences in all analysis with further grouping according to SCAR phenotype and race. Figure 3-6 shows frequencies of HLA-A and HLA-C class I alleles in rifampicin ELISpot positive SCAR and matched tolerant controls. After Bonferroni correction, we did not observe any significant differences in the frequencies of HLA-A and HLA-C alleles in cases versus tolerant controls.

Table 3-4: Frequencies of individual or combined loci of HLA-B*44:03/04 extended haplotype in patients with FLTD-induced SCAR, FLTD tolerant controls, and general population controls

Genotype	Group	RIF SCAR	RIF Tolerant controls	Odds ratio (95% CI)	*P value*	General population control[1,2] *n=192*	Odds ratio (95% CI)	*P value*
HLA-B*44:03	1	7/10 (70)	5/41 (12)	16.8 (3.2-87)	**0.0008**	19/192 (10)	21.2 (5.1-89.1)	**<0.0001**
	2	9/14 (64)	5/54 (9)	17.6 (4.2-73.6)	**0.0001**		16.4 (5-54)	**<0.0001**
	3	11/25 (44)	9/92 (10)	7.2 (2.5-20.7)	**0.0002**		7.2 (2.8-18)	**<0.0001**
HLA-B44 Supertype	1	9/10 (90)	15/41 (37)	15.6 (1.8-135.5)	0.0127	60/192 (31)	19.8 (2.5-159.8)	0.0051
	2	12/14 (86)	20/54 (37)	10.2 (2.1-50.3)	**0.0043**		13.2 (2.9-60.8)	**0.0009**
	3	15/25 (60)	29/92 (32)	3.3 (1.3-8.1)	0.0112		3.3 (1.4-7.8)	0.0063
HLA-B*15:01	1	2/10 (20)	0/41 (0)	24.4 (1.1-555.5)	0.0451	6/192 (3)	7.8 (1.3-44.6)	0.0218
	2	3/14 (21)	0/54 (0)	33.2 (1.6-687.1)	0.0235		8.5 (1.9-34.4)	0.0057

Numbers in parenthesis indicate percentage

Group 1 - rifampicin was identified as the single offending drug by SDC or exclusion, patients were back on other three FLTD and had rifampicin ELISpot ≥20 SFU/million cells.

Group 2 - patients reacting to rifampicin and other FLTD and rifampicin ELISpot ≥20 SFU/million cells were added to patients in group 1.

Group 3 – patients reacting to rifampicin and other FLTD and rifampicin ELISpot <20 SFU/million cells (ELISpot negative) were added to patients in group 2.

RIF – rifampicin, SCAR – severe cutaneous adverse reactions, CI- confidence interval, n – number of participants. The Bonferroni corrected P value for multiple comparisons Pc=0.004.

[1]Loubser, S., M. Paximadis, N. L. Gentle, A. Puren, and C. T. Tiemessen. 2020. 'Human leukocyte antigen class I (A, B, C) and class II (DPB1, DQB1, DRB1) allele and haplotype variation in Black South African individuals', *Hum Immunol*, 81: 6-7.

[2]Loubser, S., M. Paximadis, and C. T. Tiemessen. 2017. 'Human leukocyte antigen class I (A, B and C) allele and haplotype variation in a South African Mixed ancestry population', *Hum Immunol*, 78: 399-400.

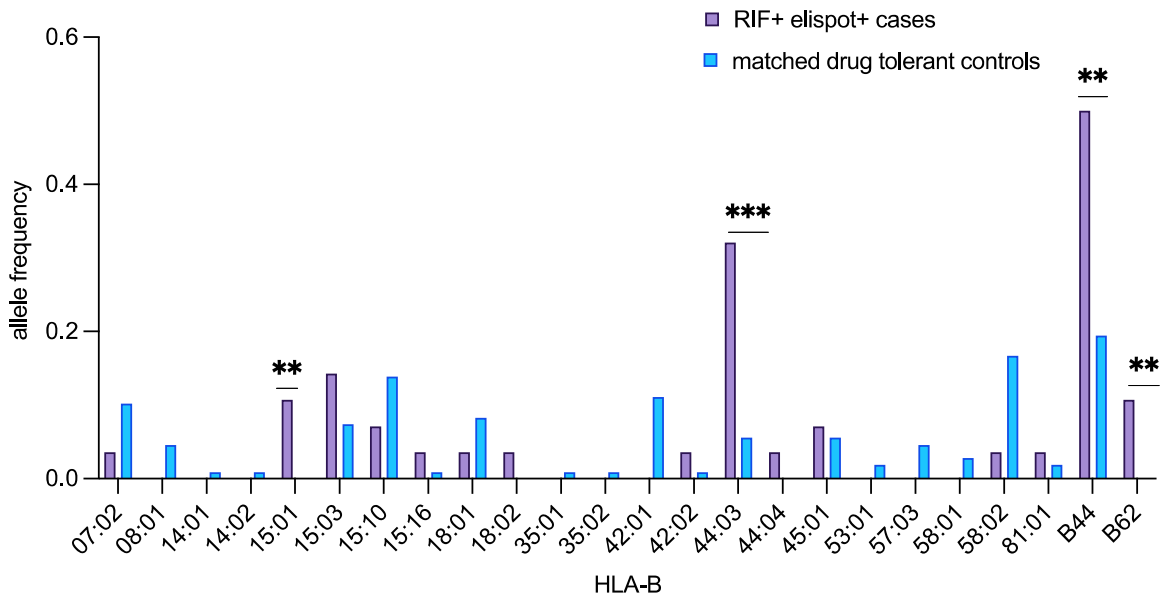

Figure 3-3: Frequencies of HLA-B alleles present in ELISpot+ rifampicin SCAR cases and matched drug tolerant controls.

Allele frequencies among group 1 and 2 cases (*n=14*) and controls (*n=54*). HLA-B*44:03 was strongly associated with rifampicin SCAR with an allele frequency of 0.321 compared to 0.056 in matched FLTD tolerant controls (P=0.0001, chi-squared test). Adjusted for HLA-B*44:03 carriage, HLA-B15:01 was another allele strongly associated with rifampicin SCAR – present in 3 of 4 (75%) rifampicin-SCAR cases and 0 of 10 matched FLTD tolerant controls (P= 0.0005, chi-squared test). Analysis is restricted to immunologically confirmed cases (ELISpot ≥20 SFU/million cells). Significant P value was set at <0.05 after Bonferroni correction for multiple comparisons (Pc=0.002). Allele frequency = (alleles/2n). RIF – rifampicin, SDC+ - sequential drug challenge positive, ELISpot+ - ELISpot positive. *B44 and *B62 here refers to the B44 and B62 supertypes respectively (Sidney et al. 2008).

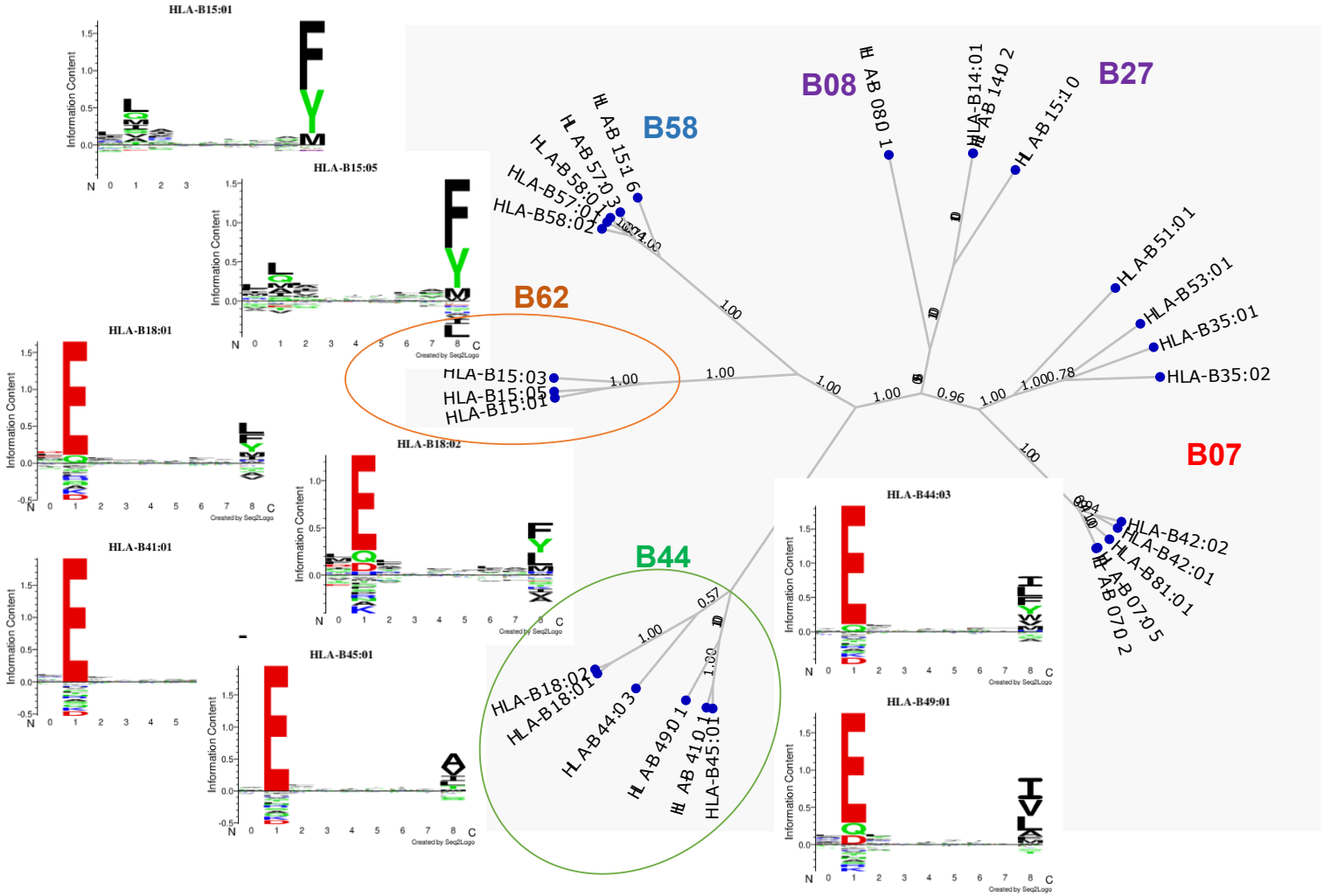

Figure 3-4: HLA-B MHCcluster and identified HLA-B supertypes

The distance tree shows sequence logos for shared predicted peptide binding sequences. HLA-B risk alleles for FLTD induced SCAR (HLA-B*44:03/04, -*45:01 and -*18:02) which belong to HLA-B44 and HLA-B62 supertypes (Sidney et al. 2008) are shown in green and orange circle respectively.

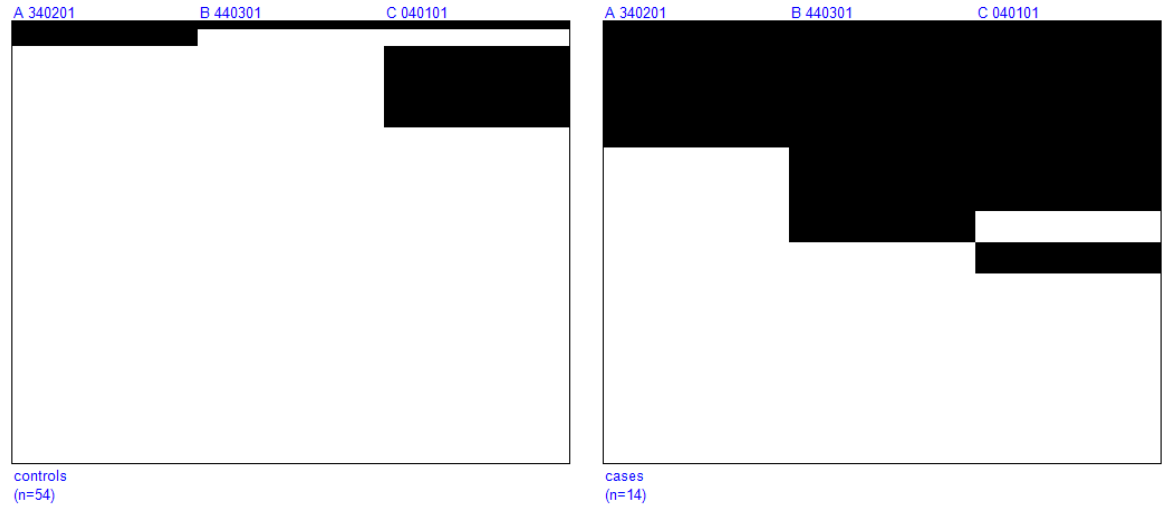

Allele(s)	Coefficient	Standard Error	Wald p-Value	Likelihood Ratio p-Value	Odds Ratio
A 340201	-36.4878519	157,016,496.698	0.9998	0.2246952	0.0000000
B 440301	40.1767314	157,016,496.698	0.9998	0.0001583	280,887,707,975,562,000.0000000
C 040101	-0.3807725	1.1362469	0.7375389	0.7283987	0.6833333

Figure 3-5: HLA class I haplotypes in rifampicin ELISpot positive SCAR cases and matched tolerant controls using Coby Gram

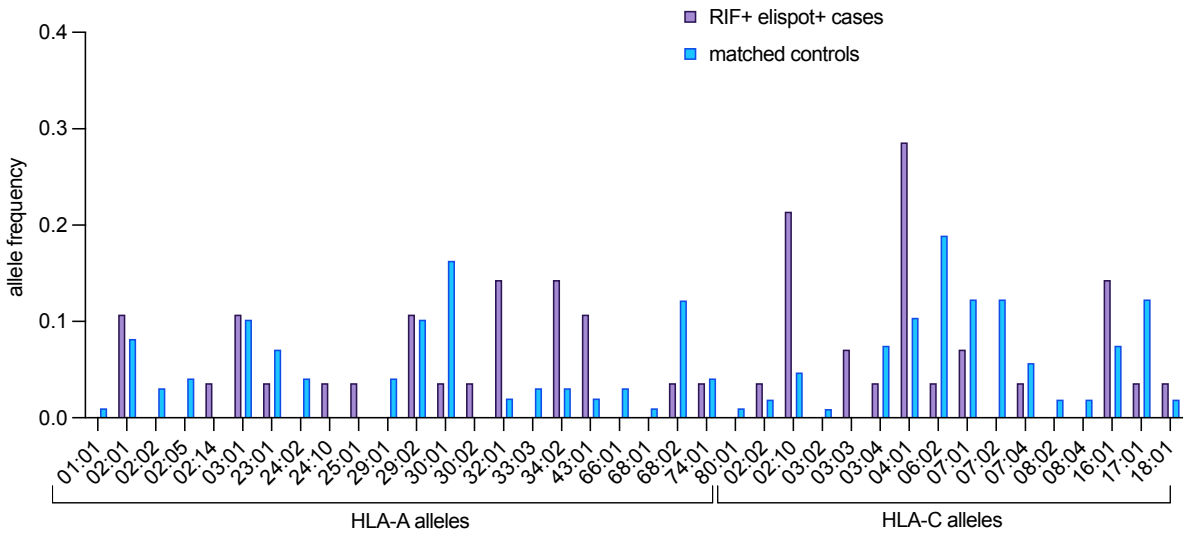

Figure 3-6: Frequencies of HLA-A and HLA-C alleles present in ELISpot+ rifampicin SCAR cases and matched drug tolerant controls.

3.3.3. Specificity of rifampicin T cell responses and binding to HLA-B alleles

We examined the functional capacity of allotypes HLA-B*44:03, -*44:04, -*45:01 and -*15:01 and how it differs from other HLA-B alleles in the cohort. We were also testing the differences in rifampicin specific responses according to risk allele status. We performed IFN-g ELISpot assay on all prospectively and retrospectively enrolled patients and drug tolerant controls with stored PBMCs. There were 9 drug tolerant controls recruited in the IMARI registry with stored PBMCs to investigate drug responses in comparison to participants with FLTD-SCAR in specific immunologic studies. Of the 25 rifampicin-SCAR cases, 14 (56%) had an IFN-g ELISpot response >=20 SFU/million cells compared to 0 of 9 (0%) drug tolerant controls (P=0.0032). ELISpot positivity was 10 of 14 (71%) among patients carrying HLA-B*44:03/04. Only one drug tolerant control carried HLA-B*44:03. In samples with sufficient cell numbers, PBMCs were routinely tested against all FLTD, and concurrently administered medications potentially implicated in development SCAR – such as TMP-SMX). Two HLA-B*44:03 patients with negative rifampicin ELISpot had >=20 SFU/million cells to isoniazid 50ug/ml and 4-Nitro-sulfamethoxazole 10ug/ml (major TMP-SMX metabolite) respectively – and these drugs had the highest Naranjo scores along with rifampicin.

After adjusting for HLA-B44:03/04 carriage, 1 of 2 (50%) patients carrying HLA-B*45:01 had a positive ELISpot. The negative ELISpot in the second patient could be explained by blood collection 5 years post rifampicin SCAR onset. The last three rifampicin ELISpot positive cases carried HLA-B*15:01 (figure 3-7A). ELISpot positivity was 12 of 14 (86%) among patients carrying one or more allele that belongs to the HLA-B44 supertype (Table 3-4) and compared to patients carrying other HLA-B alleles, there was a significant difference in the SFU with a P value of 0.0020 (figure 3-7A). After adjusting for HLA-B*44:03, -*44:04, -*45:01 and -*15:01 carriage, the remaining eight cases carried the following alleles, HLA-B*14:01, 81:01, 42:02, 53:01,08:01, 15:03, 07:02, 58:02, 15:10, 15:05 and 57:01 which did not activate rifampicin-specific T cells (figure 3-7B). One of the eight patients carried the HLA-B allele combination 15:05 and 57:01. Interestingly, HLA-B*15:05 has a similar peptide binding motif as HLA-B*15:01 (figure 3-9). The negative ELISpot results in this case, could also be attributed to blood collection 2-year post rifampicin-SCAR (Table 3-5). Using CD4 count as a measure immune status and HIV progression, we did not observe any significant differences between ELISpot positive and negative patients stratified by HLA-B allele (Table 3-5).

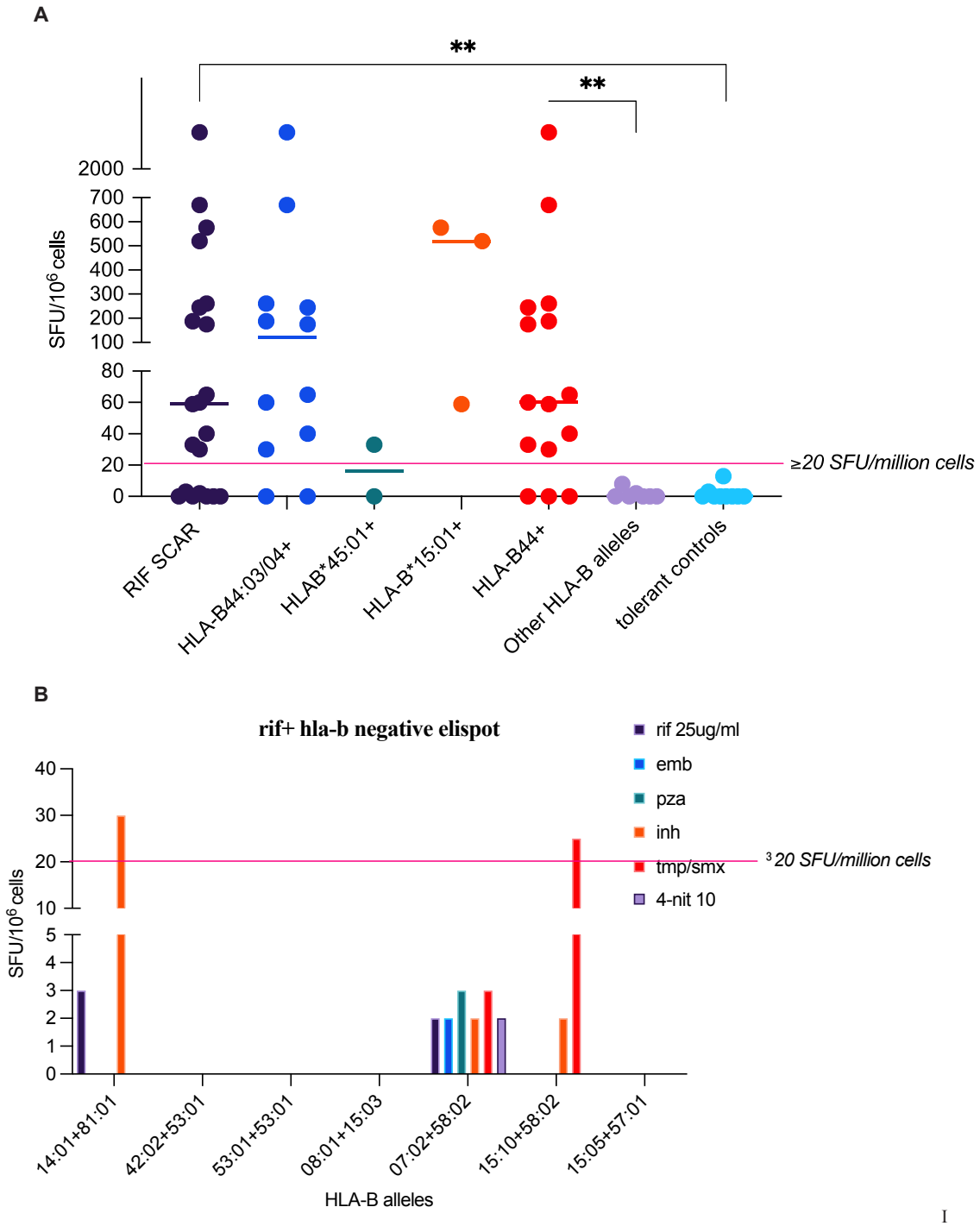

I

Figure 3-7: IFN-γ ELISpot responses in RIF SCAR cases stratified by HLA risk allele carrier status

A) IFN-y ELISpot responses in rifampicin SCAR (RIF SCAR) cases (*n=25*) and tolerant controls (*n=9*) after stimulation with 25ug/ml of rifampicin results. There were significant differences between cases and controls (P=0.0020, t-test). Rifampicin SCAR cases were stratified by HLA risk allele carriage. The risk allele carriage in tolerant controls was *n= 1* HLA-B44:03, *n=2* HLA-B45:01, *n= 2* HLA-B*18:01. There was no carriage of HLA-B*15:01 tolerant controls with stored PBMCs. Means of replicates are plotted. In patients with blood collected at different at time points, the highest ELISpot results are plotted. Spot forming units (SFU) per million cells above 20 after the removal of background (unstimulated cells) were considered positive (positive ELISpot threshold indicated by pink line). **B)** In samples with sufficient cell numbers, PBMCs were routinely tested against all FLTD. Results of these other tested drugs for rifampicin cases with negative rifampicin ELISpot – patients identified by HLA-B alleles on the x-axis.

Table 3-5: ELISpot results stratified by HLA-B allele and HIV status

HLA-B allele	ELISpot positive	HIV positive (if ELISpot positive)	Median CD4 count	ELISpot negative/SDC positive	HIV positive (if ELISpot negative)	Median CD4 count
B44:03/04	10	9	101	2	2	80
B45:01	1	0	-	1	1	457
B44	11	9	101	3	3	141
B15:01/05	3	0	-	1	0	-
Other HLA-B alleles	0	0	-	7	6	127

3.3.4. Models of Rifampicin docking onto risk HLA B alleles (with peptide)

The chemical structure of three mycobactericidal rifamycin are shown in figure 3-8A. Rifampicin ($C_3H_{58}N_4O_{12}$) is a polyketide belonging to a chemical class of compounds termed ansamycins, named for the heterocyclic structure containing a naphthoquinone core spanned by an aliphatic ansa chain; it is a relatively large, small-molecule drug with a molar mass of 822.95 g/mol^{-1}. Given the relatively large size of the small molecule rifampicin and the putative risk alleles HLA-B*44:03 and -B*15:01, we applied molecular docking (CD-Dock2 – cavity detection guided blind docking) to determine potential binding sites for rifampicin. CB-Dock predicts binding sites of a submitted protein and performs docking with a popular docking program, AutoDock Vina (Watanabe et al. 2017). We carried out docking of rifampicin ligand (National Center for Biotechnology Information (2023). PubChem Compound Summary for CID 135398735, Rifampicin. Retrieved June 5, 2023 from https://pubchem.ncbi.nlm.nih.gov/compound/Rifampicin) with HLA-B*44:03 (PDB ID: 3DX7) and HLA-B*1501 (PDB ID: 6UZP) peptide complexes.

The docking model showed rifampicin interacting at the highest vina score to HLA-B*4403-peptide complex (-7.1 Kcal/mol) and HLA-B*1501-peptide complex (-8.3 Kcal/mol) (figure 3-8D-E) at conserved positions responsible for overall structural stability. These include positions 6, 8, 27, 98, 102 and 113 located in the β-sheet floor of the binding groove or in α-1 and α-2 domains contacting the β-sheet floor (figure 3-8B-C) (Haliloglu, Gul, and Erman 2010; Serçinoğlu and Ozbek 2020). The model also showed rifampicin interacting via hydrogen bonds with residues ARG48, ALA49, PRO50, TRP51, residues that are in close vicinity to position 45, 63 and 67 which contribute to antigen specificity of the peptide binding B-pocket (figure 3-8D-E).

Thus, in the subsequent analyses we have considered both drug-pMHC models. Initially we considered the possibility of direct interaction with peptides and hence examine shared-binding specificities between the group of risk B alleles noted in our rifampicin SCAR cases compared to controls, focused on key amino acid positions that determine differential peptide-binding specificity. Linked to this we have explored whether known polymorphisms in endoplasmic reticulin aminopeptidase 1 and 2 – important enzymes in peptide trimming and hence peptide repertoires – improve predictive value of these class I risk alleles. Subsequently, we explore whether risk alleles potentially sort or interact with other pMHC complexing machinery, in particular the relationship between risk alleles and tapasin dependency.

A

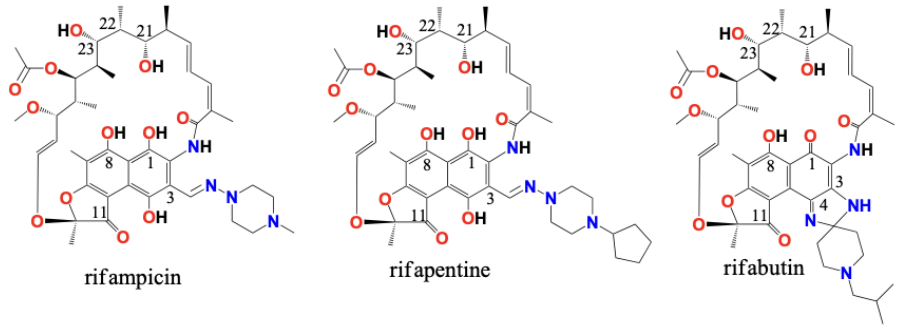

Scheme 1. Exemplary structures of known and used in antibacterial and antitubercular therapy *ansa*-macrolides – semisynthetic derivatives of 3-formylrifamycin SV.

B

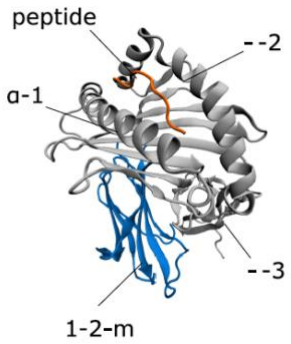

C

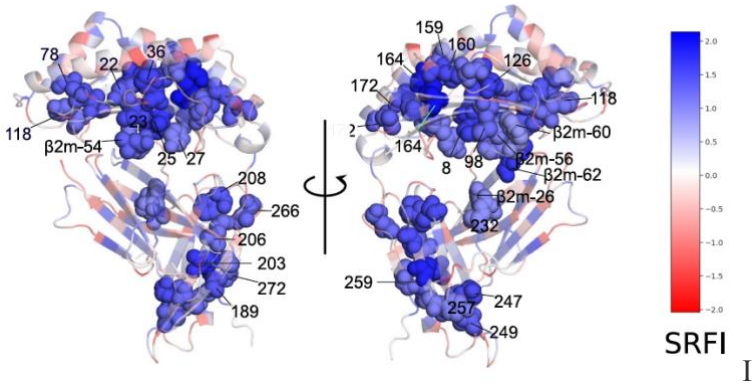

I

D

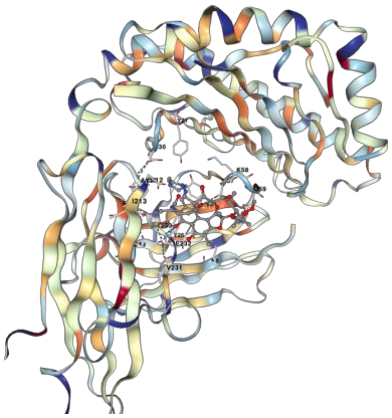

HLA-B*44:03

CurPocket ID: C1
Cavity volume (Å^3): 3850
Vina score: -7.1
Contact residues:
Chain A: TYR27 ASP30 ALA211 GLU212 ILE213 VAL231 GLU232 THR233 PHE241 LYS243
Chain B: LYS6 TYR26 SER57 LYS58 ASP59 TYR63

E

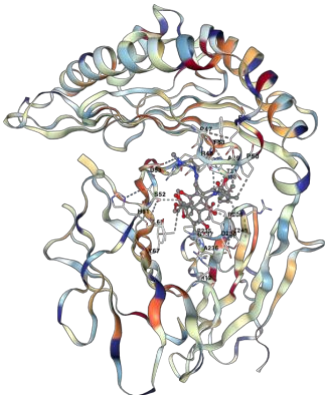

HLA-B*15:01

CurPocket ID: C1
Cavity volume (Å^3): 1820
Vina score: -8.3
Contact residues:
Chain A: ASP30 THR31 GLN32 PHE33 ARG48 ALA49 PRO50 TRP51 THR178 PRO235 GLY237 ASP238 ARG239
Chain B: ARG12 PHE22 GLU50 SER52 ASP53 LEU65 TYR67

Figure 3-8: Models of rifampicin docking onto risk HLA B alleles (with peptide)

A) Exemplary structures of rifamycin. Three-dimensional structure of pMHC (**B**) and conserved positions within the HLA structure **(C).** Adapted from (Czerwonka et al. 2016) and (Serçinoğlu and Ozbek 2020)CB-Dock results for HLA-B*44:03 **(D)** and *15:01 **(E).**

3.3.4. The effects of individual amino acids in the peptide binding groove

HLA-class I alleles typically interact with two amino acids in the peptide chain – amino acid 2 and 9 which corresponds to pocket B and F as locations of anchor residues. The type of sidechain bound by each pocket depends upon the class I allotype, more specifically on the residues at positions of polymorphism that line the pockets. The size, shape and polarities of pockets determine the peptide sidechains they bind. We therefore asked whether similarities exist between binding specificities for the identified HLA-B risk alleles (HLA-B44 and -B62 supertypes) (figure 3-4). We used IMGT/HLA database (http://www.ebi.ac.uk/ipd/imgt/hla) to determine the characteristic motifs across pockets A-F which makes the peptide binding groove of class I molecule (figure 3-1).

We found that the association with HLA-B*44:03 and other B44 and B62-associated polymorphisms, may be explained by commonality in certain critical B-pocket residues such as position 67 (figure 3-9A). The position 67 forms part of the HLA-B peptide-binding groove, located in the B pocket, which anchors the side peptide position 2 whose specificity is also influenced by the residues at polymorphic amino acid positions 9, 45 and 63 of the class I heavy chain. HLA-B44 and B62-associated polymorphisms were also grouped by commonality of residues 7Tyr 22Phe 34Val 66Ile 70Thr 99Tyr of the anchor B pocket. These alleles also differed at several B pocket positions Tyr9His Thr24Ser/Ala Lys45Thr/Met Glu63Asn (figure 3-9A). This polymorphic position 67 carries as many as five different amino-acid residues in the cohort, differing in charge and polarity (figure 3-9C), and each conferring different degree of risk (or protection) to rifampicin SCAR, consistent with the analysis of HLA-B allele frequencies (figure3-3). Serine, a neutral polar amino acid, at position 67 (predominantly found in HLA-B44 alleles) was increased in rifampicin SCAR patients than tolerant controls ($P<0.0001$); and phenylalanine, a neutral non-polar amino acid (found in HLA-B53 alleles), was found increased in tolerant controls than rifampicin SCAR cases ($P=0.0032$). Amino acid position 45 of HLA-B alleles and the type of amino acid seemed to support and strengthen signals at position 67.

Most alleles in the HLA-B44 supertype share a preference for peptides with negatively charged glutamic acid (Glu, E) at anchor position 2 and polar and hydrophobic residues at the C terminus (Marsh, Parham, and Barber 1999). Alleles most prevalent in the drug tolerant group (HLA-B*42:01, -*57:03 and *58:02) (figure 3-3) differ from the HLA-B44 alleles by three amino acids (45E, 63N, 67Y – HLA-B*42:01) and two amino acids (45M/T, 67M – HLA-B*57:03, -*58:02) in the B pocket (figure 3-9A). The difference in position 67 and the similarities between HLA-B44 alleles and HLA-B*15:01 at position 67 suggests rifampicin specificity is particularly sensitive to the B-pocket architecture, namely residue 67. In the B pocket of the characteristic motif HLA-B*44:03 the positively charged polar lysine at position 45 is reported to select peptides having negatively charged glutamic acid at position 2 (Madden 1995). The difference in HLA-B44 residues at position 45 shows

the environment of the B pocket and its ability to accommodate glutamic acid at P2 depends on all residues in polymorphic positions. Therefore position 67 may not the only be key residue forming the B-pocket anchor site for rifampicin, the amino acid substitutions positions 45 and 63, could also influence recognition of rifampicin. In particular, the presence of T at position 45 in HLA-B*18:01/02, in common with HLA-B*58:02 potentially explains the slight increase in the frequency of HLA-B*18:01 in controls and that although it shares similarities with HLA-B44:03, in our cohort, its association with rifampicin-SCAR is dependent on HLA-B*44:03 and HLA-B15:01 carriage (Table 3-1). In addition, Ser67 could be the most probable site where rifampicin may be influencing the B pocket, especially for HLA-B*15:01 since it differentiates it from HLA-B57:03 (Met67). However, the interaction could also be controlled by neighbouring residues including substitution with a neutrally charged Met45 in HLA-B15:01 which counter charge the negative charge - while the presence of Glu45 in HLA-B*42:01, in combination with varied residues at position 67 (figure 3-9A) completely blocks the binding of glutamic acid in the B pocket. In our AutoDock modelling, we observed rifampicin interactions with residues in close vicinity to these polymorphic positions for HLA-B*44:03 and HLA-B*15:01 (figure 3-8D-E).

A

	B pocket residues								
HLA-B alleles	7	9	22	24	34	45	63	66	67	70	99
B*44:03:01:01	**Y**	**Y**	**F**	**T**	**V**	**K**	**E**	**I**	**S**	**T**	**Y**
B*18:01:01:01	.	H	.	S	.	T	N	.	.	.	.
B*18:02:01	.	H	.	S	.	T	N	.	.	.	.
B*41:02:01:01	.	H	.	.	.	.	.	.	.	.	.
B*45:01:01:01	.	H	.	.	.	.	.	.	.	.	.
B*49:01:01:01	.	H	.	.	.	.	.	.	.	.	.
B*15:01:01:01	.	.	.	A	.	M	.	.	.	.	.
B*15:03:01:01	.	.	.	S	.	E	.	.	.	.	.
B*15:05:01:01	.	.	.	A	.	M	.	.	.	.	.
B*15:16:01:01	.	.	.	A	.	M	.	N	M	F	.
B*57:01:01:01	.	.	.	A	.	M	.	N	M	S	.
B*57:03:01:01	.	.	.	A	.	M	.	N	M	F	.
B*58:01:01:01	.	.	.	A	.	T	.	N	M	S	.
B*58:02:01:01	.	.	.	A	.	T	.	N	M	S	.
B*08:01:01:01	.	S	.	S	.	E	N	.	.	.	.
B*14:01:01:01	.	.	.	S	.	E	N	.	C	.	.
B*14:02:01:01	.	.	.	S	.	E	N	.	C	.	.
B*15:10:01:01	.	.	.	S	.	E	N	.	C	.	.
B*35:01:01:01	.	.	.	A	.	T	N	.	.	.	.
B*35:02:01:01	.	.	.	A	.	T	N	.	.	.	.
B*51:01:01:01	.	.	.	A	.	T	N	.	.	.	.
B*53:01:01:01	.	.	.	A	.	T	N	.	F	.	.
B*07:02:01:01	.	.	.	S	.	E	N	.	Y	Q	.
B*07:05:01:01	.	.	.	S	.	E	N	.	Y	Q	.
B*42:01:01:01	.	.	.	S	.	E	N	.	Y	Q	.
B*42:02:01:01	.	H	.	S	.	E	N	.	Y	Q	.
B*81:01:01:01	.	.	.	S	.	E	N	.	Y	Q	.

	F pocket residues												
74	77	80	81	84	95	97	114	116	123	133	143	146	147
Y	N	T	A	Y	I	R	D	D	Y	W	T	K	W
.	S	N	L	.	L	.	.	S	.	.	.	.	.
.	S	N	L	.	L	M	.	S	.	.	.	.	.
.	S	N	L	.	L	S	N	Y	.	.	.	.	.
.	S	N	L	.	W	.	N	L	W	.	.	.	.
.	.	I	.	.	W	.	N	L	.	.	.	.	.
.	S	N	L	.	L	.	.	S	.	.	.	.	.
.	S	N	L	.	L	.	.	S	.	.	.	.	.
.	S	N	L	.	L	.	.	S	.	.	.	.	.
.	.	I	.	.	W	.	.	S	.	.	.	.	.
.	.	I	.	.	.	V	.	S	.	.	.	.	.
.	.	I	.	.	.	V	N	Y	.	.	.	.	.
.	.	I	.	.	.	.	.	S	.	.	.	.	.
.	.	I	.	.	L	W	.	S	.	.	.	.	.
D	S	N	R	.	L	S	N	Y	.	.	.	.	.
D	S	N	L	.	L	W	N	F	.	.	.	.	.
D	S	N	L	.	L	W	N	F	.	.	.	.	.
.	S	N	L	.	L	.	.	Y	.	.	.	.	.
.	S	N	L	.	.	.	.	S	.	.	.	.	.
.	S	N	L	.	.	.	N	Y	.	.	.	.	.
.	.	I	.	.	W	T	N	Y	.	.	.	.	.
.	.	I	.	.	.	.	.	S	.	.	.	.	.
D	S	N	L	.	L	S	.	Y	.	.	.	.	.
D	S	N	R	.	L	S	N	Y	.	.	.	.	.
D	S	N	L	.	L	S	N	Y	.	.	.	.	.
D	S	N	L	.	L	S	N	Y	.	.	.	.	.
D	S	N	L	.	L	S	N	Y	.	.	.	.	L

B

	A pocket									C pocket					D pocket							E pocket				
HLA-B alleles	5	7	59	63	66	99	159	163	167	171	9	70	73	74	97	99	113	114	155	156	159	160	97	114	147	152	156
B*44:03:01:01	**M**	**Y**	**Y**	**E**	**I**	**Y**	**Y**	**L**	**S**	**Y**	**Y**	**N**	**T**	**Y**	**R**	**Y**	**Y**	**D**	**Q**	**L**	**Y**	**L**	**R**	**D**	**W**	**V**	**L**
B*18:01:01:01	.	.	.	N	.	.	.	T	W	H	H	.	.	.	.	.	H	.	.	.	.	.	.	.	.	.	.
B*18:02:01	.	.	.	N	.	.	.	T	W	H	H	.	.	.	M	.	H	.	.	.	.	.	M	.	.	.	.
B*41:02:01:01	.	.	.	.	.	.	E	W	.		H	.	.	.	R	.	H	N	.	.	.	.	R	N	.	.	.
B*45:01:01:01	.	.	.	.	.	.	.	.	.	.	H	.	.	.	.	.	.	N	.	D	.	.	.	N	.	.	D
B*49:01:01:01	.	.	.	.	.	.	.	W	.		H	.	.	.	.	.	.	N	.	.	.	.	.	N	.	E	.
B*15:01:01:01	.	.	.	.	.	.	.	W	.		.	.	.	.	.	.	H	.	.	W	.	.	.	.	.	E	W
B*15:03:01:01	.	.	.	.	.	.	.	W	.		.	.	.	.	.	.	H	.	.	.	.	.	.	.	.	E	.
B*15:05:01:01	.	.	.	.	.	.	.	W	.		.	.	.	.	.	.	H	.	.	.	.	.	.	.	.	.	.
B*15:16:01:01	.	.	.	.	N	.	.	W	.		.	S	.	.	.	.	H	.	.	.	.	.	.	.	.	E	.
B*57:01:01:01	.	.	.	.	N	.	.	W	.		.	S	.	.	V	.	H	.	.	.	.	.	V	.	.	.	.
B*57:03:01:01	.	.	.	.	N	.	.	W	.		.	S	.	.	V	.	H	N	.	.	.	.	V	N	.	.	.
B*58:01:01:01	.	.	.	.	N	.	.	W	.		.	S	.	.	.	.	H	.	.	.	.	.	.	.	.	.	.
B*58:02:01:01	.	.	.	.	N	.	.	W	.		.	S	.	.	W	.	H	.	.	.	.	.	W	.	.	.	.
B*08:01:01:01	.	.	.	N	.	.	.	T	W	.	D	.	.	D	S	.	H	N	.	D	.	.	S	N	.	.	D
B*14:01:01:01	.	.	.	N	.	.	.	T	W	H	.	.	.	D	W	.	.	N	.	.	.	.	S	N	.	E	.
B*14:02:01:01	.	.	.	N	.	.	.	T	W	H	.	.	.	D	W	.	.	N	.	.	.	.	W	N	.	E	.
B*15:10:01:01	.	.	.	N	.	.	.	.	W	.	.	.	.	.	.	.	H	.	.	.	.	.	.	.	.	E	.
B*35:01:01:01	.	.	.	N	.	.	.	.	W	.	.	.	.	.	.	.	H	.	.	.	.	.	.	.	.	.	.
B*35:02:01:01	.	.	.	N	.	.	.	.	W	.	.	.	.	.	.	.	H	N	.	.	.	.	.	N	.	.	.
B*51:01:01:01	.	.	.	N	.	.	.	.	W	H	.	.	.	.	T	.	H	N	.	.	.	.	T	N	E	.	.
B*53:01:01:01	.	.	.	N	.	.	.	.	W	.	.	.	.	.	.	.	H	.	.	.	.	.	.	.	.	.	.
B*07:02:01:01	.	.	.	N	.	.	.	E	W	.	.	Q	.	D	S	.	H	.	.	R	.	.	S	.	.	E	R
B*07:05:01:01	.	.	.	N	.	.	.	E	W	.	.	Q	.	D	S	.	H	N	.	R	.	.	S	N	.	E	R
B*42:01:01:01	.	.	.	N	.	.	.	T	W	.	.	Q	.	D	S	.	H	N	.	D	.	.	S	N	.	.	D
B*42:02:01:01	.	.	.	N	.	.	.	T	W	.	H	Q	.	D	S	.	.	N	.	D	.	.	S	N	.	.	D
B*81:01:01:01	.	.	.	N	.	.	.	E	W	.	.	Q	.	D	S	.	H	N	.	.	.	.	S	N	L	.	.

C

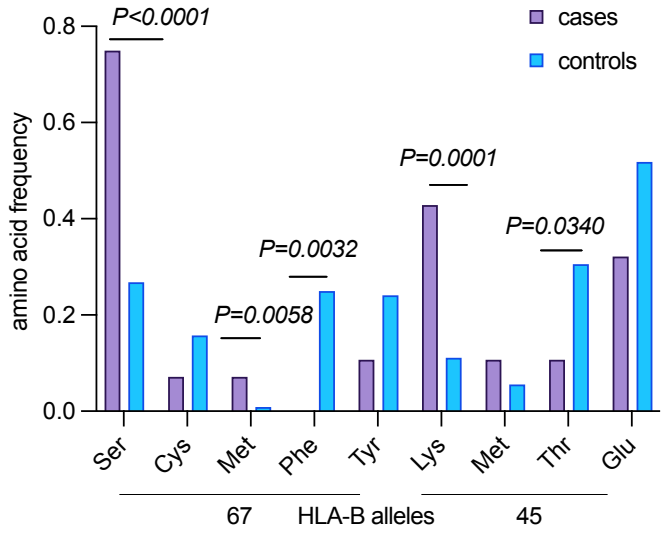

D

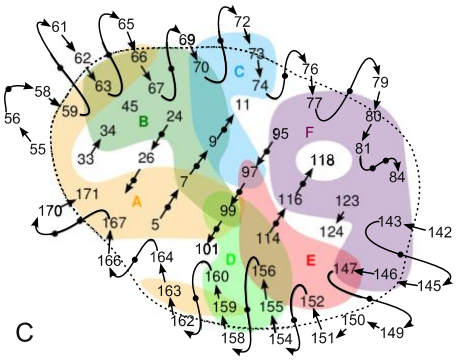

Figure 3-9: HLA-B alleles frequencies and binding pockets associated with rifampicin induced SCAR

A) Alignment of HLA-B B and F pocket sequences. Yellow highlighted positions show polymorphic key residues that confer specificity and peptide preference for HLA-B allotypes. In bold font is the sequence of HLA-B*44:03 rifampicin SCAR risk allele. **B)** Alignment of HLA-B A, C, D and E pocket sequences. **C)** Amino-acid residue frequencies in *2n=28* cases and *2n=108* controls within associated amino-acid positions of HLA-B alleles. **D)** Schematic overview of the binding groove showing amino acids positions that make up each pocket. As defined in HLA-A2. *Adapted from (van Deutekom and Keşmir 2015)*

3.3.5. Investigating ERAP polymorphism in rifampicin-SCAR

Our HLA data suggests that rifampicin-SCAR is associated with HLA-B44 and B62 alleles. However, in comparison to other HLA-drug-ADR pairs the odds ratios are modest (12-30 versus >100), and HLA-B44 risk alleles are found amongst rifampicin tolerant controls suggesting that other genomic risks may be necessary either outside of the HLA region or modifying the HLA-peptide-TCR complex interactions. In autoimmune and inflammatory diseases, polymorphisms in the endoplasmic reticulum aminopeptidase (ERAP) 1 and 2 genes have been found to be important in association with HLA-class I risk alleles (Evans et al. 2011; Strange et al. 2010; Reeves et al. 2014). ERAP1 is an enzyme responsible for ER N-terminus peptide trimming, and polymorphisms are associated with differential trimming activities and thus altered peptide presentation or HLA-peptide stability (Falk and Rötzschke 2002). ERAP 1 and 2 are in almost complete linkage disequilibrium and ERAP genes (on chromosome 5) are epistatically linked to HLA. We thus hypothesised that ERAP1 and 2 may be important candidate genes, linked to class I HLA risk alleles driving the occurrence of FTLD-SCAR in affected individuals. We selected 19 SNPs located across ERAP1 and ERAP2 to investigate.

To assess their association with the development of rifampicin SCAR, we investigated their frequencies in HLA-B risk allele positive and negative rifampicin SCAR cases and matched tolerant controls. Twenty-four rifampicin SCAR cases and 80 matched tolerant controls were ERAP typed. Table 3-6 shows the allelic frequencies of these SNPs and *P* values. There were significant differences in the frequency of genotype CT of rs27529 (P=0.0522), AG of rs30187 (P=0.0522) and AG of rs17482078 (P=0.0312) in HLA-B risk allele positive cases compared to controls. In HLA-B risk allele negative cases and controls, significant differences were observed in CC of rs27434 (P=0.0315), CC of rs27529 (P=0.0315) and GG of rs30187. After Bonferroni correction (Pc=0.001) for multiple comparisons, no significant differences were observed. Additionally, we did not observe any differences in an independent HLA non-restricted analysis.

In comparisons with >30% differences where the effect size will be increased with a larger sample size, we investigated the robustness of non-synonymous variants, rs30187 and rs17482078 in ERAP 1 on rifampicin SCAR predisposition and pathogenesis. ERAP1 genotype AG in rs30187 (odds ratio: 3.5; 95% CI: 0.97-12.9; P=0.0548) and genotype AG in rs17482078 (odds ratio: 12.0; 95% CI: 0.58-247.4; P=0.1082) were associated with rifampicin SCAR in cases carrying at least one HLA-B risk allele than HLA-B risk positive matched controls. Whereas genotypes GG in rs30187 (odds ratio: 8.0; 95% CI: 0.87-73.6; P=0.0662) had an effect in HLA-B risk allele negative rifampicin SCAR cases compared to matched controls (figure 3-10A-B). These differences were not observed between HLA-B risk allele positive and negative matched tolerant in terms of frequency (Table 3-6). Our data suggests interaction between HLA-B-risk alleles and ERAP1 even heterogenous genotypes rs30187

and rs17482078 are associated with rifampicin SCAR while homozygosity of rs30187 and rs17482078 are protective against SCAR in HLA-B risk allele positive controls and lack of drug specific IFN-γ responses in HLA-B risk allele negative SCAR cases (figure 3-10-A-B). For ERAP haplotype and analyses by activity of peptide "trimming" we used amino acid positions relevant to impute ERAP1 allotype based on (Reeves et al. 2013) and (Ombrello, Kastner, and Remmers 2015) to assign ERAP1 trimming efficiency as efficient, hyperactive or hypoactive as indicated in figure 3-10C and appendix, section 3.2. Analysis of ERAP1 functionality based on haplotype analysis showed an increased carriage of hypoactive allotypes in HLA-B risk allele negative cases (P=0.0362), whereas no significant differences were observed between HLA-B risk allele positive cases and controls (figure 3-10D).

Table 3-6: Rifampicin ERAP

			HLA-B risk allele positive			HLA-B risk allele negative		
Locus	**SNP**	**Genotype**	**Cases *n=18* freq.**	**Controls *n=26* freq.**	***P* value**	**Cases *n=6* freq.**	**Controls *n=54* freq.**	***P* value**
ERAP 1	rs3734016	AG	0,000	0,077	0.2242	0,000	0,093	0.4472
		GG	1,000	0,923		1,000	0,870	
	rs73148308	CT	0,111	0,115	0.9198	0,000	0,130	0.3513
		TT	0,889	0,885		1,000	0,833	
	rs26653	CC	0,000	0,154	0.0888	0,333	0,185	0.4234
		CG	0,611	0,462	0.3330	0,500	0,481	0.9265
		GG	0,389	0,385	1.0000	0,167	0,296	0.5078
	rs26618	AA	0,944	0,846	0.3597	0,833	0,778	0.7791
		AG	0,056	0,154		0,167	0,185	0.9061
	rs27895	AA	0,056	0,115	0.5103	0,333	0,111	0.1342
		AG	0,500	0,385	0.4744	0,500	0,537	0.8534
		GG	0,333	0,500	0.2683	0,167	0,315	0.4528
		IR	0,111	0,000		0,000	0,000	
	rs2287987	AA	0,722	0,808	0.4884	1,000	0,815	0.2603
		AG	0,167	0,115	0.6427	0,000	0,130	0.3513
		GG	0,000	0,077	0.2242	0,000	0,019	0.7289
		IR	0,111	0,000		0,000	0,000	
	rs27434	CC	0,167	0,346	0.1944	0,833	0,370	**0.0315**
		CT	0,611	0,423	0.2205	0,167	0,481	0.1510
		TT	0,111	0,231	0.3149	0,000	0,111	0.3960
		IR	0,111	0,000		0,000	0,000	
	rs73144471	AT	0,111	0,077	0.7382	0,000	0,148	0.3118
		TT	0,889	0,923		1,000	0,815	0.2603
	rs27529	CC	0,167	0,385	0.1217	0,833	0,370	**0.0315**
		CT	0,722	0,423	**0.0522**	0,167	0,519	0.1066
		TT	0,111	0,192	0.4787	0,000	0,074	0.5068
	rs30187	AA	0,111	0,192	0.1217	0,000	0,074	0.5068
		AG	0,722	0,423	**0.0522**	0,167	0,519	0.1066
		GG	0,167	0,385	0.4787	0,833	0,370	**0.0315**
	rs10050860	AA	0,000	0,077	0.2242	0,000	0,019	0.7289
		AG	0,167	0,115	0.6427	0,000	0,130	0.3513
		GG	0,778	0,808	0.8097	1,000	0,815	0.2603
		IR	0,056	0,000		0,000	0,000	
	rs17482078	AA	0,000	0,077	0.2242	0,000	0,000	
		AG	0,167	0,000	**0.0312**	0,000	0,074	0.5068
		GG	0,833	0,923	0.3663	1,000	0,889	0.3960
	rs27044	CC	0,111	0,115	0.9198	0,000	0,037	0.6208
		CG	0,444	0,385	0.7431	0,167	0,370	0.3339
		GG	0,444	0,500	0.6985	0,833	0,556	0.2064
ERAP 2	rs2549782	GG	0,111	0,192	0.4787	0,500	0,296	0.3232
		GT	0,500	0,577	0.6043	0,500	0,426	0.7450
		TT	0,389	0,231	0.2582	0,000	0,241	0.1790
	rs2248374	AA	0,111	0,192	0.4787	0,500	0,296	0.3232
		AG	0,500	0,577	0.6043	0,500	0,426	0.7450
		GG	0,389	0,231	0.2582	0,000	0,241	0.1790

A

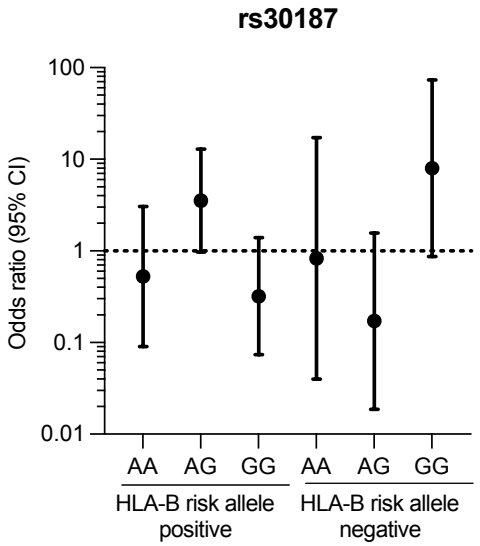

B

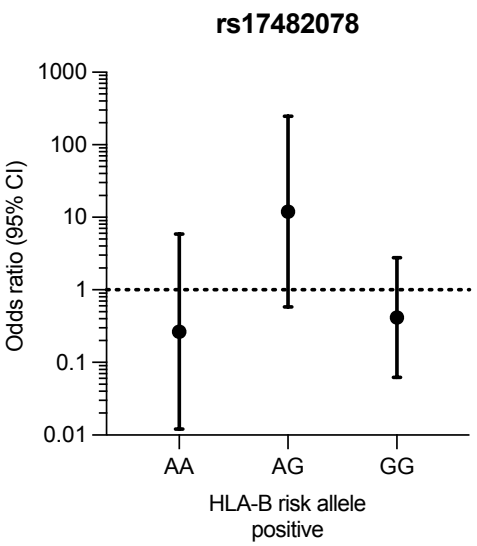

C

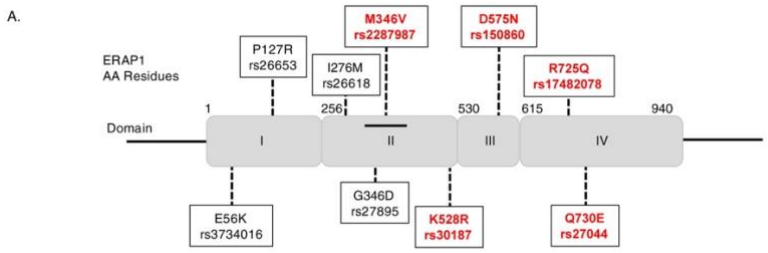

B.

		E56K	P127R	I276M	G346D	M349V	K528R	D575N	R725Q	Q730E	PT+ ABC HSS (%)	Tolerant (%)	Phenotype
ALLOTYPE Reeves et al 2013	WT					M	K	D	R	Q	0.33	0.25	Efficient
	K528R/Q730E					M	R	D	R	E	0.38	0.41	Hypoactive
	M349V/K528R					V	R	N	Q	E	0.13	0.25	Hypoactive
	MKDRE*					M	K	D	R	E	0.14	0.07	ND
ALLOTYPE Ombrello et al 2015	Hap1	E	P	I	G	M	K	D	R	Q	0.19	0.19	Efficient
	Hap2	E	R	I	G	M	K	D	R	Q	0.15	0.02	Efficient
	Hap4	E	R	I	G	M	R	D	R	E	0.01	0.04	Hypoactive
	Hap5	E	R	I	D	M	R	D	R	E	0.04	0.06	Hypoactive
	Hap6	E	P	I	G	M	R	D	R	E	0.12	0.04	Hypoactive
	Hap7	K	P	I	G	M	R	D	R	E	0.02	0.02	Hypoactive
	Hap8	E	P	M	G	M	R	D	R	E	0.20	0.26	Hypoactive
	Hap10	E	P	I	G	V	R	N	Q	E	0.16	0.32	Hypoactive
	Hap3	E	R	I	G	M	K	D	R	E	0.13	0.09	ND

D

		HLA-B risk allele positive					HLA-B risk allele negative				
Phenotype		**Cases *n=16***	**Freq.**	**Controls *n=31***	**Freq.**	***P* value**	**Cases *n=6***	**Freq.**	**Controls *n=53***	**Freq.**	***P* value**
WT WT	Efficient	2	0,125	5	0,161	0.7870	0	0,000	5	0,094	0.4473
WT Under	Efficient	11	0,688	15	0,484	0.1748	1	0,167	28	0,528	0.0974
Under Under	Hypoactive	3	0,188	5	0,161	0.7975	5	0,833	20	0,377	**0.0362**

Figure 3-10: Association findings for ERAP1 SNPs rs27529, rs30187 and rs17482078 stratified by the rifampicin HLA-B risk alleles and ERAP1 allotype analysis

A) rs30187 **B**) rs17482078. **C**) Amino acid positions relevant for the ERAP1 allotype nomenclature. Adapted from (Pavlos et al. 2020). **D**) ERAP1 allotype frequency for HLA-B risk allele positive and negative rifampicin SCAR cases and matched tolerant controls.

3.3.6. Exploratory analysis of KIR genes in patients with rifampicin SCAR

Our rationale for separately assessing KIR, is the known strong interactions between KIR and HLA alleles (Lanier 1998). KIR and HLA class I are known to have actively co-evolved and evidence exists that prevalent KIR, HLA and ERAP alleles have co-evolved in Africans under the selective pressure of infectious diseases such as malaria (Garamszegi 2014; Yindom et al. 2012). KIR binding specificity and affinity to HLA class I molecules, and consequently patterns of resistance to specific diseases are influenced by complex interactions of allelic polymorphisms of both KIR and HLA class I genes.

Twenty-four rifampicin SCAR cases and 78 matched tolerant controls were KIR genotyped. We analysed KIR genotypes in *n=18* rifampicin SCAR cases and *n=26* tolerant controls carrying either one or two HLA-B risk alleles outlined in section 3.3.2 and *n=6* rifampicin SCAR cases; *n=52* tolerant controls negative for HLB44 and HLA-B62 risk alleles. We have concerted the allelic KIR into present or absent without the resolution to look at the full allelic level and we are aware not all alleles are expressed at the cell surface. Table 3-7 shows the frequencies and statistical associations. The presence of KIR2DL3 (odds ratio: 9.3; 95%CI: 1.8-49.1; P=0.0084) and KIR2DS3 (odds ratio: 12; 95%CI: 2.6-55.7; P=0.0014) had a significantly increased effect in HLA-B risk allele positive rifampicin SCAR cases than controls. After multiple test analyses using Bonferroni correction, the association was only significant for the presence of the activating KIR2DS3 (Pc=0.003). The frequencies of KIR haplotypes in the same groups are outlined in Table 3-8. The number of KIR centromeric A/B haplotype (odds ratio: 3.5; 95%CI: 1-12.5; P=0.0498) was increased in HLA-B risk allele positive cases than controls, whereas centromeric B/B haplotypes (odds ratio: 0.13; 95%CI: 0.02-0.66; P=0.0140) was significantly increased in controls than cases. HLA-B risk allele negative cases had a significantly increased number of centromeric B/B haplotypes (odds ratio: 6.7; 95%CI: 1.1-40.9; P=0.0406) compared to controls.

KIR3DL1 is the only KIR locus that encodes for activating allotype KIR3DS1 and several inhibitory alleles. KIR3DL1 allotypes ligands are HLA-B molecules that contain the Bw4 motif at position 80 (figure 3-7). Although there was no difference in the presence of KIR3DL1 and KIR3DS1 between cases and controls (Table 3-7), we still looked at the allele frequency of KIR3DL1 and KIR3DS1 given the high frequency of Bw4 alleles in SCAR patients than controls. We next compared frequency of Bw4 alleles by the amino acid encoded at position 80 and observed that cases had increased frequency of Bw4-80T allotypes (influenced by HLA-B*44:03 carriage), whereas controls had an increased frequency of Bw4-80I allotypes. KIR3DL1 has a higher avidity for isoleucine80 (Bw4-80I) than threonine80 (Bw4-80T) (Alter et al. 2007). HLA-B*44:03 was the only rifampicin HLA-B risk allele in the Bw4 group while the other HL-B44 and HLA-B62 risk alleles belonged to the Bw6 motif (figure 3-12).

KIRs act to regulate cytotoxic NK and T cells responses with specificity for the interacting peptide (Hertzman et al. 2021; Thananchai et al. 2007). Although we cannot completely rule out the possibility of Bw4-80I protection in controls, we calculated the KIR3DL1 and haplotypes frequencies in combination with Bw4-80T ligands based on the proposed peptide preference for Bw4-80T molecules in rifampicin SCAR. Analysis of various KIR-HLA-Bw4-80T combinations revealed no significant differences between rifampicin SCAR patients and tolerant controls. The frequency of KIR centromeric B/B and HLA-Bw4-80T (odds ratio: 0.1; 95%CI: 0.01-0.78; P=0.0281) was significantly increased in tolerant controls than rifampicin cases (Table 3-9).

To perform its inhibitory function, KIR3DL1 must be expressed at the cell surface. The level of allotype expression at this locus is divided into three groups: high (KIR3DL1*001, *002, *003, *008, *009, *015 and *020), low (KIR3DL1*005, *006 and *007), and not expressed (KIR3DL1*004) which represents an unusual allele as it encodes a protein that is retained within the cell. In individuals with Bw6/Bw6 risk alleles, it does not matter which KIR3DL1 subtype is present because the ligand is absent, so the KIR3DL1 molecule is non-functional – therefore we focused our subtype analysis on KIR3DL1+Bw4-80T rifampicin SCAR patients and tolerant controls. Overall, there was no difference between cases and controls in the expression of KIR3DL1 inhibiting allotypes. The most notable result was some of the highly expressed allotypes such as KIR3DL1*001, *002, *020 were only expressed in controls (figure 3-12) and thus any protective effect of KIR3DL1 interacting with Bw4-80I molecules would most likely be seen in tolerant controls.

Table 3-7: Frequencies of KIR genes in rifampicin SCAR cases and matched FLTD tolerant controls

	HLA-B risk allele positive					HLA-B risk allele negative				
Allele	**Cases *n=18***	**Controls *n=26***	**OR**	**95% CI**	**P value**	**Cases *n=6***	**Controls *n=52***	**OR**	**95% CI**	**P value**
KIR-2DL1	1,000	1,000	0.6981	0.0132 - 36.7945	0.8590	1,000	1,000	0.1238	0.0023 - 6.7857	0.3065
KIR-2DL2	0,722	0,808	0.6190	0.1497 - 2.5599	0.5079	0,833	0,712	2.0270	0.2181 - 18.8382	0.5345
KIR-2DL3	0,889	0,462	**9.3333**	1.7747 - 49.0844	**0.0084**	0,333	0,692	0.2222	0.0369 - 1.3399	0.1008
KIR-2DL4	1,000	0,962	2.1765	0.0839 - 56.4787	0.6397	1,000	0,923	1.2062	0.0580 - 25.0728	0.9036
KIR-2DL5	0,611	0,692	0.6984	0.1978 - 2.4662	0.5771	0,667	0,481	2.1600	0.3634 - 12.8400	0.3971
KIR-2DP1	0,889	0,654	4.2353	0.7914 - 22.6660	0.0917	0,833	0,865	0.7778	0.0788 - 7.6805	0.8297
KIR-2DS1	0,278	0,308	0.8654	0.2299 - 3.2580	0.8307	0,167	0,096	1.8800	0.1817 - 19.4516	0.5964
KIR-2DS2	0,667	0,769	0.6000	0.1573 - 2.2890	0.4546	0,833	0,538	4.2857	0.4677 - 39.2717	0.1979
KIR-2DS3	0,611	0,115	**12.0476**	2.6047 - 55.7234	**0.0014**	0,500	0,231	3.3333	0.5936 - 18.7172	0.1714
KIR-2DS4	1,000	0,962	2.1765	0.0839 - 56.4787	0.6397	1,000	0,923	1.2062	0.0580 - 25.0728	0.9036
KIR-2DS5	0,611	0,615	0.9821	0.2860 - 3.3730	0.9772	0,667	0,519	1.8519	0.3115 - 11.0082	0.4980
KIR-3DL1	0,889	0,885	1.0435	0.1561 - 6.9738	0.9650	1,000	0,808	3.2118	0.1673 - 61.6552	0.4389
KIR-3DL2	1,000	0,885	5.5106	0.2675 - 113.5105	0.2688	0,333	0,096	4.7000	0.6811 - 32.4340	0.1164
KIR-3DL3	1,000	0,846	2.1765	0.0839 - 56.4787	0.6397	1,000	0,923	1.2062	0.0580 - 25.0728	0.9036
KIR-3DP1	0,944	0,923	1.4167	0.1187 - 16.9101	0.7831	0,833	0,885	0.6522	0.0648 - 6.5669	0.7168
KIR-3DS1	0,167	0,115	1.5333	0.2725 - 8.6273	0.6277	0,000	0,077	0.8291	0.0399 - 17.2336	0.9036

Table 3-8: KIR haplotype frequencies in rifampicin SCAR

	HLA-B risk allele positive					HLA-B risk allele negative				
Allele	**Cases *n=18***	**Controls *n=26***	**OR**	**95% CI**	**P value**	**Cases *n=6***	**Controls *n=52***	**OR**	**95% CI**	**P value**
Cen-A/A	0,278	0,154	2.1154	0.4802 - 9.3193	0.3220	0,167	0,212	0.7455	0.0787 - 7.0575	0.7978
Cen-A/B	0,611	0,308	**3.5357**	1.0013 - 12.4850	**0.0498**	0,167	0,481	0.2160	0.0236 - 1.9787	0.1751
Cen-B/B	0,111	0,500	0.1250	0.0238 - 0.6567	**0.0140**	0,667	0,231	**6.6667**	1.0846 - 40.9760	**0.0406**
Tel-A/A	0,611	0,615	0.6044	0.1828 - 1.9983	0.4092	0,833	0,673	2.4286	0.2627 - 22.4477	0.4342
Tel-A/B	0,278	0,269	0.5495	0.1337 - 2.2575	0.4062	0,167	0,115	1.5333	0.1523 - 15.4394	0.7168
Tel-B/B	0,111	0,077	1.4118	0.1806 - 11.0338	0.7424	0,000	0,115	0.5503	0.0276 - 10.9572	0.6955

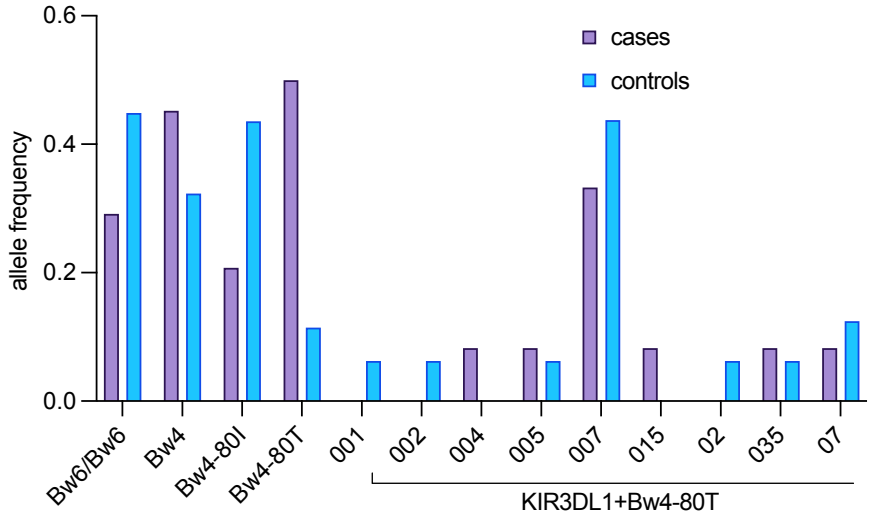

Figure 3-11: Allele frequency of KIR3DL1 alleles and HLA-Bw4/Bw6 subtypes

The frequency of each variable except Bw4-80I and -80T (frequency of Bw4) is shown for KIR3DL1 positive cases carrying rifampicin HLA-B risk alleles and matched drug tolerant controls

Table 3-9: Effects of KIR3DL1 and HLA-Bw4-80T combinations in rifampicin SCAR

KIR-HLA-B combination	**Cases, *n=12***	**Freq.**	**Controls, *n=9***	**Freq.**	**OR**	**95% CI**	***P* value**
KIR3DL1+Bw4-80T	11/12	0,917	7/9	0,778	3.1429	0.24 - 41.51	0.3845
KIR3DS1+Bw4-80T	2/12	0,167	0/9	0,000	4.5238	0.19 - 106.7	0.3493
KIR haplotype-HLA-B combination							
Cen-A/A+Bw4-80T	3	0,250	1	0,111	2.6667	0.2289 - 31.0708	0.4337
Cen-A/B+Bw4-80T	7	0,583	2	0,222	4.9000	0.7000 - 34.3014	0.1094
Cen-B/B+Bw4-80T	2	0,167	6	0,667	0.1000	0.0128 - 0.7812	**0.0281**
Tel-A/A+Bw4-80T	9	0,750	6	0,667	1.5000	0.2233 - 10.0769	0.6765
Tel-A/B+Bw4-80T	2	0,167	1	0,111	1.6000	0.1219 - 20.9943	0.7205
Tel-B/B+Bw4-80T	1	0,083	2	0,222	0.3182	0.0241 - 4.2024	0.3845

3.4. Discussion

In this chapter we investigated associations between specific immunogenomic genes important in adaptive immune responses and antigen processing and their association with FLTD associated DRESS and SJS/TEN. This study and ability to phenotype the culprit drug was facilitated by optimisation of an ELISpot assay to identify FLTD-specific IFN-γ producing T cells. The immunogenomic genes included a focus on HLA class I alleles previously shown to be strongly associated with SCAR reactions as well as ERAP and KIR. Genetic polymorphisms in KIR in particular have been previously associated with many diseases of evolutionary importance in African populations (Norman et al. 2013) as well as cutaneous diseases (Margolis et al. 2021; Margolis et al. 2023). ERAP polymorphisms have also been associated with abacavir hypersensitivity in the context of HLA-B*57:01 and nevirapine SJS/TEN in the context of HLA-C*04:01. In both cases hypoactive trimming phenotype was protective against a hypersensitivity reaction (Hertzman et al. 2021). There are limited data on genetic factors that cause predisposition to FLTD induced-SCAR, especially in HIV-TB co-infected endemic settings. Published genetic association studies also highlighted the influence of ethnicity and specific risk allele frequencies in study population to the strength of the association.

Primary findings elucidated in this chapter include an association of HLA-B*44:03 with development of rifampicin SCAR in Black and South African mixed ancestry individuals. Of interest is the strength of the association is highest in cases where rifampicin was identified as the primary clinical culprit and positive on SDC and ELISpot. Detailed analysis of the HLA-B*44:03 peptide binding groove, guided by positive rifampicin ELISpot in rifampicin SCAR patients not carrying HLA-B*44:03 revealed key HLA-B*44:03 risk polymorphic positions in the pathology of rifampicin SCAR. These alleles belong primarily to the HLA-B44 and HLA-B62 supertypes (Sidney et al. 2008). We also applied a detailed analysis of the peptide binding groove which revealed that the HLA-B44 and HLA-B62 supertypes share commonality in the polymorphic positions that determine the specificity of the peptide binding groove. A hypothesis from the virtual modelling is that HLA-B44 and HLA-B62 supertypes share a similar B-pocket confirmation for rifampicin binding and peptide presentation capable of activating T cells. Virtual analysis of the peptide groove has previously been applied to great success in nevirapine hypersensitivity to study shared peptide binding specificities across different HLA class I and II supertypes in different ethnicities (Pavlos et al. 2017).

In our model docking findings, we observed potential mechanistic differences in the development of rifampicin SCAR between PLHIV and HIV negative cases. With HLA-B*15:01, our virtual modeling findings suggest possible parent drug interacts with the peptide binding groove at higher affinity for presentation and induction of drug specific responses, whereas, in HLA-B*44:03, rifampicin may be

present in the ER and as a tapasin dependent allotype (appendix, section 3.1) (Bashirova et al. 2020), rifampicin may bind to conserved tapasin related positions to provide structural stability for high pMHC complex presentation. However, future invitro based studies will be highly important to prove physiological relevance of these possible interactions. Given the long incubation time (median, 29 days), these could be peptide with unknown T cell epitopes now stabilised by rifampicin for presentation. Although further analysis is required, our docking model results provides support compatible with pMHC complex stability required in peptide ligand presentation. In addition, in view of the fact that our HIV uninfected populations are underrepresented, and that race and ethnicity factors come into play we cannot rule out the role of a founder population effect on the HLA-B*15:01 analysis.

Our results confirm general findings seen with all other associations between HLA class I alleles and drug hypersensitivity reactions in that we believe that HLA-B*44 supertype may be an important risk factor for the development of rifampicin SCAR. However, it is not sufficient for the development of rifampicin SCAR and additional experimental work is required to ascertain other risk factors that may be important in the PPV of HLA-B*44:03 for rifampicin SCAR. Intriguingly one model may be that rifampicin SCAR is an HLA class I-restricted CD8+ T cell mediated reaction which can be correlated to the loss of immune tolerance seen in advanced HIV immunosuppression (McMichael and Rowland-Jones 2001). This is a similar to the hypothesis tested by Cardone et al in a mouse model that showed in immunocompetent HLA-B*57:01 animals, abacavir induces CD8+ T cells with an anergy-like phenotype that did not lead to ADRs (Cardone et al. 2018).

Additional risk factors included in an exploratory of other genes which from part of antigenic processing and the immune response synapse such as ERAP, and KIR which have been implicated in the development of SCAR to other drugs (Hertzman et al. 2021). Our results also signified the importance of HLA-B44 and HLA-B62 interaction with ERAP1 in the peptide generation and presentation.

Due to type one error, we did not observe any significant differences in ERAP analysis. However, with a larger sample size, the presence of genotype and AG at rs30187 and AG at SNP rs17482078 may potentially increase the aminopeptidase activity with more peptides presented which may account for the increased number of rifampicin specific CD8+ T cells and potentially the lack of drug specific responses (measured by ELISpot) in other HLA-B risk allele positive cases not carrying this genotype. Additionally, the increased presence of hypoactive ERAP allotypes in HLA-B risk allele negative may also explain the lack of rifampicin specific ELISpot responses in these SCAR cases. These SNPs have been demonstrated to be correlated with modifications in peptide length and

trimming specificity of peptides generated from HIV and HCV antigens (Saulle et al. 2020). These are viral epitopes implicated in the development of DRESS (Duong et al. 2017).

After establishing the frequencies of HLA-B risk alleles among rifampicin cases and tolerant controls, we employed KIR typing to analyse the association between KIRs with HLA-B cognate ligands and development of rifampicin SCAR or NK and CTLs tolerance in controls. Combinations of HLA-Bw4 and KIR3DL1 and KIR3DS1 have been reported to correlate with the occurrence of autoimmune diseases (Zvyagin et al. 2010) and HIV progression (Alter et al. 2007). We found no differences in the presence of KIR3DL1 and KIR3DS1 in HLA-B risk allele positive cases and matched controls. Given alleles in the HLA-B44 supertype are the primary contributors to the Bw4 motif, we looked at the frequency of KIR3DL1 alleles to study the strength of inhibitory signals in cases versus controls. Although Bw4 motif with threonine at position 80 has been shown to have low affinity for KIR3DL1 (Lanier 1998), the increased frequency of highly expressed KIR3DL1 alleles in controls suggests stronger inhibitory signals between KIR3DL1 and HLA-Bw4-80T may be sufficient to confer NK and CTLs tolerance in HLA-B risk allele positive controls. The protective function of KIR3DL1*001, *002 and *02 has been reported in the pathogenesis of autoimmune diseases (Zvyagin et al. 2010) and infectious disease control and progression (Martin et al. 2002; Alter et al. 2007). Whereas KIR3DL1*004, *005 and *015 present at high frequencies in cases than controls are associated with unregulated inflammation and autoimmunity. However, functional studies are necessary to support KIR variants and SCAR outcome.

A couple of limitations need to be addressed. Firstly, the total number of isoniazid, pyrazinamide and ethambutol were even lesser than rifampicin SCAR cases and therefore excluded from further genetic testing analysis. Secondly, for any genetic association study, the population ethnicity is important in matching cases and tolerant controls. The susceptibility HLA-B*15:01 we discovered in HIV uninfected cases was present only in SAM and has higher allele frequencies in SAM than Black African populations. The inclusion of general healthy population as a control group where SAM participants are well represented was helpful in this instance. However, to confirm this allele as the reason for rifampicin SCAR susceptibility in this group, we need to improve the numbers of SAM drug tolerant controls and include race and ethnicity in our matching criteria. Thirdly, modelling studies in ADRs (Ostrov et al. 2012; Pavlos et al. 2017; Thomas et al. 2017) and many other common diseases (Khodadoust et al. 2017; Nair et al. 2006; Madden 1995) have provided the best evidence of proteins and gene-gene interactions. However, these are still virtual analyses for hypothesis generation and functional studies are necessary to provide novel insights in our understanding of molecular mechanisms involved in the development of rifampicin SCAR.

Chapter 4 - Single cell immune profiling of rifampicin DRESS contrasting HIV infected and uninfected cases

4.1. Introduction

A key element of T cells responses in SCARs is activation of T cells and the generation of specific proinflammatory, cytotoxic molecules. We identified the HLA class I B - HLA-B*44:03, and the HLAB44 supertype as associated with rifampicin induced SCAR. However, not all individuals who carry HLA-B*4403 and HLA-B44 risk alleles will develop a hypersensitivity reaction to rifampicin. Those identified in our control group, completed their FLTD anti-TB treatment without adverse events. HIV-associated chronic immune activation is characterized by an increase in proinflammatory mediators, dysfunctional T regulatory cells, and a pattern of T-cell-senescent phenotypes similar to those seen in the elderly (figure 4-1). At present, the extent of immune system dysfunction associated with advanced HIV, its contribution to the SCAR pathogenesis, especially with concomitant TB disease are understudied. In fact, many studies have reported SCARs are more common and severe in HIV infected patients, a few have focused on delineating the immune factors that are associated with increased susceptibility and overcoming immune tolerance in these patients and elucidating the cellular mechanisms that govern transition from tolerance to allergic reaction – particularly given the phenotypic variability and drug exposure latency in these patients (Cardone et al. 2018).

We hypothesize, mechanisms that regulate cytotoxic immune responses (previously shown to drive these reactions and cause tissue injury) are defective due to the lack of CD4+ T regulatory cells in HIV. Therefore, the balance between recognition of drugs and regulation of immune responses are impaired. To broadly characterize this immune state, we used high-dimensional CyTOF and single cell RNA sequencing to assess and characterise the overall lymphocyte and myeloid cell population of PBMCs, the abundance to T cells, NK cells, monocytes and DCs, their differentiation and functional differences. Here, we compared immune profiles in longitudinally collected blood samples from rifampicin DRESS patients, alongside a cohort of drug tolerant patients at more than eight weeks on treatment. This was to identify immune signatures specific to reaction timepoint (pre-SDC, post-SDC and recovery), those specific to anti-TB drug induced DRESS by analysing HIV negative DRESS patients and lastly drug tolerant controls where we expected to only observe pathogen-associated immune profile. Understanding why some patients with HLA-B*4403 develop rifampicin SCAR, whereas others do not, the differences, if any between SCAR in HIV positive and negative patients, is crucial for accurate diagnosis and management of drug allergy.

HIV is associated with aCD4+ T cell depletion, marked differential immune profiles and cytokine production from innate and adaptive immune responses. A study by Cardone et al which relied on

animal models showed patient specific conditions may determine the outcome of responses to abacavir (Cardone et al. 2018). In this study, the in vivo depletion of CD4+ T cells prior to abacavir administration enhanced DC maturation to induce systemic abacavir-specific CD8+ T cells with an effector-like and skin-homing phenotype and CD8+ infiltration and inflammation in the skin of mice. A combination of two high-dimensional analyses will allow us to comprehensively explore the immune state of HIV infected patients at each reaction timepoint and determine whether reactions are fleeting flare-ups with the possibility of tolerance upon the expansion of functional immunoregulatory factors or there is sustained immune memory after drug sensitization. Additionally, we will understand the relationship between presence of viral antigens, viral reactivation, and the immunological mechanisms of DRESS.

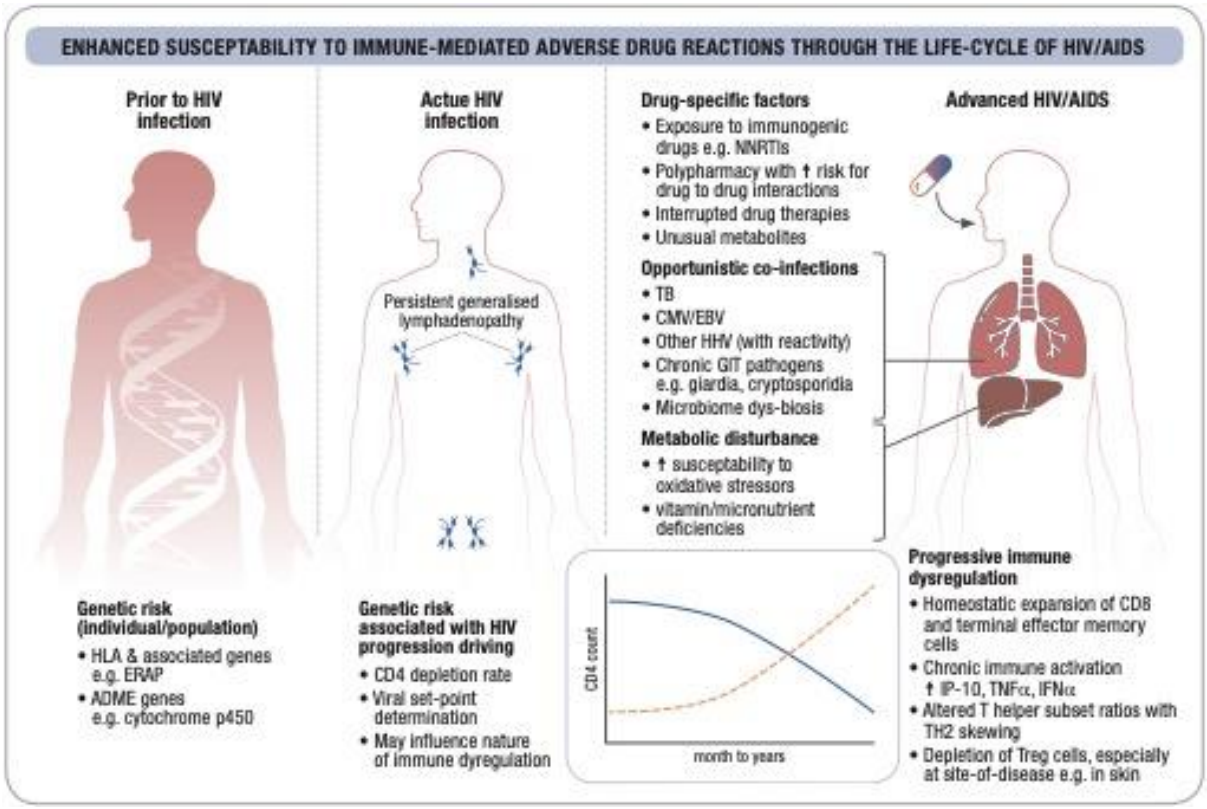

Figure 4-1: HIV associated immune dysfunction

Adapted from (Peter, Choshi, and Lehloenya 2019)

4.2. Materials and Methods

4.2.1. Patients and controls participants selection

In this hypothesis generating and initial characterisation of FLTD SCAR with high-dimensionality approaches, we decided to select representative grouping of available patients. We aimed to include rifampicin induced DRESS cases, HIV infected and uninfected cases from the IMARI registry, drug-tolerant controls matched for HIV-related immunosuppression (CD4 counts) and active TB disease from the PredART cohort. We also included a group of healthy controls without DRESS, HIV, and active TB to serve as an experimental control for our mass cytometry panel in normal peripheral blood mononuclear cells (appendix 4.4). Table 4-1 summarizes the demographic and clinical characteristics of SCAR cases and matched drug-tolerant matched controls used for mass cytometry stratified by HIV status. Majority of the participants (73%) were female with a median (IQR) age of 35 years (32-38 yrs.).

For inclusion in this CyTOF experiment cases (*n=4*) needed to meet the following criteria:

- RegiSCAR criteria meet as possible, probable, or definite DRESS
- Sequential drug challenge reaction to rifampicin
- Rifampicin ELISpot positive (≥20 SFU/million cells)
- Known HIV status and CD4 cell count if applicable

Drug tolerant controls (*n=4*)

- Matched to cases w.r.t self-identified race, age, gender, HIV status and CD4 cell count
- Tolerated at least eight weeks of all four first-line anti- TB drugs (rifampicin, isoniazid, ethambutol, and pyrazinamide) and at least more than 12 weeks for controls also on TMP-SMX
- No history of any cutaneous or other immune-mediated adverse drug reactions during treatment

Healthy controls (*n=3*)

- No prior exposure to FLTD
- HIV and TB uninfected

A total of four rifampicin DRESS cases were included and matched to four FLTD tolerant controls and three healthy controls. Three cases were HIV+ with a median (IQR) CD4 count of 101 cells/mm^3 (70-111 cells/mm^3). One HIV- rifampicin DRESS cases were selected to study the role of HIV in the development of SCAR. Four HIV+ tolerant controls with a median CD4 cell count of 81 cells/mm^3 (56-114 cells/mm^3) were included to allow differentiation of SCAR specific responses from HIV/TB associated immune dysfunction. The demographic data, medical history, symptoms, signs, main laboratory findings and major reaction details for each SCAR case were captured on a case record form into the IMARI patient registry password-protected redcap database, and detailed case

descriptions with photographs, Naranjo/ALDEN scoring, ELISpot and HLA data is shown in (figure 4-6A-B).

Table 4-1: CyTOF patients and control participants

Group	Sample ID	Gender	Age	CD4 count	Offending drug	SCAR validated phenotype
DRESS HIV+	10001	M	35	101	rifampicin	Probable DRESS
	10085	F	41	39	rifampicin	Definite DRESS
	10092	F	37	121	rifampicin	Possible Dress
DRESS HIV-	10020	M	33	-	rifampicin	Probable DRESS
Drug tolerant controls HIV+	SN048	F	42	56	-	-
	SN050	F	27	56	-	-
	SN091	F	29	106	-	-
	SN155	M	35	138	-	-
Healthy controls	201	F	37	-	-	-
	202	F	46	-	-	-
	203	F	28	-	-	-

4.2.2. Sample Collection

Peripheral venous blood was collected from each participant into tubes containing EDTA as an anti-coagulant (BD Vacutainer). Figure 4-2 below shows the timeline of blood sampling allowing comparison between cases. Bloods was collected at one baseline for controls and different stages of the reaction for rifampicin DRESS cases. There were four reaction timepoints for blood collection 1) during the acute stage of the reaction (<6 days since first symptoms onset), 2) once the patient laboratory findings have settled and SDC is about to be started (pre-SDC), 3) when the patient is having a positive reaction to any FLTD and 4) during recovery which ranges 3-24 months for cases selected. Blood was processed within 3 hours of collection and PBMCs were stored as outlined in section 2.2.2.

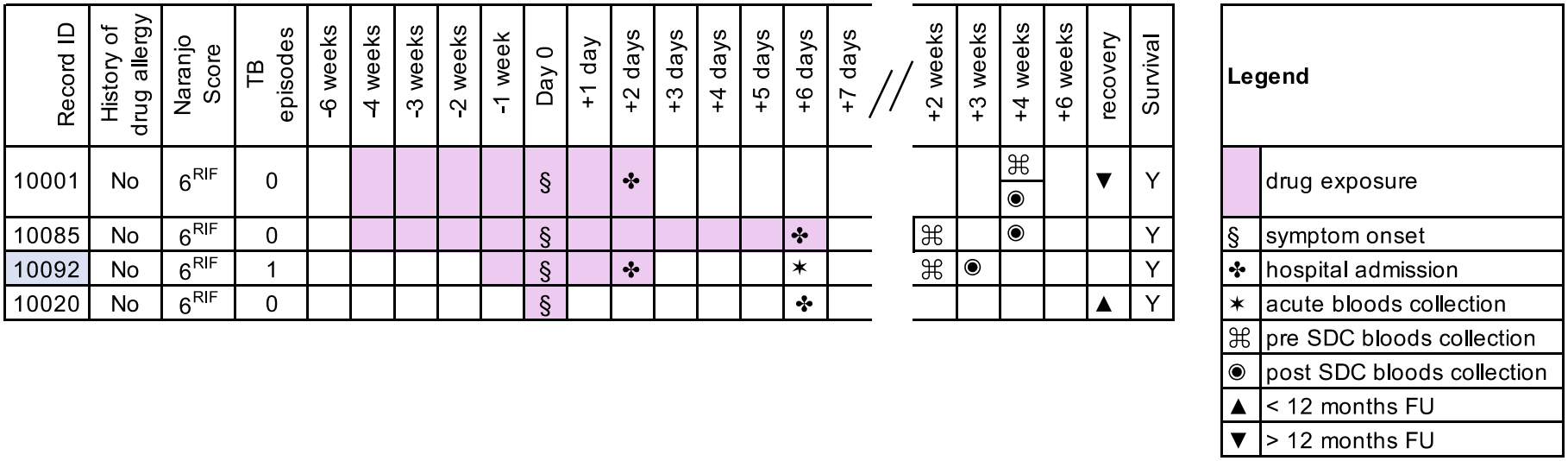

Figure 1-2: Drug reaction history and sample collection timepoints for mass cytometry

RIF- rifampicin, SDC – sequential drug challenge, FU – follow up

4.2.3. Mass cytometry by time of flight (CyTOF)

The initial immune characterisation of SCAR has been conducted with flow cytometry; however, the number of immune markers is restricted with this approach. Consequently, we worked with our mass cytometry core facility at the University of Cape Town to develop a multiparameter mass cytometry by time-of-flight panel to allow for the broadest possible immune profiling that was locally available and funded at the time of this work. In mass cytometry, fluorescent labelling of antibodies used in flow cytometry are replaced by heavy metal ion labels. Advantages of mass cytometry include increased numbers of simultaneous markers that can be tested at once, without loss of sensitivity and lack of spill-over between mass channels that is normally experienced between fluorochromes which requires complex compensation matrices to control. Our collaborators at Vanderbilt University Medical Centre had developed and optimised a mass cytometry antibody panel to study ADRs - we combined this antibody panel with the one developed by our core facility at UCT to study tuberculosis responses and totalled 33 surface and intracellular markers. Fourteen antibodies with new heavy metal ion labels or new clones were titrated to determine their optimal concentration for detection and resolution. Four serial dilutions were done for each antibody and the stimulation index calculation was used to choose concentration. In the subsequent run we tested the full antibody panel, and the results are reported in appendix, section 4.4.

CyTOF sample preparation

Figure 4-3 provides a schematic outline of the mass cytometry workflow and 33 marker immune panel. In brief, frozen PBMCs, as per the sampling in section 4.2.2 were thawed, rested, stimulated at 1-2 x10^6 cells/ml and incubated for 18-20 hours at 37°C, 5% CO_2 as outlined in section 2.2.3 and 2.2.4. Monensin and Brefeldin A were added an hour after incubation to block the release of intracellular markers in all in vitro stimulation conditions. Following overnight incubation, cells were washed with 1ml of 2% EDTA in 1X PBS, then incubated with 500µl of Rh103 (fluidigm) solution for 10 minutes at room temperature. Cells were washed with cell staining media (CSM, fluidgim) in preparation for antibody staining. Extracellular antibody cocktail (appendix, section 4.1 and 4.2) was prepared in CSM, filtered through 0.1um column, 50µl was added in each tube and incubated for 45 minutes at 4°C. Prior to intracellular staining, cells were washed with CSM, 200µl of perm/fix (fluidigm) was added and incubated for 20 minutes at room temperature. Cells were washed after with perm/wash buffer (BD Biosciences). Intracellular antibody cocktail was prepared in perm/wash, filtered through 0.1µm column and 50µl was added in each tube, incubated for 45 minutes at 4°C. Washed twice with perm/wash and added 1ml of 1/6000 dilution of Ir191/193 for overnight incubation at 4°C. On acquisition day, cells were washed twice with de-ionised (milliQ) water, pelleted on ice and transported to the CyTOF2 lab (figure 4-3).

Acquisition and processing of CyTOF data

When the CyTOF2 was ready, cells were resuspended in 500µl of 1/10 dilution of EQ™ four element in de-ionised (milliQ) water. The sample was injected into the cytometer for acquisition of approximately 0.5 - 1 million events and normalized with the with Helios normalizer software (Fluidigm version 6.7.1014). Data were uploaded to Cytobank.org for analysis and visualization. Data were processed to remove calibration beads, debris, and dead cells. In DRESS cases and tolerant controls, we analysed 53 613 with an average of 5957 per sample. For T cells metacluster and manual gating analysis, T cells were defined as CD3+CD19-CD14-CD16- and gated as such. For manual gating analysis, 33300 CD3+ T cells were further stratified as CD4+ or CD8+ T cells. T cells subpopulations were defined as follows: CD45RA+CD28+CD27+; central memory are CD45RA-CD28+CD27+/-; effector memory are defined by the lack of expression of CD45RA-CD28+/-CD27+/-; terminal differentiated effector memory are CD45RA+/-CD28-CD27+/- (Martin and Badovinac 2018) and CD56+ T cells (appendix, section 4.3, CyTOF gating strategy).

Analysis of CyTOF data

Data were analysed and visualised in Cytobank.org and R-based semi-automated pipeline developed at Vanderbilt University Mass Cytometry Centre of Excellence. The pipeline uses UMAP (McInnes, Healy, and Melville 2018) for dimensional reduction visualization, FlowSOM (Van Gassen et al. 2015) as an automated clustering tool and marker enrichment modelling (Diggins et al. 2017) algorithm for independent identification of cell clusters. Statistical analysis of cell population frequencies between sample groups were identified by calculating the fold change between mean event count across groups. P values were calculated using unpaired, two-tailed Student's t-test and Bonferroni correction for multiple comparisons and Wilcoxon test were done with GraphPad Prism 10.

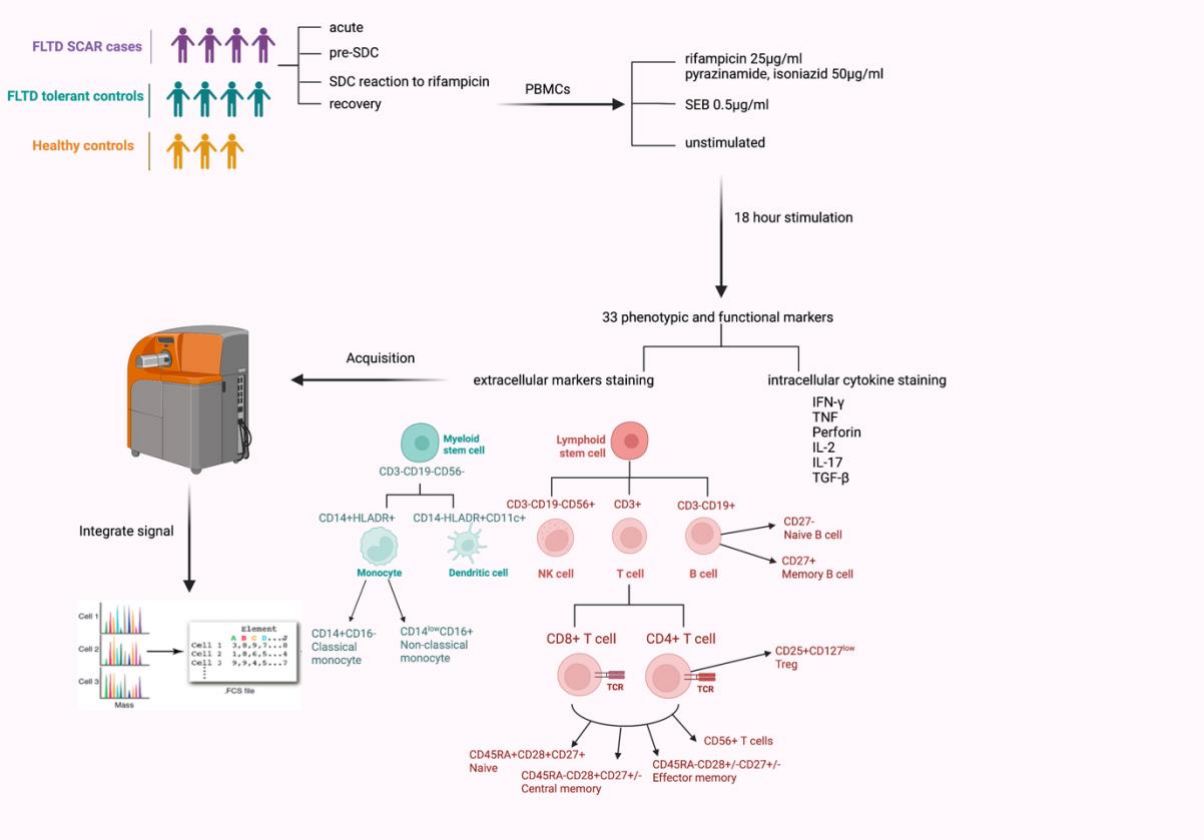

Figure 1-3: Schematic representation of the CyTOF experimental workflow

Cryopreserved PBMCs from *n=4* HIV+/- rifampicin DRESS cases and *n=4* HIV+ tolerant controls were thawed and underwent 18-20h stimulation with media (unstimulated control), FLTD (rifampicin 25ug/ml, ethambutol 50ug/ml, pyrazinamide 50µg/ml – drug specific stimulation) and SEB (non-specific stimulation - positive control). Samples were stained with a panel of antibodies including 26 surface markers and 8 intracellular markers and analysed with mass cytometer 2. For data analysis, we used a combination of manual gating and unsupervised computational analyses for reductionality, clustering and visualisation to identify immune cells and their functionality between included clinical groups.

4.2.4. Cite-seq and ScRNA-seq

Cite-seq sample preparation

Cryopreserved PBMCs, as per the sampling in section 4.2.2 were thawed, rested, with each timepoint sample divided into two for unstimulated and rifampicin stimulated in vitro conditions and incubated for 18-20 hours at 37°C, 5% CO_2 as outlined in section 2.2.3 and 2.2.4. After incubation, cells were collected into 15ml tubes and wshed with 10-12ml of 1XPBS and spun at 300g for 10 minutes. The second washed was done with 5ml of cell staining buffer (Cat. No. 420201), spun at 400g for 10min. The supernatant was removed and pelleted cells were resuspended in 50µl cell staining buffer. Cells were then blocked with the addition of 5µl of human TruStain FcX™ Fc blocking reagent to the recommended number of cells in 22.5µl cell staining buffer and incubated for 10 min at 4°C. The lyophilized antibody cocktail was (BioLegend Cat. No. 399905) (appendix, section 4.5 for Cite-seq antibodies) was prepared following manufacturer's instructions for staining. To perform staining, FcX blocked cells were transferred to 12 x 75 mm tubes and 25µl of reconstituted antibody cocktail to each tube and incubated for 30min at 4°C (on ice). The 1ul of hashtag antibody per sample according to the experimental plan. After staining incubation, cells were washed with three times with cell staining buffer, spun at 400g for 5min. Cells were then resuspended in 200µl of 1XPBS and counted using trypan blue viability staining in a countess. Cells were pooled based on the countess numbers to get 36000 cells in 37.8µl for 10X genomics. The single cell suspensions were processed through the 10X genomics Chromium Next GEM Single Cell 5′ Reagent Kits v2 to prepare ScRNA-seq and TCR-seq libraries according to the manufacturer's instructions (10X Genomics) (figure 4-4). Next, Illumina sequencing was applied.

Cell Ranger version 6.0.1 (10X Genomics) was used to process the data from the 5' ScRNA-seq and TCR-seq experiments using human reference genome version GRCh38. Gene counts were normalized with Seurat v4 using SCtransform and scale-factor transform methods. Genes with >0 counts in fewer than three cells and low-quality cells that either contained less than 100 genes or more than 25% mitochondrial content were filtered out. Seurat's CellCycleScoring function was used for determining cell-cycle phases. Joint analysis of merged samples was performed using R package Harmony. Identification of clusters of single cells was performed by dimensional reduction using PCA and by applying graph clustering algorithms to the reduced components. Visualization of the results was performed with uniform manifold approximation and projection (UMAP) and t-distributed stochastic neighbour embedding (t-SNE). The clusters were annotated by cell types derived using ScMatch and SingleR with the help of FANTOM5 and human cell atlas reference datasets. Antibody count matrix was derived using the Cell Ranger's feature barcoding analysis pipeline. TotalSeqC antibody barcodes corresponding to the 142 features (5 hashtags and 137 antibodies) was supplied as the reference. The filtered counts were later imported in Seurat R package and subjected to centered-log-ratio (CLR)

normalization. The values returned were superimposed over RNA derived clusters (tSNE /UMAP) for visualization. TCR results were exported and visualized through VGAS.

Cite-seq differential gene expression and GO enrichment analyses

Differential gene expression (DGE) analysis was performed among (1) pre-SDC versus post-SDC samples, (2) unstimulated versus rifampicin stimulated cells in both pre- and post-SDC samples, (3) comparison with recovery samples in patient 10001 with longitudinal data. Differential gene expression was calculated using UMI normalized gene expression data and genes were considered for analysis if they were expressed in two or more cells per cell subset. DGE analysis was performed using our in-house VGAS analysis which incorporates Bioconductor R packages for ScRNA-seq analysis. Differential expression was calculated using t-test with FDR for multiple comparisons correction. DGEs were considered statistically significant with an adjusted (FDR) P value of >0.05 and fold change >0.6. To find the function of DGEs in each sample groups, we used biological pathway enrichment analysis. The top ≤2000 DEGs in the identified cell clusters were investigated with the gene enrichment analysis tool with function enrichGO (OrgDb = "org.Hs.eg.db", keyType = "SYMBOL", ont = "BP") of ClusterProfiler (Yu et al. 2012) and plotted the top 20 enriched pathways. The terms from the functional libraries were plotted using adjusted p values and gene count as bar height and colour.

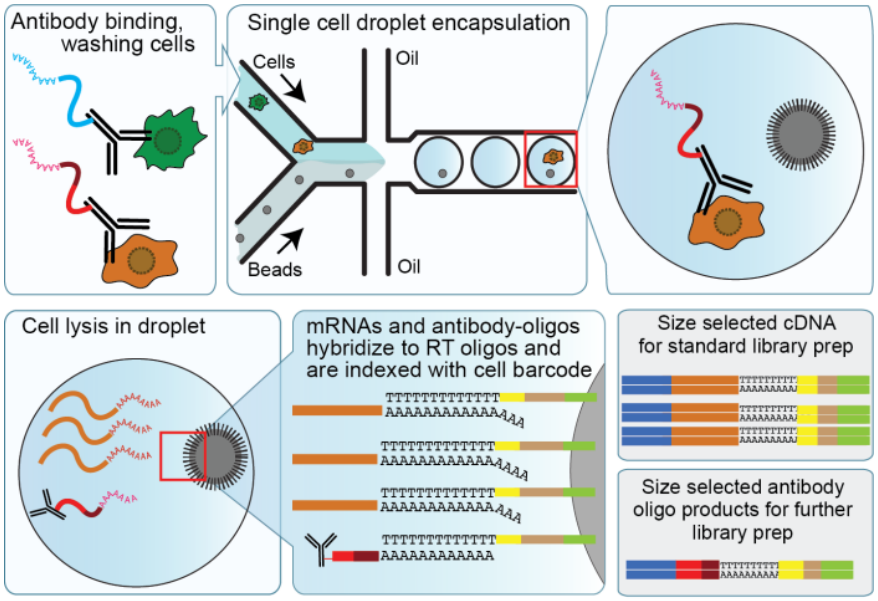

Figure 4-4: Schematic diagram of Cellular Indexing of Transcriptomes and Epitopes by Sequencing (CITE-seq)

Adapted from cite-seq.com

4.3. Results - CyTOF

4.3.1. Chapter 4 sample selection and experiment guideline

Chapter four of this thesis details characterization of T cells in rifampicin-induced DRESS. We used two single cells methods in an integrated manner to investigate the cell phenotype, function and TCR clonotypes. Patient samples were collected at various reaction timepoints. Figure 4-5 was designed as a reference tool to better understand the samples available, their time-points across the course of case acute DRESS, and sequential drug rechallenge and positive reaction to Rifampicin. These timing we consider important in understanding the biological differences within the analyses and between patients. Importantly, in this laboratory study sampling is opportunistic based on the clinical care of the case which is managed by the treating clinicians.

A subset of four adults from the FLTD-SCAR cohort were selected for single cell analyses - *n=3* HIV positive and *n=1* HIV negative with SDC confirmed rifampicin reaction and *n=4* matched drug tolerant controls (figure 4-2, Table 4-1). Oral SDC were performed in all cases according to standardized protocols (Lehloenya et al. 2020b) and as detailed in chapter 2, to confirm rifampicin reaction. All cases had skin and systemic symptoms including sore throat, fever, cough, dyspnoea, and chest pain at the start of major reaction. The diagnosis of active rifampicin-susceptible TB disease was confirmed in all cases during admission with the detection of MTB DNA (GeneXpert) in sputum and chest x-ray for patient 10092. The latency between commencement of rifampicin based FLTDs and onset of DRESS rash was 28, 39, 13 and 15 days in patient 10001, 10085, 10092 and 10020 respectively; case 10092 is notable in the shorter latency between drug exposure and DRESS onset. This is best explained in that case 10092 had previous TB (2012) and received FLTDs without any adverse reaction; notably the patient was HIV negative at the time of this previous TB drug exposure (HIV positive from 2014). Our CyTOF experiments we analysed one case (10092) with a sample collected within the first week since onset of DRESS; one case (10085) with samples collected pre- and post- a positive *in vivo* rifampicin sequential drug challenge (SDC) reaction; one case (10001) we analysed sample collected at 24 months post the onset of DRESS well into the recovery phase and the one HIV negative rifampicin DRESS case (10020), we analysed sample collected at three months post the onset of DRESS (figure 4-5). In all three cases of PLHV with rifampicin DRESS, in our Cite-Seq data we analysed samples from pre- and post- a positive *in vivo* rifampicin SDC reaction, with times ranging from day 11-28 (pre SDC) and 17-62 (post-positive rifampicin reaction). The time from rifampicin exposure to the onset of positive drug challenge reaction was 1, 5, and 1 days in cases 10001, 10085, and 10092 respectively. Case 10001 we also analysed a sample in the recovery period at 24 months following the onset of DRESS (figure 4-5). Figure 4-6 (A-D) describe clinical characteristics with photographs, ELISpot and rechallenge reactions and timelines. Details about all drug exposures and HIV and TB disease are also highlighted.

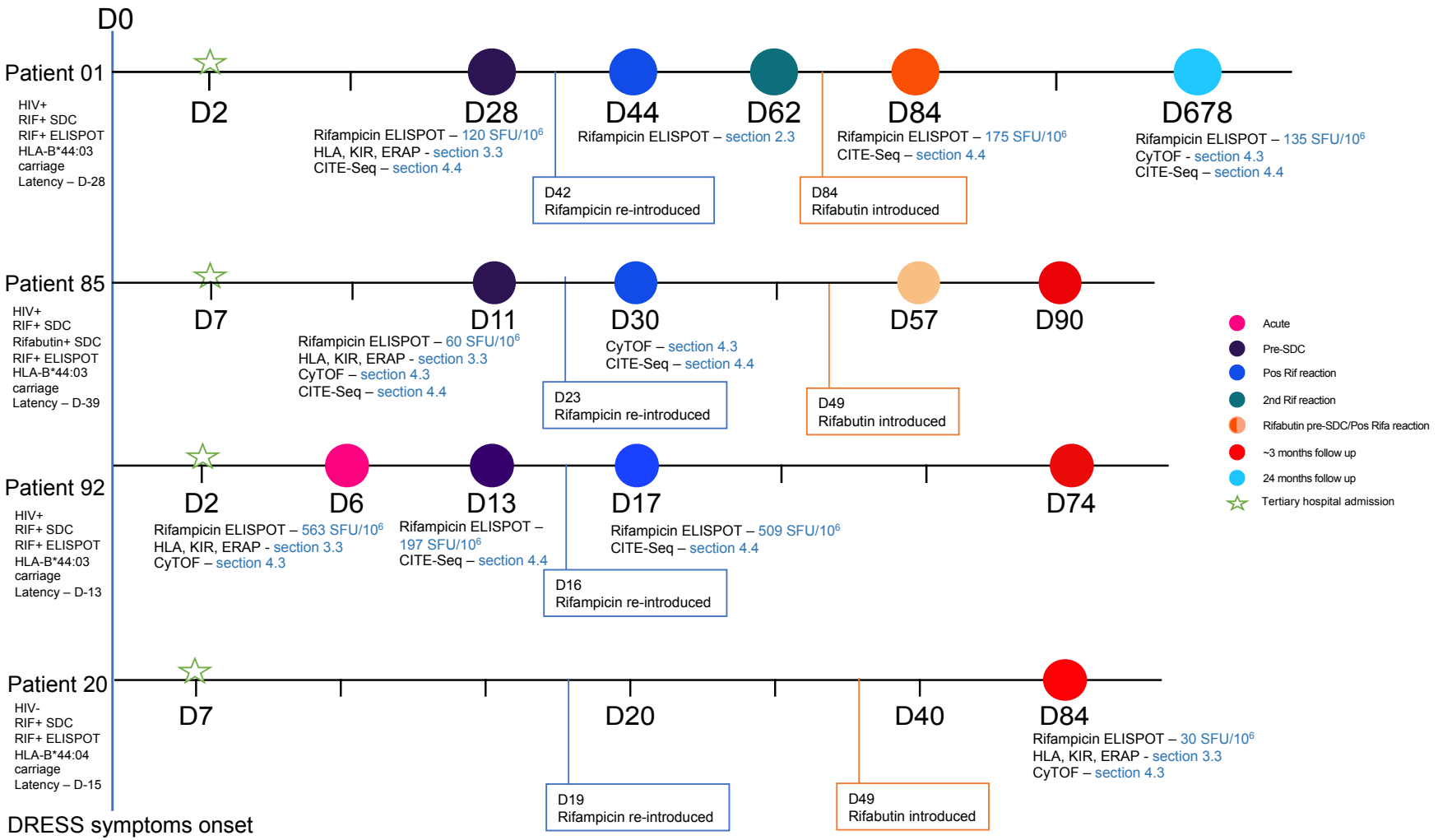

Figure 1-5: Sample collection and experiment guide to chapter 4

Days with no symbols represents the lack of samples at that reaction timepoint. SDC – sequential drug challenge, CITE-seq – cellular indexing of transcriptomes and epitopes, CyTOF – mass cytometry by time of flight, RIF - rifampicin.

A

D-33
Pulmonary TB Sputum GeneXpert
2018/12/14

D-26
Rifafour started
2018/12/21

D0
First skin symptoms
Peeling, stripping, Erythema, DILI, AKI
2019/01/16

D2
All drugs stopped
Backbone started (moxifloxacin, ethionamide, ethambutol)
2019/01/18

D54
1st Discharge regimen
2019/03/11
Rifampicin
INH
EMB
Moxifloxacin

D91
Final Discharge regimen
2019/04/17
Rifabutin
INH
EMB
Moxifloxacin

ART initiated
2019/07/26
Tenofovir, Emtricitabine, Efavirenz

CD4 cell count 63 2019/06/04
HIV Viral Load 40 2019/11/21
HIV Viral Load <50 2020/07/29
HIV Viral Load LDL 2021/07/27

Patient 1 – Definite DRESS

D28
Pre rechallenge bloods, saliva
2019/02/13 11:17:00

D44
RIF reaction bloods
2019/03/01 11:17:00

D62
2nd RIF reaction/ Re-admission bloods
2019/03/19 12:00:00

D84
Pre rechallenge bloods
2019/04/10 12:04:00

24-month FU bloods
2020/11/24 09:29:00

D-33
HIV diagnosis
2018/12/14

D-33
CD4 count = 101
2018/12/14

Patient was not on ART or Bactrim at time of reaction

HLA-A 03:01:01G + 32:01:01G
HLA-B 81:01:01G + 44:03:02G
HLA-C 02:10:01G + 04:01:01G

ELISPOT
RIF 25ug/ml = 120
EMB 50, 500ug/ml = 27
PZA 500ug/ml = 5
INH 500ug/ml = 0
CyTOF

D28
Isoniazid rechallenge
2019/02/13 11:29:00
No reaction

D42
RIF rechallenge
2019/02/27 11:31:00

D43
RIF reaction (24 hours)
2019/02/28
Oedema face/hands
Visible rash.
RIF not stopped
Decision was made to treat through

D59
2nd RIF reaction and hospital re-admission (17 days since rechallenge)
2019/03/16
Fever
Visible rash

ELISPOT
RIF 25ug/ml = 175
EMB 50, 500ug/ml = 0
PZA 500ug/ml = 0
INH 500ug/ml = 0
CyTOF

D84
Rifabutin rechallenge
2019/04/10 12:12:00
No reaction

ELISPOT
RIF 25ug/ml = 132
EMB 50, 500ug/ml = 0
PZA 500ug/ml = 0
INH 500ug/ml = 0
CyTOF

	Normal Range	Acute SCAR 2019/01/17 13:23	Pre-oral SDC 2019/02/13 10:53	Post Oral SDC Rifampicin 2019/02/28 11:45	Reaction (Readmission) 2019/03/22 11:43
Eosinophils	0.00 – 0.8x109/L	0.6	0.21	0.73	2.65
Atypical Lymphocytes		Yes	Yes	Not seen	Yes
ALT	7 – 35U/L	2333	63	64	401
AST	13 – 35U/L		81	76	640
ALP	53 – 128U/L	116	174	139	93
HHV6 PCR		Neg	Neg	Neg	Neg
EBV VL (copies/mL)		-	544	-	<detectable limit
CMV VL (IU/mL)		-	<62	-	290

B

D-30
TB Diagnosis Pulmonary TB - Gene Xpert
2019/09/17

D-32
Rifafour started
2019/09/19

D0
First skin symptoms
Itching, burning, exanthema, erythema
2019/10/21

D7
All drugs stopped
2019/10/28

ART regimen?

D60
Discharge regimen
2019/12/20
INH
PZA
EMB

CD4 count 866 2018/09/25
CD4 count 39 2019/09/16
CD4 count 23 2021/05/25

HIV Viral Load LDL 2016/16/08
HIV Viral Load 3475 2017/05/10
HIV Viral Load 70746 2021/09/22

Patient 85 – Definite DRESS

D11
Pre rechallenge bloods, saliva
2019/11/01 12:51:00

D30
RIF reaction bloods, skin biopsy
2019/11/20 10:20:00

D57
Rifabutin reaction bloods
2019/12/17 11:00:00

-3 years
HIV diagnosis
2016/01/01

D-30
CD4 count = 39
2019/09/17

Patient was not on ART or Bactrim at time of reaction

HLA-A 02:01:01G + 68:02:01G
HLA-B 15:10:01G + 44:03:02G
HLA-C 03:04:02G + 07:01:01G

ELISPOT
RIF 25ug/ml = 60
EMB 50, 500ug/ml = 0
PZA 500ug/ml = 18
INH 500ug/ml = 0
Rifabutin – 0
CyTOF

D15
Isoniazid rechallenge
2019/11/05 11:52:00
No reaction

D23
RIF rechallenge
2019/11/13 10:10:00

D25
EMB rechallenge
2019/11/15 10:39:00
No reaction

D28
RIF reaction (5 days)
2019/11/18
Itching, Burning, visible rash

D29
RIF stopped
2019/11/19 10:41:00

CyTOF

D42
PZA rechallenge
2019/12/02 11:08:00
No reaction

D49
Rifabutin rechallenge
2019/12/09 10:03:00

D55
Rifabutin reaction
2019/12/15
Increased eosinophils, visible rash

Rifabutin stopped
2019/12/15 08:41:00

No PBMCs recovered

	Normal Range	Acute SCAR 2019/10/28 11:30:00	Pre-oral SDC 2019/11/01 10:19:00	SDC Rifampicin Reaction 2019/11/19 09:05:00	SDC Rifabutin Reaction 2019/12/15 09:31:00
Eosinophils	0.00 – 0.8x109/L	1.49	0.01	0.80	1.99
Atypical Lymphocytes		Not seen	Not seen	Not seen	Not seen
ALT	7 – 35U/L	68	56	13	29
AST	13 – 35U/L	118	69	38	53
ALP	53 – 128U/L	68	-	-	-
HHV6 PCR		-	Neg	Neg	Neg
EBV VL (copies/mL)		-	<detectable limit	<detectable limit	<detectable limit
CMV VL (IU/ml)		-	11231	20180	1233

C

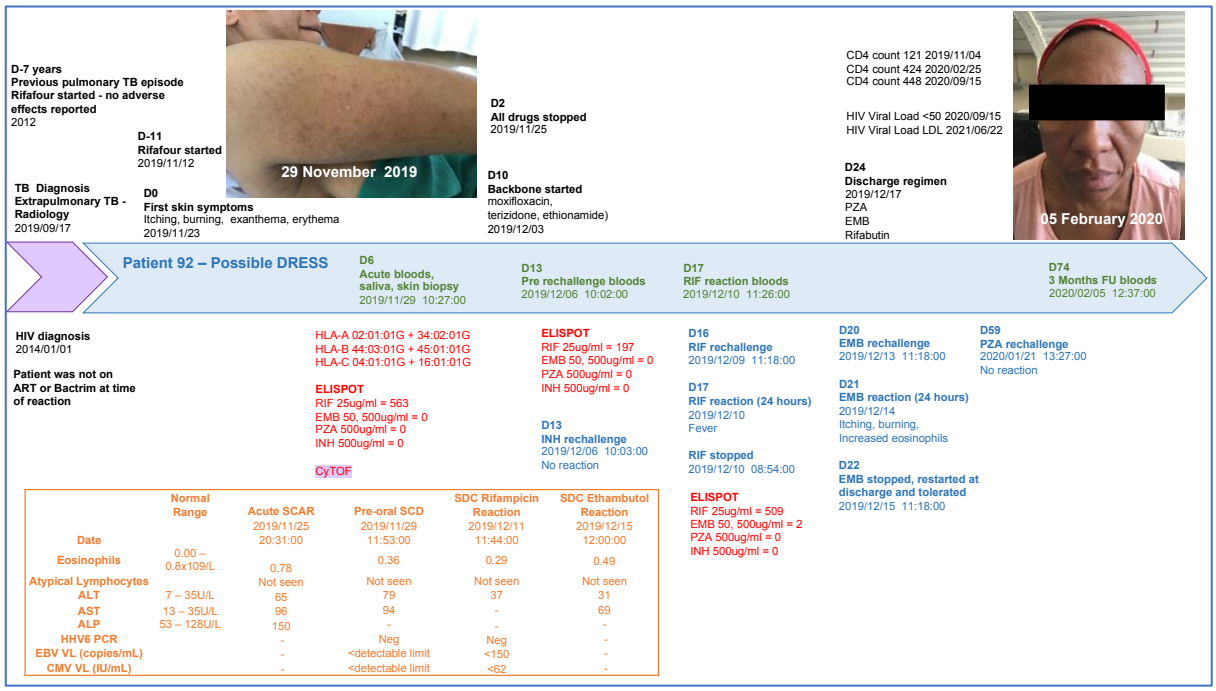

D

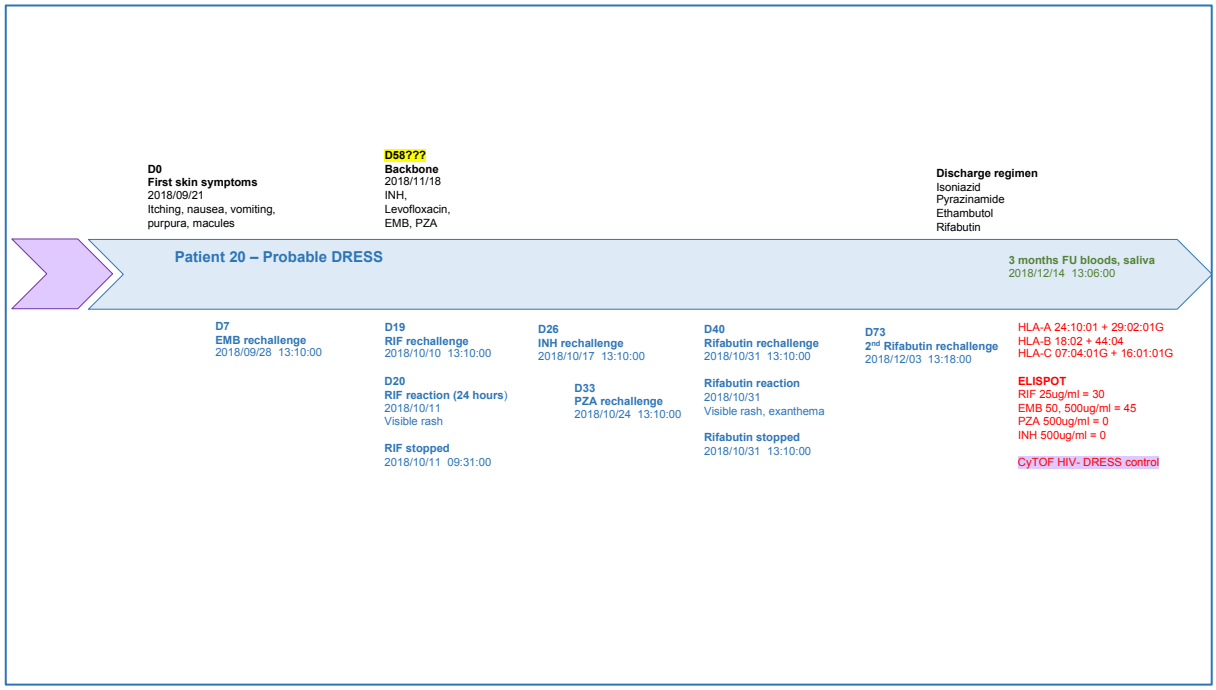

[1]

Figure 1-6: CyTOF and CITE-Seq patients' reaction timelines

Detailed patient reaction timeline including medical history, medication history, laboratory findings, sample collection and experiments performed at relevant timepoints.

[1] Patient 10020 was recruited at 3 months post rifampicin DRESS symptoms and reaction pictures are not available. Probable DRESS validated phenotype was made prospectively.

4.3.2. Immune profiling FLTD induced DRESS by unsupervised analysis

To determine the proportions and phenotypes of unstimulated cells between PLHV and uninfected rifampicin-induced DRESS cases (n=4) and HIV infected drug-tolerant controls (n=4), we performed uniform manifold approximation and projection (UMAP) based on a total 53 613 unstimulated live cells and 14 known major immune cell lineage markers (figure 4-3). Major immune cells were resolved, and we used FlowSOM (Van Gassen et al. 2015) coupled with marker enrichment modelling (Diggins et al. 2017) to unbiasedly cluster cells by shared proteins and determine the number of phenotypically distinct populations in each individual patient.

Secondary clustering identified 10 meta clusters (MC) and the cells were colour highlighted by their respective FlowSOM cluster (figure 4-7A). All major immune cells were identified in cases and controls and based on the expression of lineage markers (figure 4-7B), the clusters were classified into the following 10 cell types: CD4+ T cells (CD3+CD4+ CD25+ CD127+, *MC1*); naïve CD8+ T cells (CD3+ CD8+ CD45RA+, *MC2*); memory CD8+ T cells (CD3+ CD8+ CD45RA−, *MC12*) (Martin and Badovinac 2018; Mahnke et al. 2013); gamma-delta (γδ) T cells (CD3+ TCRgd+, *MC5*); CD8+ CD4+ T cells (*MC4*); B cells (CD3− CD19+ HLADR+, *MC6*); NK cells (CD3− CD19− CD14− CD56+, *MC7*); CD56+ T cells (CD3+ CD56+ TCRgd+, *MC8*); CD14+ monocytes (CD3- CD19- CD14+ CD11c+ HLADR+, *MC10*), and CD16+ monocytes (CD3− CD19− CD56− CD16+ CD11c+, *MC9*) (Maecker, McCoy, and Nussenblatt 2012). The frequencies of each cluster, stratified by reaction timepoint are shown in figure 4-7C, with each slice representing the percent of live cells – the legend shows the contribution of each marker to the cluster.

Comparing distributions of unstimulated cell populations between HIV+ rifampicin DRESS cases (10092; 10085 pre- and post-SDC; 10001), HIV- rifampicin DRESS (10020) at different timepoints of the reaction and HIV+ FLTD tolerant control, we noted memory CD8+ T cells (MC3) were specially enriched in the acute (day 6) sample of 10092 and during *in vivo* Rifampicin exposure (day 11) and positive reaction sample of 10085 (day 30 following 6 days of re-exposure to rifampicin). The highest frequencies of naïve CD8+ T cells (MC2) were observed in the early (day 84, case 10020) and late recovery (day 678, case 10001) samples of DRESS regardless of offending drug and HIV status. High frequencies of both naïve and memory CD8+ T cells (MC2 and 3) were also noted in the drug tolerant PLHV control samples. TCR gamma delta T cells were the only non-conventional immune cells more abundant in HIV- rifampicin DRESS (day 84, 10020). An increase in the percent of CD14+ and CD16+ monocytes was noted in 10085 pre-SDC (day 11), 10020 HIV- (day 84) and late recovery (day 678, 10001) samples. The CD4+ CD8- (MC1) cluster was not further differentiated by unsupervised analysis and the highest frequency of this cluster was observed in HIV- rifampicin DRESS. Although we noted these differences in PBMC frequencies between reaction timepoints;

overall, there was considerable interindividual variations and no consistent differences between HIV+ DRESS cases and tolerant controls, although the HIV negative DRESS patient stands out due to the lack of CD4 T cell depletion. Thus, all differences in PBMC count difference noted can be attributed to effects of HIV on the immune system (Kazer et al. 2020), rather than across the disease course of DRESS or treatment of active TB disease (Table 4-2, figure 4-7C).

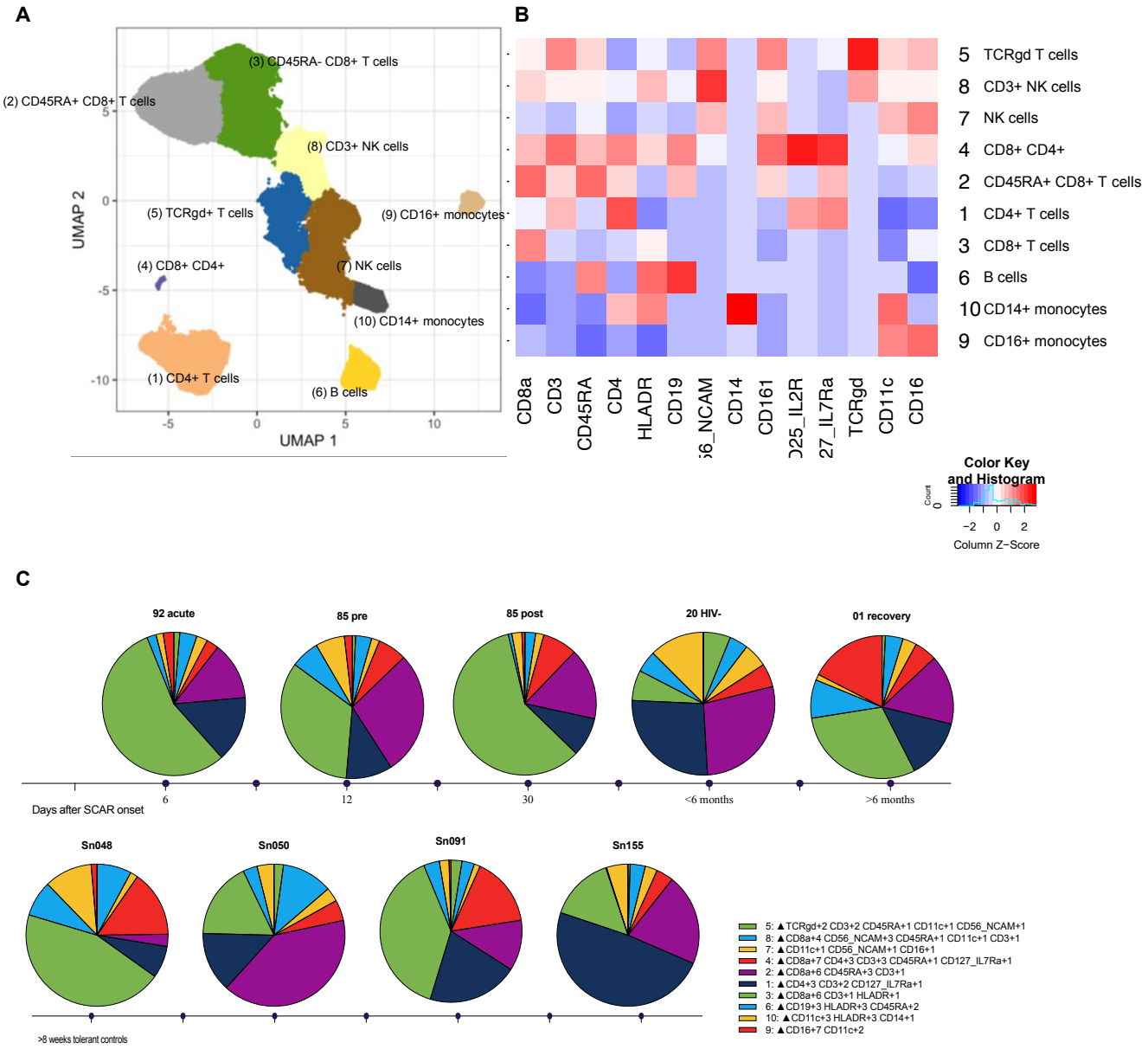

Figure 1-7: Immune cell profiling of unstimulated PBMCs from FLTD DRESS and tolerant controls

Uniform Manifold Approximation and Projection (UMAP) clustering of live PBMCs derived from HIV+ and HIV- rifampicin DRESS cases (n=4) and drug tolerant controls (n=4). **A**) Unsupervised clustering with FlowSOM identified ten major immune cells in unstimulated PBMCs. Parentheses indicate the metaclusters. **B**) heatmap of the median expression of 14 lineage markers used to generate MEM labels which highlights the expression levels on each cell subset. **C**) Pie charts representing relative frequency of major immune cell populations in each participant, stratified by clinical outcome, reaction, and baseline sampling timepoint for tolerant controls. NK, natural killer cell.

Table 4-2: Summary of cell frequencies (% of parent population) by manual gating and unsupervised clustering

Parent population	Cell population	10092	10085 pre SDC	10085 post SDC	10020	10001	Sn048	Sn050	Sn091	Sn155
Live cells	CD4 T cells	14,82	10,48	8,86	26,64	7,30	13,67	20,67	48,64	14,82
	CD8 T cells	68,56	61,84	75,22	34,80	47,54	57,56	50,55	35,61	68,56
	NK cells	6,37	5,44	4,28	9,67	9,55	14,77	4,23	6,25	6,37
	Monocytes	4,05	8,40	2,95	12,51	12,28	3,88	2,66	4,92	4,05
	B cells	2,08	6,49	0,81	4,92	8,11	3,24	3,59	0,17	2,08
	TCRgd T cells	1,33	0,75	0,00	6,14	0,06	2,14	2,49	0,46	1,33
	CD4 CD8 T cells	2,78	6,60	7,87	5,33	15,17	4,75	15,81	3,94	2,78
CD8 T cells	Naive CD8 T cells	13,09	28,08	16,21	27,97	2,78	40,07	11,52	20,85	13,09
	Memory CD8 T cells	55,47	33,76	59,00	6,83	44,76	17,49	39,03	14,77	55,47
NK cells	CD3+ CD56+	3,88	3,65	2,43	4,23	7,82	11,58	2,84	3,47	3,88
	CD56+ NK cells	2,49	1,80	1,85	5,44	1,74	3,18	1,39	2,78	2,49
Monocytes	CD14+ monocytes	1,62	6,60	2,26	12,45	10,94	3,82	2,20	4,81	1,62
	CD16+ monocytes	2,43	1,80	0,69	0,06	1,33	0,06	0,46	0,12	2,43

SDC – sequential drug challenge

4.3.3. Characterization of T cell subsets

We next studied the CD4+ and CD8+ T cells in DRESS patients and controls to identify distinct cell populations that contribute mostly to the reaction. Data analysis included manual gating and unsupervised analysis. Firstly, we used manual gating to identify CD3+ T cells (appendix, section 4.3, gating strategy) – after removal of beads, the first gate was set on time and viability, then we identified CD3+ T cells in the second gate set on parameters CD3 and CD19. We followed by unsupervised analysis on this population of interest which considers the entire T cell landscape and characterisation of CD4+ and CD8+ T cells. It is the same approach as in section 4.3.2 which uses UMAP for dimension reductionality and FlowSOM coupled with MEM for clustering. We looked at markers associated with differentiation, senescence and exhaustion, activation, and regulation.

In figure 4-8A-C, we identified CD4+ and CD8+ T cells in 33 300 CD3+ T cells from 4 rifampicin DRESS cases (two timepoint for 10085) and 4 tolerant controls with three stimulation conditions. Unsupervised analysis revealed five subpopulations of CD8+ T cells including naïve CD8+ T cells as defined by the expression CD45RA+CD28+CD27+ (MC15); central memory are CD45RA-CD28+CD27+/- (MC13); effector memory are defined by the lack of expression of CD45RA-CD28+/-CD27+/- (MC11); terminal differentiated effector memory are CD45RA+/-CD28-CD27+/- (MC8, 16) (Martin and Badovinac 2018) and CD56+ T cells (MC12, 14) (figure 4-8D-E). Although DRESS cases and tolerant controls displayed comparable levels of total CD8+ T cells, with subpopulation we discovered distinct phenotypic groups enriched in HIV+ cases versus HIV+ controls. Specifically, the three DRESS enriched clusters (MC2, 8 and 16) (MC2 mean of 3% in cases versus 1% in controls; $p=0.00413$, MC8 mean of 36% in cases versus 21% in controls; $p=0.000132$ and MC16 mean of 1% in cases versus 0% in controls $p=0.00371$) (figure 4-8F) were all memory CD8+ T cells. For MC16, the co-expression of CD4 was heterogenous between individuals. Further, MC16 T cells increased in cases following stimulation with rifampicin and SEB (figure 4-8G).

The CD4+ T cells compartment was comprised of four major clusters, including naïve CD4+ T cells (MC11), memory CD4+ T cells (MC10). Two CD4+ T cells subpopulations (MC7, 9) were significantly more abundant in HIV+ controls than HIV+ cases (MC7 mean of 1% in cases versus 5% in controls; $p= 0.00743$). For MC9 the differences were noted in the mean event of 6 cells in cases versus 14 cells in controls, $p= 0.000822$ (figure 4-8F). Regulatory T cells (Treg) are best identified by the expression of FoxP3, which is not included in our panel. Since they were not distinctly clustered in FlowSOM analysis, we used the expression of CD127 (low), CD25 (high) and CCR4 (high) to identify a Tregs metacluster (figure 4-8E). The comparison of frequency between cases and controls for all stimulation conditions is shown in figure 4-7J. No differences were not in the frequency of MC

7 and 9 based on stimulation conditions. However, we noted a higher frequency of MC7 in 10020 (HIV- DRESS) and 10001 (late recovery) as compared to other DRESS cases (figure 4-8G).

We further investigated if expanded T cell subpopulations were due to HIV or reaction specific by comparing enrichment between HIV+ and HIV- DRESS (figure 4-8H); between HIV+ participants (cases and controls combined) and HIV- participant (figure 4-8J). The data suggest, expansion of MC8 may be the effect of HIV. Since MC2 is commonly expanded in DRESS irrespective of HIV co-infection, could be a rifampicin specific enriched population. MC16 was still uniquely only enriched in HIV+ DRESS. The expansion of and MC7,9 was shared between HIV- DRESS and HIV+ tolerant controls. The two unconventional T cell phenotypes were CD45RA+ and CD45RA- gamma-delta cells (MC3, 6) and MC constituted mean of 2% in HIV+ DRESS and mean of 6% in HIV- DRESS, $p= 0.000124$. Similarly, comparison of HIV+ and HIV- showed a mean difference with 3%, $p= 0.117$ in HIV+ participants (figure 4-8H, J).

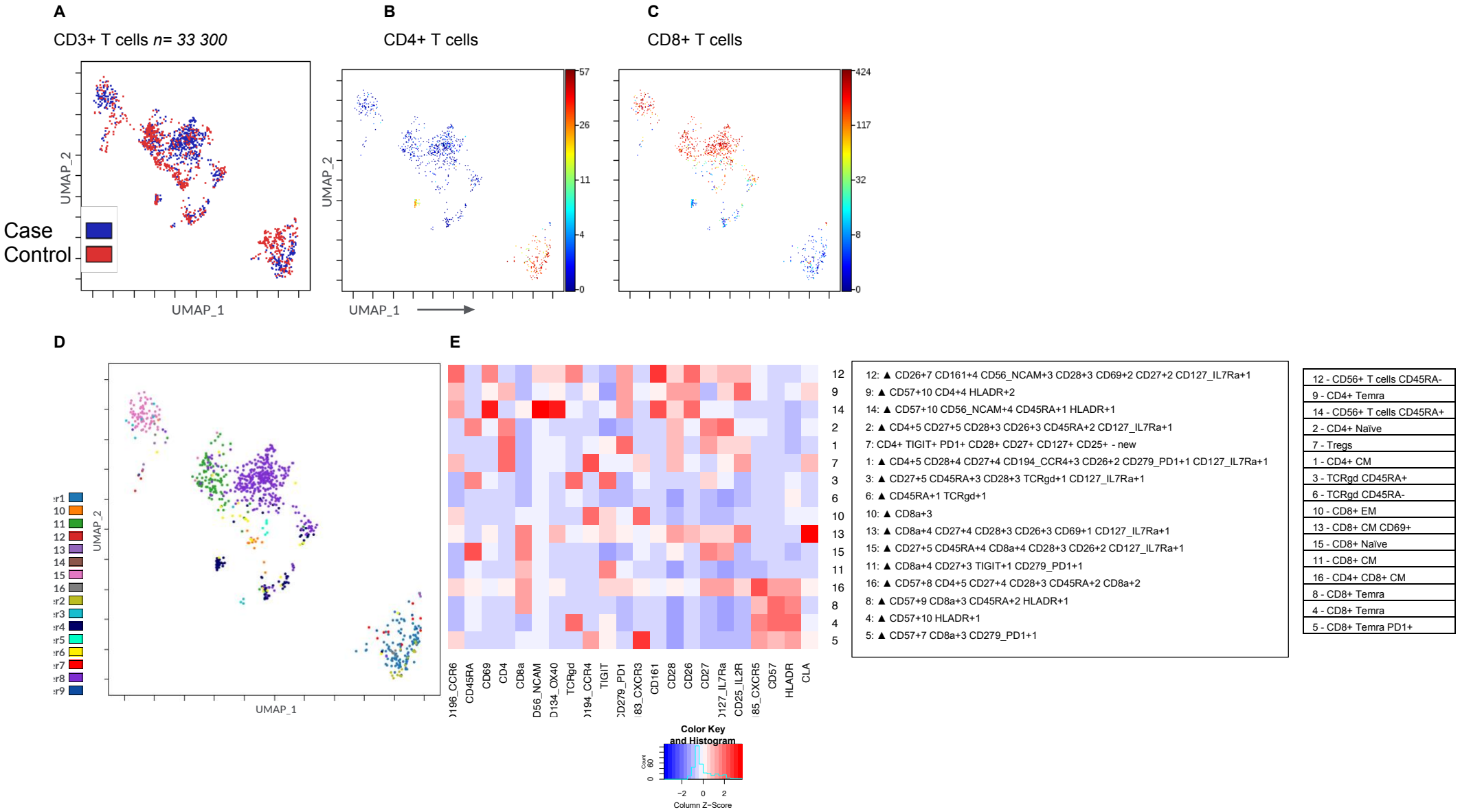
A
CD3+ T cells n= 33 300
B
CD4+ T cells
C
CD8+ T cells
Case
Control
UMAP_2
UMAP_1
57
26
11
4
0
424
117
32
8
0
D
E
UMAP_2
UMAP_1
12: ▲ CD26+7 CD161+4 CD56_NCAM+3 CD28+3 CD69+2 CD27+2 CD127_IL7Ra+1
9: ▲ CD57+10 CD4+4 HLADR+2
14: ▲ CD57+10 CD56_NCAM+4 CD45RA+1 HLADR+1
2: ▲ CD4+5 CD27+5 CD28+3 CD26+3 CD45RA+2 CD127_IL7Ra+1
7: CD4+ TIGIT+ PD1+ CD28+ CD27+ CD127+ CD25+ - new
1: ▲ CD4+5 CD28+4 CD27+4 CD194_CCR4+3 CD26+2 CD279_PD1+1 CD127_IL7Ra+1
3: ▲ CD27+5 CD45RA+3 CD28+3 TCRgd+1 CD127_IL7Ra+1
6: ▲ CD45RA+1 TCRgd+1
10: ▲ CD8a+3
13: ▲ CD8a+4 CD27+4 CD28+3 CD26+3 CD69+1 CD127_IL7Ra+1
15: ▲ CD27+5 CD45RA+4 CD8a+4 CD28+3 CD26+2 CD127_IL7Ra+1
11: ▲ CD8a+4 CD27+3 TIGIT+1 CD279_PD1+1
16: ▲ CD57+8 CD4+5 CD27+4 CD28+3 CD45RA+2 CD8a+2
8: ▲ CD57+9 CD8a+3 CD45RA+2 HLADR+1
4: ▲ CD57+10 HLADR+1
5: ▲ CD57+7 CD8a+3 CD279_PD1+1
CD45RA
CD69
CD4
CD8a
CD56_NCAM
TCRgd
TIGIT
CD161
CD28
CD26
CD27
CD25_IL2R
CD57
HLADR
CLA
Color Key and Histogram
Count
Column Z-Score
12 - CD56+ T cells CD45RA-
9 - CD4+ Temra
14 - CD56+ T cells CD45RA+
2 - CD4+ Naïve
7 - Tregs
1 - CD4+ CM
3 - TCRgd CD45RA+
6 - TCRgd CD45RA-
10 - CD8+ EM
13 - CD8+ CM CD69+
15 - CD8+ Naïve
11 - CD8+ CM
16 - CD4+ CD8+ CM
8 - CD8+ Temra
4 - CD8+ Temra
5 - CD8+ Temra PD1+

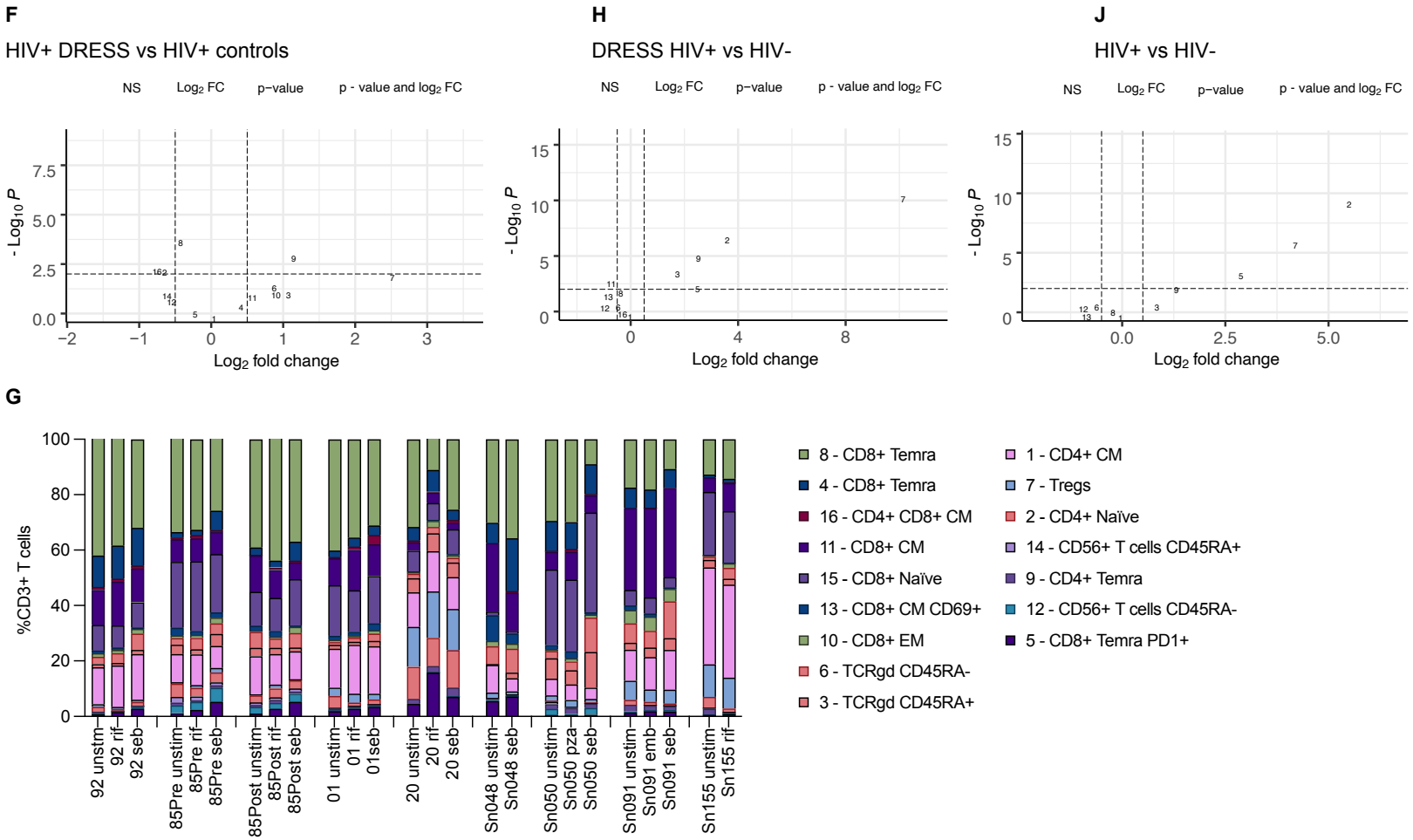

Figure 1-8: Diversity of T cell population in HIV+ DRESS

A-D) Metaclustering of CD3+ T cells from concatenated cells from 4 DRESS cases and 4 tolerant controls at all stimulation conditions: representative UMAP of clustered T cells (*n = 33 300 cells*) overlaid by clinical outcome (**A**), spectral colours indicating protein expression of the T cell markers CD4+ (**B**) and CD8+ (**C**) and with the respective T cell subpopulations clustered by FlowSOM (metacluster numbers indicated in the corresponding population colours) (**D**). **E**) Cluster heatmap showing protein marker expression in each metacluster – independently labelled using MEM (middle) and the canonical annotation of these subsets (left). **F**) Volcano plot of the foldchange of metacluster event count in HIV+ DRESS (right) and HIV+ tolerant controls (right). P values were calculated using a paired, two-sided Student's t-test and corrected using Bonferroni. G) Bar chart of the relative frequency of T cell metaclusters in cases and controls, stratified by reaction timepoint and invitro stimulation condition. H) Volcano plot of the foldchange of metacluster event count in HIV+ DRESS (right) and HIV- DRESS (right). J) H) Volcano plot of the foldchange of metacluster event count in HIV+ participants (right) and HIV- participant (right).

4.3.4. Analysis of T cells enriched in HIV+/- DRESS cases and HIV+ tolerant controls

Within the CD4+ and CD8+ subpopulations, we looked at markers commonly related to T cells activation (CD69, OX40 and HLA-DR), senescence and exhaustion (CD57, PD1, TIGIT), differentiation (CD45RA, CD28 and CD27). Metacluster 8 and 9 CD8+ and CD4+ T cells respectively had high expression of CD57 and no expression of co-stimulation markers CD28, CD27, suggesting a senescent non-replicative population possibly due to chronic antigen stimulation related to tuberculosis and HIV (figure 4-8E). Therefore, we focused functional investigations on metaclsuter 2, 16 enriched in HIV+/- rifampicin DRESS and metacluster 7 in HIV+ tolerant controls.

Firstly, we assessed the expression of CD69 as a marker of early activation, OX40 which plays a major role in promoting T cell clonal expansion and cytokine production and human leukocyte antigen-DR isotype. CD69 expression was high and uniform in a stimulation dependent manner in cases versus tolerant controls. HLA-DR expression was high in resting cells; however, we noted an increased stimulation dependent expression in participant 20, 85 pre SDC and 92. OX40, while of low expression in resting and drug stimulated cells for cases and controls, notably increases uniformly upon non-specific SEB stimulation in cases. These data suggest that cells of MC 16 CD8+ T cells subset in cases are more activated than controls and present a heterogenous spectrum of activation. The magnitude of activation seems to be driven by sampling timepoint; with the highest expression observed in samples collected in the acute stage of the reaction compared to recovery in HIV+ cases (figure 4-9A).

Metacluster 16 had a high expression of CD57 in cases and controls regardless of HIV status and stimulation condition, suggesting replicative senescence and minimal antigen induced T cell apoptosis. Additional markers of exhaustion, PD1 and TIGIT showed no consistent changes between cases and controls, reaction timepoint and stimulation conditions (figure 4-9B). Regarding the effector memory compartment, CD8 T cells are grouped into two distinct clusters based on the expression of CD57 and CD28, CD27 (figure 4-8E). Co-stimulatory molecules (CD28, CD27) expressed by CD8+ T cells are important for T cell activation, formation, and survival of memory subsets. Their presence is vital for induction of immune response and clonal expansion after antigenic stimulation. Co-stimulatory molecules (CD27, CD28) were highly expressed in cluster 16 in cases and controls and all stimulation conditions (figure 4-9C). Increased expression of CD57 and decreased expression of CD27 and C28 are markers of senescent memory CD8+ T cells associated with cytotoxic effector responses and produce interferon-γ. Metacluster 16 cells exhibited a chronically activated (HLA-DR) and differentiated phenotype (CD57), the high levels of co-stimulatory molecules. These findings along with the re-expression of CD45RA on memory phenotype upon stimulation (which is re-

expressed in cell subsets that simultaneously initiate an exhaustion reprogramming in response to antigenic stimulation) (figure 4-9C) suggest proliferative capabilities in addition to the inflammatory and cytotoxic responses. We did not observe any clinical outcome, reaction timepoint or invitro stimulation specific differences in expression of selected markers in metaclusters 2.

In metacluster 7, regulatory T cells (CD4+ $CD127_{low}$ CD25+) we looked at functional characterisation of Tregs based on differential expression of HLA-DR and CCR6. Drug tolerant controls showed a higher expression of HLA-DR than rifampicin DRESS cases, with a significantly higher median expression noted in drug stimulated cells (figure 4-9E). This data suggests an early contact and suppressive activity of Tregs with high FoxP3 expression (Peiser, Becht, and Wanner 2007; Baecher-Allan, Wolf, and Hafler 2006). CCR6 expression on Tregs is associated with activation, memory, and expansion that are indicative for an effector memory function (Kleinewietfeld et al. 2005). The expression of CCR6 was variable in tolerant, however, the median expression was still higher than in rifampicin DRESS cases (figure 4-9F).

Given the well characterised role of T cells at the site of disease in SCAR, we interrogated the expression of chemokines as key regulators of leukocytes trafficking expressed on functionally distinct T cell subsets, including Th2 and Tregs. As indicated in figure 4-9D, no differences were noted in the expression of CCR6, CCR4, CXCR3 and CXCR5 in cluster 16 cells between cases and controls, reaction timepoint and stimulation conditions. However, manual gating using the gating strategy outlined in appendix, section 4.3, showed a lower percentage of CD4+ T cells expressing CXCR3, CCR4 and CCR6 in cases as compared to controls (figure 4-10A). These data suggest an increased attraction and movement of CD4+ T cells to areas of inflammation and immune surveillance with a potential regulatory function in controls than cases. Although not significant, the opposite was observed in CD8+ T cells with a higher mean percentage expression of CXCR3, CCR4 and CCR6 in cases than controls (figure 4-10B) – suggesting trafficking of activated and cytotoxic (higher mean percentage of CD8+ T cells expressing OX40 (CD134) and perforin in cases than controls – figure 4-10C) CD8+ T cells to the site of disease mediating DRESS and associated tissue damage (Peter et al. 2017).

A
Activation

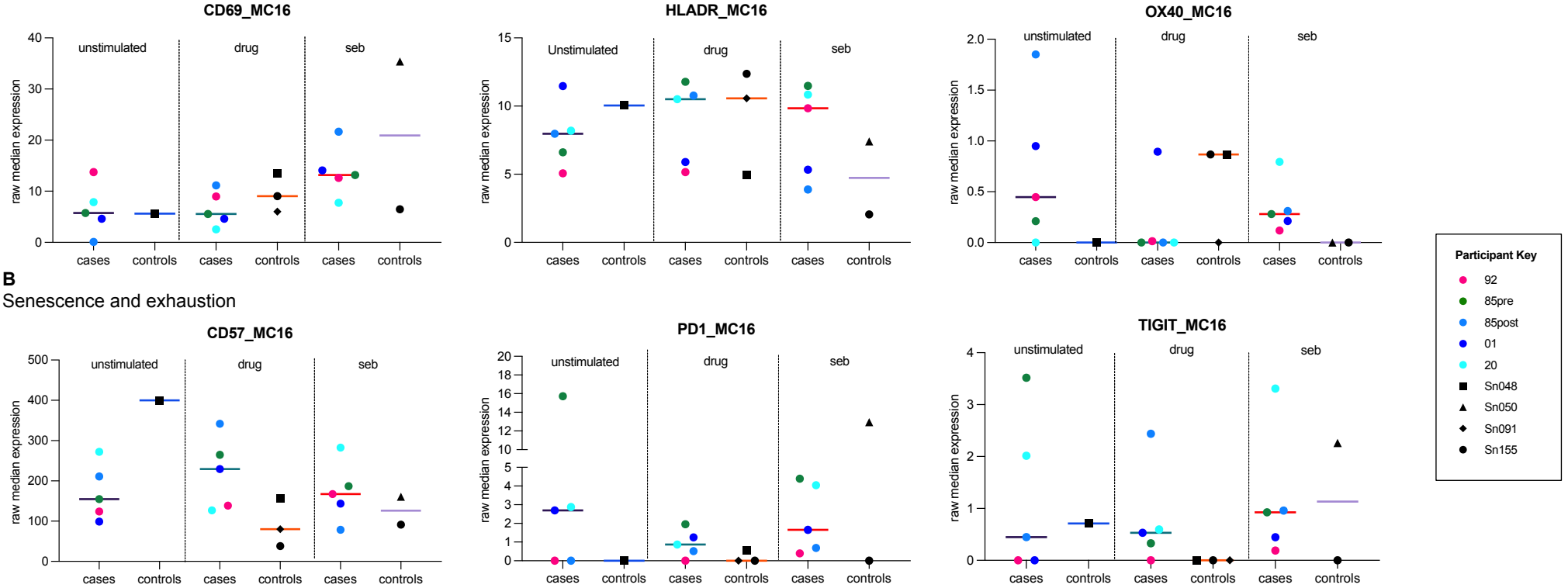

B
Senescence and exhaustion

C
Differentiation

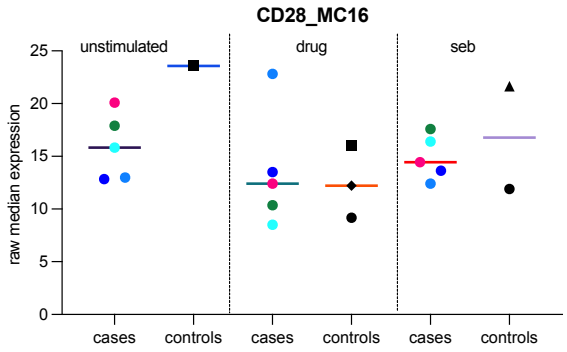

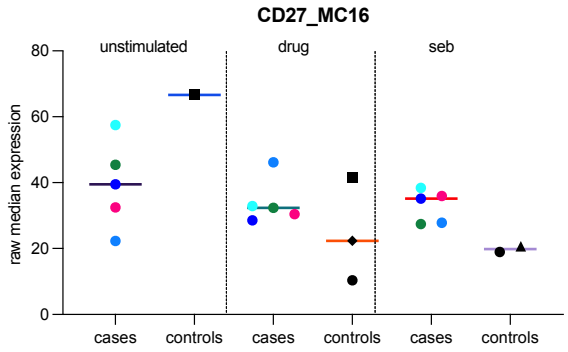

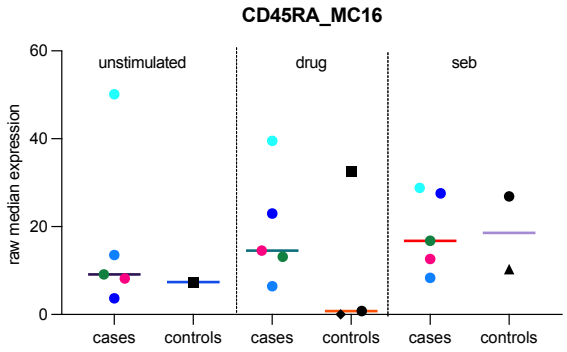

D
Chemokines and skin homing

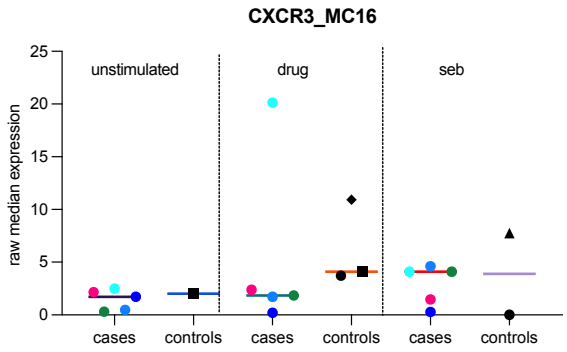

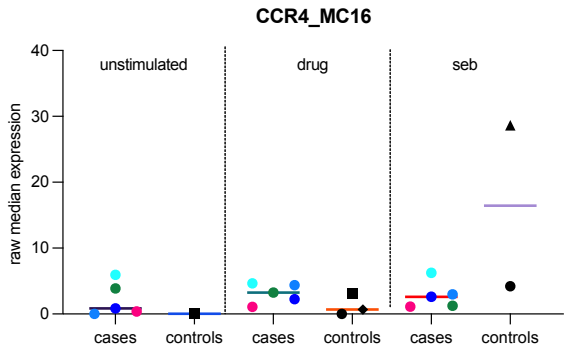

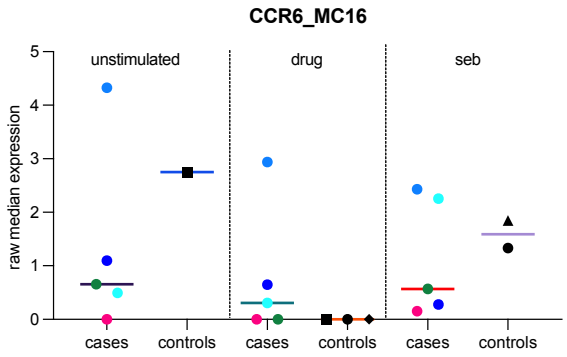

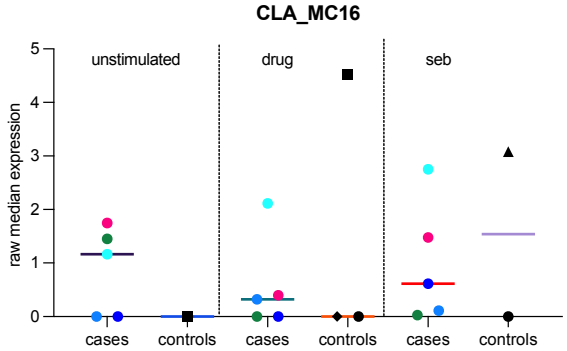

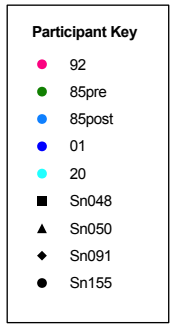

E
Activated regulatory T cells

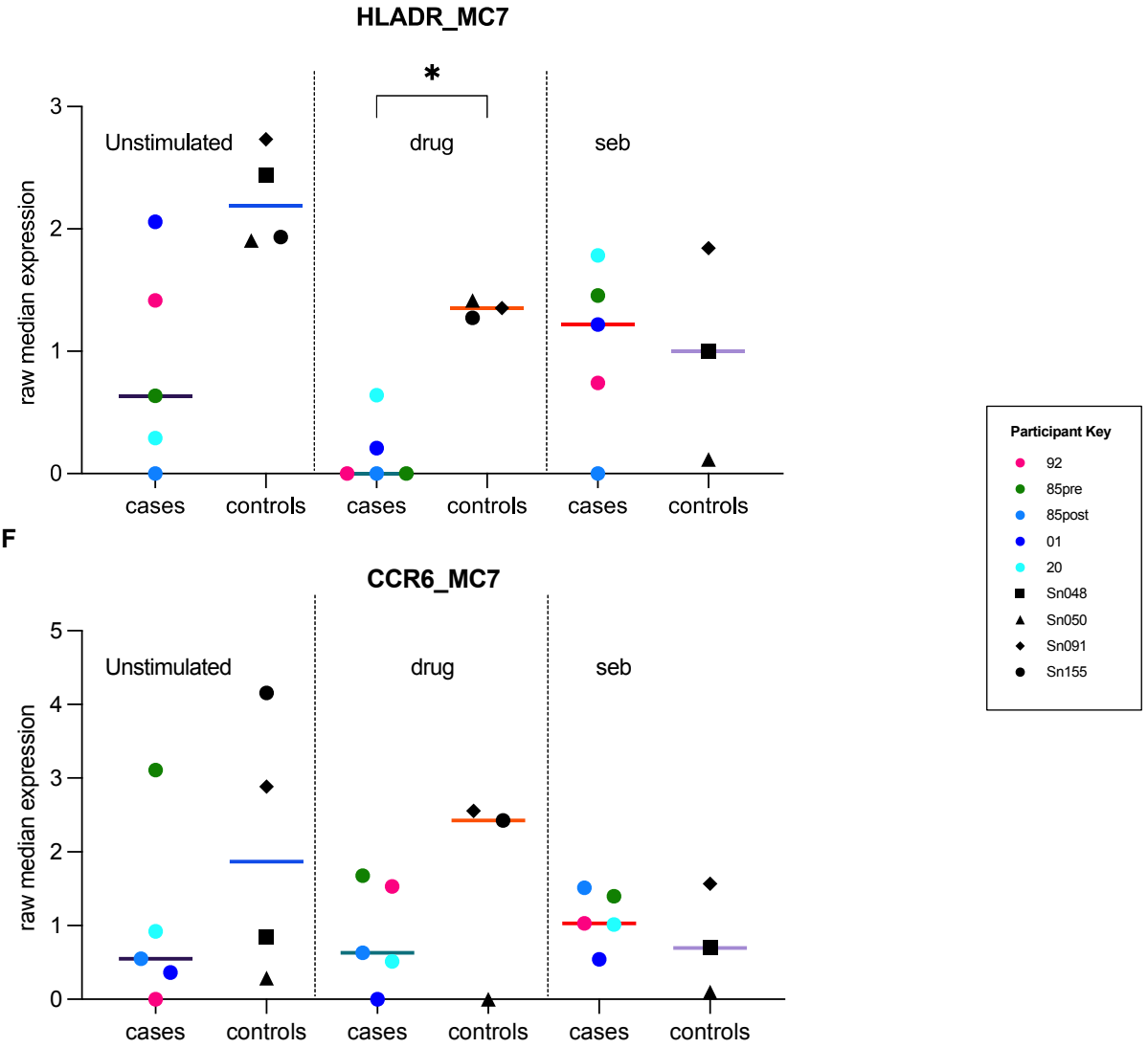

Figure 1-9: Unique T cell signature in DRESS cases compared to tolerant controls.

A-D) Median expression of selected markers in FlowSOM generated immune cluster 16 (CD4+ CD8+ effector memory T cells) and metacluster 7 (regulatory T cells) for each timepoint and in vitro stimulation condition (data for individual HIV+/- DRESS cases (*n=4*) are shown in specific colour. Participants numbers that begin with Sn and are coloured in black, different shapes are HIV+ tolerant controls *n=4*). **A**) Markers related to T cell activation are CD69, HLA-DR and OX40. **B**) Senescence and exhaustion markers are CD57, PD1 and TGIT. **C**) T cell differentiation into naïve and memory subsets is indicated by CD28, CD27 andCD45RA. **D**) Chemokines and skin homing markers included CXCR3, CCR4, CCR6 and CLA. Median expression of HLA-DR (**E**) and CCR6 (**F**) in MC. P value of >=0.05 was considered significant and if not indicated, p value is not significant.

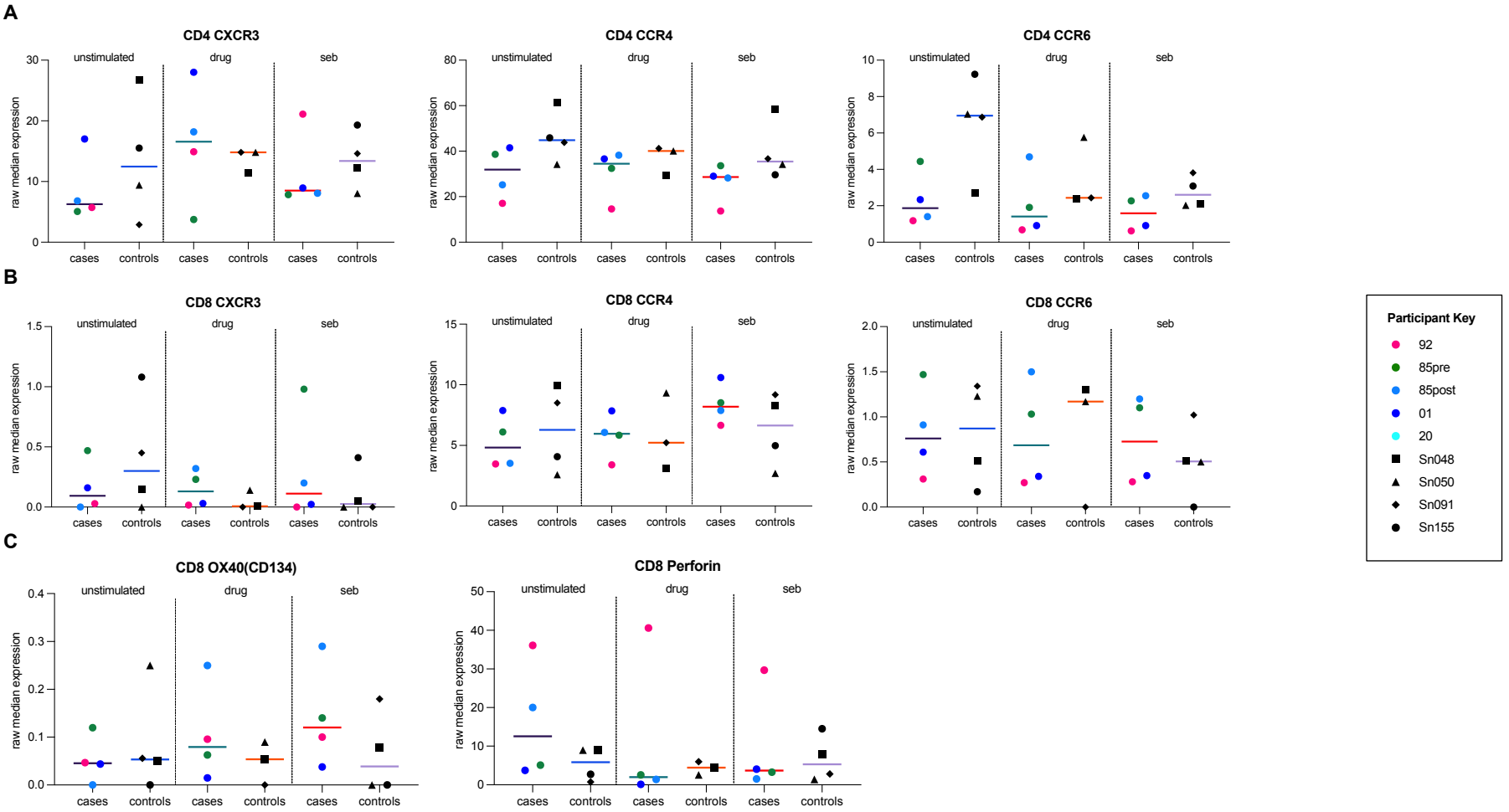

Figure 1-10: Percentage of T cells expressing chemokines and cytokines.

A-C) Representative dot plots expression of different chemokine receptors and effector markers in manually gated CD3+CD4+ and CD3+CD8+ T cells from rifampicin DRESS cases and tolerant controls. The frequency of cells expressing the indicated markers are determined for each participant and in vitro stimulation conditions (each colour represent stimulation condition in HIV+/- cases *n=4* and HIV+ tolerant controls *n=4*). Data represent individual values (dots), mean (centre bar). Mann-Whitney unpaired t-tests were used to compare between cases and tolerant controls with stimulation conditions combined. P value of >=0.05 was considered significant and if not indicated, p value is not significant.

4.3.5. In vitro production of proinflammatory and cytotoxic molecules

We next studied the functionality of CD4+ (MC7) and CD8+ (MC2, 16) T cells enriched in cases and controls, including the production of IFN-γ, IL-17, IL-2, TNF-α, TGF-β and perforin in resting cells and following stimulation with FLTD and SEB. Figure 4-11 shows the raw median expression of intracellular cytokines in metacluster 7, 2 and 16. Based on our ELISpot results, IFN-γ production is dependent on drug specific and non-specific stimulation. In comparison to drug tolerant controls, metacluster 16 cells from cases (10092, 10085 pre, 10085 post and 10020) had a higher and uniform expression of IFN-γ in a stimulation dependent manner. Similarly, to ELISpot results, there was no IFN-γ production in unstimulated, and rifampicin stimulated cells for patient 10001 bloods collected in recovery stage of the reaction (24 months since onset of symptoms). A similar trend of stimulation dependent expression was present in patient 10092, 10085 pre, 10085 post and 10020 with the production of TNF-α (figure 4-11A) and IL-2 (excluding 85 pre). The co-expression of these inflammatory and proliferative cytokines suggests polyfunctionality of cells in this cluster. Perforin was most abundant in DRESS cases than tolerant controls and the expression was similar in all stimulation conditions (figure 4-11B). Analysis of metacluster 2, majority of HIV+ DRESS and HIV+ tolerant controls showed no functionality in response to drug and non-specific stimulation (SEB). This confirmed this population has little to no activity in these participants because of HIV related CD4+ effector dysfunction. HIV- rifampicin DRESS cases had the highest production of IFN-γ, TNF-α, IL-2 and perforin in response to drug and SEB stimulation (figure 4-11C-D). We observed no differences in the expression of IL-17, TGF-β for metacluster 2 and 16.

To investigate whether any functional differences that determine FLTD tolerance, we compared the expression of cytokines in metacluster 7 enriched in drug tolerant controls. There was a high abundance of TGF-β in resting metacluster 7 cells for tolerant controls and interestingly, we also noted higher expression in cases with samples collected when lab findings are within normal range (early recovery – 10085 pre, 3 months – 10020 and 24 months – 10001) relative to samples collected in the acute stage of the reaction (10092, 10085 post) (figure 4-11C). Because immune homeostasis and tolerance is characterised by TGF-β inhibiting expansions and functions of components of the immune system, the general upregulation of markers associated with T cell regulation in tolerant controls suggests expansion of metcacluster 7 influences clinical phenotype. Following stimulation, cells in metaclusters 7 showed no differences in the expression of TGF-β (figure 4-11E) and overall, for other included cytokines. These trends from the unsupervised analysis were confirmed when comparing the median IFN-γ levels in manually gated effector memory CD8+ HLA-DR+ T cells and CD4+ T cells. Comparison of manually gated percentage of expression reflected a similar trend and differences were also not significant.

A

Inflammatory cytokines, proliferative and cytotoxic molecules

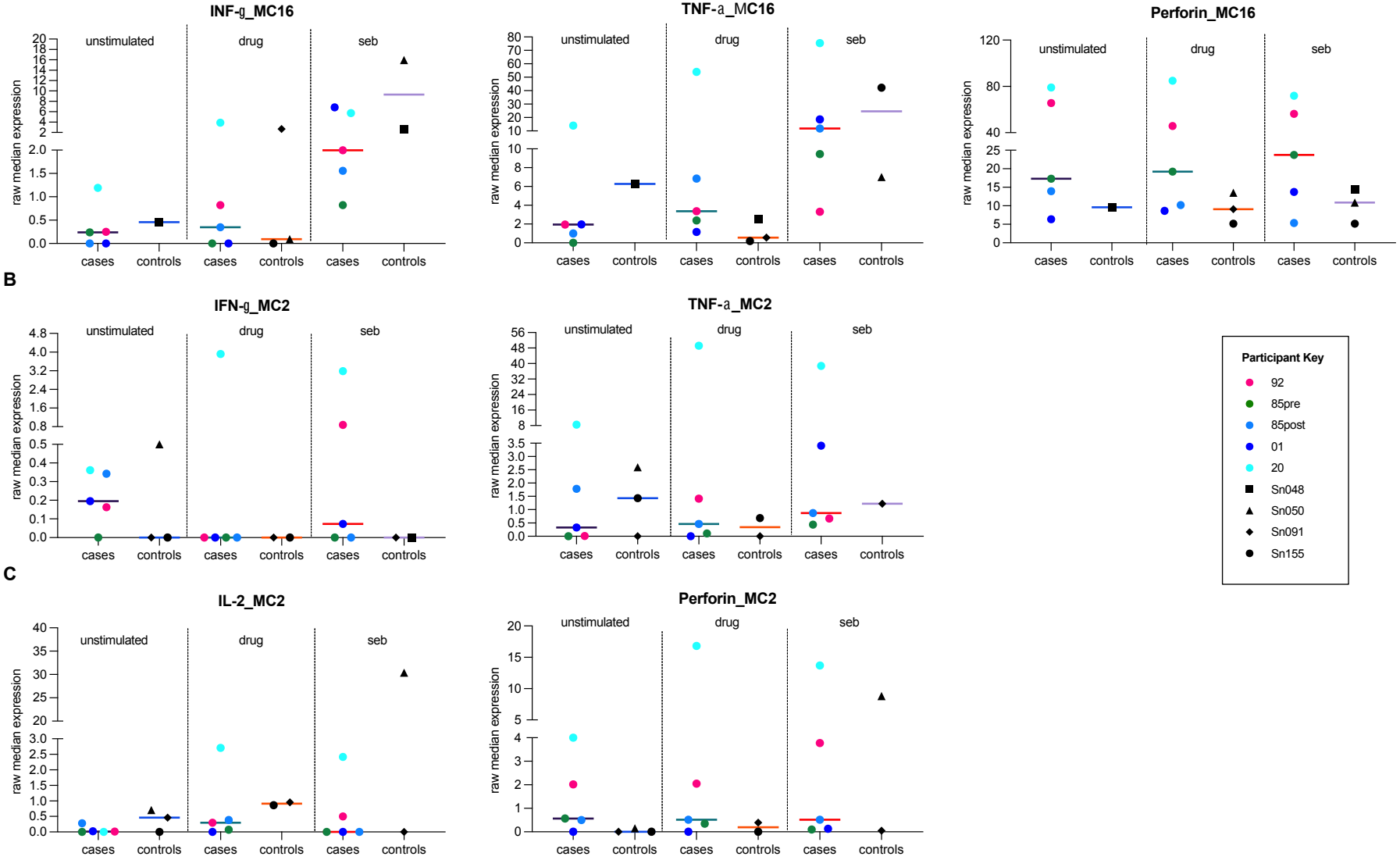

D
Regulatory molecule

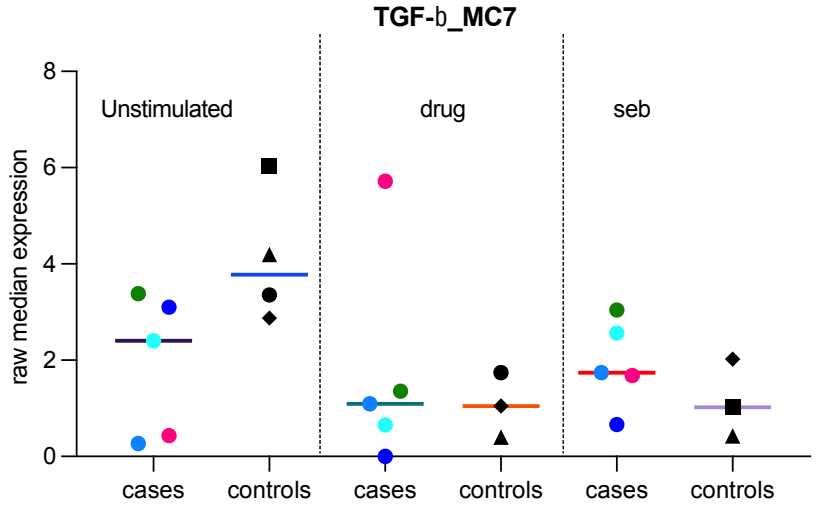

Figure 1-11: Cytokine production by CD4+ and CD8+ T cells after in vitro stimulation with rifampicin and SEB

A-D) Representative dot plots of median expression of intracellular cytokines in FlowSOM generated immune cluster 16 (CD4+ CD8+ effector memory T cells), metacluster 2 (CD4+ effector memory T cells) and metacluster 7 (regulatory T cells) of HV+/- rifampicin DRESS cases and HIV+ tolerant controls after invitro stimulation with drug and SEB. Case and control, stimulation condition and reaction timepoint comparison between the median expression of IFN-γ and TNF-α and perforin (**A**) in metacluster 16. Case and control, stimulation condition and reaction timepoint comparison between the median expression of IFN-γ and TNF-α (**B**), IL-2 and perforin (**C**) in metacluster 2. **D**) Case and control comparison between the median expression of TGF-beta in metacluster 7.

4.3.6. Innate immune responses specific to rifampicin DRESS

We next looked at the differentiation and functionality of CD3- lymphoid cells. We used UMAP generated in section 4.3.3 and NK cells were further were resolved into two clusters (CD45RA+ and C45RA-) while there was no further differentiation of CD14+ classical and CD16+ non-classical monocytes (figure 4-12A-B). CD45RA- NK cells were distinguished as a proliferative, activated cluster with high levels of non-antigen specific production of inflammatory and cytotoxic molecules. Although we did not observe any differences based on stimulation conditions, CD45RA+ NK cells showed a more activated, inflammatory, and cytotoxic response in cases than tolerant controls (figure 4-12C-D). Both clusters had a higher median expression of TIGIT in cases than tolerant controls. NK cells with low levels of TIGIT expression are associated with higher cytokine secretion and cytotoxic potential. This finding may reflect a key component of NK cell mediated innate immune responses in rifampicin DRESS cases and drug tolerance in controls with diminished cytotoxic capabilities.

We observed the strongest changes in CD16+ non-classical monocytes, with an upregulation of TNF-α and IL-2 upon drug and SEB stimulation in cases than controls. The highest drug specific stimulatory responses of this cluster were noted in HIV- DRESS and HIV+ DRESS samples collected in the acute stage of the reaction (10092 and 10085 post) (figure 4-12E-G).

A

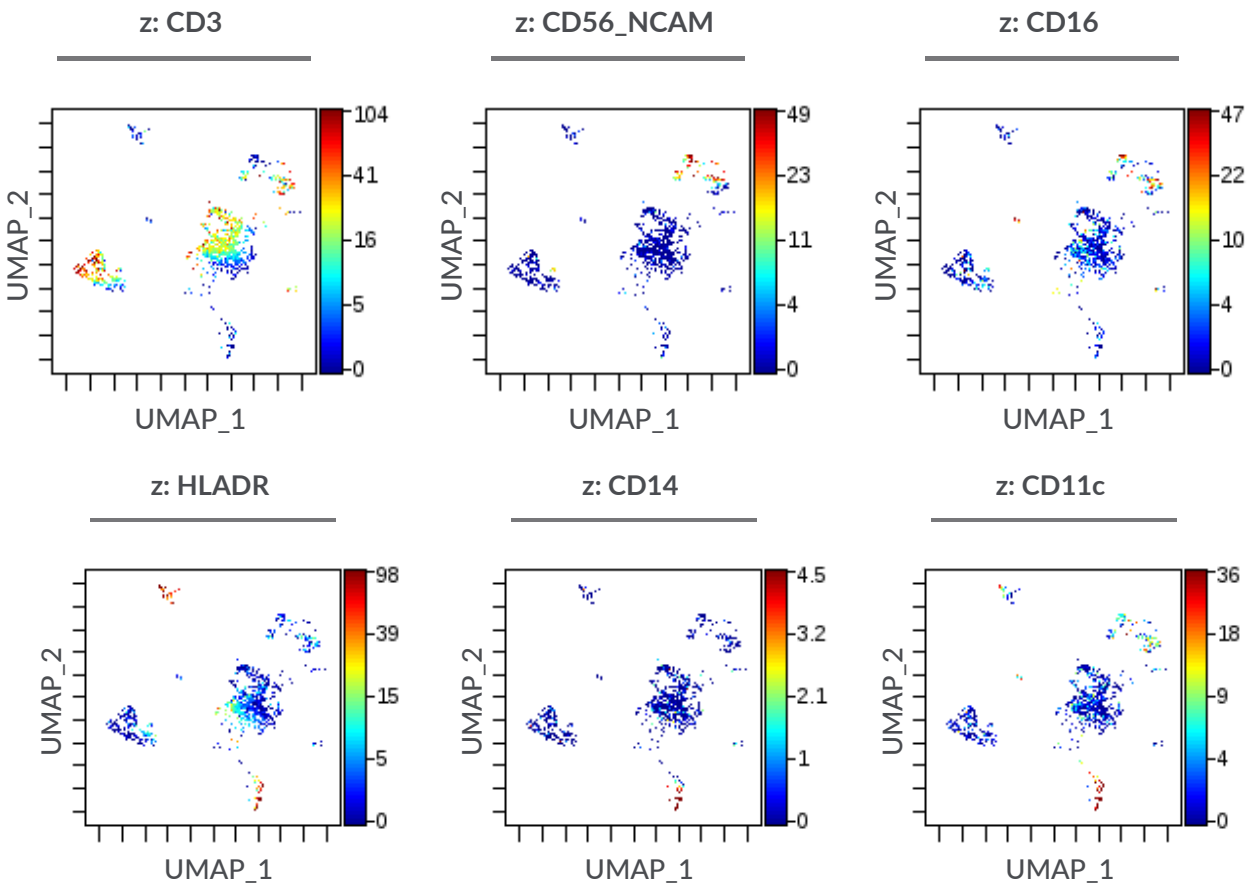
z: CD3
z: CD56_NCAM
z: CD16
z: HLADR
z: CD14
z: CD11c
UMAP_1
UMAP_2
104
41
16
5
0
49
23
11
4
47
22
10
98
39
15
4.5
3.2
2.1
1
36
18
9

B

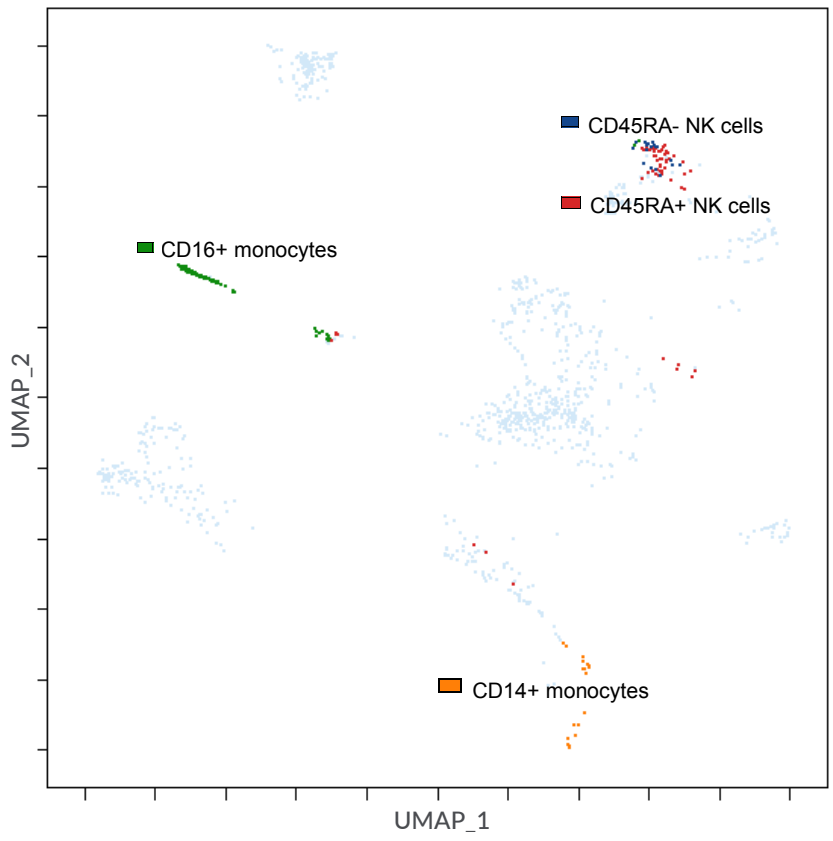
CD45RA- NK cells
CD45RA+ NK cells
CD16+ monocytes
CD14+ monocytes
UMAP_1
UMAP_2

C

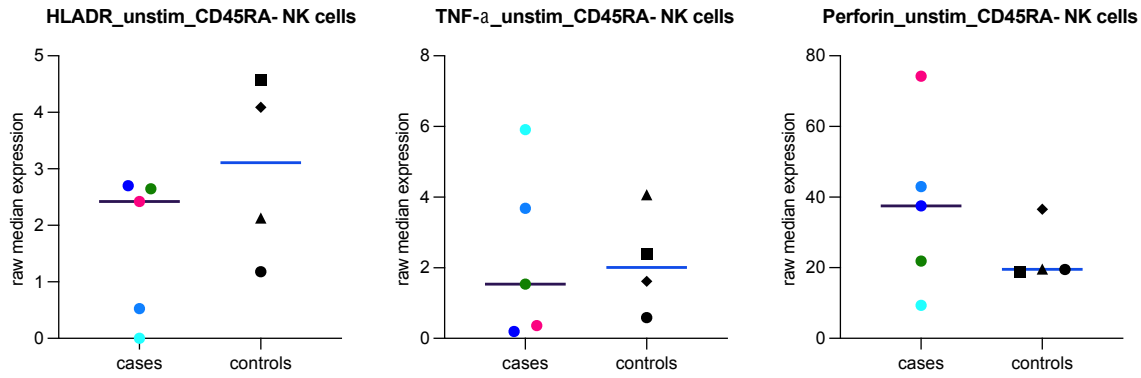
HLADR_unstim_CD45RA- NK cells
TNF-a_unstim_CD45RA- NK cells
Perforin_unstim_CD45RA- NK cells
raw median expression
cases
controls

D

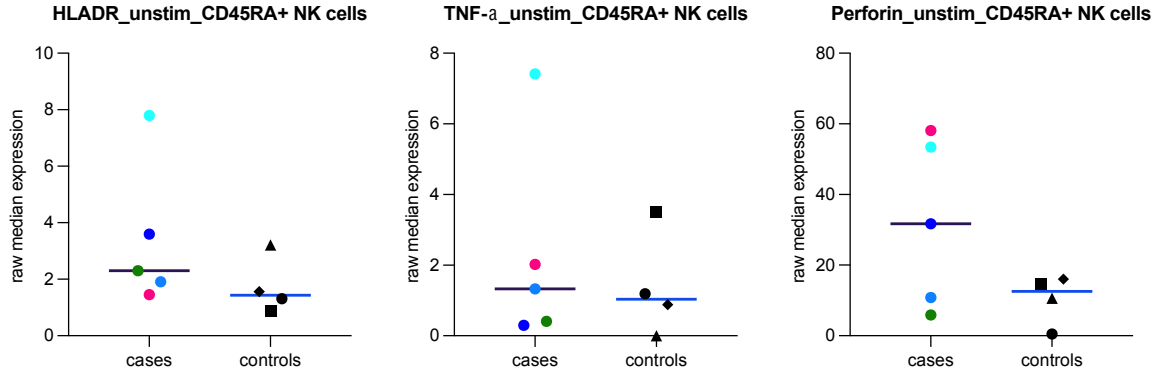
HLADR_unstim_CD45RA+ NK cells
TNF-a_unstim_CD45RA+ NK cells
Perforin_unstim_CD45RA+ NK cells
raw median expression
cases
controls

E

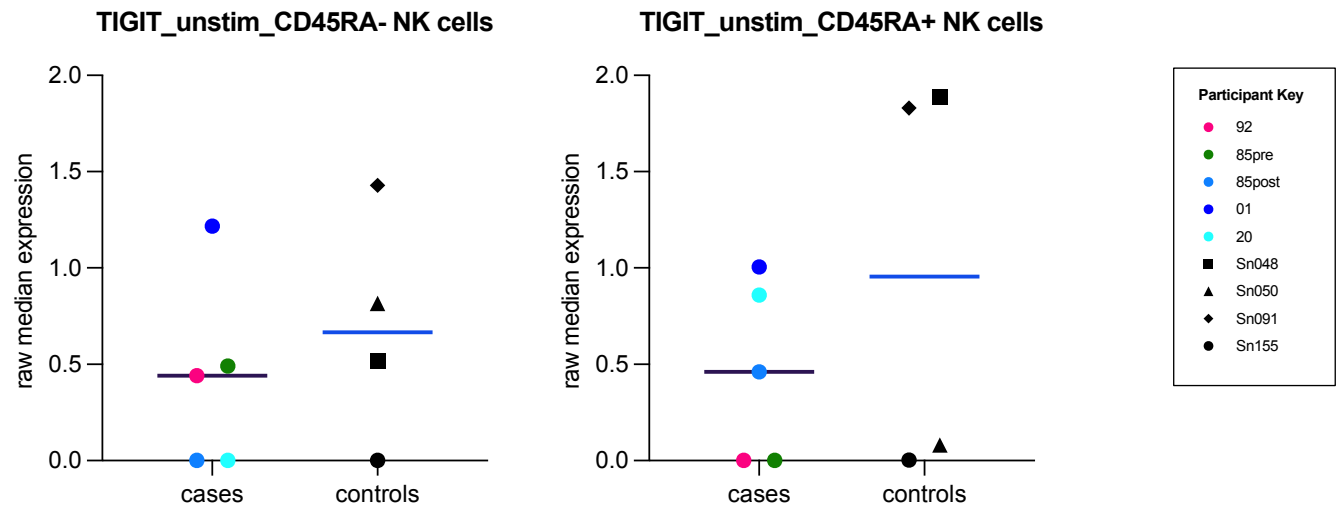
TIGIT_unstim_CD45RA- NK cells
TIGIT_unstim_CD45RA+ NK cells
raw median expression
cases
controls
Participant Key
92
85pre
85post
01
20
Sn048
Sn050
Sn091
Sn155

F

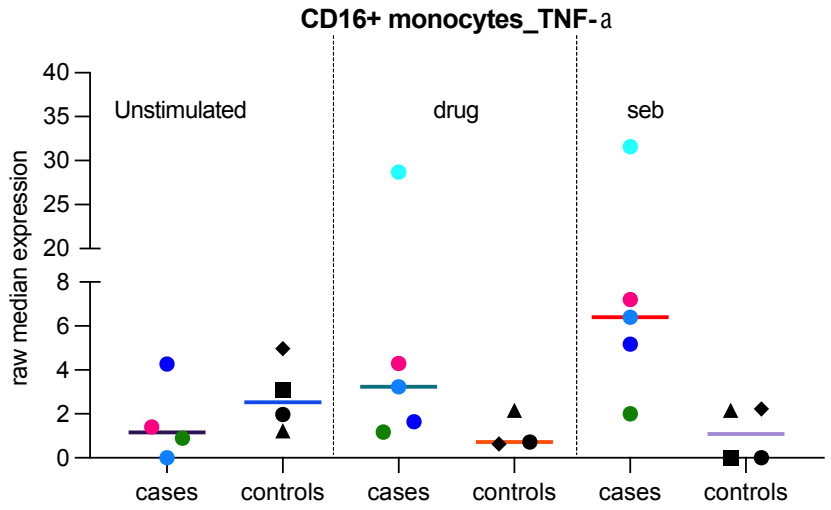

G

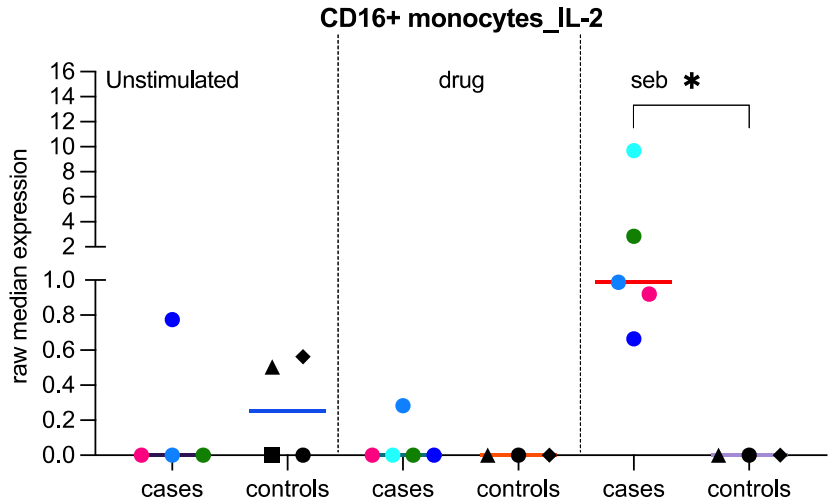

Figure 1-12: Monocytes and NK cells in rifampicin DRESS

A) UMAP of spectral colours indicating protein expression of the CD3- cell markers CD56+ (NK cells) CD14+CD11c+ (CD14 monocytes and CD16+CD11c+ (CD16 monocytes). **B**) UMAP with the respective populations clustered by FlowSOM (metacluster labelled and identified by colour). **C-D**) Representative dot plots showing median expression of HLA-DR, TNF, and perforin in CD45RA- NK cells (**C**) and in CD45RA+ NK cells (**D**). **E**) Representative dot plot indicating expression of regulatory molecule TIGIT in CD45RA+ and CD45RA- NK cells. **F**) TNF **G**) IL-2 expression in CD16+ monocytes. *p < 0.05, **p < 0.01, ***p < 0.001, and ****p < 0.0001, Mann-Whitney test, Bonferroni correction and if not indicated, p value is not significant.

4.4. Results – Cite-seq

4.4.1. Cite-seq immune profiling

To further decipher key differences in immune molecular mechanisms and signalling pathways in pre vs post SDC and recovery bloods, we analysed immune cells using Cite-seq, a method that quantifies proteomic and transcriptomic data within a single cell readout (Stoeckius et al. 2017). We collected data from 55916 cells pre- and post-SDC in three rifampicin DRESS patients (10001, 10085 and 10092) and in the recovery stage (patient 10001) of the reaction (see figure 4-5). In our Cite-seq analysis we only looked at HIV infected rifampicin DRESS cases. 5′sc-TCR-RNA-Cite-seq collects data on pre-selected surface protein marker expression, transcriptomics and TCRs of individual cells. We identified and clustered groups of cells using canonical genes and surface antibody expression of lineage markers resulting in 10 clusters organised into populations including B cells, CD4+ T cells, CD8+ T cells, dendritic cells, erythrocytes, hematopoietic stem cells (HSC), macrophages, monocytes, neurons, and natural killer (NK) cells (figure 4-13A).

Consistent with our CyTOF results in HIV infected patients, majority of immune cells were CD8+ T cells (figure 4-13B). All cell subsets were compared between reaction timepoints and following *in vivo* drug stimulation. The CD8+ T cells were significantly enriched in post-SDC bloods compared to pre-SDC in all three patients regardless of in vitro stimulation conditions ($p=0.0022$) (figure 4-13C). In contrast, monocytes and macrophages were more abundant in pre- than post-SDC samples ($p=0.0260$) with minimal to no differences between stimulation conditions (figure 4-13D). After Bonferroni correction for multiple comparisons, only CD8+ T cells differences between pre-SDC and post-SDC were significant.

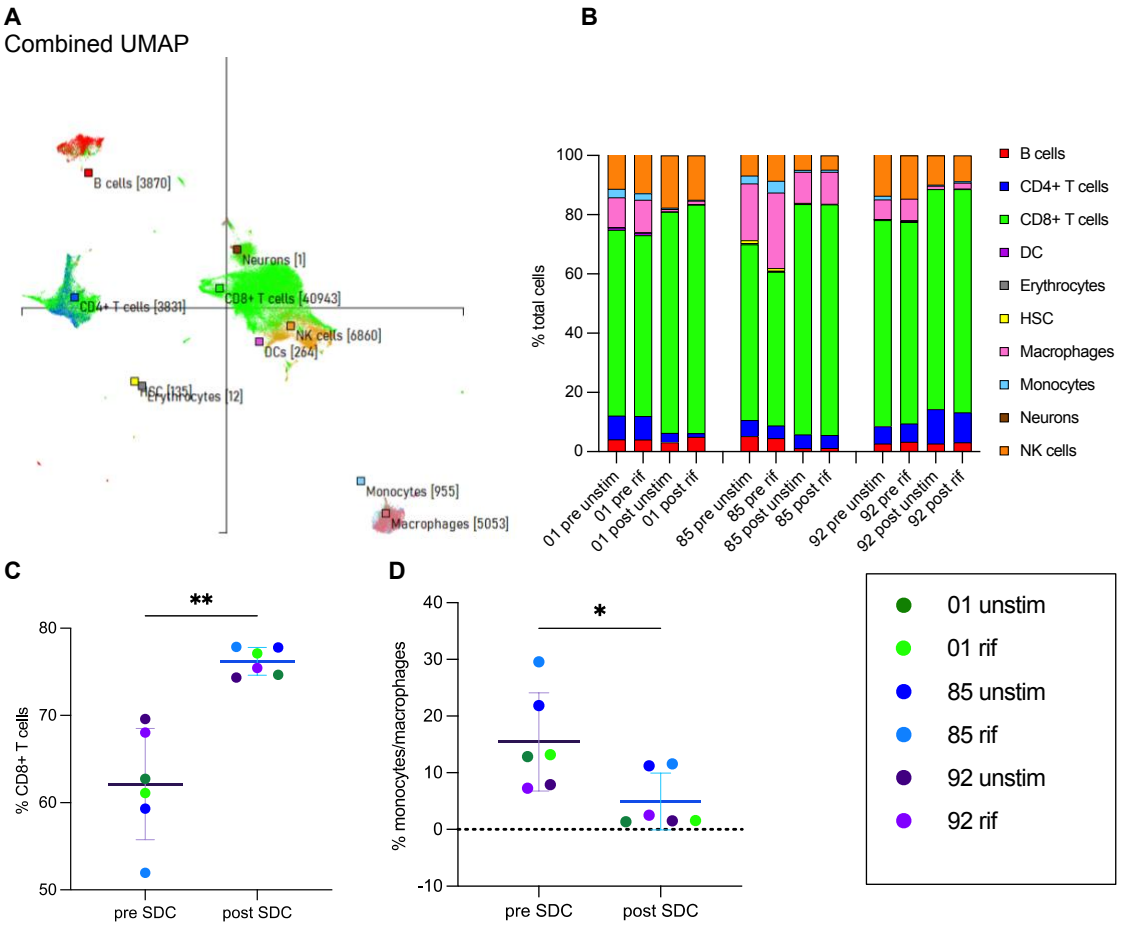

Figure 1-13: Analysis of pre and post rifampicin SDC bloods using Cite-seq

A) Combined UMAP plot (n = 55916 cells) clustered by antibody expression and overlaid by cell type. **B)** Bar chart of cell type frequencies in unstimulated and rifampicin stimulations at pre and post SDC timepoints (01 pre unstim n = 3410, 01 pre rif n = 4230, 01 post unstim n = 2001, 01 post rif n = 2452, 85 pre unstim n = 2340, 85 pre rif n = 3154, 85 post unstim n = 2158, 85 post rif n = 2002, 92 pre unstim n = 2272, 92 pre rif n = 3280, 92 post unstim n = 1937, 92 post rif n = 3557). Scatter plot showing frequency of CD8+ T cells (**C**) and monocytes/macrophages (**D**). All cell types were compared between reaction timepoints and stimulation conditions. The approximate P values were determined using a two-sided Mann-Whitney test, lines indicate the mean. Unstim – unstimulated cells, rif – 25ug/ml rifampicin stimulated cells, SDC – sequential drug challenge, NK cells – natural killer cells.

4.4.2. Landscape of circulating T cells in rifampicin induced DRESS

We further classified T cells from the 5′sc-TCR-RNA-Cite-seq profiling based on the expression of canonical genes (figure 4-14A-B). CD8+ and CD4+ T cells subsets showed distinct expansions and alterations in functional states. Pre SDC and recovery samples have a higher percentage of naïve and central memory T cells. Differentially expressed genes (DEGs) were projected on the T cell UMAP to show high expression of naïve and central memory markers (CCR7, SELL, CD27) in pre SDC samples (figure 4-14E). Post-SDC samples showed an expected expansion of CD8+ effector memory T cells (figure 4-14C). We noted a high amount of interindividual variability of regulatory T cells between patients and stimulation conditions (figure 4-14D).

Although both pre and post SDC unstimulated T cells showed gene expression consistent with chronic viral infection (Kazer et al. 2020), post SDC samples display an increase in activation and cytotoxicity markers compared to pre SDC which likely represents the T cell activation associated with in vivo rifampicin exposure at the time of sampling (figure 4-14F); DEGs with fold change >0.6 and P adjusted >0.05 are labelled and include: cytotoxic molecules (GZMB, GNLY, GZMH, NKG7 and CST7) and proinflammatory chemotaxis CCL5 which is expressed on recently activated T cells via TCR (Swanson et al. 2002) and is a chemoattractant of eosinophils (Daugherty et al. 1996) (figure 4-14F). Signalling pathway analysis in pre-SDC unstimulated T cells highlighted viral processing and viral specific responses whereas activation and effector functions were expressed in post-SDC unstimulated T cells. The genes in the alpha-beta T cell activation (ZNF683/TRBC2/TRBC1/ TBX21/RORA/PTPRC/PTGER4/PRDM1/NKG7/IL2RG/HMGB1/EOMES/CD3G/CD3D/BCL11B/ ANXA1), cell killing (SLAMF7/ SH2D1A/PTPRC/PRF1/NKG7/KLRD1/HMGN2/GZMB/GNLY/ GAPDH/FCGR3A/CX3CR1/CTSC/CD2) and TCR signalling (TRGC2/TRBC2/TRBC1/THEMIS/ SH2D1A/PTPRJ/PTPRC/CD8A/CD3G/ CD3D/BTN3A1) are consistent with recent antigen interaction and effector phenotype (figure 4-14G). These data confirm our CyTOF observations where in post-SDC unstimulated samples and during *in vivo* rifampicin stimulation there is evidence of differing degrees of activation that overlap with exhaustion and is evident despite the background state of HIV-driven perturbations of the T-cell compartment and activation state. The expression of CCL5, IL2RG and cytotoxic effector molecules (PRF1, GZMB, GNLY) indicate effector differentiation, suggestive of replicative, inflammatory, and cytotoxic responses despite the hybrid or co-expression of exhaustive markers.

A

Combined UMAP - T cells differentiation

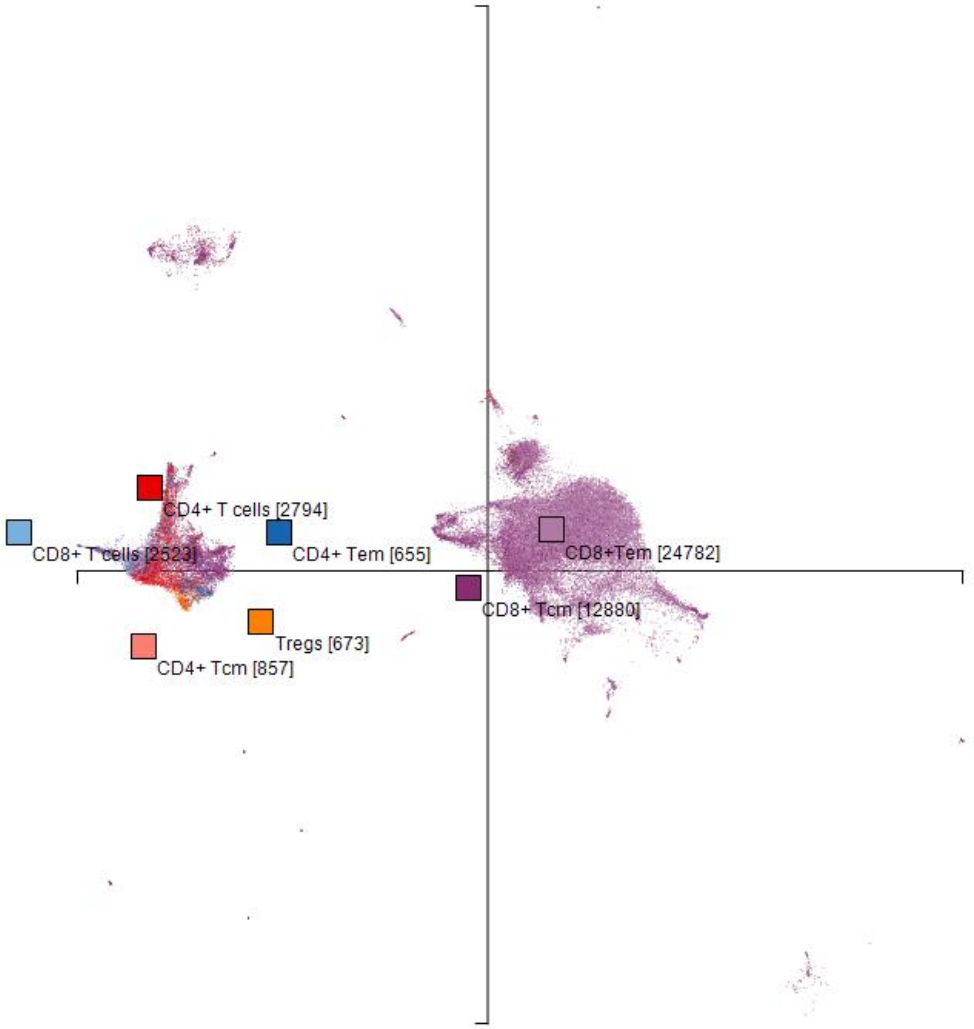

B

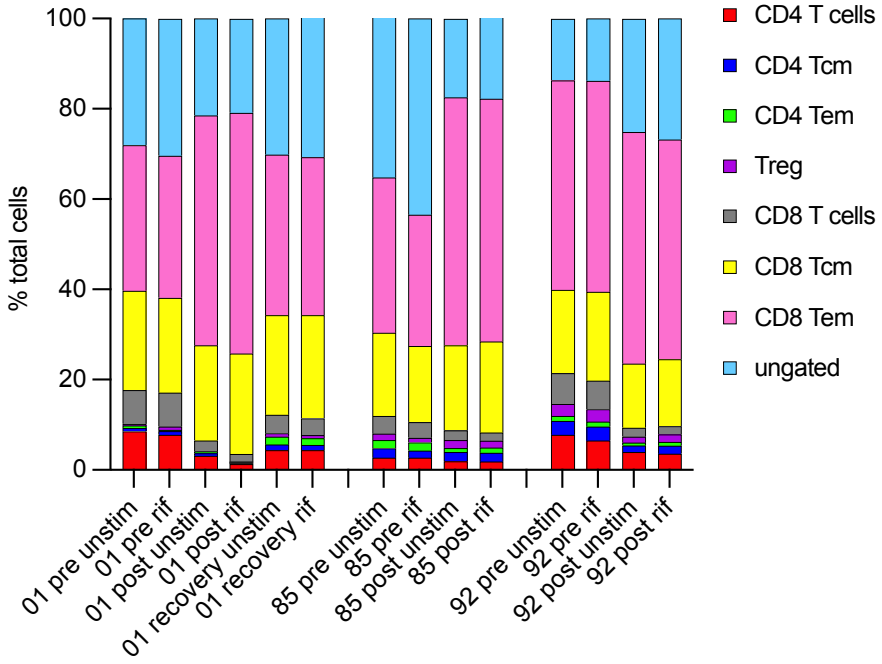

C

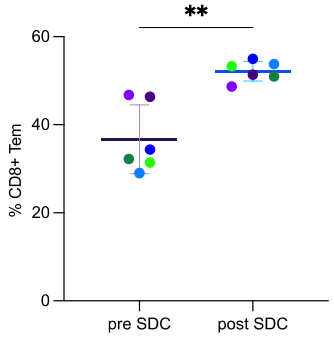

D

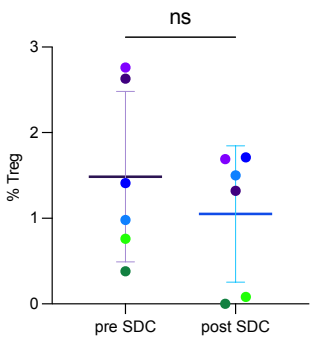

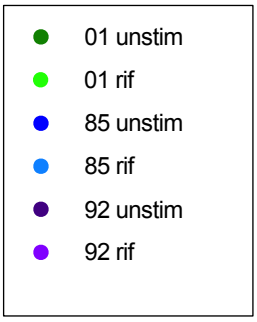

E

Combined pre and post unstimulated heatmap

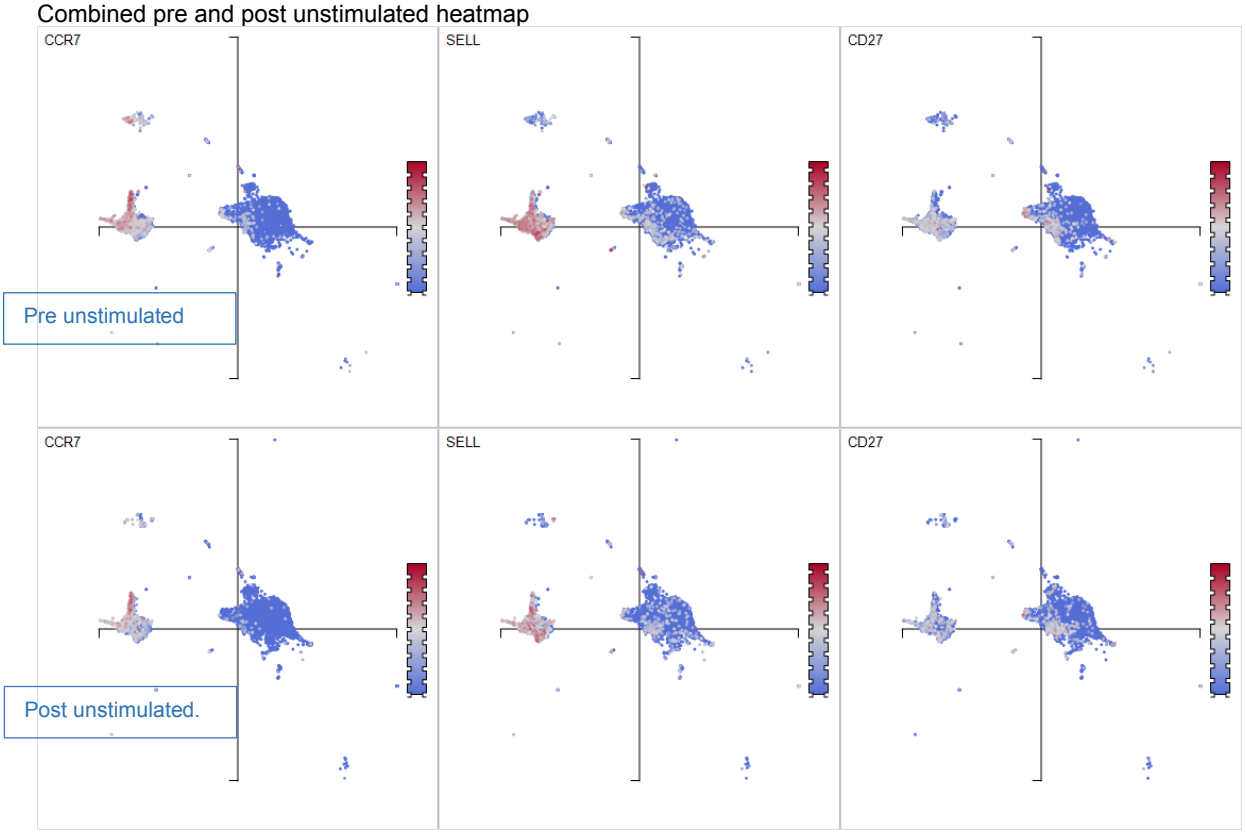

F

Combined pre- and post-SDC unstimulated T cells

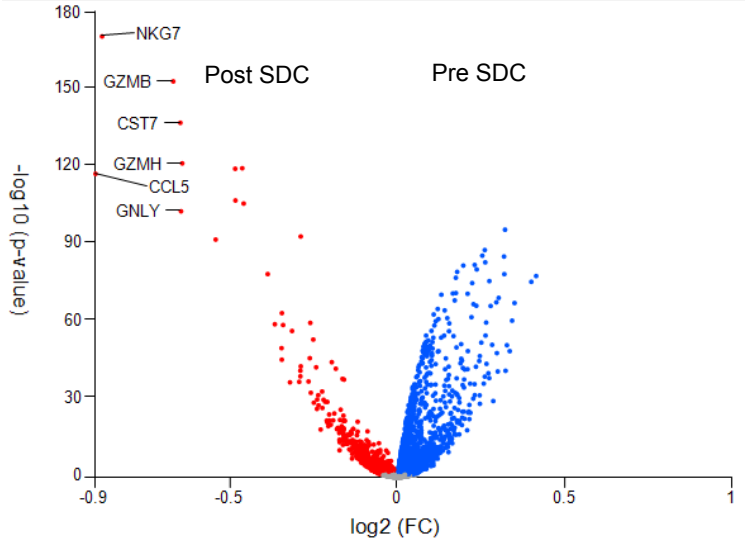

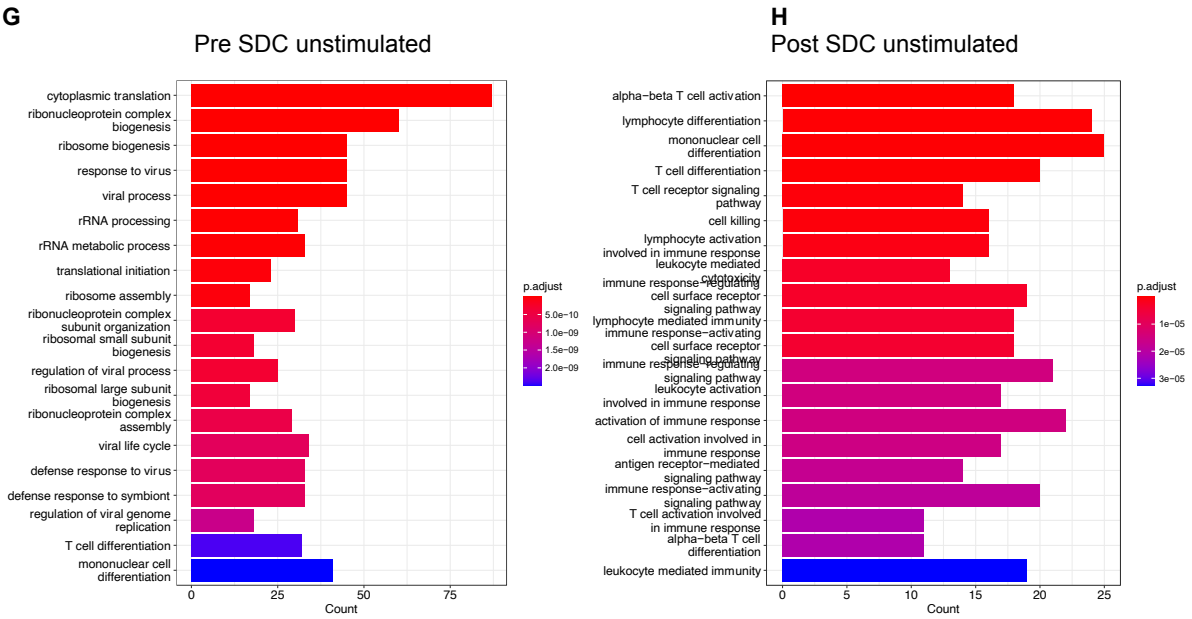

Figure 1-14: Characteristics of circulating T cells in rifampicin induced DRESS

A) UMAP plot clustered by canonical genes and antibody derived expression and overlaid by T cell subset. **B**) Bar chart of T cell frequencies in three DRESS patients, two reaction timepoints and two in vitro stimulation conditions. **C-D**) Scatter plots showing population percentage of effector memory CD8+ T cells and regulatory T cells (Treg) stratified by reaction timepoint, and each patient annotated by dot colour. Data were analysed with the Mann-Whitney test. Values are mean with standard deviation and P value <0.05 was considered significant after Bonferroni correction for multiple comparisons. All T cell subpopulations were compared between reaction timepoints and stimulation conditions. **E**) UMAP plots showing the expression of T cell differentiation markers in pre- and post-SDC unstimulated cells. **F**) Volcano plot of DEGs determined by two-sided t-test and FDR correction in unstimulated T cells of pre- and post-SDC samples. **G-H**) Pathway analysis of T cell DEGs with q value <0.05 upregulated in pre- (**G**) and post-SDC (**H**) unstimulated cells. Q values determined by FDR correction. rRNA – ribosomal RNA, SDC – sequential drug challenge.

The preceding sections of this chapter (CyTOF and Cite-seq) has demonstrated that patients with HIV and rifampicin DRESS show HIV-related CD4 T cell depletion (with some differences in naïve versus memory populations and activation and exhaustion states). Similarly, there is expansion of the CD8 T cell compartment with predominance of an effector memory phenotype, with features of chronic activation and exhaustion across time-points – features which are likely contributed to by both HIV, DRESS, and even differential states of active TB disease. Although interindividual variability is present and sample size is small, there are suggestive trends that with in vivo drug stimulation (SDC) there is evidence in the peripheral blood of expansion in the CD8 effector memory, activated and cytotoxic cells compared to prior to drug reintroduction. Thus, we thought that it would be worthwhile to further attempt to define the specific cytotoxic T cells with the *ex vivo* stimulation conditions and through TCR repertoire analyses.

4.4.3. Characteristics of CD4+ T cell subset after *ex vivo* rifampicin stimulation

We did sub-analysis of CD4+ T cell responses to rifampicin stimulation *in vitro* for pre and post SDC samples, attempting to dissect out regulatory from effector CD4 T cell responses and confirm some of the suggestive regulatory T cell response data from mass cytometry. We performed pathway enrichment analysis with DEGs obtained from comparison of unstimulated and invitro rifampicin stimulated cells in pre-SDC samples from three DRESS patients and two stimulation conditions. Figure 4-15A shows top 20 enriched biological processes in CD4+ T cells from pre-SDC samples and majority of pathways mainly signal CD4+ T cell responses to HIV as the primary cell target for infection (Nishimura et al. 2005). We identified enrichment of genes associated with lymphocyte mediated immunity, proliferation, and differentiation. Particularly, genes associated with regulation of T cell immune responses and NK mediated cytotoxicity (FOXP3, TIGIT, IL10RA, FCRL3, ZFP36) were overexpressed in unstimulated than rifampicin stimulated cells (figure 4-15C). Although expression was not uniform in all patients, CD4+ T cells from patient 85 showed a distinct functional regulatory pathway with the highest expression of TGFB1 observed in pre-SDC unstimulated, followed by pre-SDC rifampicin stimulated cells and minimal expression in post-SDC samples. Upregulated in pre-SDC rifampicin stimulated cells were genes which interact with cytokine receptors to mediate lymphocyte function, provide co-stimulatory signals for expansion and effector differentiation of activated T cells (IL2RG, IL4R, STAT5A, TUBAIB) and genes involved in CD4+ T cell exhaustion (PDCD1, CTLA4 and TIGIT) (figure 4-15C). Interindividual variability was truly vast and as such we did not identify a conclusive effector or regulatory transcriptional profile in pre-SDC rifampicin stimulated cells.

In the post-SDC samples, enriched biological processes in relation to immune function and responses included regulation of lymphocytes apoptosis, differentiation, and cellular response to interleukin 4

(figure 4-15B). Interleukin-4 (IL-4) induces differentiation of CD4+ T cells into T-helper 2 (Th2) cells. IL-4 is one of the central cytokines regulating allergic inflammation as it occurs in DRESS syndrome (Musette and Janela 2017). Genes enriched in pathway regarding cellular responses to IL-4 were not enhanced by *in vitro* rifampicin stimulation as no uniform differences were observed in the levels of expression between rifampicin stimulated cells and unstimulated (figure 4-15C). The upregulation of STAT6, IL4R and GATA3 in post-SDC unstimulated (in vivo drug stimulation) cells contributed most to the IL-4 signalling pathway observed in post-SDC samples. Genes such as IL-5, IL13, CCR8; related to Th2 phenotype and eosinophilic inflammation in the skin during allergic disease (Endo et al. 2014), were minimally expressed in our dataset. The regulation of immune effector process was in part driven by genes which negatively impact the regulation of Th2 responses, plasmacytoid dendritic cells cytokine production, NK and T cell mediated cytotoxicity (ANXA1, BST2, CD96, FGL2) (figure 4-15C). Again, not all genes in these immune response regulatory pathways were upregulated in a drug specific manner. Patient 10001 recovery samples presented an overall downregulation of gene expression.

Changes related to lymphocyte proliferation and Th2 responses were largely observed in the CD4+ TEM cluster (figure 4-15D). The highest inhibitory and regulatory transcriptomic changes were noted in the Treg cluster – a population that was lower in post compared to pre SDC samples, although interindividual variability dominated (figure 4-14D). Furthermore, analysis of surface expression of IL4-R+ (CD124) and CCR6- (CD196) confirmed a Th2 phenotype as observed in DEG analysis and in response to in vitro rifampicin stimulation for post-SDC cells (figure 4-15E).

A
Pre-SDC CD4+ T cells (816 DEG)

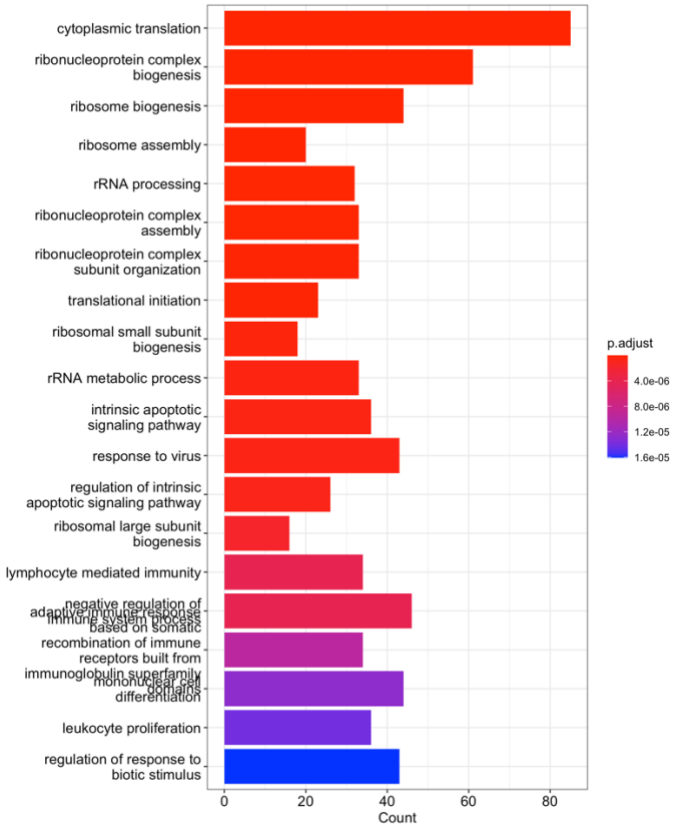

B
Post-SDC CD4+ T cells (224 DEG)

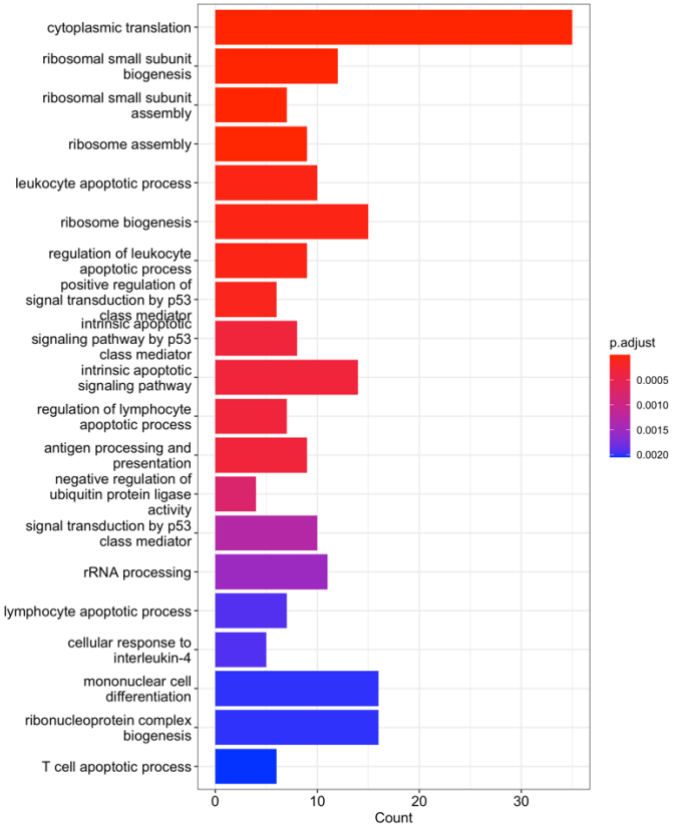

C

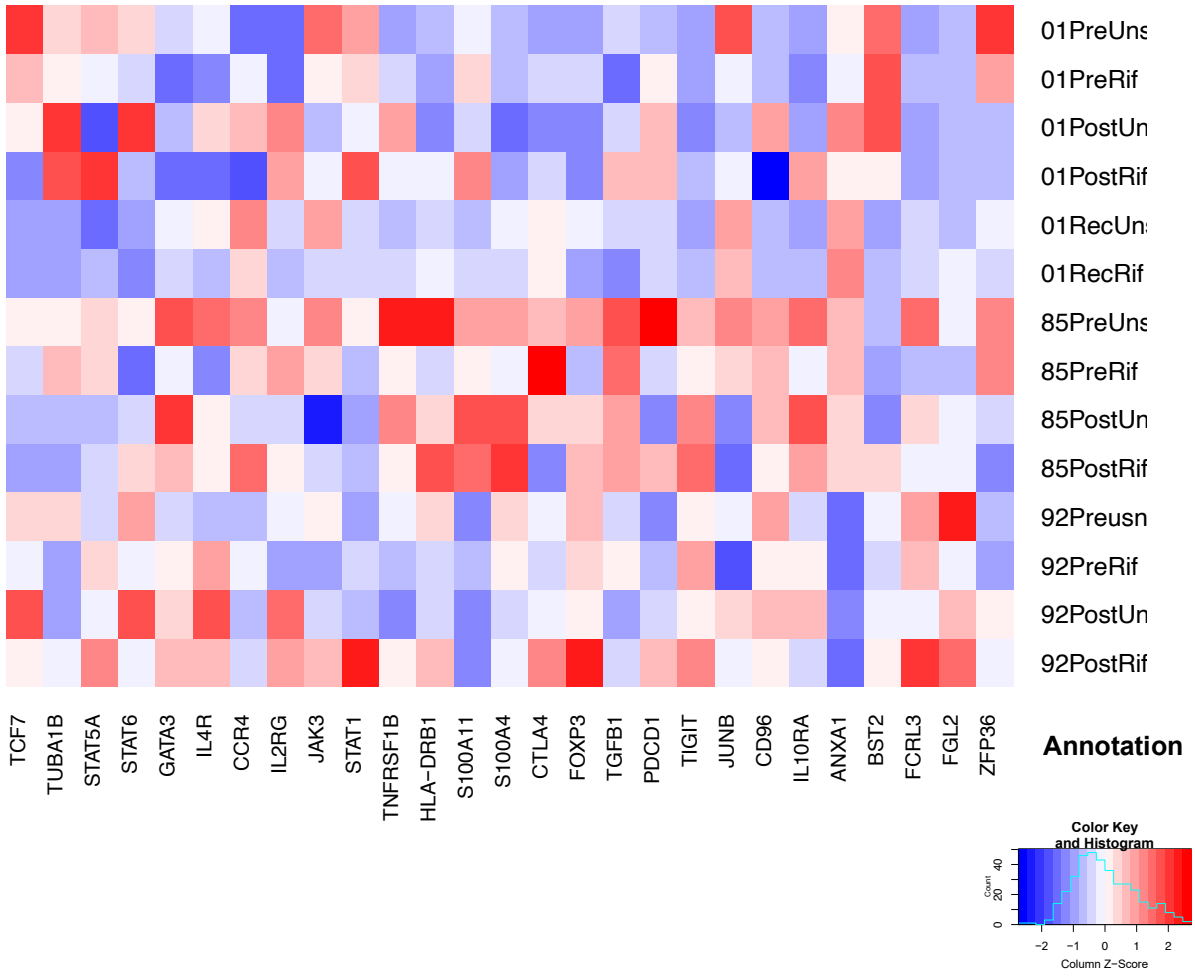
01PreUns
01PreRif
01PostUn
01PostRif
01RecUns
01RecRif
85PreUns
85PreRif
85PostUn
85PostRif
92Preusn
92PreRif
92PostUn
92PostRif
TCF7
TUBA1B
STAT5A
STAT6
GATA3
IL4R
CCR4
IL2RG
JAK3
STAT1
TNFRSF1B
HLA-DRB1
S100A11
S100A4
CTLA4
FOXP3
TGFB1
PDCD1
TIGIT
JUNB
CD96
IL10RA
ANXA1
BST2
FCRL3
FGL2
ZFP36
Annotation
Color Key and Histogram
Count
0
20
40
−2
−1
0
1
2
Column Z−Score

D

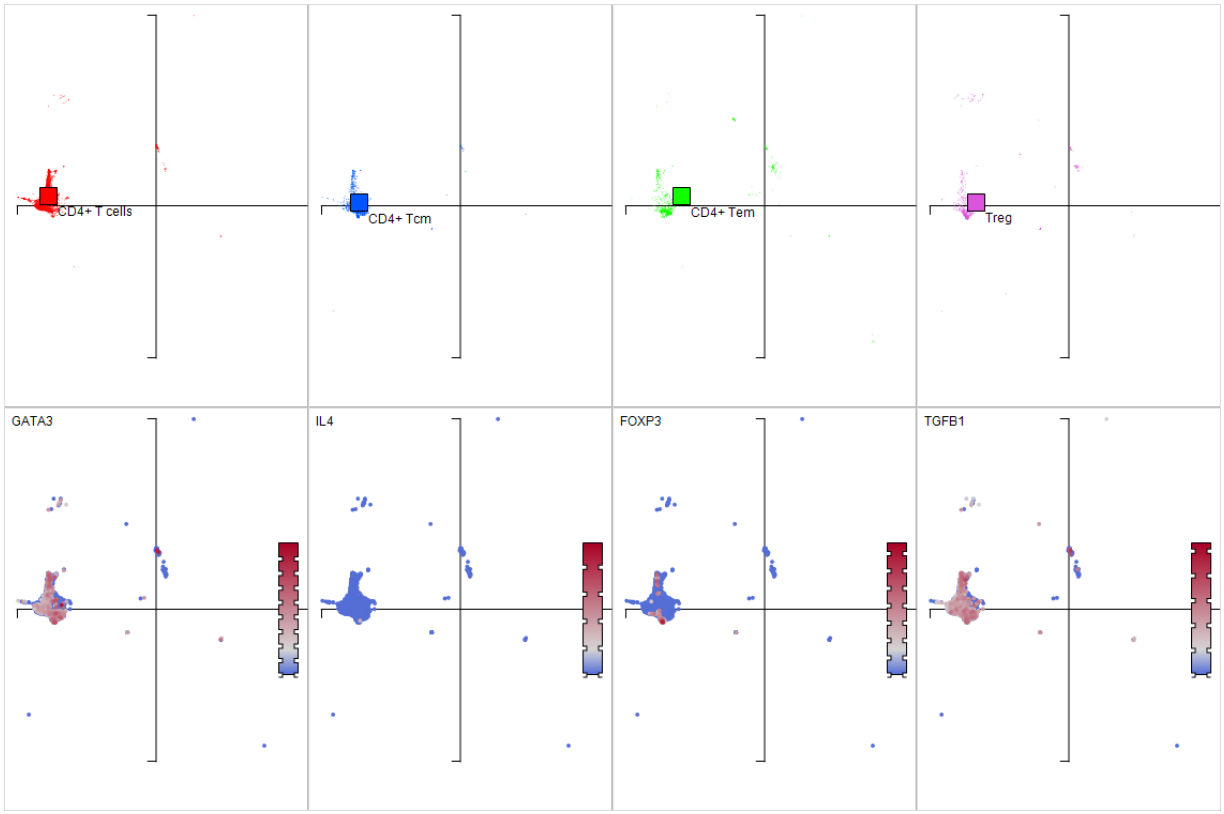
CD4+ T cells
CD4+ Tcm
CD4+ Tem
Treg
GATA3
IL4
FOXP3
TGFB1

E

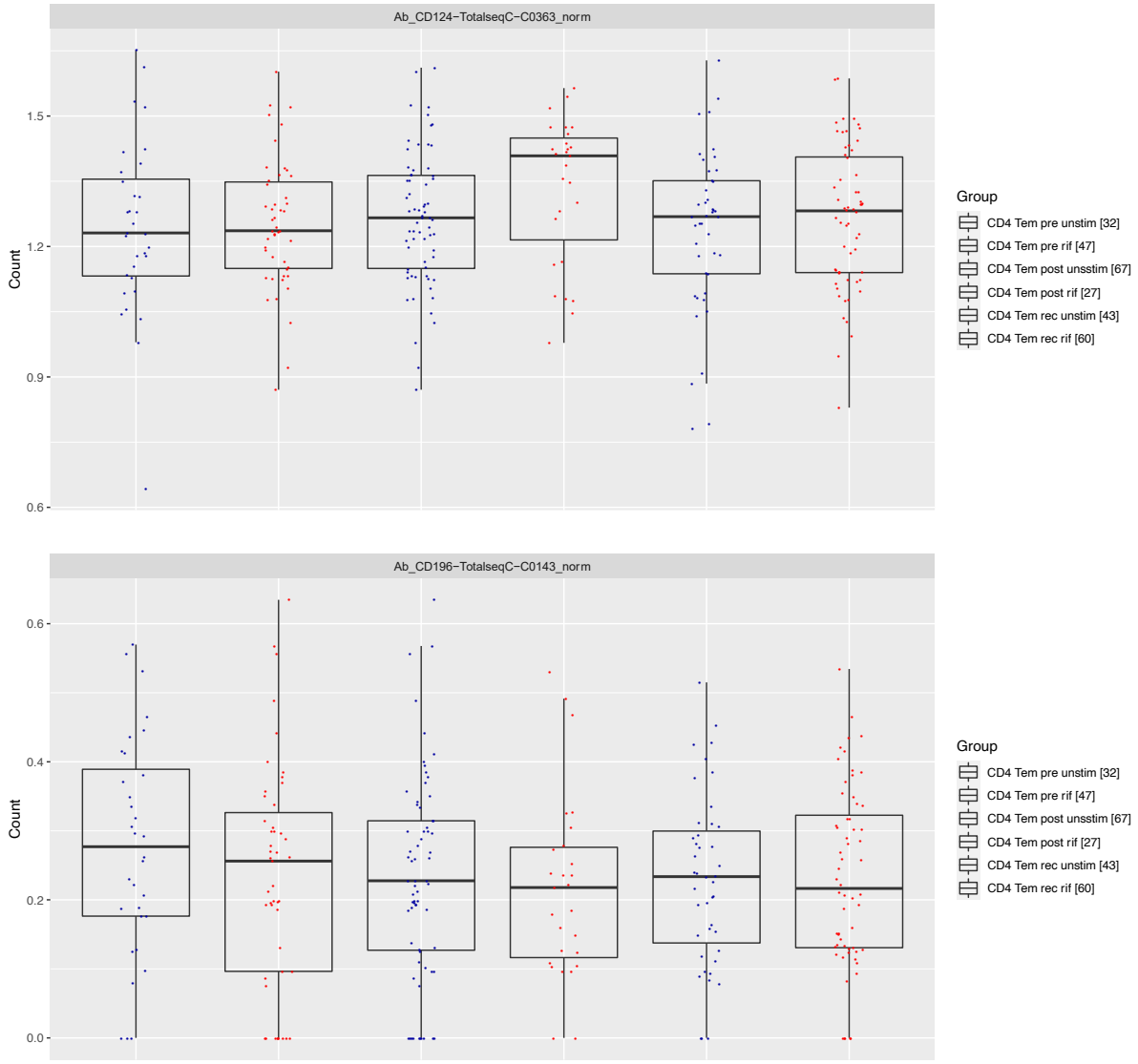

Figure 1-15: CD4+ T cells Cite-seq

Pathway analysis of CD4+ T cell DEGs (816 genes in pre-SDC and 224 genes in post-SDC) upregulated in pre- (**A**) and post-SDC (**B**) samples. The q values were determined using the FDR correction for multiple comparisons. **C**) Heatmap of the variable genes contributing the highest to the annotation of biological pathways related to immune responses and effector functions across timepoints and in vitro stimulation conditions. Columns show log2 counts, averaged and scaled per gene. **D**) Scaled gene expression to identify effector and regulatory CD4+ T cells and the co-expression of Th2 (GATA3, IL-4R) and regulatory (FoxP3, TGFB1) markers. **E**) Tagged antibody expression of CD124 and CD196 in responses to rifampicin in pre- and post-SDC samples.

4.4.4. CD8+ T cells

A sub-analysis of CD8+ effector memory T cells showed a pattern consistent with the hyperactive immune state in HIV (Kazer et al. 2020). We performed enrichment pathway analysis and we focused on co-stimulatory and co-inhibitory signals essential for innate and adaptive immunity with an emphasis on T lymphocyte responses. Pre- and post-SDC samples shared many of the same top 20 enriched pathways, highlighting similar coexistence of activated, pro-inflammatory and exhausted CD8+ T cells phenotype (figure 4-16A-B).

Distinct gene expression and signalling pathways (leukocyte mediated cytotoxicity, cell killing, leukocyte migration) indicated specific chemotactic and cytotoxic functions of CD8+ T cells in post-SDC samples with the highest enrichment noted in rifampicin stimulated cells for both pre- and post-SDC samples Pre- and post-SDC rifampicin stimulated cells were characterised by unique set of genes including CXCL3, CXCL5, CXCL13, CCL2, IL1B, TNF-α, PRF1, TNFRSF9 (CD137) and TNFRSF4 (OX40) (figure 4-16C). These genes were upregulated in a drug specific manner in pathways related to T cell activation, migration, and cytotoxic responses (figure 4-16B). T cell exhaustion is characterised by gradual depletion of effector functions in response to chronic inflammation and the identification of concomitant action of exhaustion markers (LAG3, CD160 and EOMES) and expression of CX3CR1 suggests that these highly cytotoxic CD8+ T cells undergo exhaustion reprogramming to also display a higher proliferative capacity and promote long lasting immunity in tissues with the upregulation of IL15RA; reported to enhance cell proliferation and expression of apoptosis inhibitor BCL2 (Wu et al. 2002; Herndler-Brandstetter et al. 2018). These findings are consistent with our CyTOF observations that terminally differentiated effector memory CD8+ T cells that drive drug specific responses are reprogramed and re-directed towards proliferative and pro-inflammatory responses with possible migration to the skin which is supported by the expression of CCR10 in this subset of CD8+ T cells (figure 4-16C). Although T cell exhaustion marks chronic and persistent inflammation, it has been reported in drug induced immune responses generated in CD4 depletion (Cardone et al. 2018). Additionally, upregulation of genes such as TNFRSF4 (OX40) and ZAP70 support a recent TCR ligation with present antigen and most likely reflect rifampicin-induced immune responses specific to DRESS syndrome. Similar to CD4+ T cell cluster, patient 10001 recovery samples presented an overall downregulation of gene expression.

A
Pre-SDC CD8+ T cells (2000 DEG)

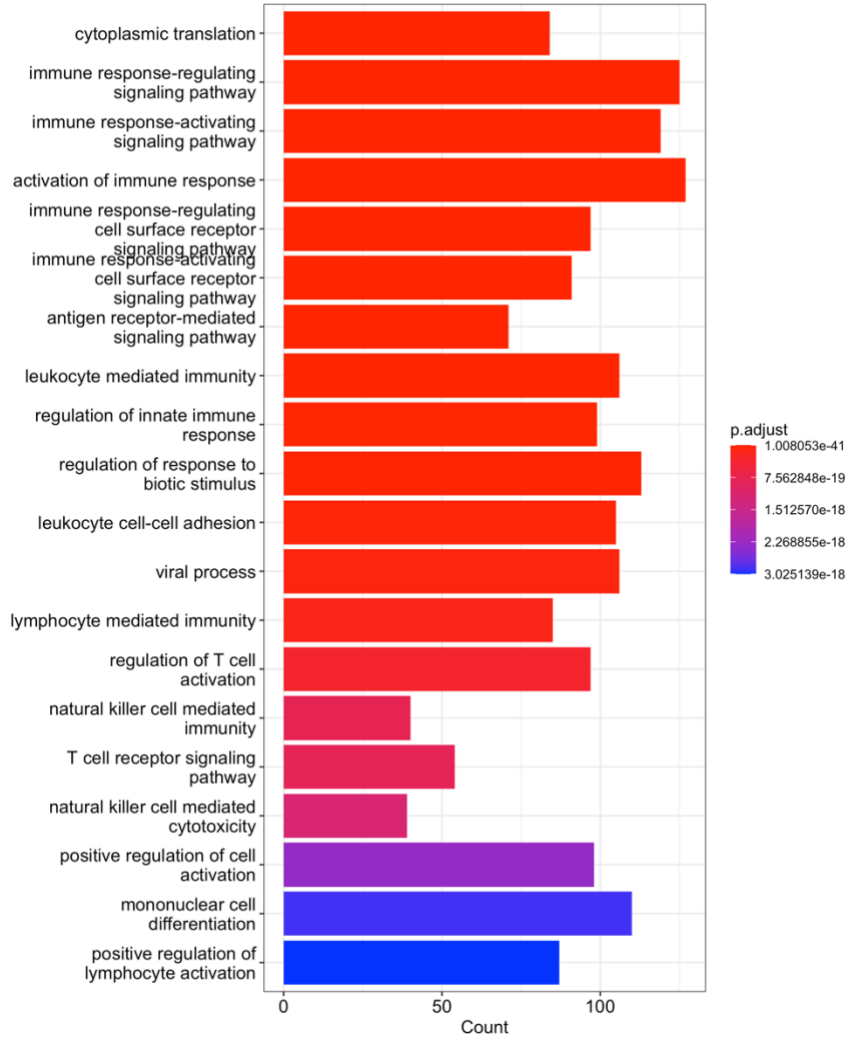

B
Post-SDC CD8+ T cells (2000 DEG)

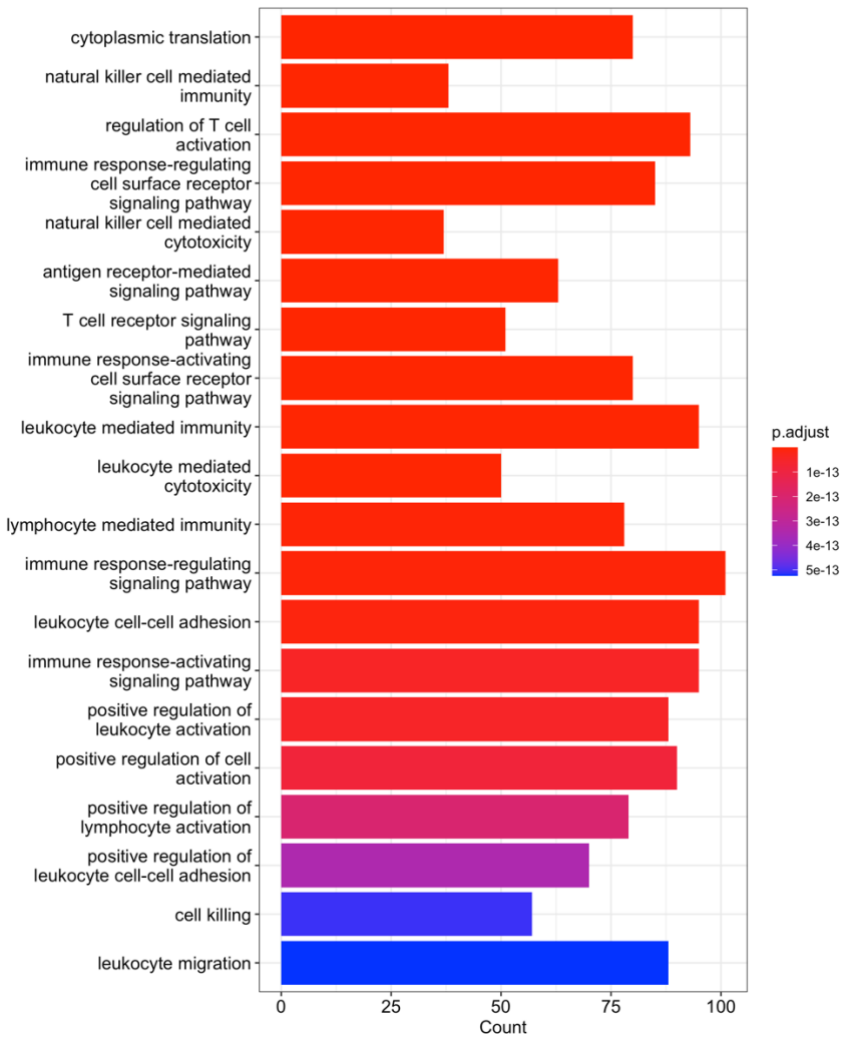

C

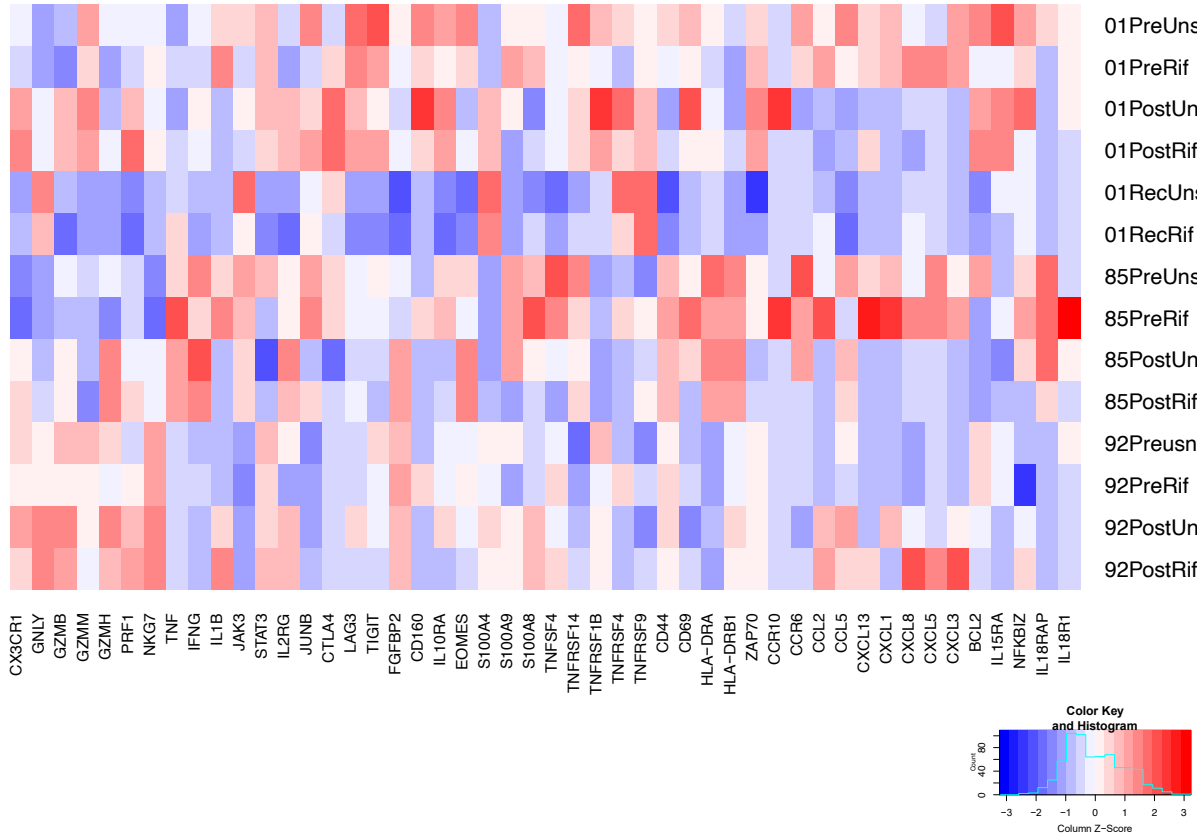

Figure 1-16: CD8+ T cells Cite-seq

Pathway analysis of the top 4000 DEGs of effector memory CD8+ T cells upregulated in pre- (**A**) and post-SDC (**B**) samples. The q values were determined using the FDR correction for multiple comparison. **C**) Heatmap of the variable genes contributing the highest to the annotation of biological pathways related to immune responses and effector functions across timepoints and in vitro stimulation conditions. Columns show log2 counts, averaged, and scaled per gene.

4.4.5. Analysis of TCR clonotypes

The immunological synapse combination of peptide-MHC complex interacting with TCR is at the centre of SCAR pathogenesis (figure 1-7). Relevant examples include public TCRαβ from the cytotoxic T lymphocytes of patients with carbamazepine-SJS/TEN, with its expression showing drug specificity and bias for HLA-B*15:02 (Pan et al. 2019). In allopurinol-induced SCAR, private but dominant TCR clonotypes were identified in HLA-B*58:01 positive allopurinol SJS/TEN patients from Southeast Asia. (Chung, Pan, et al. 2015). Thus, given our findings of HLA-B*44:03 as a risk allele for rifampicin DRESS, and the fact that all three of the patients including in our 5′sc-TCR-RNA-Cite-seq analyses carried HLA-B*44:03 we sought in the following analyses to characterise the TCR repertoires of these three patients.

We mapped the V–J junction and CDR3αβ pairings and looking at the top 100 clones, we found each patient had a unique TCR repertoire, and the clonally expanded cells were overrepresented in the CD8+ T cell clusters (figure 4-17A-C). One exception to this was that TRAV14/DV4/TRBV6-2 was unique to patient 10001 recovery samples but given the long period between the day 62 and day 678 samples, this is not surprising. The percentage frequency of the top 100 peripheral blood clonotypes were similar among in pre- and post-SDC samples. In each patient, we observed differences in the percentage frequency across time-points with higher differences observed in pre- and post-SDC compared to recovery samples of patient 10001 – again mainly due to the long period since onset of symptoms, SDC and recovery. There were no differences within in vitro stimulation conditions (figure 4-17D).

Next, we evaluated phenotypic characteristics of dominant TCR clonotypes to identify specific clones responsible for the highly inflammatory, proliferative, and cytotoxic microenvironment observed among CD8+ T cells from pre- and post-SDC cells stimulated with rifampicin. We performed TCR profiling in all cells from the three patients pre and post SDC samples and analysed the top 5/100 expanded clones. None of the V-J combinations and CDR3αβ pairings showed significant transcriptional profile consistent with highly inflammatory, proliferative, and cytotoxic microenvironment observed among CD8+ T cells from pre- and post-SDC cells stimulated with rifampicin – even when restricted to CD8+ effector memory T cells. Therefore, we next performed analysis to identify cells with identical TCRβ sequences and significant responses to rifampicin that could be attributed to DRESS syndrome.

A
10001

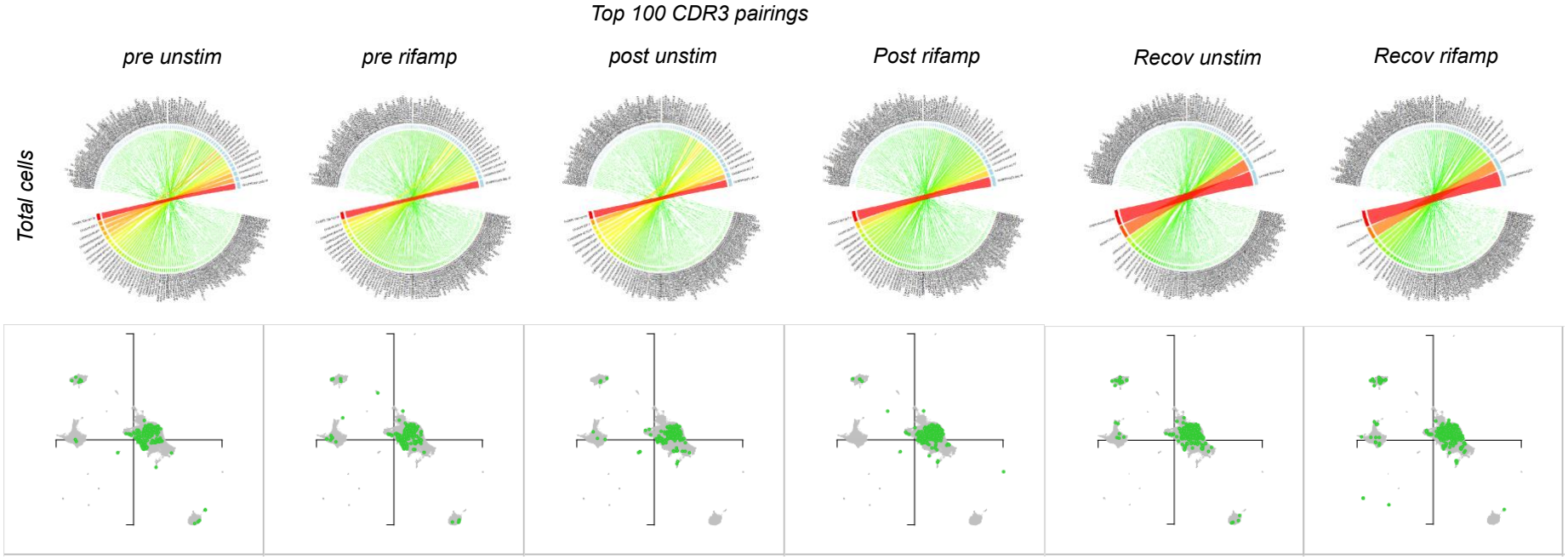
Top 100 CDR3 pairings
pre unstim
pre rifamp
post unstim
Post rifamp
Recov unstim
Recov rifamp
Total cells

B
10085

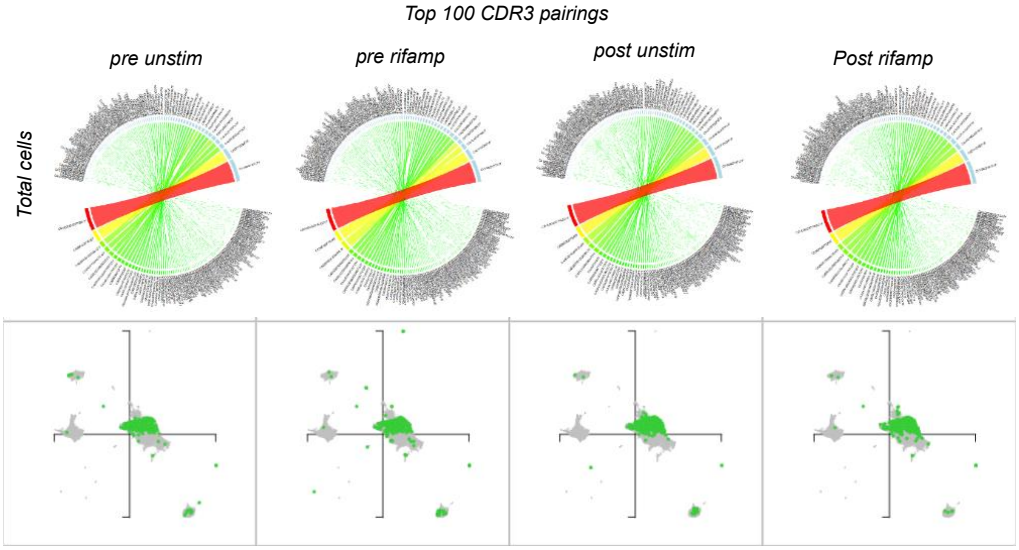

C
10092

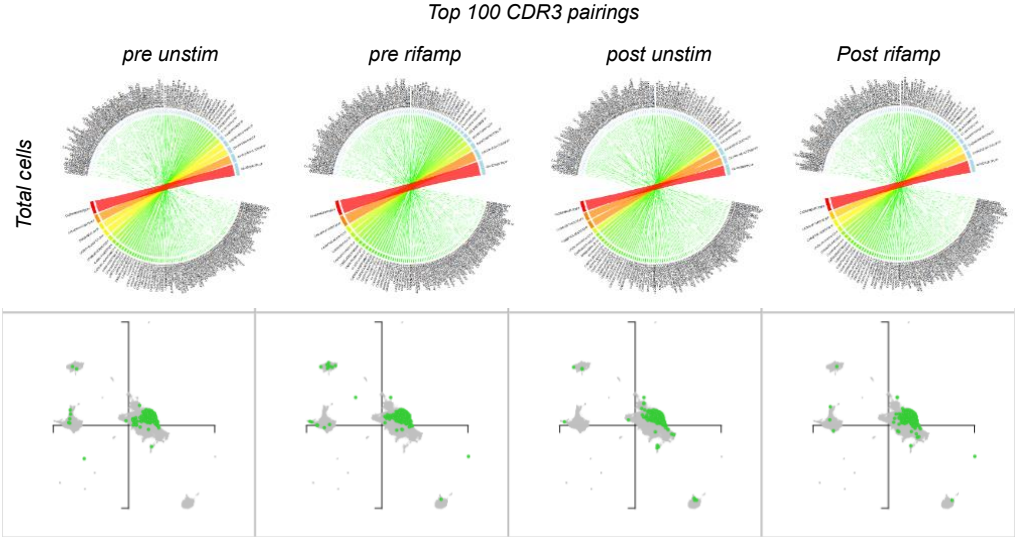

D

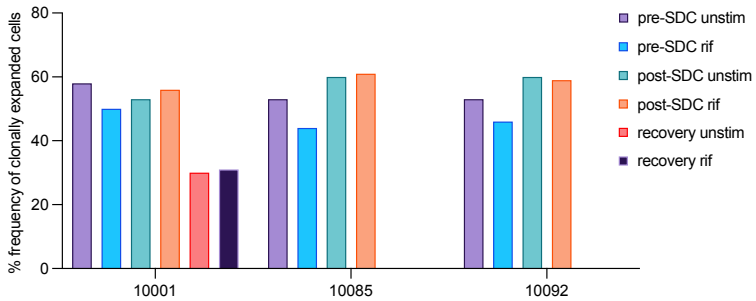

Figure 1-17: T cell receptor clonotype analysis across different patients, timepoints and stimulation conditions

A-C) A representative TRAV–TRBV Circos plot of PBMCs of each rifampicin induced DRESS patient, reaction timepoint and in vitro stimulation condition 10001 (**A**), 10085 (**B**), 10092 (**C**). Ribbons represent alpha/beta pairings with sizes scaled to pairing frequency. Also represented under Circos plots for each patient are UMAPs with the top 5 clones highest – majority in the CD8+ effector memory cluster. **D**) Distribution of the top 5 clonotypes per patient, reaction time point and in vitro stimulation condition – represented as mean percentage frequency. The top 5 clonotypes were unique in each patient. SDC – sequential drug challenge.

4.4.6. Defining shared TCR specificity groups for rifampicin specific T cells in DRESS

Although it is possible that we may be missing a public TCRαβ in the affected skin of these patients, in the above sections, we identified inflammatory, proliferative, and cytotoxic T cells responses in vivo rifampicin exposure and following *in vitro* rifampicin stimulation. This transcriptional profile of highly expanded CD8+ T cells suggests the presence of individual TCRαβ clonotypes in peripheral blood that share common peptide-binding features and are drug-specific and responsible for driving DRESS pathology.

Shared TCRα and TCRβ clonotypes in three patients are absent. In chapter 3 we discussed a model where rifampicin may stabilise and increase the surface expression of HLA-B*4403. We deduce distinct TCR sequences from proliferative and cytotoxic T cells recognise the same pMHC ligand. Therefore, we explored grouping of lymphocyte interactions by paratope hotspots (GLIPH2) algorithm that groups TCR sequences based on shared peptide-binding specificity (Glanville et al. 2017; Huang et al. 2020; Musvosvi et al. 2023) to find commonalities between the three HLA-B*4403 restricted patients. GLIPH2 identifies shared specificity groups based on identical amino acid sequence motifs or global homologies within the complementarity-determining region 3 (CDR3) of the TCRβ chain.

We had a dataset of 8518 distinct CDR3β sequences from 14 PBMCs samples (three patients, two timepoints – pre and post SDC, recovery and two stimulation conditions – unstimulated and 25ug/ml rifampicin). After applying GLIPH2, we identified 2264 specificity groups with 29 recognised as clonally expanded motifs. TCR similarity groups shared by all three participants at least one of the timepoints were further examined for DGE following *in vitro* rifampicin stimulation. This filtering resulted in eight (LGGF, LINE, SQVP, QVPG, FYNS, GLIN, TDSS and SIWG) TCR similarity groups (figure 4-18A-B) which showed no significant association with HLA-B*44:03. The absence of TCR similarity group: HLA-B*44:03 combinations could be due to the preselection of patients with shared HLA-B allele as there were TCR groups significantly associated with HLA-A*0201 carried by two patients (10085 and 10092). The number of CDR3β sequences in each GLPH2 group and number of cells contributing to each group are reported in figure 4-18C.

We were particularly interested in three TCR groupings: LGGF and SQVP TCR groups which were enriched in patient 10001 and 10085 at both pre- and post-SDC timepoints and stimulation conditions; and then the SIWG TCR group present only in post-SDC rifampicin stimulated cells, but consistently across all three patients (figure 4-18D). Differential gene expression analysis included all cells that contribute to each TCR group. The SIWG group showed increased expression in differentiation gene

markers (CCR7) associated with naïve and central memory phenotype observed more in pre-SDC samples and an upregulated expression of IL-4R related to IL-4 signalling pathways observed in CD4+ T cell cluster. The LGGF group showed a cytotoxic and inflammatory profile with the upregulation of GZMK, GZMA, CXCL13, CXCL1, CCL5 and CCL2. However, the markedly increased expression of LAG3, CTLA4 and IL10RA suggest direct inhibition of T cell function. SQVP TCR group showed consistent effector memory phenotype (KLRG1+ CX3CR1+ CCR7-) characterised by inflammatory (IL2RG, CCL4, CCL5, CXCL5) and the highest expression of cytotoxic molecules including GNLY, GZMB, GZMH, NKG7). Most importantly, T cell clones in the SQVP group were the only ones expressing IFNG – an analyte measured in our ELISpot data to confirm the specificity of rifampicin induced immune responses (figure 4-18E). Patient 10085 was the only participant with SQVP TCR group present in pre- and post-SDC unstimulated and rifampicin stimulated cells. We observed a similar trend toward increased inflammatory (IFNG, CCL4) and cytotoxic (GZMB, NKG7, GZMH) molecules in rifampicin stimulated cells compared with unstimulated (figure 4-18F-G).

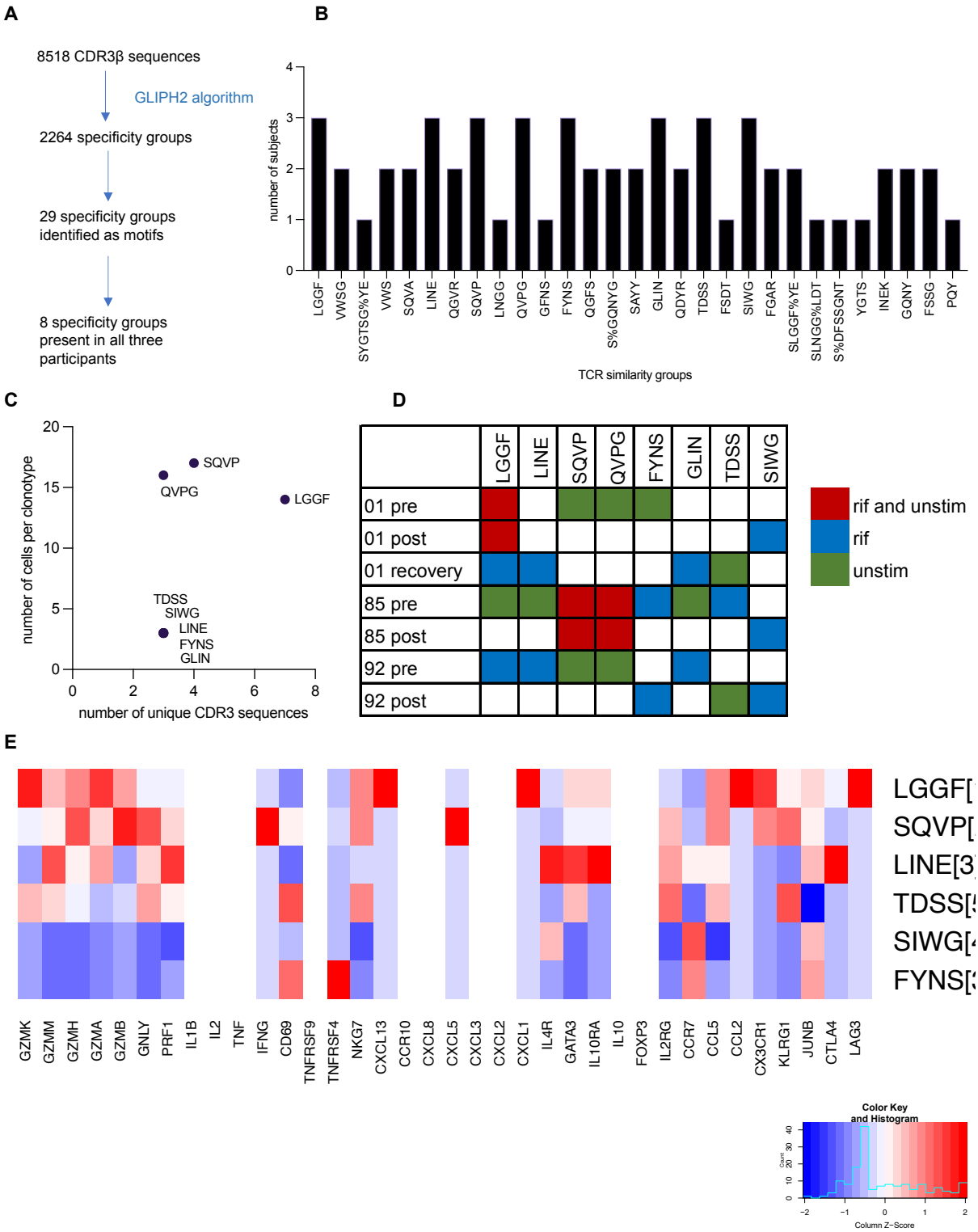
A
8518 CDR3β sequences
GLIPH2 algorithm
2264 specificity groups
29 specificity groups identified as motifs
8 specificity groups present in all three participants
B
number of subjects
TCR similarity groups
LGGF
VWSG
SYGTSG%YE
VWS
SQVA
LINE
QGVR
SQVP
LNGG
QVPG
GFNS
FYNS
QGFS
S%GQNYG
SAYY
GLIN
QDYR
TDSS
FSDT
SIWG
FGAR
SLGGF%YE
SLNGG%LDT
S%DFSSGNT
YGTS
INEK
GQNY
FSSG
PQY
C
number of cells per clonotype
number of unique CDR3 sequences
SQVP
QVPG
LGGF
TDSS
SIWG
LINE
FYNS
GLIN
D
LGGF
LINE
SQVP
QVPG
FYNS
GLIN
TDSS
SIWG
01 pre
01 post
01 recovery
85 pre
85 post
92 pre
92 post
rif and unstim
rif
unstim
E
GZMK
GZMM
GZMH
GZMA
GZMB
GNLY
PRF1
IL1B
IL2
TNF
IFNG
CD69
TNFRSF9
TNFRSF4
NKG7
CXCL13
CCR10
CXCL8
CXCL5
CXCL3
CXCL2
CXCL1
IL4R
GATA3
IL10RA
IL10
FOXP3
IL2RG
CCR7
CCL5
CCL2
CX3CR1
KLRG1
JUNB
CTLA4
LAG3
LGGF[
SQVP[
LINE[3
TDSS[
SIWG[
FYNS[
Color Key and Histogram
Count
Column Z-Score

F

SQVP specificity group

10085 pre-RIF versus Unstim

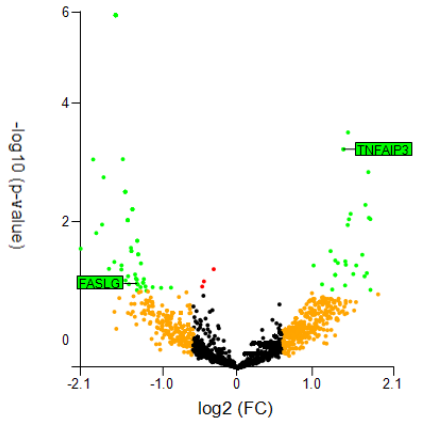

10085 post-RIF versus Unstim

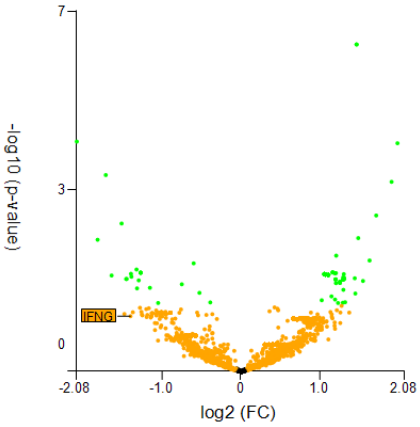

G

Upregulated in pre rifampicin stimulated SQVP expressing T cells *n=5*	
Gene	log2 Fold Change
GZMB	1,3571
NKG7	1,092
GNLY	1,0384
CD96	1,0116
Upregulated in pre unstimulated SQVP expressing T cells *n=4*	
TNFAIP3	1,4167
GZMM	1,3612
ANXA6	1,2792
S100A4	1,3223
HLA-F	1,2299
CXCR3	1,054
ZAP70	1,0321
STAT6	1,0313
PRF1	0,9569
CD74	0,9578
STAT4	0,9599

Upregulated in post rifampicin stimulated SQVP expressing T cells *n=4*	
Gene	log2 Fold Change
IFNG	1,4015
GNLY	1,0525
SELL	0,9547
CXCR3	0,7705
HLA-DRB1	0,759
CD74	0,724
CCL4	0,6771
Upregulated in post unstimulated SQVP expressing T cells *n=5*	
ANXA6	1,191
TGFB1	0,9508

Figure 1-18: Establishing specificity groups with CDR3b sequences and phenotypic characterization of grouped clones

A) Flow diagram of analysis of shared T cell specificities with GLIPH2 algorithm. **B**) The bar plot depicts the number of patients with CDR3β sequences that belong to the similarity group indicated on the x-axis. The similarity groups are denoted by the amino acid motif that is shared by TCR sequences clustered together. Similarity groups including '%' marks the GLIPH2 wildcard in identifying the shared amino acid motif. **C**) Scatterplot of the correlation between the number of unique CDR3β sequences in a TCR group and the number of T cells contributing to the group. **D**) Summary of the patient level TCR specificity from three patients. Each patient and reaction timepoint studied is shown in a row; each TCR group occupies a column. Column colours mark response in one or more stimulation conditions for a patient possessing the TCR group at a specific reaction timepoint. **E**) A heatmap display with log2 counts (averaged and scaled per gene) of 36 gene related to function and differentiation of T cells in TCR groups present in the three patients. **F**) Volcano plots and **G**) genes and foldchange for the DGE in SQVP specificity group present in patient 10085 pre- and post-SDC rifampicin and unstimulated cells.

4.4.7. Rifampicin induces activated and inflammatory monocytes/macrophages

As (markers associated with antigen presentation) were differentially expressed across T cells, we established whether there was a relationship between antigen presenting cells and drug specific T cell mediated immunity. Antigen presenting cells, and their pro/anti-inflammatory phenotype are important drivers/modifiers of effector T cells responses, and have been linked to the optimal co-stimulation for drug to induce drug-reactive CD8+ T cells (Cardone et al. 2018) and keratinocyte killing in SCAR (de Araujo et al. 2011; Tohyama et al. 2012). The transcriptional analysis of monocytes/macrophages identified revealed a greater functional heterogeneity compared to the two CD14+ and CD16+ subsets detected in our CyTOF analysis. Here, using antibody expression and canonical genes, further subclassification included (M1, M2 macrophages and subclassification of monocytes based on the expression of CD14+ classical monocytes and CD16+ non-classical monocytes) (figure 4-19A-B). However, this subclassification reduced the number of cells per patient and stimulation condition, therefore, we looked at the whole monocytes and macrophage populations.

Differentially expressed genes were identified by comparing rifampicin stimulated and unstimulated cells at pre and post SDC timepoints in each DRESS patient (pre- or post- SDC, unstimulated vs rifampicin stimulated). Labelled genes had a fold change >0.6 and *P* adjust <0.05. Patient 10001 and 10085 had a downregulation of gene expression (figure 4-19C-D), whereas in patient 10092, markers associated with activation and enhanced antigen presentation (HLA-DR, HLA-DR-B1), which control the expression of proinflammatory cytokines such as TNF and its receptors, through which monocytes my interact with CD4+ and CD8+ T cells (STAT1) were upregulated in rifampicin stimulated cells than unstimulated (figure 4-19E). We also noted an upregulation CD14+ along with calgranulin genes (S100A4, S100A6), and RNase1 expression associated with antiviral and antimicrobial activity in post-SDC unstimulated cells. There was also downregulation of gene expression in macrophages, especially in rifampicin stimulated cells and post-SDC unstimulated. This showed the unrelatedness of the cells to drug induced immune responses, as non-drug factors were dominating, and macrophages were therefore excluded from further analysis.

The signalling pathway analysis of genes upregulated in pre- and post-SDC monocytes showed enrichment of biological processes related to bacterium responses and interactions with lymphocytes. One of the unique characteristics of the top enriched pathways in pre-SDC samples - cytokine signalling pathway and the response to lipopolysaccharide and molecule of bacterial origin was the enriched expression of CD14 in the latter. In post-SDC cells and rifampicin stimulated pre-SDC cells we recognised a higher expression of CX3CR1 and enrichment of genes contributing to cytokine signalling pathway such as CCL3, CCL4 expressed within a couples of hours after stimulation to attract myeloid and effector T cells to inflamed sites were induced in post-SDC cells including CCL5

induced in the later stage of inflammation seen in rifampicin stimulated cells. We also detected that rifampicin stimulated monocytes showed high expression of NFKBIA, STAT1, STAT2 which control the expression of proinflammatory cytokines such as TNF and its receptors, through which monocytes my interact with CD4+ and CD8+ T cells (figure 4-19F-H). We noted an increased expression of IL-10 in unstimulated cells from pre- and post-SDC samples. Interleukin-10 has been shown to directly inhibit CD8+ T cell function in chronic viral infection such as HIV, by enhancing N-glycan branching to decrease antigen sensitivity. Looking further at this proposed mechanism, we noted an increase in the expression of MGAT5, a gene also implicated in the down regulation of TCR signalling by increasing the antigenic threshold required for T cell activation (Smith et al. 2018). The downregulation of IL-10 and MGAT5 by rifampicin suggests the assembly and surface expression of p-MHC is compromised to various degree by drug – adding the proposed mechanisms of rifampicin and MHC class I molecules interactions discussed in chapter three of this thesis.

A
Combined UMAP – Monocytes

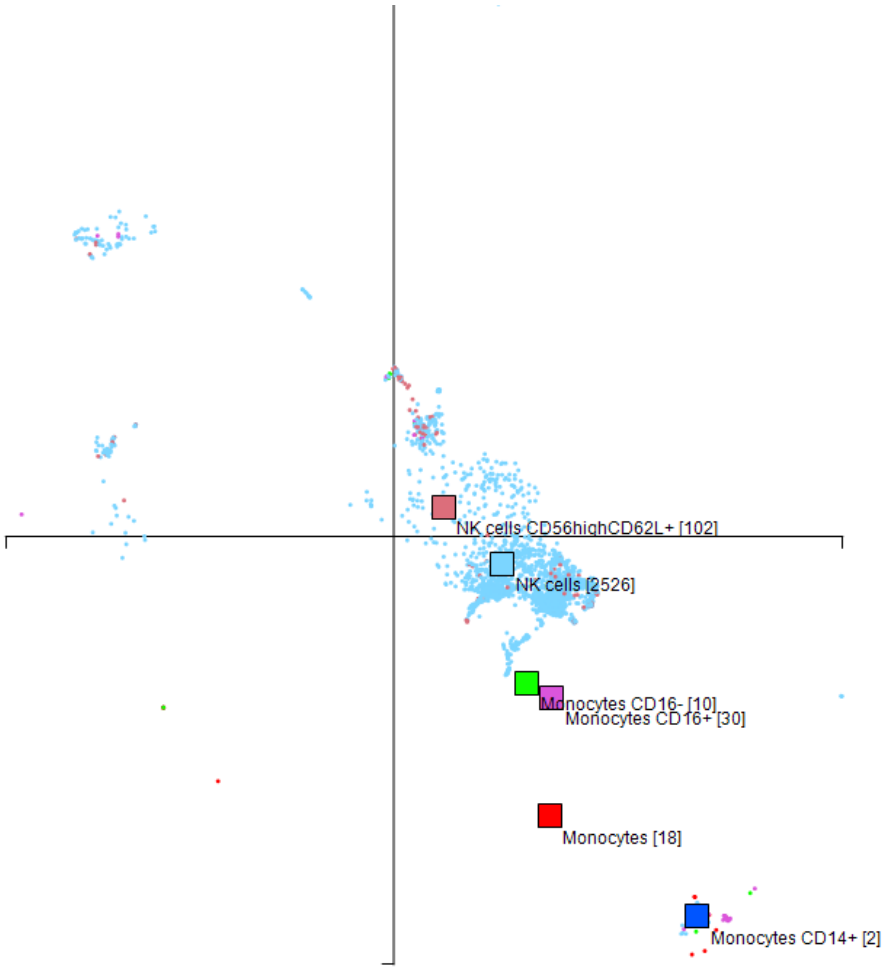

B
Combined UMAP - Macrophages

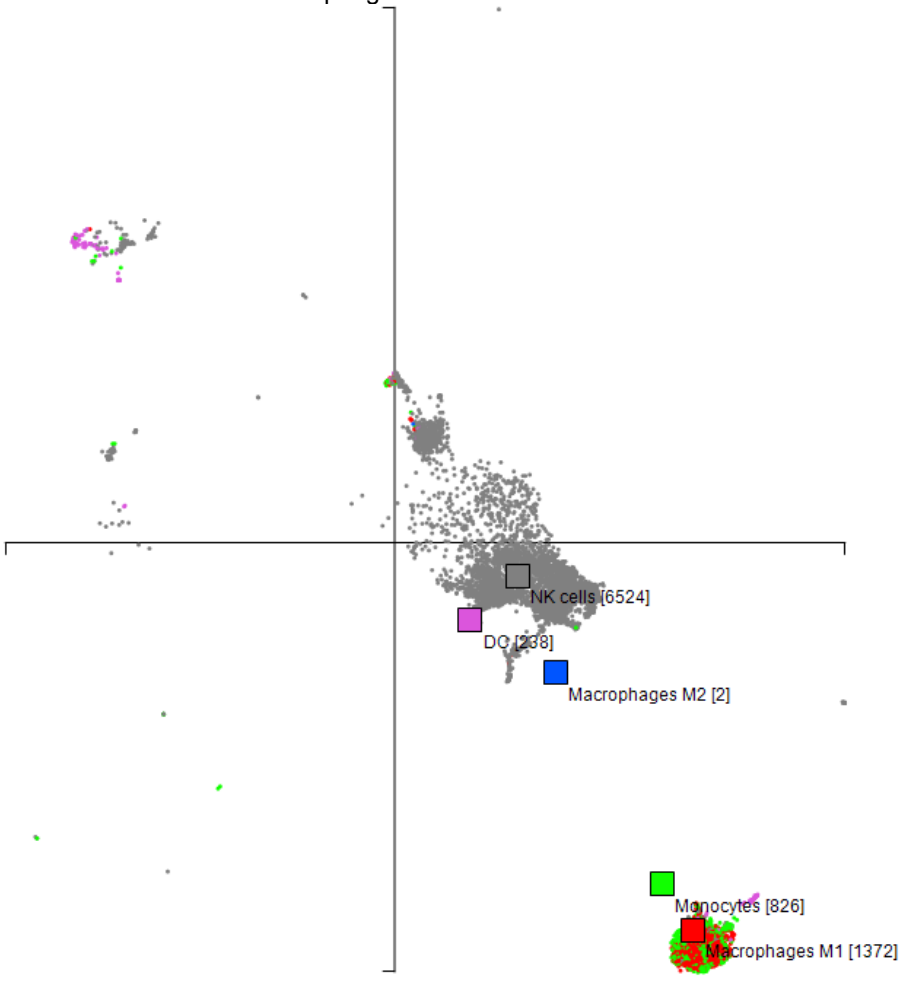

C

10001 pre-RIF versus Unstim

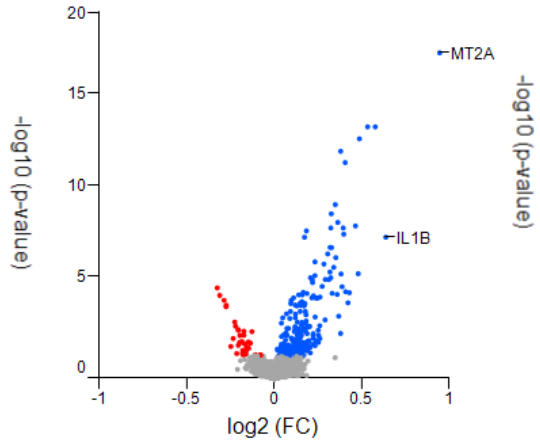

10001 post-RIF versus Unstim

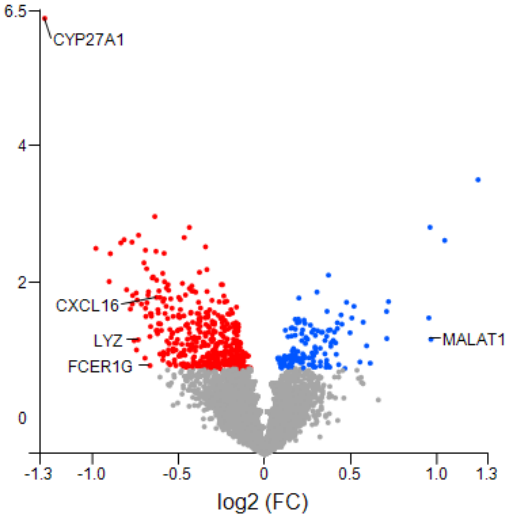

D

10085 pre-RIF versus Unstim

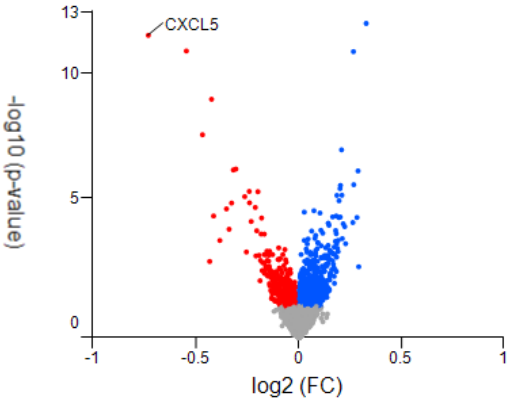

10085 post-RIF versus Unstim

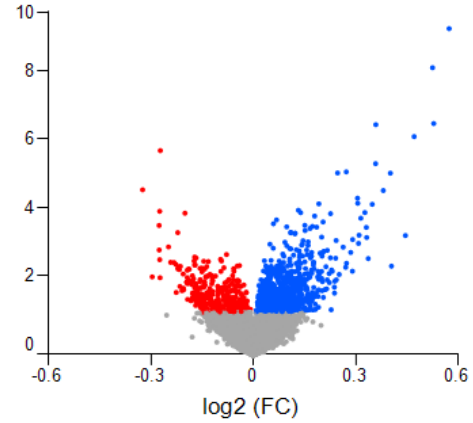

E

10092 pre-RIF versus Unstim

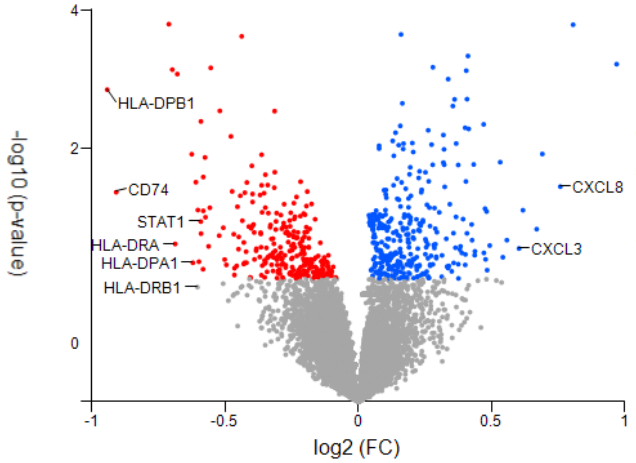

10092 post-RIF versus Unstim

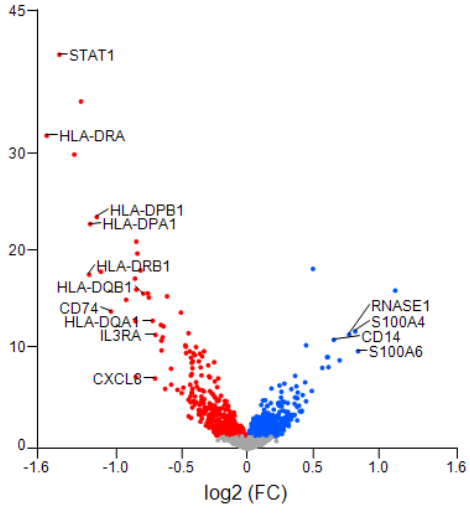

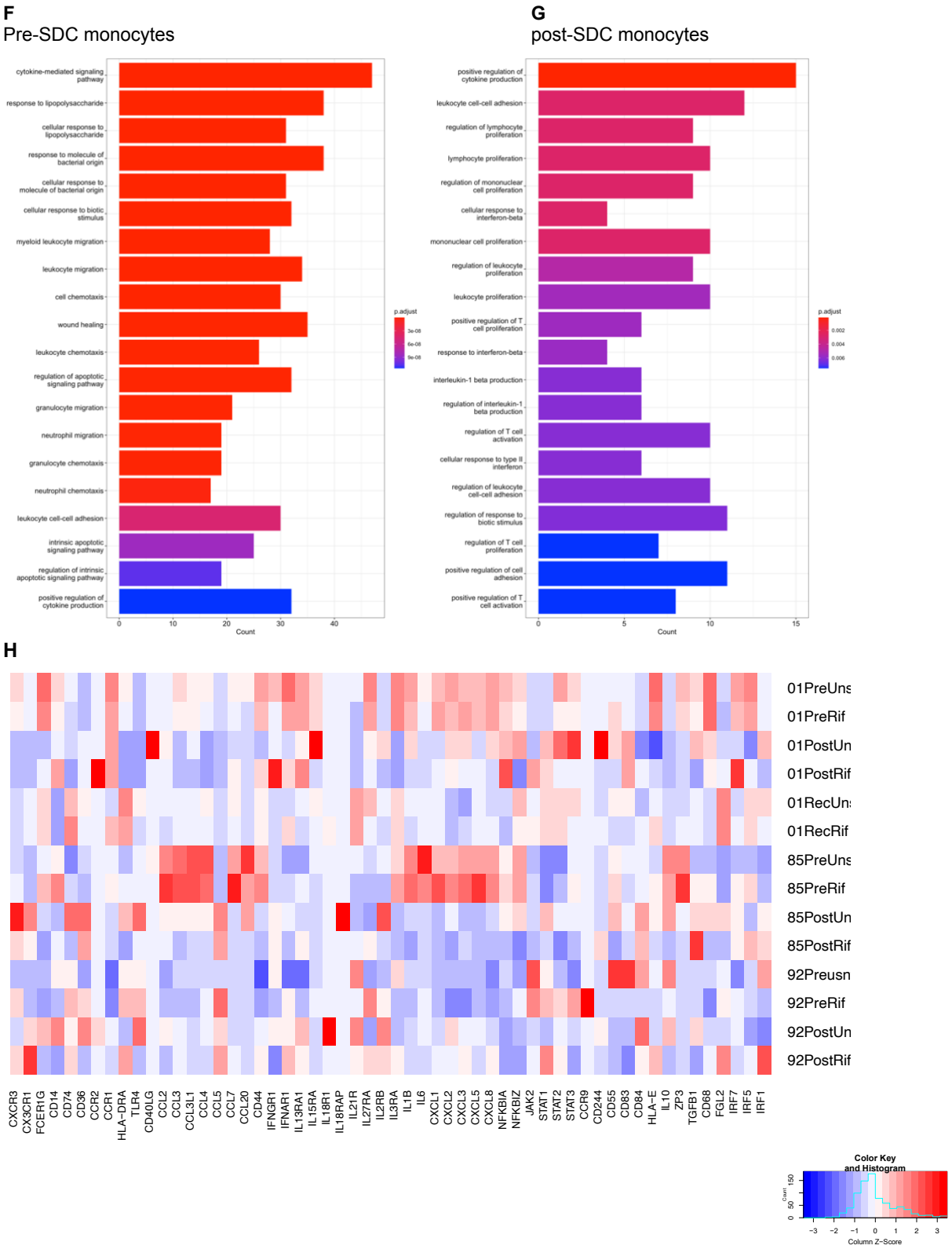

Figure 1-19: Gene expression characterisation associated with monocyte/macrophages in rifampicin induced DRESS

A-B) UMAP plots showing monocytes (**A**) and macrophages (**B**) subpopulations into CD14+/-, CD16+/- monocytes and M1, M2 macrophages. **C-E**) Volcano plots showing DEGs between monocytes/macrophage population for patient 10001 (**C**), 10085 (**D**), 10092 (**E**) in rifampicin or unstimulated cells. **F-G**) Bar plots of GO annotations enriched in monocytes from pre- (**F**) or post-SDC (**G**) samples. Q values were calculated using two-sided t-test and the FDR correction for multiple comparisons. **H**) Heatmap of the DEGs in immune function related pathways in **F** and **G**.

4.4.8. Rifampicin enhances a mature and activated DCs and NK cells phenotype

After defining adaptive responses and characterizing the T cells landscape of rifampicin DRESS, we next looked at features specific to innate responses and their relation to proinflammatory and cytotoxic rifampicin specific T cells. The number of DCs were not sufficient in our dataset for further subpopulation into myeloid and plasmacytoid DCs. We initially focused on surface markers to define mature and immature DCs (CD40, CD54, CD58, CD83), co-stimulation (CD24, CD86), viral receptors (CD4, CD46 [RNASeq]), DC signalling (CD88), antigen presenting (HLA-A-B-C, HLA-DR, CD1c), antigen uptake (CD32, CD64), homing (CD11a, CD11b, CD11c, CD44, CD49d) as outlined in a review by Banchereau et al (figure 4-20A) (Banchereau and Steinman 1998) and co-inhibitory receptors (CD274 (PD-L1), PDCD2L [RNASeq], CD80 [RNASeq]) involved T cell tolerance. DC maturation as characterised by upregulation of CD40, CD54, CD58, HLA-DR occurred more in the presence of rifampicin than in unstimulated cells for both pre- and post-SDC samples (figure 4-20B, yellow box). rifampicin stimulated DCs also had a higher expression of antigen presenting markers HLA-A-B-C, HLA-DR and CD1c, with the highest significance of this relationship seen in the pre-SDC samples of patient 10001 and 10085 (figure 4-20B, green box). When expression was scaled by rows (each patient, timepoint and stimulation condition), in unstimulated pre- and post-SDC cells, we observed upregulation and uniform expression of DCs ligands (CD274, PDCD2L, CD80) that largely modulate activated T cell inhibition and suppress adaptive immune responses through interaction with PDCD1 and CTL4 on T cells. The highest significance of this relationship was seen in the post-SDC samples of patient 10001 and 10092 (figure 4-20C, purple box).

The data demonstrated a functional dendritic cell compartment enhanced by presence of drug – the high level of co-stimulation markers and CD40 suggests interaction with CD28 and CD40LG for drug specific T cell activation. The upregulation of co-inhibitory ligands in unstimulated cells is also an interesting observation potentially related to the regulation of pre-existing memory CD8+ T cells specific to either self of foreign (viral) antigens – a now source of drug responsive T cells after culprit drug viral reactivation (Cardone et al. 2018; Picard et al. 2010; Cho, Yang, and Chu 2017b). We noted the contribution of Th2 cells to rifampicin induced DRESS in section 4.4.3 of this thesis. Here, we also looked at DC transcriptional changes required for optimal Th2 priming in vivo (Walker and McKenzie 2018). The increased expression of IRF4 and KLF4 in rifampicin stimulated cells suggests participation of DCs in the development of Th2 cell subset (figure 4-20B). These transcriptional factors (IRF4, KLF4) directly activate the expression of Il-10, IL-33 and can be induced by various stimuli including allergen, alarmins and inflammatory stimuli. Interestingly, IRF4 expression does not correlate with expression of IL-10 in rifampicin stimulated cells (figure 4-20B). This is similar to the observation made in monocytes and possible relation to antigen presentation in rifampicin reactions.

Finally, analysis of unstimulated versus rifampicin stimulated cells in pre- and post-SDC did not reveal any drug specific responses in the NK cell compartment. We then compared unstimulated cells in pre- and post-SDC samples to study the effect of in vivo drug exposure. We saw an upregulation of genes associated with cytotoxic NK responses (GZMB, GZMH, GNLY) in highly inflammatory conditions (CCL4, CD74, CCL4L2) (figure 4-20 D-F). The post-SDC unstimulated cells of patient 10085, showed a phenotype of CD56+ T cells with a high expression of T cell co-receptor CD3E. Whereas, pre-SDC unstimulated cells were marked by increased expression of inhibitory molecule TGFB1 (figure 4-20E) consistent with our CyTOF data where unstimulated cells from pre-SDC and recovery samples, along with drug tolerant controls had an increased expression of regulatory molecules (figure 4-11E).

A

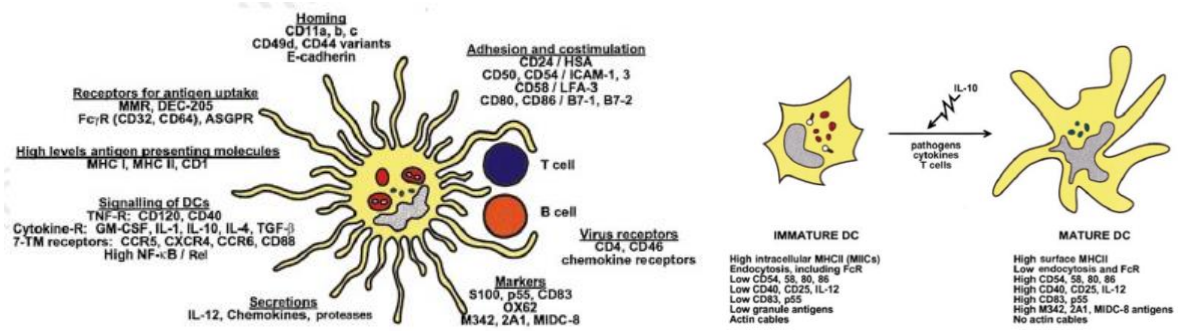

B

Scaled by column

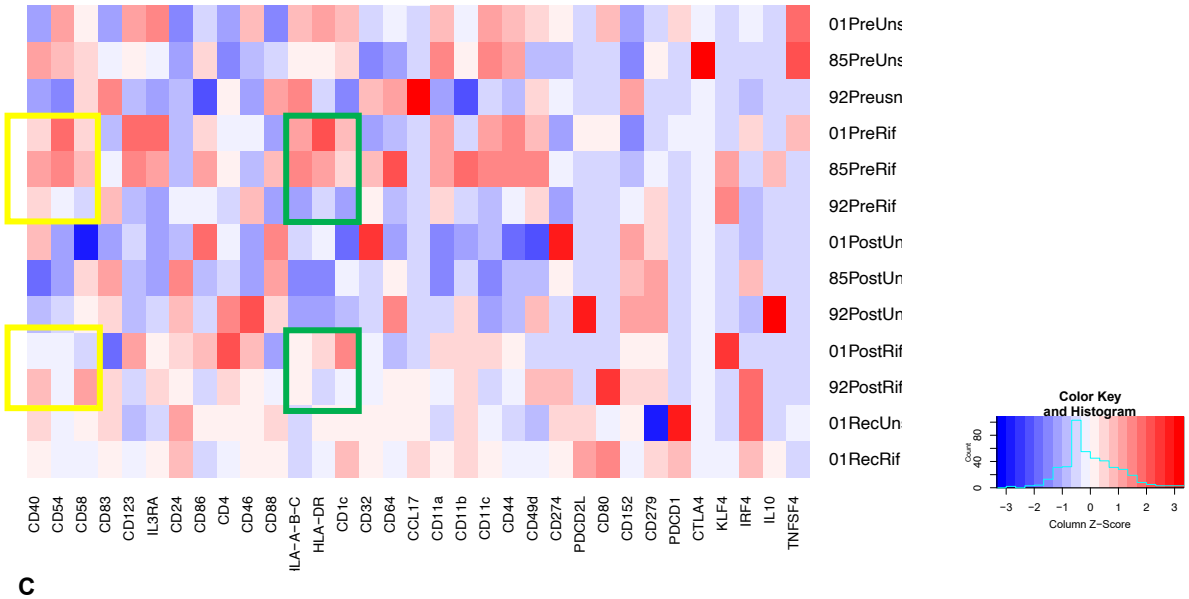

C

Scaled by row

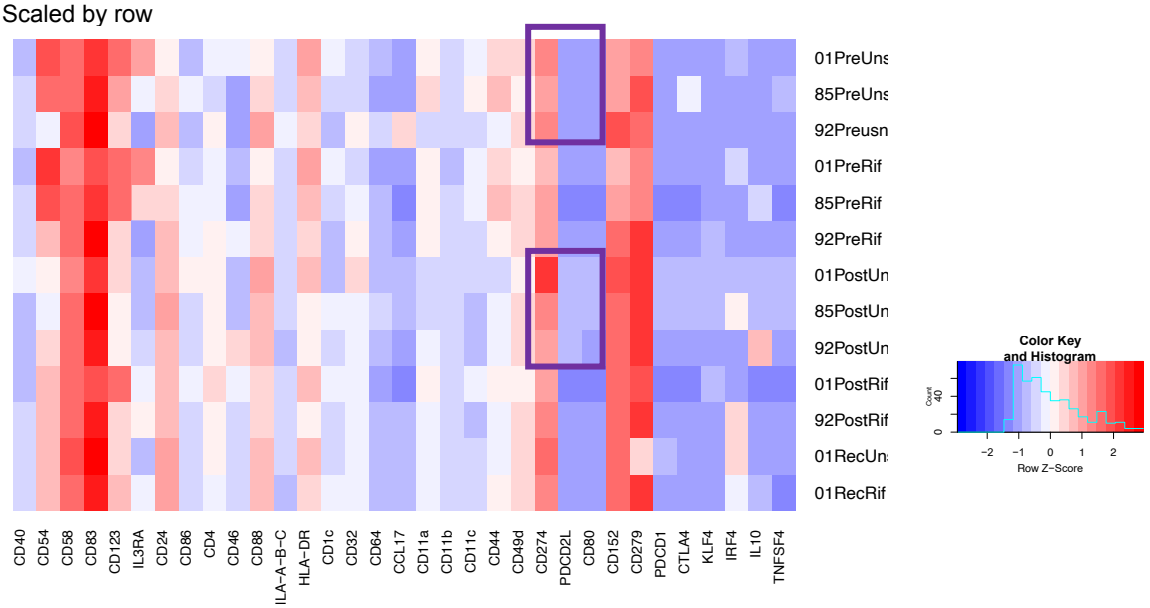

D

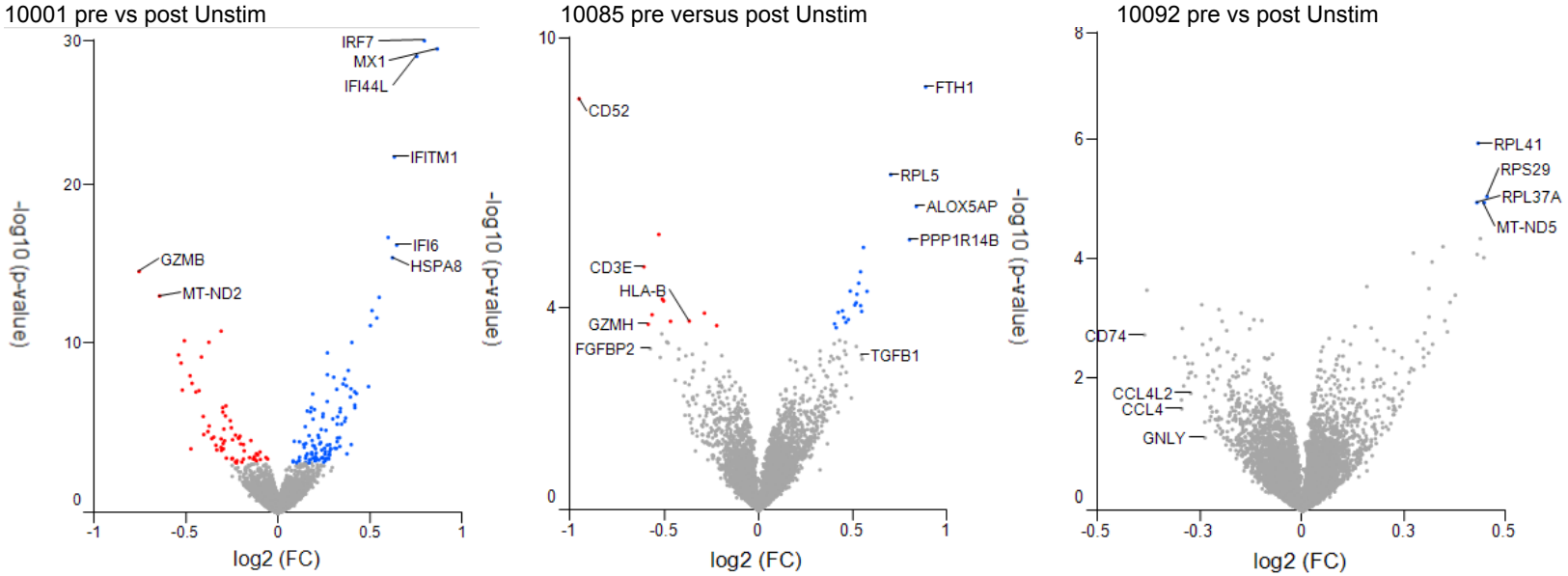

Figure 1-20: innate immune signatures in rifampicin DRESS

A) DC analysis approach. Features useful in the identification and characterisation of DCs. *Adapted from (Banchereau and Steinman 1998)*. **B**) Heatmap shows Z-score transformed expression of log2 counts (averaged and scaled per gene and antibody) of 6 genes and 22 antibody surface markers related to function and differentiation of DCs (as specified in section 4.4.8) in three patients, two timepoints and two in vitro stimulation conditions. Yellow box highlights expression of markers related to DC maturation in rifampicin stimulated cells. Green box highlights expression of markers related to antigen presentation in rifampicin stimulated cells **C**) Heatmap scaled by patient, timepoint and in vitro stimulation condition. Purple box highlights markers related to T cell inhibition and immune tolerance in pre- and post-SDC unstimulated cells **D**) Volcano plot of gene expression in NK cells from unstimulated pre- compared to post-SDC samples. Genes from the pre-SDC cells up signature are highlighted in blue and genes upregulated in post-SDC unstimulated cells are highlighted in red for patient 10001, 10085, 10092. Genes with a fold change >0.6 are labelled – excluding patient 10092 genes contributing to up signature in post-SDC unstimulated cells.

4.5. Discussion

The functional studies in chapter two and three of this thesis confirm the immunological basis of rifampicin SCAR, the presence of drug-specific T cells, and putative risk HLA alleles. However, HLA risk allele show modest odds ratio and there were considerable numbers of drug-tolerant controls carrying the risk HLA allele. This is like several other drug-HLA risk allele combinations and has been characterised in the literature as the 'positive predictive gap' (Peter et al. 2017). Herein, we have tried to further characterise the immune profile and the possible presence in the peripheral blood of drug specific TCR in the pathogenesis of rifampicin DRESS. This exploratory work aimed to better understand the immunological factors that may contribute to tolerance versus allergy – especially in the context of HIV. The challenge though has been to disentangling rifampicin-specific cells from the complex immune dysregulated environment associated with advanced HIV (Phillips and Mallal 2007; Peter, Choshi, and Lehloenya 2019) as well as the acute immune activation associated with acute DRESS. We aimed to detect consistent patterns between profiling Cite-seq profiling and CyTOF analyses, and use both *in vitro* drug stimulation conditions, drug tolerant controls, and samples across *in vivo* drug rechallenge and positive reactions to rifampicin to uncover relevant immune cell subsets and a more accurate assessment of the functional properties of rifampicin-specific T cells.

First examining cell counts across sampling conditions, we noted increased frequencies of CD8+ T cells post SDC. CD8+ T cells were not only prominent in post-SDC samples, but showed a more activated, exhausted, and terminally differentiated effector memory phenotype compared to pre-SDC samples. This is consistent to other studies reporting pre-existing memory CD8+ T cells, directed against either self or foreign antigens as potential sources of drug responsive T cells (Picard et al. 2010; Adam et al. 2014). Post-SDC T cells expressed high levels of CD57, a marker of terminally differentiated, exhausted and senescent T cells upregulated in chronic inflammation or aging (Pinti et al. 2016), and this CyTOF expression was consistent with a terminally differentiated and exhausted gene expression signature (KLRG1, PD-1, CTLA4, EOMES, LAG3 and TIGIT) in Cite-Seq. Expanded, exhausted T cells are well reported in advanced HIV (Wherry and Kurachi 2015; Lopez Angel et al. 2021; Ndhlovu et al. 2015). In contrast, T cells from pre-SDC samples showed a more naïve and central memory phenotype with high expression of CCR7, SELL and CD27. It has been suggested that CD57+ cells secrete cytokines after activation, however, due to increased susceptibility to antigen-induced cell death, they are unable to undergo cell proliferation (Focosi et al. 2010). However, there was no difference in the expression of exhausted T cell markers between unstimulated and rifampicin stimulated T cells *in vitro*, making it unlikely that antigen-induced apoptosis is responsible for the CD57 expression (Brenchley et al. 2003). A subset of CD4+ and CD8+ T cells with co-expression of CD27, CD28, CD45RA and CX3CR1 suggested the presence of activated T

cells with high capacity for proliferation, proinflammatory and cytotoxic responses after antigenic stimulation (Herndler-Brandstetter et al. 2018; Horiuchi et al. 2001; Tian et al. 2017). In CyTOF analysis, this co-expression was not observed for drug tolerant controls.

In vitro stimulation with rifampicin significantly increased CD8+ T cell responsiveness in pre- and post-SDC samples. In our CyTOF data, analysis of intracellular cytokine production following FLTD and SEB stimulation both showed an increased expression IFN-γ, TNF-α and IL-2 in T cells enriched in DRESS patients than tolerant controls. An excessive inflammatory response characterised by elevated levels of proinflammatory cytokines and chemokines and extensive keratinocyte death has been described in DRESS patients (Duong et al. 2017), with circulating CD8+ T cells known to be the greatest producers of IFN-γ and TNF-α (Cho, Yang, and Chu 2017b). In our DRESS patients, transcriptional expression of many cytotoxic, proinflammatory cytokines and chemokines including CXCL3, CXCL5, CXCL13, CCL2, IL1B, TNF-α, PRF1; were dramatically increased upon drug stimulation. Interestingly, a more potent activation was seen in post- than pre-SDC samples where upregulated gene expression responses following in vitro rifampicin stimulation mapped towards viral processing rather than only activated and cytotoxic responses (NKG7, GZMB, GZMH, GNLY) seen in post-SDC samples, related to in vivo rifampicin stimulation. High levels of CCL17 and CCL22, ligands of CCR4 and indicators of T cell recruitment and subsequent antigen presentation mediated by monocytes upon exposure to the culprit drug have been reported in a DRESS patient, and our data is consistent with this (Kim et al. 2020).

DRESS is thought to have a Th2 phenotype, with Th2 cytokines like IL-5 and IL-13 driving tissue eosinophilia (Cacoub et al. 2011). We noted The CD4+ T cells showed enrichment of genes in the cellular responses to IL4 pathway in response to both *in vivo* and *in vitro* rifampicin stimulation. These included TCF7, a transcription factor that promotes Th2 differentiation (Walker and McKenzie 2018). We also found a significantly increased *in vitro* responsiveness of Th2 cells to rifampicin in the CD4+ effector T cells subpopulation, confirmed by surface expression of IL4R (CD124) and minimal expression of CCR6 (CD196). Surprisingly, we did not observe a corresponding increased expression of typical Th2 cytokines such as IL-4, IL-5, IL-10, and IL-13. Expression of chemokine CXCR3 and CD62L have been used to subdivide effector memory TH2 T cells into four distinct subpopulation, and on antigen stimulation each had diverse cytokine production, with not all sub-populations showing robust cytokine production (Endo et al. 2014). Therefore, our Th2 cells may represent low cytokine producing subpopulations, or the lack of robust cytokine production may also suggest limited drug-specific response amongst the CD4 T-cell compartments.

Elegant murine studies in abacavir hypersensitivity, have shown that CD4+ T cell depletion increases DC maturation, thereby providing increased co-stimulatory signals which enable a break in immune tolerance in the presence of drug and generation of clinical hypersensitivity (Cardone et al. 2018). For this reason, we wanted to explore the phenotype and activation state of peripheral blood antigen presenting cells, especially in the HIV infected DRESS samples. Exploring cell numbers, we found a decreased frequency of monocytes in post-SDC samples, with increases in pre-SDC and drug tolerant controls; a subset of CD16+ monocytes were uniquely enriched in DRESS recovery samples. In cases compared to drug-tolerant controls, monocytes overproduced TNF-α and IL-2 following nonspecific SEB stimulation. An increased production of inflammatory cytokines from myeloid cells have previously been shown in peripheral blood and site of disease for SCAR patients (de Araujo et al. 2011; Tohyama et al. 2012), however non-specific monocyte responsiveness and variability in monocyte cell numbers may also reflect non-drug/DRESS changes but rather relate to TB disease state. Active TB is known to cause increases in circulating monocytes and induce disease-specific immunosuppression (Lastrucci et al. 2015).

Cite-seq analysis on pre- and post-SDC immune cells, using canonical genes and antibody expression, identified two subsets of macrophages resembling classical M1 mainly involved in inflammatory responses and M2 phenotype involved in anti-inflammatory responses (Yunna et al. 2020). In addition, we identified CD14+ classical and $CD14^{dim}$ CD16+ non-classical monocytes. Although there was more resolution at transcriptional level, to maintain substantial number of cells for comparison, we analysed whole monocytes and macrophages populations. Monocytes in pre-SDC samples with an increased expression of CD14, expressed genes involved in bacterium responses, whereas in post-SDC samples showed an inflammatory transcriptional signature enriched with genes related to cytokine signalling and attraction of effector T cells to the sites of inflammation (Shi and Pamer 2011). These data shows drug-specific monocytes subset responses even without prior resolution by canonical genes and surface protein markers into CD14+ and CD16+ monocytes. Monocytes from pre-SDC samples showed enrichment of wound healing pathway which signifies this early recovery stage, with settled laboratory and clinical findings following acute DRESS and prior to SDC. We also examined T cell ligands that indicate recent TCR ligation with the present antigen and found upregulation of CD40 and HLA-DR which may indicate cell-cell interaction for the activation of rifampicin specific T cells – indicating co-ordinated innate and adaptive communication in the presence of drug. Additionally, we defined the possible role of DCs in the priming and development of Th2 cells implicated in the pathogenesis of DRESS. We also observed the lack of IL10 expression which highlights DCs as possible ignitors of immune responses and their neglect of immunity control in the presence of rifampicin.

Very few data exist on the changes in the T regulatory cell compartments in patients affected by SCAR, particularly in HIV infected patients Consequently, we looked at regulatory T cells and their functionality in the presence of drug. Regulatory T cells are crucial for regulating immune homeostasis and self-tolerance. They express transcription factor Foxp3, but can also be identified by surface expression of CD25 and low or null expression of CD127 (Buckner 2010). They maintain peripheral tolerance by becoming activated, producing inhibitory cytokines and modulating DC maturation and function to suppress antigen-specific responses. They also function in a homeostatic manner to downregulate immune responses against invading pathogens and tumours – this can be deleterious by limiting infection sterilization or anti-tumour immunity (Vignali, Collison, and Workman 2008). The was considerable inter-individual variation in the numbers of Tregs, but we did note the post-SDC samples to have lower percentages of Tregs compared to HIV infected drug tolerant controls, pre-SDC and recovery samples from HIV infected and uninfected DRESS patients. Interestingly, drug-tolerant controls show higher expression levels of activation marker (HLA-DR) and chemokines (CCR6) regulating trafficking to sites of inflammation. These data, along with the increased expression of TGFβ suggests that drug-tolerant controls carrying at risk HLA alleles may have more Tregs functionality, but considerable further work is necessary to confirm this hypothesis.

With scRNA-seq, we were also able to look at V(D)J sequences for paired T cell receptors and provide a detailed characterization of expanded clones from T cell repertoires and identify strong drug specific immune responses that shape the entire immune repertoire in rifampicin DRESS. In a study explaining the interaction between HLA, carbamazepine and TCR in SCAR, they found public αβTCR with a bias for HLA risk allele. The oligoclonal clonotypes overexpressed cytotoxic and T cell activation markers in comparison to healthy controls (Pan et al. 2019). In contrast, our data demonstrated interindividual heterogeneity of TCR repertoire and T cell clones overrepresented in the CD8+ T cell clusters with multiple phenotypes and functionally divergent. In an attempt to explore for any shared antigen-specificity between the TCR repertoires of our patients, we used the GLIPH2 algorithm applied to the three rifampicin DRESS patients. We inferred HLA restrictions by only analysing patients with HLA-B*4403. We then prioritised TCR specificities groups shared among three patients and present the pre- and post SDC timepoints and unstimulated and rifampicin stimulated conditions, with interesting hypothesis generating results. T cells bearing TCRs with the SQVP group were found across all three patients and had a massive production of cytokines similar to what have seen ELISpots and single cell immune profiling following drug stimulation. When cells from one patient were stimulated with rifampicin, we observed an increased expression of IFN-γ and cytotoxic molecules as compared to unstimulated cells. This indicates that T cells with TCRs from SQVP group, have a higher ability to respond *in vitro* to rifampicin stimulation producing molecules that drive inflammatory responses and T cell mediated apoptosis. None of the TCR similarity groups overlapped with the TCR groups associated with MTB disease outcomes (Musvosvi et al. 2023) and

CMV TCR repertoire (Attaf et al. 2020). However, comparisons to clonotypes driven by HIV antigens and other HHVs remains unknown.

Several studies described the upregulation of granzyme B, perforin and granulysin among other cytotoxic and inflammatory markers and they have been suggested as biomarkers of severity (Peter et al. 2017; Chung et al. 2008). These cytotoxic markers can be linked to NK as well as T cells, and thus we explored NK cell populations as part of our analyses. Indeed, we found a more activated, inflammatory, and cytotoxic NK compartment in the post-SDC compared to the pre-SDC unstimulated cells demonstrating the immune activation of in vivo drug exposure. However, we did not observe any differences between unstimulated and rifampicin stimulated cells *in vitro*. Therefore, it was unclear if the emerging cytotoxic pattern in NK cells was the results of general immunopathology induced by SCAR and non-specific NK responses in an hyperactivated microenvironment or results of an innate lymphoid response relevant to DRESS immunopathogenesis.

This part of the study has several limitations. Firstly, we had low numbers of DRESS patients and drug tolerant controls in our CyTOF data, therefore having insufficient statistical power for grouped analyses. Similarly, in our scRNA-seq analysis, we had only three patients, who were chosen on the basis of similar clinical characteristics and presence of HLAB44:03 carriage, limited any comparison to those without HLA-B*4403 carriage, or to HIV negative rifampicin DRESS and drug tolerant controls. Secondly, due to the fact that oral sequential drug challenge was not standardised, and rifampicin was re-introduced at different times across the time course of both DRESS and TB disease, some of the differences that we have noted may not relate to drug, but rather acute DRESS and recovery, or active TB disease with different amounts of exposure to sterilising medications. Furthermore, the post-SDC sampling time-point did not always occur immediately at the onset of symptoms, being performed hours to days following onset of symptoms and reaction to rifampicin on re-exposure. This may also add additional complexity to the interpretation of this data. Thirdly, our CyTOF antibody panel did not include surface markers for a thorough subpopulation of T cell phenotypes, or identification of all innate and innate-like immune cells or unconventional T cells subsets such as MAIT cells. To an extent this was mitigated by the expanded cell phenotyping afforded by Cite-seq.

In conclusion, in rifampicin DRESS patients, we have found: i) both T cells lineages with increased expression of activation, exhaustion and senescence markers; ii) skewing of CD4+ T cell activation towards Th2 functional phenotype; iii) increased CD8+ effector T cells; iv) high expression levels of a variety of cytokines and chemokines, from proinflammatory to cytotoxicity in active reaction (post-SDC and rifampicin stimulated cells), to those that inhibit immune responses largely in early recovery (pre-SDC unstimulated cells); v) T cell clones with a shared TCR specificity group with increased

inflammation upon rifampicin *in vitro* stimulation; and vi) a mature innate immune cell compartment that promotes activation of T cells, not induction of peripheral tolerance. Our analyses provide an the first in depth characterisation of DRESS in persons living with HIV, and an introductory understanding to immunological factors that mediate transitions from drug tolerance to reaction in rifampicin DRESS. It offers a framework for future in-depth investigations into the roles of innate immune cells, drug specific T cells influx at the site of disease and confirm tissue specificity of T cell clones bearing SQVP TCR specificity group.

Chapter 5 - Site of disease

5.1. Introduction

In chapter 4 we examined the peripheral blood compartment of three SCAR patients. The limitations of this compartment compared to site-of-disease samples meant that we actively tried to collect skin biopsies for Cite-seq immune profiling to match with our peripheral blood compartment findings. The only patient where this was possible was patient 10085 transcriptional profile in rifampicin induced DRESS.

Site of disease samples shown to have enriched populations of infiltrated and pathogenic lymphocytes (Chung et al. 2008; Kim et al. 2020). Skin infiltrating T cells express genes involved in T cell activation, proliferation, and migration such as (JAK3, STAT1, IL2RG, MKI67 and CCR10) (Kim et al. 2020). However, little is known about the comprehensive expression programs and functional states of skin-infiltrating T cell populations, particularly in an immune state complicated by HIV TB co-infection. In this chapter we attempted to profile and characterized the types and states of skin-infiltrating T cells isolated from frozen lesioned and non-lesioned skin biopsies collected during an oral additive sequential drug challenge.

5.2. Materials and Methods

5.2.1. Patient characteristics – 10085 affected and non-affected skin

A 41-year female diagnosed with HIV in 2018, developed skin and systemic signs and symptoms associated with adverse drug reaction thirty-two days after starting Rifafour – a fixed drug combination for the treatment of drug susceptible tuberculosis. The patient presented at a primary care hospital with a 55% body surface area skin rash characterised by exanthema, erythema, epidermal necrolysis which affected the trunk, legs, arms, palms, and soles. The patient was antiretrovirals naïve and the most recent CD4 count, measured close the onset of major reaction was 39 cells/mm^3. Notable laboratory findings were high eosinophils in the acute stage of the ADR (7 days since symptoms onset) and on SDC reaction to rifabutin, liver enzymes were also elevated in the acute stage, pre-SDC and post-SDC rifampicin and rifabutin reactions. We measured the viral copies of HHV6, EBV and CMV in the plasma samples collected longitudinally and observed detectable levels on CMV in all samples with the highest viral load noted in the post-SDC rifampicin reaction plasma (figure 4-6B). Sequential drug challenge is the gold standard for diagnosis and management of FLTD induced ADRs at Groote Schuur hospital. The first of the four FLTD to be re-introduced was isoniazid followed fifteen days after symptoms onset, followed by rifampicin after twenty-three days. Five days later, the patient reacted to rifampicin and clinical manifestations included itching, burning and visible rash characterised by exanthema and erythema (figure 4-6B).

5.2.2. Skin biopsy collection

Patient 85 4mm across and 6mm deep skin biopsy of lesioned skin was sampled within 24 hours of the positive reaction to rifampicin re-exposure (figure 5-1A). This was 30 days after the acute onset of systemic and skin signs and symptoms. Three (2X lesioned and 1X non-lesioned) skin biopsies were collected in R10 media for cryopreservation (1X lesioned and 1X non-lesioned) and formalin (1X lesioned) for histology.

5.2.3. Immunohistochemistry and immunofluorescence

Skin biopsy for histopathology was prepared and analysed as reviewed and detailed here (Chimbetete et al. 2022; Chimbetete et al. 2023). We used basic immunohistochemistry (IHC) to stain CD3, CD4, CD8 and CD45RO+ T cells. We also established an immunofluorescence assay in our laboratory to further identify T cell subpopulations, including regulatory T cells and their location in the skin. Confocal microscopy was used for visualization and visual semi-quantitative analysis scoring systems or a quantitative analysis counting positive cells per high powered field were the two quantification methods used (Chimbetete et al. 2022; Chimbetete et al. 2023).

5.2.4. Skin biopsy cryopreservation and shipping to VUMC for analysis

For cryopreservation, skin biopsies were transferred into 1ml cryovial containing 20% DMSO in foetal bovine serum (FBS) and stored in strata cooler at -80°C overnight and transferred to cryobox the next day for long term storage. The cryopreserved skin biopsies were shipped on dry ice to VUMC in February 2020, with non-optimal cold chain in transit – which could have possibly had an effect on the low cell numbers after thawing and single cell suspension.

5.2.5. Single cell suspension, TCR sequencing, Cite-seq/Total Seq

To achieve single cell suspension for Cite-seq including TCR sequencing, we collaborators at VUMC performed skin digestion using collagenase P enzyme (Sigma). The skin biopsy was thawed in August 2021, following 20 months of cryopreservation. Collagenase P solution was prepared by dissolving 60mg of lyophilized powder in 10ml of sterile 1XPBS to make 6mg/ml stock concentration. Cryovials of affected and non-affected skin biopsies were thawed in 37°C water bath. The FBS/DMSO was removed, and biopsies were washed with R10 media then transferred to a petri dish, chopped with scissors until finely minced. The skin bits were transferred to 15ml conical tube and topped up with R10 to bring the volume to 5ml. One millilitre of collagenase P (6mg/ml) and 25ul of DNase I (20mg/ml) were added. The tubes were incubated at 37°C for 90 minutes with gentle agitation. After digestion, cells were passed through a 70µm strainer using a syringe plunger. To wash the cells, 15ml of 1XPBS was added and centrifuged at 400g for 7 minutes. Cells were lysed for 3 minutes with 3ml ACK lysis buffer (life technologies) and then washed again with 30ml 1XPBS. Cells were counted,

pelleted and the 10X genomics sample preparation and staining were followed as outlined in section 4.2.4.

5.2.6. Data analysis – Cite-seq

Data analyses including normalization, clustering, visualization, and differential analysis were performed as outlined in section 4.2.4.

5.3. Results

5.3.1. Histopathology and immunohistochemistry report

The haematoxylin and eosin (H&E) staining showed the dermis with an interstitial and perivascular lymphohistiocytic dermatitis with pigmentary incontinence and oedema with no eosinophils. The pathological diagnosis was an interface, erythema multiforme-like dermatitis of the vacuolar degeneration type (appendix, section 5.1, histology report). In comparison, a skin biopsy of an HIV-infected drug tolerant control showed no histopathological and morphological changes in both dermal and epidermal compartments, as well as a low distribution of inflammatory infiltrates compared to those observed for patient 85 lesioned skin (figure 5-1B).

Immunohistochemistry of the same skin biopsy stained with anti-CD3, CD4, CD8, CD45RO and a triple staining immunofluorescence panel of CD3+CD4+FoxP3+ specific for Tregs; confirmed infiltration of T cells to the site of disease. Majority of skin infiltrating T cells were found in the superficial dermis, and minimally at the dermo-epidermal junction and in the epidermis. Overall, dermal (and epidermal) CD4+ T cell infiltrates were lower when compared to CD8+ T cells, with an average number of positive cells per high-powered field of 26 versus 67 dermal T cells respectively, $P=0.03$. Expression of effector memory T cells was assessed using the CD45RO marker. CD45RO+ T cells predominated across CD3+ T cell infiltrates in the dermis, although no dual staining was carried out to determine which T cell sub-population (CD4, CD8) displayed a higher effector memory phenotype. The average density of Tregs in the dermis (number of CD3+CD4+FoxP3+ Tregs divided by the average dermal area) and frequency (CD3+CD4+FoxP3+ Tregs as a percentage of dermal CD3+CD4+ T cells present) over three high-powered field (X60) stitched panel images was low and very sparse, with almost none appearing in the epidermis. Overall, the few Tregs observed were in the superficial dermis, appearing in clusters of CD3+CD4+ T cells, with an average density and frequency of 10 cells/mm^2 and 20%, respectively (figure 5-1C).

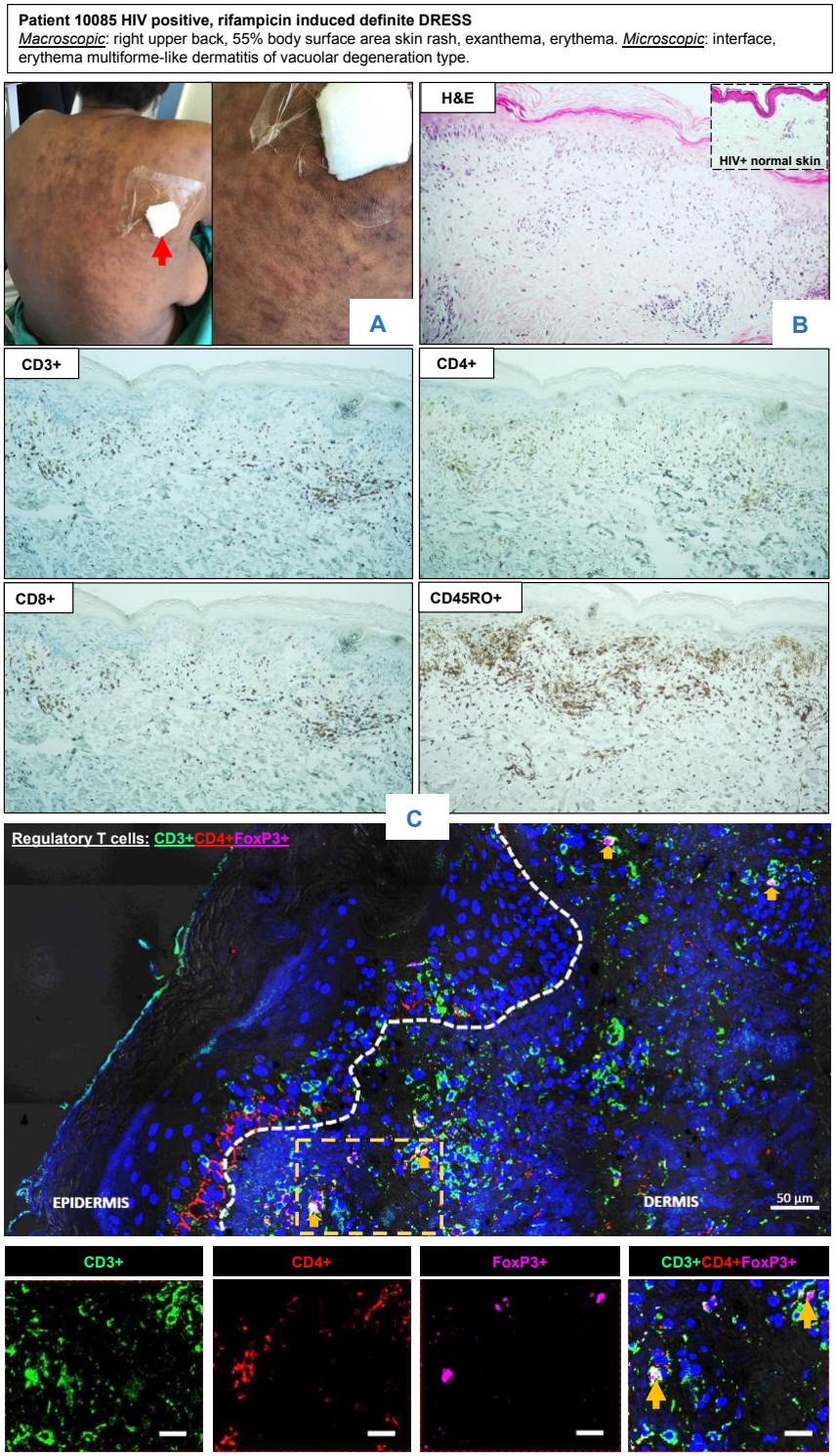

Figure 1-1: Rifampicin DRESS affected skin biopsy histology and immunohistochemistry

A) Post-SDC reaction to rifampicin skin biopsy site. Skin biopsy collected 24 hours after SDC reaction to rifampicin, at day 30 after onset of systemic and skin symptoms. Signs and symptoms on rifampicin re-exposure were similar to onset, including itching, burning and rash characterised by exanthema and erythema. **B**) Haematoxylin and eosin staining of punch skin biopsy from patient 10085 and normal skin from HIV+ drug tolerant control (top right corner of H&E image). **C**) Second and third panels illustrate immunohistochemistry results of the same skin biopsy stained with CD3, CD4, CD4 and C45RO antibodies for detection of T cell subsets infiltrating the dermis and epidermis of patient 10085 (rifampicin DRESS). Lower two panels are immunofluorescence staining with CD3, CD8, CD4 and FoxP3 to detect T cells and further subpopulation to quantify regulatory T cells among CD3+CD4+ T cells (Chimbetete et al. 2023).

5.3.2. Cite-seq immune profiling in affected and unaffected skin biopsy.

In our affected and unaffected skin biopsy ScRNA-seq experiments we targeted 5000 cells in affected and unaffected skin. However, only 203 major immune cells were recovered after removal of doublets and normalization (figure 5-2B), making our findings in this experiment of limited value. Nevertheless, we conducted cautionary exploratory analyses of the small number of cells, focused on T cells and monocytes enriched in both affected and unaffected samples. Unsupervised clustering and the UMAP shows clusters of cells found in the skin – determined by expression of canonical genes and lineage surface expression markers (figure 5-2A).

CD8+ T cells.

Consistent with our analysis of drug specific peripheral T cells in sc-RNAseq and CyTOF data, CD8+ T cells in affected skin showed a significant upregulation of genes related to memory phenotype and maturation (IL7R – CD127, IL2RG, CD52) (Martin and Badovinac 2018), co-stimulation markers highlight monocyte-T cell interaction for T cell activation (CD2, LINC01871) (Binder et al. 2020) and proliferation regulation (MT2A, SH3BGRL3) (Subramanian Vignesh and Deepe 2017) (figure 5-2C).

Monocytes.

Monocytes/macrophages in the affected skin biopsy were more activated, proinflammatory (IL1B, CCL3, CCL4, TIMP-1), and expressed neutrophil attracting chemokines (CXCL2, CXCL8), which extravasate in the vicinity of perivascular macrophages (Heath and Carbone 2013). Affected skin monocytes also highly expressed known mediators of IL1B production (NFKBIA) (Sutterwala, Haasken, and Cassel 2014), monocytes migration (CXCL3, CCL2), T cells chemoattractant (CCL3L1, CCL20) (Kupper and Fuhlbrigge 2004) (figure 5-2D).

TCR clonotypes.

We had limited number of cells with TCR α- chain and TCR β-chain to define clonotypes for downstream analysis.

A

Cells in unaffected *n=5* (left) and affected *n=198* (right) skin.

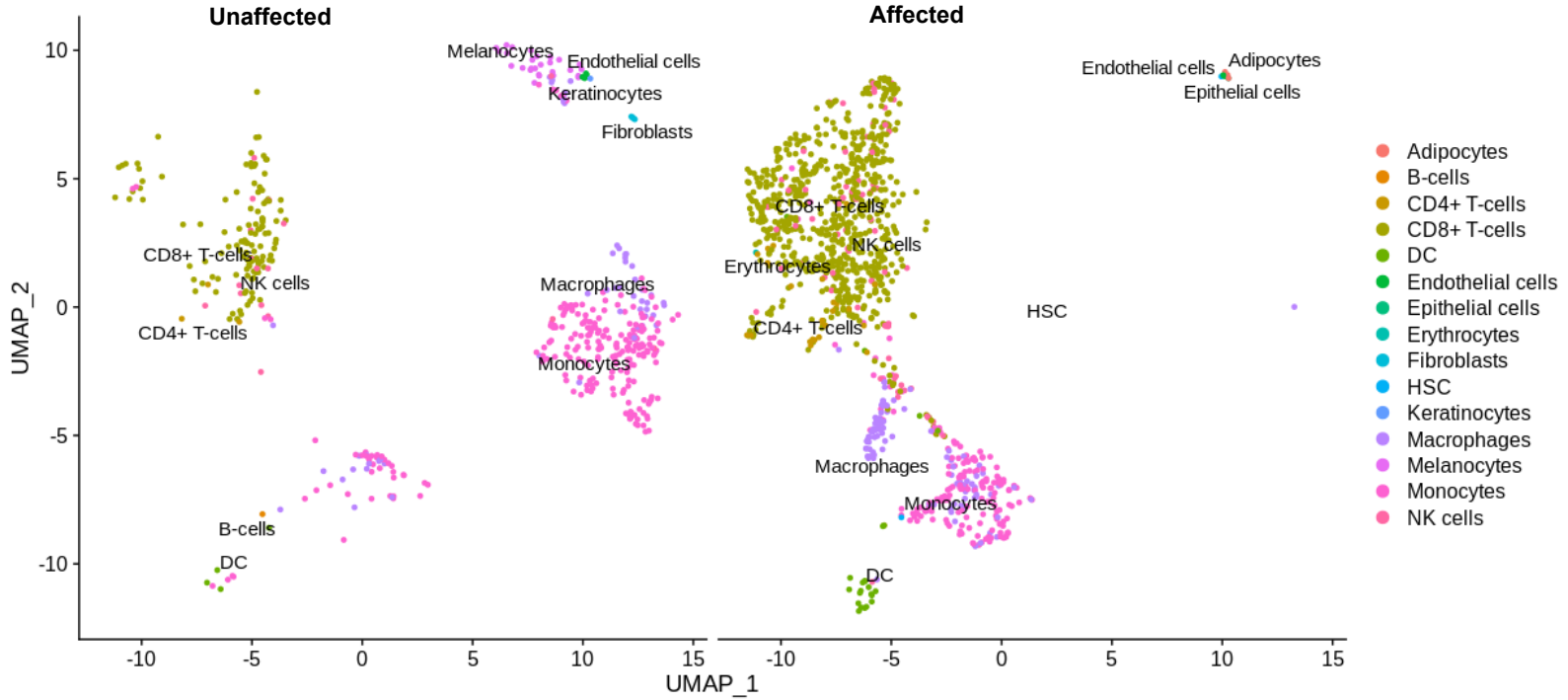

B

	AFFECTED	UNAFFECTED
CD8+ T cells	32	0
DC	1	0
Endothelial cells	3	0
Erythrocytes	1	0
Macrophages	26	0
Monocytes	121	4
NK cells	14	1

C

CD8: Up-Regulated Genes Per Cluster

Name	Aff		P-Value	Unaff
IL7R	2.08	***	2.51e-3	-2.08
LINC01871	1.49	**	4.20e-2	-1.49
MT2A	1.35	*	6.95e-2	-1.35
CD2	1.02		6.63e-1	-1.02
IL2RG	0.95		9.51e-1	-0.95
SH3BGRL3	0.35		1.00e+0	-0.35
CD52	0.77		1.00e+0	-0.77

D

Status: Up-Regulated Genes Per Cluster

Name	Aff		P-Value	UnAff
IL1B	9.98	****	4.11e-80	-9.98
CXCL8	9.25	****	3.63e-79	-9.25
CXCL3	8.23	****	2.81e-62	-8.23
SERPINB2	11.36	****	3.01e-61	-11.36
CXCL2	8.20	****	3.14e-61	-8.20
CCL3L1	8.23	****	2.52e-52	-8.23
CCL3	6.06	****	2.04e-50	-6.06
CCL20	10.53	****	9.89e-46	-10.53
CCL4L2	7.14	****	1.10e-41	-7.14
CCL4	5.26	****	4.71e-38	-5.26
PLAUR	4.88	****	1.14e-36	-4.88
THBS1	4.73	****	1.41e-29	-4.73
CCL2	5.35	****	9.27e-29	-5.35
SOD2	3.65	****	3.28e-27	-3.65
TIMP1	3.65	****	1.83e-24	-3.65
CTSL	3.31	****	5.79e-21	-3.31
S100A9	3.22	****	2.44e-18	-3.22
CSTB	2.77	****	8.24e-16	-2.77
NFKBIA	2.62	****	5.14e-15	-2.62

Figure 1-2: Single cell gene expression of profiling of immune cells in affected skin biopsy of rifampicin induced DRESS

A) The UMAP projection of skin cells from rifampicin induced DRESS skin biopsies, showing the formation of 15 clusters in different colors. The description of each cluster is determined by expression of canonical genes. Cells on the left are from affected skin biopsy and right were from unaffected skin biopsy. **B**) Major immune cell numbers in affected and unaffected skin. **C**) Differential gene expression of CD8+ T cells in affected compared unaffected skin. Reported are the genes highly and significantly (after FDR correction for multiple comparisons) expressed in the CD8+ T cells cluster in affected skin. **D**) Differential gene expression of monocytes in affected compared unaffected skin. Reported are the genes highly and significantly (after FDR correction for multiple comparisons) expressed in the monocytes cluster in affected skin.

5.4. Discussion

Here, we attempted to demonstrate and characterise immune cells that drive rifampicin DRESS pathology. The histopathology results forms part of the work published in our lab (Chimbetete et al. 2023). Our Cite-seq data were heavily limited by skin biopsy storage and shipping, digestion techniques and the amount of skin at the start of digestion to achieve single cell suspension. Experiments could not be repeated to the lack of paired site of disease samples for the participants included in this thesis. Therefore, we are very cautious to form any conclusive remarks based on these limitations. Future experimental plans to look at the site of disease are outlined in section 6.16 of this thesis.

Chapter 6 – Future directions and Conclusion

6.1. Future directions

In this thesis we have presented genetic, immunological, and viral factors related to development of SCAR in HIV-TB co-infected patients. An easy performance *in vitro* assay (ELISpot) allowed us to establish the immunological basis of first line anti-tuberculosis drug induced SCAR, and this optimized assay has already impacted patient care and received international recognition. We identified and substantiated the importance of HLA risk alleles in the development of SCAR suggesting a putative risk HLA-B allele for rifampicin DRESS, and specificity of drug responsive T cells. High dimensional single cell analysis including CyTOF and sc-RNAseq afforded the first insights and exploration of DRESS in the context of HIV and TB co-infection, with advancement in our understanding of phenotype, differentiation, and functions of drug-specific T cells. The inclusion of drug tolerant controls carrying HLA risk alleles greatly contributed to the exploration of immune state associated with drug allergy and tolerance, in the context of HIV.

6.1.1. Drug-specific T cells to first-line anti-tuberculosis drugs

In Chapter 2, we discussed our efforts to optimize an ELISpot assay to confirm the specificity of drug responsive T cells and identify causative drug in a multi-drug regimen. In terms of diagnostics, an important aspect of SCAR management is the early withdrawal of causative drugs and supportive therapy to reduce life threatening complications. Causative drugs with long half-lives remain a dreaded complication associated with major morbidity and mortality (Rajaratnam et al. 2010). Traditional diagnostics to identify causative drug in SCAR have included chronology of drug exposure, patch testing and oral drug rechallenge if multiple drugs have been taken. These remain limited by the time they can be conducted and the risk of severe relapse on drug re-introduction.

ELISpot, LTT and cytometry-based assays are *in vitro* tests used to measure peripheral blood mononuclear cell responses to culprit drugs in patients with SCAR. In our study we focused on ELISpot assay, and even in our best performing drug, namely Rifampin, several limitations remain including sensitivity, specificity, reproducibility, and standardization for routine testing. Although rifampicin ELISpot is already proving clinically useful despite limited sensitivity, the other three FLTD (pyrazinamide, ethambutol, and isoniazid) could not be linked *in vitro* to the immunological mechanism of SCAR. Thus, further ELISpot optimization and development is required. The next steps we are considering and working on include: i) immune augmentations such as addition of IL-2 (Kato et al. 2017), or alpha-galacotsylceramide (Klaewsongkram et al. 2021); ii) longer drug incubations (Chessman et al. 2008) to improve antigenicity in immunoassays; iii) use of fresh rather than frozen PBMCs; and iv) the use of metabolites. To date, others have examined the use of

adjuvants but found issues of high background and false positive results (Janetzki et al. 2015), emphasizing the need to interpret laboratory results in the context of clinical testing, and continue trying several different optimization strategies.

6.1.2. Pharmacogenomic risk for FLTD-associated SCAR

In recent years, population specific predictive testing for HLA risk prior to starting a certain SCAR offending drugs has been introduced into routine clinical practice. The best examples is HLA-B*57:01 prior to starting abacavir which has nearly eliminated DHS secondary to abacavir (Mallal, Phillips, Carosi, Molina, Workman, Tomazic, Jägel-Guedes, et al. 2008), but HLA-B*15:02 prior to carbamazepine use is also used in many Asians countries (Ferrell and McLeod 2008). In these HLA risk alleles, the associations were very strong with odds ratios >100 and 100% negative predictive value. Furthermore, with abacavir the positive predictive value is more than 50% meaning in populations with high HLA-B*57:01 prevalence number needed to test is as low as 30. However, many HLA risk associations, similar to what we have noted in this thesis, show more modest odds ratio and low positive predictive values, limiting immediate clinical use and likely indicating important aspects of immunopathogenesis such as that risk may relate to certain shared features across groups of HLA risk alleles e.g., peptide binding specificities. In our context, given the lower-than-expected odds ratio for HLA-B*44:03 and HLA-B*15:01, our immediate next steps are a larger sample sizes of cases to validate these risk alleles conclusively. Similarly, we are looking to increase our numbers for other FLTD-SCAR combinations so that we have adequate power to uncover risk alleles for the other three first-line anti-TB drugs, as well as considering whether any of our multiple drug hypersensitivity phenotypes we see have unique HLA associations. Understanding the positive predictive gap, in this thesis we also examined for any other gene polymorphisms that contribute to hypersensitivity or tolerance including ERAP and KIR genes that have strong epistatic associations with HLA. We did note differences including higher frequency of efficient ERAP1 functional haplotypes in rifampicin SCAR compared to tolerant controls and possible regulation of NK and CTL responses in tolerant controls through KIR inhibitory receptor and HLA-B risk alle cognate ligand, however all were underpowered. Thus, enlarging our sample size will be critical to allow us to make more definitive conclusions of how HLA gene risk, ERAP polymorphisms and KIR haplotypes impact outcomes following rifampicin exposure. There have also been pharmacogenomic associations between adverse drug reactions and ADME genes. For instance, NAT2 polymorphism have been associated with FLTD DILI (Huang et al. 2002). Further work will explore if polymorphism that change drug concentration also increase the risk of hypersensitivity in at-risk individuals.

6.1.3. How Rifampicin interacts with the peptide-MHC:TCR immune synapse

This thesis work has detected drug-specific T cells recognizing the parent drug rifampicin, identified putative HLA and possible ERAP pharmacogenomic risk, as well as suggesting groups of TCRs that may be involved. Using in silico modeling tools we have several possible locations for rifampicin to bind HLA-B*44:03 and HLA-B*15:01; the highest sites include interacting with peptide, and between the HLA α-chain and β2-microglobulin in a manner that suggests it might stabilize the peptide-MHC complex. In-depth *in vitro* work is now planned to better understand where rifampicin binds to the peptide-MHC:TCR complex, if antigen processing is required, and if our suggested TCR grouping does in fact represent the offending clones. We will use two approaches for investigation: i) a Jurkat reporter cell line, electroporate with TCRs of interest (including SQVP TCR specificity group). These T cells will be cultured with patient B cell line or single antigen cell line expressing HLA-B*44:03 and HLA-B*15:01 pulsed with peptides including CMV and HIV antigens in the presence of rifampicin. In this assay different in vitro conditions will allow to monitor drug specific T cell activation as well as inhibition ii) a T cell cloning assay to expand drug specific T cells stimulated with rifampicin. The proliferative drug specific T cells will also be co-cultured with APCs and under different in vitro stimulation conditions, we will investigate the interaction of rifampicin with proteins involved in the antigen processing and presentation and required peptides (if any) for T ell recognition.

6.1.4. Changing co-stimulatory phenotypes in antigen presenting cells in person living with HIV

Many questions remain regarding how diverse co-stimulatory and inflammatory signals influence antigen presenting cells to shape the transcriptional and functional landscape in a manner that favours tolerogenic versus cytotoxic T cells in drug hypersensitivity. The elegant murine studies by the Norcross laboratory first examining how CD4 T-cell depletion leads to increased DC co-stimulation and consequent generation of cytotoxic CD8 T cells causing SCAR, and more recently in the role of tissue-resident Kupffer cells of the liver in suppressing flucloxacillin-reactive CD8 T cells preventing drug-induce liver injury highlight i) the important influence of APCs on drug hypersensitivity outcomes, ii) that APCs can be both beneficial and harmful, and iii) that several factors influence APC phenotypes (Cardone et al. 2018; Ananthula et al. 2023). In Chapter 4 we also explored circulating antigen presenting cells showing drug-stimulated activation of monocytes and cytokine production, as well as changing phenotypes across the time-course our samples. However, it is hard to dissect the drivers of these phenotypes and what direct they influence drug-specific T cells and the clinical phenotype. We are currently discussing and considering the best future methods for studying this important aspect of drug hypersensitivity pathogenesis in the context of HIV. Potential options include an HLA-B*44:03 transgenic murine model, while the other involves a shift to focus on drug tolerant persons carrying the risk HLA alleles during the first six weeks of anti-TB treatment. The

volume of TB patients in South Africa allows consideration of such an approach, but sample size and resource requirement would be considerable. In addition, given both the flucloxacillin DILI mechanistic work, as well as elegant spatial transcriptomic work in atopic dermatitis highlighting the exceptionally small number, yet profound influence of only a few resident antigen presenting cells in driving AD pathology, study of skin is critical (Schäbitz et al. 2022). We now have a major focus to study antigen presenting cells and their phenotypes at the site-of-disease in rifampicin DRESS skin biopsies using high dimensionality approaches such as imaging mass cytometry or spatial transcriptomics.

6.1.5. A critical role for regulatory T cells for ensuring tolerance to Rifampicin.

Immune homeostasis is maintained by FoxP3+ Tregs and other immune cells producing suppressive cytokines such as IL-10 and TGF-β which counter responses of autoreactive T cells and provides negative regulation of cytotoxic responses (Vignali, Collison, and Workman 2008). In fact, regulatory T cells have also been shown to be dramatically expanded and functional in the acute stage of DRESS, whereas in SJS/TEN they were diminished. Another student in our laboratory, using immunofluorescence staining for CD4, CD25 and FoxP3+ demonstrated no differences in T-regulatory numbers in the skin of HIV infected compared to uninfected DRESS cases, including rifampicin DRESS. Furthermore, in a DRESS patient with a slow onset of positive drug reaction symptoms following rifampicin re-exposure, Treg infiltrates were very high, likely demonstrating their homeostatic role to counteract effector T-cell responses (Chimbetete et al. 2023). These findings are consistent with the variable number of T-regs in the peripheral blood compartment of the rifampicin DRESS patients in this cohort. However, in our exploratory analyses of T-reg functionality there was a suggestion of increase HLA-DR activation amongst Tregs from drug-tolerant and recovering DRESS, and reduced expression of TGF-β and transcription factors T-bet, IRF4 and STAT3 in Tregs from rifampicin DRESS patients. Tregs with this profile are likely unable to suppress Th1 and Th2 responses (Zheng et al. 2009; Schietinger and Greenberg 2014). Based on this we hypothesize that peripheral lymphoid derived FoxP3+ Tregs infiltrating the skin, lack distinct tissue and drug specific molecular signature to control drug specific inflammatory and cytotoxic responses. This hypothesis needs to be explored in future work, including by characterisation of Tregs at the site of disease (skin and blister fluid) of both acute and recovery DRESS patients to examine their suppressive capabilities in localised inflammation across longitudinal sampling, as well as compared to drug tolerant controls. In fact, similar to the work examining the polarity of antigen presenting cells, the ideal studies to conduct our prospective cohorts across the first six weeks of anti-TB treatment in at risk individuals. Additional questions that we will consider during the course of this planned future work, includes: i) what are the molecular alterations in signalling that would account for Treg hypo responsiveness in at risk individuals? ii) what functions, if any may Tregs that are functionally deficient have in response to drug specific cytotoxic cells? and iii) is the functional

deficiency a consequence of advanced HIV-related immune suppression (in other words confined to persons living with HIV)?

6.1.6. Cutaneous immune cells and drug specific responses in the skin

During the course of this thesis, we worked hard to optimise shipping and sample processing methods for handling rifampicin DRESS skin biopsies. However, this has not yet been successful, and until recently we lacked 10X genomic capabilities at the University of Cape Town. We attempted shipping and processing of skin biopsy sample from patient 10085, however, due to suboptimal freezing conditions when shipping frozen skin biopsies to out collaborators at Vanderbilt University Medical Centre for processing and Cite-seq, there was a huge loss of cells during skin processing and considerable cell clumping. Thus, although we present some exploratory analysis of the sample, we were unable to perform most of our downstream analyses involving major immune cells. We have now optimised these methods and await the appropriate patient for sampling and analyse. In that initial analysis, the focus will be on examining the site-of-disease TCR repertoire to see if we can confirm tissue specificity of T cells bearing TCRs with the SQVP motif. Furthermore, the detection and characterisation of antigen presenting cells will also be important as we continue to study the interplay between the innate immune system and promotion of drug responsive T cells.

6.2. Conclusion

SCARs remain one the most challenging syndromes to diagnose, understand and treat, especially in HIV TB co-infected individuals. In this thesis we have begun to detail the immune phenotype of rifampicin SCAR in the context of HIV TB co-infection, using our unique setting of supportive care (not oral corticosteroids) and in vivo drug provocation to allow insights into drug-stimulated immune activation. We noted differences in several relevant immune compartments, including antigen presenting cells, regulatory T cells, and drug-specific T-cell clonotypes. Examining for HLA risk associations, we have noted an association with HLA-B*44:03 possibly modulated by ERAP haplotypes. However, all our genetic exploratory work needs larger sample sizes for confirmation, while our mechanistic work requires site-of-disease single-cell study. Considerable further in vitro mechanistic work as mapped out in this chapter is also required to confirm putative mechanisms for how rifampicin interacts with pMHC:TCR. Furthermore, additional larger studies both in humans and with animal models are warranted to explore immune tolerance in those carrying at risk HLA alleles, and the critical roles of antigen presenting cell phenotypes and regulatory T-cell functionality in drug tolerance and hypersensitivity.

References

Adam, Jacqueline, Natascha Wuillemin, Stephan Watkins, Heidi Jamin, Klara K. Eriksson, Peter Villiger, Stefano Fontana, Werner J. Pichler, and Daniel Yerly. 2014. 'Abacavir Induced T Cell Reactivity from Drug Naïve Individuals Shares Features of Allo-Immune Responses', *PLoS One*, 9: e95339.

Adler, N. R., A. K. Aung, E. N. Ergen, J. Trubiano, M. S. Y. Goh, and E. J. Phillips. 2017. 'Recent advances in the understanding of severe cutaneous adverse reactions', *Br J Dermatol*, 177: 1234-47.

Almudimeegh, A, C Rioux, H Ferrand, B Crickx, Y Yazdanpanah, and V Descamps. 2014. 'Drug reaction with eosinophilia and systemic symptoms, or virus reactivation with eosinophilia and systemic symptoms as a manifestation of immune reconstitution inflammatory syndrome in a patient with HIV?', *British Journal of Dermatology*, 171: 895-98.

Alter, G., M. P. Martin, N. Teigen, W. H. Carr, T. J. Suscovich, A. Schneidewind, H. Streeck, M. Waring, A. Meier, C. Brander, J. D. Lifson, T. M. Allen, M. Carrington, and M. Altfeld. 2007. 'Differential natural killer cell-mediated inhibition of HIV-1 replication based on distinct KIR/HLA subtypes', *J Exp Med*, 204: 3027-36.

Alvestad, Silje, Stian Lydersen, and Eylert Brodtkorb. 2008. 'Cross-reactivity pattern of rash from current aromatic antiepileptic drugs', *Epilepsy research*, 80: 194-200.

Ananthula, S., K. Krishnaveni Sivakumar, M. Cardone, S. Su, G. Roderiquez, H. Abuzeineh, D. E. Kleiner, M. A. Norcross, and M. Puig. 2023. 'Development of mouse models with restricted HLA-B∗57:01 presentation for the study of flucloxacillin-driven T-cell activation and tolerance in liver injury', *J Allergy Clin Immunol*, 152: 486-99.e7.

Attaf, Meriem, Julia Roider, Amna Malik, Cristina Rius Rafael, Garry Dolton, Andrew J. Prendergast, Alasdair Leslie, Thumbi Ndung'u, Henrik N. Kløverpris, Andrew K. Sewell, and Philip J. Goulder. 2020. 'Cytomegalovirus-Mediated T Cell Receptor Repertoire Perturbation Is Present in Early Life', *Frontiers in Immunology*, 11.

Auquier-Dunant, A., M. Mockenhaupt, L. Naldi, O. Correia, W. Schröder, and J. C. Roujeau. 2002. 'Correlations between clinical patterns and causes of erythema multiforme majus, Stevens-Johnson syndrome, and toxic epidermal necrolysis: results of an international prospective study', *Arch Dermatol*, 138: 1019-24.

Azukizawa, Hiroaki, and Satoshi Itami. 2007. 'Animal models of toxic epidermal necrolysis', *Drug Hypersensitivity*: 129-39.

Azukizawa, Hiroaki, Hiroshi Kosaka, Shigetoshi Sano, William R Heath, Isao Takahashi, Xing-Hua Gao, Yasuyuki Sumikawa, Masaru Okabe, Kunihiko Yoshikawa, and Satoshi Itami. 2003. 'Induction of T-cell-mediated skin disease specific for antigen transgenically expressed in keratinocytes', *European journal of immunology*, 33: 1879-88.

Azukizawa, Hiroaki, Shigetoshi Sano, Hiroshi Kosaka, Yasuyuki Sumikawa, and Satoshi Itami. 2005. 'Prevention of toxic epidermal necrolysis by regulatory T cells', *European journal of immunology*, 35: 1722-30.

Baecher-Allan, C., E. Wolf, and D. A. Hafler. 2006. 'MHC class II expression identifies functionally distinct human regulatory T cells', *J Immunol*, 176: 4622-31.

Bain, L. E., C. Nkoke, and J. J. N. Noubiap. 2017. 'UNAIDS 90-90-90 targets to end the AIDS epidemic by 2020 are not realistic: comment on "Can the UNAIDS 90-90-90 target be achieved? A systematic analysis of national HIV treatment cascades"', *BMJ Glob Health*, 2: e000227.

Bakkum, R. S., F. B. Waard-Van Der Spek, and H. B. Thio. 2002. 'Delayed-type hypersensitivity reaction to ethambutol and isoniazid', *Contact Dermatitis*, 46: 359.

Banchereau, J., and R. M. Steinman. 1998. 'Dendritic cells and the control of immunity', *Nature*, 392: 245-52.

Bashirova, A. A., M. Viard, V. Naranbhai, A. Grifoni, W. Garcia-Beltran, M. Akdag, Y. Yuki, X. Gao, C. O'HUigin, M. Raghavan, S. Wolinsky, J. H. Bream, P. Duggal, J. Martinson, N. L. Michael, G. D. Kirk, S. P. Buchbinder, D. Haas, J. J. Goedert, S. G. Deeks, J. Fellay, B.

Walker, P. Goulder, P. Cresswell, T. Elliott, A. Sette, J. Carlson, and M. Carrington. 2020. 'HLA tapasin independence: broader peptide repertoire and HIV control', *Proc Natl Acad Sci U S A*, 117: 28232-38.
Bejia, I. 2007. 'DRESS syndrome: case report', *Reactions*, 1141: 3.
Bekker, L. G., S. Roux, E. Sebastien, N. Yola, K. R. Amico, J. P. Hughes, M. A. Marzinke, C. W. Hendrix, P. L. Anderson, V. Elharrar, M. Stirratt, J. F. Rooney, E. Piwowar-Manning, S. H. Eshleman, L. McKinstry, M. Li, B. J. Dye, and R. M. Grant. 2018. 'Daily and non-daily pre-exposure prophylaxis in African women (HPTN 067/ADAPT Cape Town Trial): a randomised, open-label, phase 2 trial', *Lancet HIV*, 5: e68-e78.
Bellón, T. 2019. 'Mechanisms of Severe Cutaneous Adverse Reactions: Recent Advances', *Drug Saf*, 42: 973-92.
Beumont, M. G., A. Graziani, P. A. Ubel, and R. R. MacGregor. 1996a. 'Safety of dapsone as Pneumocystis carinii pneumonia prophylaxis in human immunodeficiency virus-infected patients with allergy to trimethoprim/sulfamethoxazole', *Am J Med*, 100: 611-6.
Beumont, Maria G., Amy Graziani, Peter A. Ubel, and Rob Roy MacGregor. 1996b. 'Safety of dapsone as Pneumocystis carinii pneumonia prophylaxis in human immunodeficiency virus-infected patients with allergy to trimethoprim/sulfamethoxazole', *The American Journal of Medicine*, 100: 611-16.
Bigby, M. 2001. 'Rates of cutaneous reactions to drugs', *Arch Dermatol*, 137: 765-70.
Bigby, M., S. Jick, H. Jick, and K. Arndt. 1986. 'Drug-induced cutaneous reactions. A report from the Boston Collaborative Drug Surveillance Program on 15,438 consecutive inpatients, 1975 to 1982', *Jama*, 256: 3358-63.
Binder, Christian, Filip Cvetkovski, Felix Sellberg, Stefan Berg, Horacio Paternina Visbal, David H. Sachs, Erik Berglund, and David Berglund. 2020. 'CD2 Immunobiology', *Frontiers in Immunology*, 11.
Blanchard, J. S. 1996. 'Molecular mechanisms of drug resistance in Mycobacterium tuberculosis', *Annu Rev Biochem*, 65: 215-39.
Blumenthal, Kimberly G., Jonny G. Peter, Jason A. Trubiano, and Elizabeth J. Phillips. 2019. 'Antibiotic allergy', *The Lancet*, 393: 183-98.
Boonyagars, L., P. Hirunwiwatkul, and C. P. Hurst. 2017. 'CD4 count and risk of anti-tuberculosis drug-associated cutaneous reactions in HIV-infected Thai patients', *Int J Tuberc Lung Dis*, 21: 338-44.
Borras-Blasco, J., A. Navarro-Ruiz, C. Borras, and E. Castera. 2008. 'Adverse cutaneous reactions associated with the newest antiretroviral drugs in patients with human immunodeficiency virus infection', *J Antimicrob Chemother*, 62: 879-88.
Bothamley, Graham H. 2002. 'Treatment, Tuberculosis, and Human Leukocyte Antigen', *Am J Respir Crit Care Med*, 166: 907-08.
Boudreau, Jeanette E, and Katharine C Hsu. 2018. 'Natural killer cell education in human health and disease', *Current Opinion in Immunology*, 50: 102-11.
Bradley, Philip, and Paul G. Thomas. 2019. 'Using T Cell Receptor Repertoires to Understand the Principles of Adaptive Immune Recognition', *Annual Review of Immunology*, 37: 547-70.
Brenchley, J. M., N. J. Karandikar, M. R. Betts, D. R. Ambrozak, B. J. Hill, L. E. Crotty, J. P. Casazza, J. Kuruppu, S. A. Migueles, M. Connors, M. Roederer, D. C. Douek, and R. A. Koup. 2003. 'Expression of CD57 defines replicative senescence and antigen-induced apoptotic death of CD8+ T cells', *Blood*, 101: 2711-20.
Brooks, K. M., J. M. George, A. K. Pau, A. Rupert, C. Mehaffy, P. De, K. M. Dobos, A. Kellogg, M. McLaughlin, M. McManus, R. M. Alfaro, C. Hadigan, J. A. Kovacs, and P. Kumar. 2018. 'Cytokine-Mediated Systemic Adverse Drug Reactions in a Drug-Drug Interaction Study of Dolutegravir With Once-Weekly Isoniazid and Rifapentine', *Clin Infect Dis*, 67: 193-201.
Buckner, J. H. 2010. 'Mechanisms of impaired regulation by CD4(+)CD25(+)FOXP3(+) regulatory T cells in human autoimmune diseases', *Nat Rev Immunol*, 10: 849-59.
Cacoub, P., P. Musette, V. Descamps, O. Meyer, C. Speirs, L. Finzi, and J. C. Roujeau. 2011. 'The DRESS syndrome: a literature review', *Am J Med*, 124: 588-97.

Campbell, J. J., G. Haraldsen, J. Pan, J. Rottman, S. Qin, P. Ponath, D. P. Andrew, R. Warnke, N. Ruffing, N. Kassam, L. Wu, and E. C. Butcher. 1999. 'The chemokine receptor CCR4 in vascular recognition by cutaneous but not intestinal memory T cells', *Nature*, 400: 776-80.

Cardone, M., K. Garcia, M. E. Tilahun, L. F. Boyd, S. Gebreyohannes, M. Yano, G. Roderiquez, A. D. Akue, L. Juengst, E. Mattson, S. Ananthula, K. Natarajan, M. Puig, D. H. Margulies, and M. A. Norcross. 2018. 'A transgenic mouse model for HLA-B*57:01-linked abacavir drug tolerance and reactivity', *J Clin Invest*, 128: 2819-32.

Carr, A., and D. A. Cooper. 2000. 'Adverse effects of antiretroviral therapy', *Lancet*, 356: 1423-30.

Carr, Andrew, Ronald Penny, and David A. Cooper. 1993. 'Efficacy and safety of rechallenge with low-dose trimethoprim-sulphamethoxazole in previously hypersensitive HIV-infected patients', *AIDS*, 7: 65-72.

Carr, D. F., M. Chaponda, A. L. Jorgensen, E. C. Castro, J. J. van Oosterhout, S. H. Khoo, D. G. Lalloo, R. S. Heyderman, A. Alfirevic, and M. Pirmohamed. 2013. 'Association of human leukocyte antigen alleles and nevirapine hypersensitivity in a Malawian HIV-infected population', *Clin Infect Dis*, 56: 1330-9.

Castillo, E. F., and K. S. Schluns. 2012. 'Regulating the immune system via IL-15 transpresentation', *Cytokine*, 59: 479-90.

Catt, C. J., G. M. Hamilton, J. Fish, K. Mireskandari, and A. Ali. 2016. 'Ocular Manifestations of Stevens-Johnson Syndrome and Toxic Epidermal Necrolysis in Children', *Am J Ophthalmol*, 166: 68-75.

Chang, C. C., C. C. Ng, C. L. Too, S. E. Choon, C. K. Lee, W. H. Chung, S. H. Hussein, K. S. Lim, and S. Murad. 2017. 'Association of HLA-B*15:13 and HLA-B*15:02 with phenytoin-induced severe cutaneous adverse reactions in a Malay population', *Pharmacogenomics J*, 17: 170-73.

Chang, C. H., Y. F. Chen, V. C. Wu, C. C. Shu, C. H. Lee, J. Y. Wang, L. N. Lee, and C. J. Yu. 2014. 'Acute kidney injury due to anti-tuberculosis drugs: a five-year experience in an aging population', *BMC Infect Dis*, 14: 23.

Chaponda, Mas, and Munir Pirmohamed. 2011. 'Hypersensitivity reactions to HIV therapy', *British journal of clinical pharmacology*, 71: 659-71.

Chaves, P., M. J. Torres, A. Aranda, S. Lopez, G. Canto, M. Blanca, and C. Mayorga. 2010. 'Natural killer-dendritic cell interaction in lymphocyte responses in hypersensitivity reactions to betalactams', *Allergy*, 65: 1600-8.

Chen, Pei, Juei-Jueng Lin, Chin-Song Lu, Cheung-Ter Ong, Peiyuan F. Hsieh, Chih-Chao Yang, Chih-Ta Tai, Shey-Lin Wu, Cheng-Hsien Lu, Yung-Chu Hsu, Hsiang-Yu Yu, Long-Sun Ro, Chung-Ta Lu, Chun-Che Chu, Jing-Jane Tsai, Yu-Hsiang Su, Sheng-Hsing Lan, Sheng-Feng Sung, Shu-Yi Lin, Hui-Ping Chuang, Li-Chen Huang, Ying-Ju Chen, Pei-Joung Tsai, Hung-Ting Liao, Yu-Hsuan Lin, Chien-Hsiun Chen, Wen-Hung Chung, Shuen-Iu Hung, Jer-Yuarn Wu, Chi-Feng Chang, Luke Chen, Yuan-Tsong Chen, and Chen-Yang Shen. 2011. 'Carbamazepine-Induced Toxic Effects and HLA-B*1502 Screening in Taiwan', *New England Journal of Medicine*, 364: 1126-33.

Chen, Yi-Chun, Yung-Tsu Cho, Chia-Ying Chang, and Chia-Yu Chu. 2013. 'Drug reaction with eosinophilia and systemic symptoms: A drug-induced hypersensitivity syndrome with variable clinical features', *Dermatologica Sinica*, 31: 196-204.

Chessman, D., L. Kostenko, T. Lethborg, A. W. Purcell, N. A. Williamson, Z. Chen, L. Kjer-Nielsen, N. A. Mifsud, B. D. Tait, R. Holdsworth, C. A. Almeida, D. Nolan, W. A. Macdonald, J. K. Archbold, A. D. Kellerher, D. Marriott, S. Mallal, M. Bharadwaj, J. Rossjohn, and J. McCluskey. 2008. 'Human leukocyte antigen class I-restricted activation of CD8+ T cells provides the immunogenetic basis of a systemic drug hypersensitivity', *Immunity*, 28: 822-32.

Chimbetete, Tafadzwa, Chloe Buck, Phuti Choshi, Rose Selim, Sarah Pedretti, Sherrie Jill Divito, Elizabeth Jane Phillips, Rannakoe Lehloenya, and Jonny Peter. 2022. 'HIV-Associated Immune Dysregulation in the Skin: A Crucible for Exaggerated Inflammation and Hypersensitivity', *Journal of Investigative Dermatology*.

Chimbetete, Tafadzwa, Phuti Choshi, Sarah Pedretti, Mireille Porter, Riyaadh Roberts, Rannakoe Lehloenya, and Jonathan Peter. 2023. 'Skin infiltrating T-cell profile of drug reaction with

eosinophilia and systemic symptoms (DRESS) reactions among HIV-infected patients', *Frontiers in Medicine*, 10: 1118527.
Chintu, C., C. Luo, G. Bhat, M. Raviglione, H. DuPont, and A. Zumla. 1993. 'Cutaneous hypersensitivity reactions due to thiacetazone in the treatment of tuberculosis in Zambian children infected with HIV-I', *Arch Dis Child*, 68: 665-8.
Cho, Y. T., J. W. Lin, Y. C. Chen, C. Y. Chang, C. H. Hsiao, W. H. Chung, and C. Y. Chu. 2014. 'Generalized bullous fixed drug eruption is distinct from Stevens-Johnson syndrome/toxic epidermal necrolysis by immunohistopathological features', *J Am Acad Dermatol*, 70: 539-48.
Cho, Y. T., C. W. Yang, and C. Y. Chu. 2017a. 'Drug Reaction with Eosinophilia and Systemic Symptoms (DRESS): An Interplay among Drugs, Viruses, and Immune System', *Int J Mol Sci*, 18.
Cho, Yung-Tsu, Che-Wen Yang, and Chia-Yu Chu. 2017b. 'Drug Reaction with Eosinophilia and Systemic Symptoms (DRESS): An Interplay among Drugs, Viruses, and Immune System', *International journal of molecular sciences*, 18: 1243.
Choquet-Kastylevsky, G., L. Intrator, C. Chenal, H. Bocquet, J. Revuz, and J. C. Roujeau. 1998. 'Increased levels of interleukin 5 are associated with the generation of eosinophilia in drug-induced hypersensitivity syndrome', *Br J Dermatol*, 139: 1026-32.
Chung, W. H., W. C. Chang, Y. S. Lee, Y. Y. Wu, C. H. Yang, H. C. Ho, M. J. Chen, J. Y. Lin, R. C. Hui, J. C. Ho, W. M. Wu, T. J. Chen, T. Wu, Y. R. Wu, M. S. Hsih, P. H. Tu, C. N. Chang, C. N. Hsu, T. L. Wu, S. E. Choon, C. K. Hsu, D. Y. Chen, C. S. Liu, C. Y. Lin, N. Kaniwa, Y. Saito, Y. Takahashi, R. Nakamura, H. Azukizawa, Y. Shi, T. H. Wang, S. S. Chuang, S. F. Tsai, C. J. Chang, Y. S. Chang, S. I. Hung, Consortium Taiwan Severe Cutaneous Adverse Reaction, and Consortium Japan Pharmacogenomics Data Science. 2014. 'Genetic variants associated with phenytoin-related severe cutaneous adverse reactions', *Jama*, 312: 525-34.
Chung, W. H., W. C. Chang, S. L. Stocker, C. G. Juo, G. G. Graham, M. H. Lee, K. M. Williams, Y. C. Tian, K. C. Juan, Y. J. Jan Wu, C. H. Yang, C. J. Chang, Y. J. Lin, R. O. Day, and S. I. Hung. 2015. 'Insights into the poor prognosis of allopurinol-induced severe cutaneous adverse reactions: the impact of renal insufficiency, high plasma levels of oxypurinol and granulysin', *Ann Rheum Dis*, 74: 2157-64.
Chung, W. H., S. I. Hung, J. Y. Yang, S. C. Su, S. P. Huang, C. Y. Wei, S. W. Chin, C. C. Chiou, S. C. Chu, H. C. Ho, C. H. Yang, C. F. Lu, J. Y. Wu, Y. D. Liao, and Y. T. Chen. 2008. 'Granulysin is a key mediator for disseminated keratinocyte death in Stevens-Johnson syndrome and toxic epidermal necrolysis', *Nat Med*, 14: 1343-50.
Chung, W. H., R. Y. Pan, M. T. Chu, S. W. Chin, Y. L. Huang, W. C. Wang, J. Y. Chang, and S. I. Hung. 2015. 'Oxypurinol-Specific T Cells Possess Preferential TCR Clonotypes and Express Granulysin in Allopurinol-Induced Severe Cutaneous Adverse Reactions', *J Invest Dermatol*, 135: 2237-48.
Chung, Wen-Hung, Shuen-Iu Hung, Hong-Shang Hong, Mo-Song Hsih, Li-Cheng Yang, Hsin-Chun Ho, Jer-Yuarn Wu, and Yuan-Tsong Chen. 2004. 'A marker for Stevens–Johnson syndrome', *Nature*, 428: 486-86.
Cifaldi, L., P. Romania, S. Lorenzi, F. Locatelli, and D. Fruci. 2012. 'Role of endoplasmic reticulum aminopeptidases in health and disease: from infection to cancer', *Int J Mol Sci*, 13: 8338-52.
Clayberger, C., and A. M. Krensky. 2003. 'Granulysin', *Curr Opin Immunol*, 15: 560-5.
Colebunders, R., T. Vanwolleghem, P. Meurrens, and F. Moerman. 2004. 'Efavirenz-associated Stevens-Johnson syndrome', *Infection*, 32: 306-7.
Coopman, S, Hugo Degreef, and A Dooms-Goossens. 1989. 'Identification of cross-reaction patterns in allergic contact dermatitis from topical corticosteroids', *British Journal of Dermatology*, 121: 27-34.
Copaescu, A., E. Mouhtouris, S. Vogrin, F. James, K. Y. L. Chua, N. E. Holmes, A. Douglas, M. A. Slavin, H. Cleland, C. Zubrinich, A. K. Aung, M. S. Y. Goh, E. J. Phillips, and J. A. Trubiano. 2021. 'The Role of In Vivo and Ex Vivo Diagnostic Tools in Severe Delayed Immune-Mediated Adverse Antibiotic Drug Reactions', *J Allergy Clin Immunol Pract*, 9: 2010-15.e4.

Copaescu, Ana, Phuti Choshi, Sarah Pedretti, Effie Mouhtouris, Jonathan Peter, and Jason A. Trubiano. 2021. 'Dose Dependent Antimicrobial Cellular Cytotoxicity—Implications for ex vivo Diagnostics', *Frontiers in Pharmacology*, 12.

Corbett, E. L., C. J. Watt, N. Walker, D. Maher, B. G. Williams, M. C. Raviglione, and C. Dye. 2003. 'The growing burden of tuberculosis: global trends and interactions with the HIV epidemic', *Arch Intern Med*, 163: 1009-21.

Correia, O., L. Delgado, I. L. Barbosa, F. Campilho, and J. Fleming-Torrinha. 2002. 'Increased interleukin 10, tumor necrosis factor alpha, and interleukin 6 levels in blister fluid of toxic epidermal necrolysis', *J Am Acad Dermatol*, 47: 58-62.

Coughlan, R., and S. Cameron. 2016. 'Key data from the 17th International Workshop on Co-morbidities and Adverse Drug Reactions in HIV', *Antivir Ther*, 21: 75-89.

Councils, East African-British Medical Research. 1980. 'Controlled clinical trial of four short-course regimens of chemotherapy for two durations in the treatment of pulmonary tuberculosis. Second report. ', *Tubercle*, 61: 59-69.

Czerwonka, D., J. Domagalska, K. Pyta, M. M. Kubicka, P. Pecyna, M. Gajecka, and P. Przybylski. 2016. 'Structure-activity relationship studies of new rifamycins containing l-amino acid esters as inhibitors of bacterial RNA polymerases', *Eur J Med Chem*, 116: 216-21.

Daugherty, B. L., S. J. Siciliano, J. A. DeMartino, L. Malkowitz, A. Sirotina, and M. S. Springer. 1996. 'Cloning, expression, and characterization of the human eosinophil eotaxin receptor', *J Exp Med*, 183: 2349-54.

de Araujo, E., V. Dessirier, G. Laprée, L. Valeyrie-Allanore, N. Ortonne, E. N. Stathopoulos, M. Bagot, A. Bensussan, M. Mockenhaupt, J. C. Roujeau, and A. Tsapis. 2011. 'Death ligand TRAIL, secreted by CD1a+ and CD14+ cells in blister fluids, is involved in killing keratinocytes in toxic epidermal necrolysis', *Exp Dermatol*, 20: 107-12.

De Oliveira, L, M Dias, A Jeyabalan, B Payne, C.W Redman, L Magee, L Poston, L Chappell, P Seed, P von Dadelszen, and J. M Roberts. 2018. 'Creating biobanks in low and middle-income countries to improve knowledge – The PREPARE initiative', *Pregnancy Hypertension*, 13: 62-64.

Dendrou, C. A., J. Petersen, J. Rossjohn, and L. Fugger. 2018. 'HLA variation and disease', *Nat Rev Immunol*, 18: 325-39.

Descamps, V., A. Valance, C. Edlinger, A. M. Fillet, M. Grossin, B. Lebrun-Vignes, S. Belaich, and B. Crickx. 2001. 'Association of human herpesvirus 6 infection with drug reaction with eosinophilia and systemic symptoms', *Arch Dermatol*, 137: 301-4.

Dheda, Keertan, Clifton E. Barry, 3rd, and Gary Maartens. 2016. 'Tuberculosis', *The Lancet*, 387: 1211-26.

Diggins, Kirsten E., Allison R. Greenplate, Nalin Leelatian, Cara E. Wogsland, and Jonathan M. Irish. 2017. 'Characterizing cell subsets using marker enrichment modeling', *Nature Methods*, 14: 275-78.

Duong, Tu Anh, Laurence Valeyrie-Allanore, Pierre Wolkenstein, and Olivier Chosidow. 2017. 'Severe cutaneous adverse reactions to drugs', *The Lancet*, 390: 1996-2011.

East African-British Medical Research Councils. 1974. 'Controlled clinical trial of four short-course (6-month) regimens of chemotherapy for treatment of pulmonary tuberculosis. Third report. ', *Lancet*, 2: 237-40.

El-Sadr, W. M., R. L. Murphy, T. M. Yurik, R. Luskin-Hawk, T. W. Cheung, H. H. Balfour, Jr., R. Eng, T. M. Hooton, T. M. Kerkering, M. Schutz, C. van der Horst, and R. Hafner. 1998. 'Atovaquone compared with dapsone for the prevention of Pneumocystis carinii pneumonia in patients with HIV infection who cannot tolerate trimethoprim, sulfonamides, or both. Community Program for Clinical Research on AIDS and the AIDS Clinical Trials Group', *N Engl J Med*, 339: 1889-95.

Elzagallaai, A. A., S. R. Knowles, M. J. Rieder, J. R. Bend, N. H. Shear, and G. Koren. 2009. 'In vitro testing for the diagnosis of anticonvulsant hypersensitivity syndrome: a systematic review', *Mol Diagn Ther*, 13: 313-30.

Endo, Y., K. Hirahara, R. Yagi, D. J. Tumes, and T. Nakayama. 2014. 'Pathogenic memory type Th2 cells in allergic inflammation', *Trends Immunol*, 35: 69-78.

Evans, D. M., C. C. Spencer, J. J. Pointon, Z. Su, D. Harvey, G. Kochan, U. Oppermann, A. Dilthey, M. Pirinen, M. A. Stone, L. Appleton, L. Moutsianas, S. Leslie, T. Wordsworth, T. J. Kenna, T. Karaderi, G. P. Thomas, M. M. Ward, M. H. Weisman, C. Farrar, L. A. Bradbury, P. Danoy, R. D. Inman, W. Maksymowych, D. Gladman, P. Rahman, A. Morgan, H. Marzo-Ortega, P. Bowness, K. Gaffney, J. S. Gaston, M. Smith, J. Bruges-Armas, A. R. Couto, R. Sorrentino, F. Paladini, M. A. Ferreira, H. Xu, Y. Liu, L. Jiang, C. Lopez-Larrea, R. Díaz-Peña, A. López-Vázquez, T. Zayats, G. Band, C. Bellenguez, H. Blackburn, J. M. Blackwell, E. Bramon, S. J. Bumpstead, J. P. Casas, A. Corvin, N. Craddock, P. Deloukas, S. Dronov, A. Duncanson, S. Edkins, C. Freeman, M. Gillman, E. Gray, R. Gwilliam, N. Hammond, S. E. Hunt, J. Jankowski, A. Jayakumar, C. Langford, J. Liddle, H. S. Markus, C. G. Mathew, O. T. McCann, M. I. McCarthy, C. N. Palmer, L. Peltonen, R. Plomin, S. C. Potter, A. Rautanen, R. Ravindrarajah, M. Ricketts, N. Samani, S. J. Sawcer, A. Strange, R. C. Trembath, A. C. Viswanathan, M. Waller, P. Weston, P. Whittaker, S. Widaa, N. W. Wood, G. McVean, J. D. Reveille, B. P. Wordsworth, M. A. Brown, and P. Donnelly. 2011. 'Interaction between ERAP1 and HLA-B27 in ankylosing spondylitis implicates peptide handling in the mechanism for HLA-B27 in disease susceptibility', *Nat Genet*, 43: 761-7.

Falk, K., and O. Rötzschke. 2002. 'The final cut: how ERAP1 trims MHC ligands to size', *Nat Immunol*, 3: 1121-2.

Ferreira, Leonardo Capistrano, Carlos Eduardo Maia Gomes, Priya Duggal, Ingrid De Paula Holanda, Amanda Samara de Lima, Paulo Ricardo Porfírio do Nascimento, and Selma Maria Bezerra Jeronimo. 2021. 'Genetic association of ERAP1 and ERAP2 with eclampsia and preeclampsia in northeastern Brazilian women', *Scientific reports*, 11: 1-8.

Ferrell, P. B., Jr., and H. L. McLeod. 2008. 'Carbamazepine, HLA-B*1502 and risk of Stevens-Johnson syndrome and toxic epidermal necrolysis: US FDA recommendations', *Pharmacogenomics*, 9: 1543-6.

Focosi, D., M. Bestagno, O. Burrone, and M. Petrini. 2010. 'CD57+ T lymphocytes and functional immune deficiency', *J Leukoc Biol*, 87: 107-16.

Franke, Andre, Dermot PB McGovern, Jeffrey C Barrett, Kai Wang, Graham L Radford-Smith, Tariq Ahmad, Charlie W Lees, Tobias Balschun, James Lee, and Rebecca Roberts. 2010. 'Genome-wide meta-analysis increases to 71 the number of confirmed Crohn's disease susceptibility loci', *Nature genetics*, 42: 1118-25.

Fung, EYMG, Deborah J Smyth, Joanna MM Howson, James D Cooper, Neil M Walker, H Stevens, Linda S Wicker, and John A Todd. 2009. 'Analysis of 17 autoimmune disease-associated variants in type 1 diabetes identifies 6q23/TNFAIP3 as a susceptibility locus', *Genes & Immunity*, 10: 188-91.

Ganeva, Maria, Tanya Gancheva, Roumiana Lazarova, Jeni Troeva, Ivan Baldaranov, Ivan Vassilev, Evgenya Hristakieva, and Valentina Tzaneva. 2008. 'Carbamazepine-induced drug reaction with eosinophilia and systemic symptoms (DRESS) syndrome: report of four cases and brief review', *International journal of dermatology*, 47: 853-60.

Garamszegi, L. Z. 2014. 'Global distribution of malaria-resistant MHC-HLA alleles: the number and frequencies of alleles and malaria risk', *Malar J*, 13: 349.

Gerber, B. O., and W. J. Pichler. 2004. 'Cellular mechanisms of T cell mediated drug hypersensitivity', *Curr Opin Immunol*, 16: 732-7.

Girling, D. J. 1977. 'Adverse reactions to rifampicin in antituberculosis regimens', *J Antimicrob Chemother*, 3: 115-32.

Glanville, J., H. Huang, A. Nau, O. Hatton, L. E. Wagar, F. Rubelt, X. Ji, A. Han, S. M. Krams, C. Pettus, N. Haas, C. S. L. Arlehamn, A. Sette, S. D. Boyd, T. J. Scriba, O. M. Martinez, and M. M. Davis. 2017. 'Identifying specificity groups in the T cell receptor repertoire', *Nature*, 547: 94-98.

Grobbelaar, M, G. E. Louw, S. L. Sampson, P. D. van Helden, P. R. Donald, and R. M. Warren. 2019. 'Evolution of rifampicin treatment for tuberculosis', *Infection, Genetics and Evolution*, 74: 103937.

Gupta, N., A. Mittal, and N. Nischal. 2019. 'Drug rash vs. immune reconstitution inflammatory syndrome (IRIS)-a diagnostic dilemma', *Qjm*, 112: 925-26.

Haldane, J. B. 1956. 'The estimation and significance of the logarithm of a ratio of frequencies', *Ann Hum Genet*, 20: 309-11.
Haliloglu, T., A. Gul, and B. Erman. 2010. 'Predicting important residues and interaction pathways in proteins using Gaussian Network Model: binding and stability of HLA proteins', *PLoS Comput Biol*, 6: e1000845.
Hanafusa, T., H. Azukizawa, S. Matsumura, and I. Katayama. 2012. 'The predominant drug-specific T-cell population may switch from cytotoxic T cells to regulatory T cells during the course of anticonvulsant-induced hypersensitivity', *J Dermatol Sci*, 65: 213-9.
Haro-Gabaldón, V., J. Sánchez-Sánchez-Vizcaino, P. Ruiz-Avila, J. Gutiérrez-Fernández, J. Linares, and R. Naranjo-Sintes. 1996. 'Acute generalized exanthematous pustulosis with cytomegalovirus infection', *Int J Dermatol*, 35: 735-7.
Hashizume, H., T. Fujiyama, J. Kanebayashi, Y. Kito, M. Hata, and H. Yagi. 2013. 'Skin recruitment of monomyeloid precursors involves human herpesvirus-6 reactivation in drug allergy', *Allergy*, 68: 681-9.
Heath, W. R., and F. R. Carbone. 2013. 'The skin-resident and migratory immune system in steady state and memory: innate lymphocytes, dendritic cells and T cells', *Nat Immunol*, 14: 978-85.
Herndler-Brandstetter, D., H. Ishigame, R. Shinnakasu, V. Plajer, C. Stecher, J. Zhao, M. Lietzenmayer, L. Kroehling, A. Takumi, K. Kometani, T. Inoue, Y. Kluger, S. M. Kaech, T. Kurosaki, T. Okada, and R. A. Flavell. 2018. 'KLRG1(+) Effector CD8(+) T Cells Lose KLRG1, Differentiate into All Memory T Cell Lineages, and Convey Enhanced Protective Immunity', *Immunity*, 48: 716-29.e8.
Hertzman, R. J., P. Deshpande, A. Gibson, and E. J. Phillips. 2021. 'Role of pharmacogenomics in T-cell hypersensitivity drug reactions', *Curr Opin Allergy Clin Immunol*, 21: 327-34.
Hetherington, Seth, Arlene R. Hughes, Michael Mosteller, Denise Shortino, Katherine L. Baker, William Spreen, Eric Lai, Kirstie Davies, Abigail Handley, David J. Dow, Mary E. Fling, Michael Stocum, Clive Bowman, Linda M. Thurmond, and Allen D. Roses. 2002. 'Genetic variations in HLA-B region and hypersensitivity reactions to abacavir', *The Lancet*, 359: 1121-22.
Hirahara, Kazuki, Luzheng Liu, Rachael A Clark, Kei-ichi Yamanaka, Robert C Fuhlbrigge, and Thomas S Kupper. 2006. 'The majority of human peripheral blood CD4+ CD25highFoxp3+ regulatory T cells bear functional skin-homing receptors', *The Journal of Immunology*, 177: 4488-94.
Hiransuthikul, A., T. Rattananupong, J. Klaewsongkram, P. Rerknimitr, M. Pongprutthipan, and K. Ruxrungtham. 2016. 'Drug-induced hypersensitivity syndrome/drug reaction with eosinophilia and systemic symptoms (DIHS/DRESS): 11 years retrospective study in Thailand', *Allergol Int*, 65: 432-38.
Hirsch, LJ, H Arif, EA Nahm, R Buchsbaum, SR Resor, and CW Bazil. 2008. 'Cross-sensitivity of skin rashes with antiepileptic drug use', *Neurology*, 71: 1527-34.
Holtzer, C. D., J. F. Flaherty, Jr., and R. L. Coleman. 1998. 'Cross-reactivity in HIV-infected patients switched from trimethoprim-sulfamethoxazole to dapsone', *Pharmacotherapy*, 18: 831-5.
Hoosen, K., A. Mosam, N. C. Dlova, and W. Grayson. 2019. 'An Update on Adverse Cutaneous Drug Reactions in HIV/AIDS', *Dermatopathology (Basel)*, 6: 111-25.
Horiuchi, T., M. Hirokawa, Y. Kawabata, A. Kitabayashi, T. Matsutani, T. Yoshioka, Y. Tsuruta, R. Suzuki, and A. B. Miura. 2001. 'Identification of the T cell clones expanding within both CD8(+)CD28(+) and CD8(+)CD28(-) T cell subsets in recipients of allogeneic hematopoietic cell grafts and its implication in post-transplant skewing of T cell receptor repertoire', *Bone Marrow Transplant*, 27: 731-9.
Hsu, D. Y., J. Brieva, N. B. Silverberg, and J. I. Silverberg. 2016. 'Morbidity and Mortality of Stevens-Johnson Syndrome and Toxic Epidermal Necrolysis in United States Adults', *J Invest Dermatol*, 136: 1387-97.
Huang, H., C. Wang, F. Rubelt, T. J. Scriba, and M. M. Davis. 2020. 'Analyzing the Mycobacterium tuberculosis immune response by T-cell receptor clustering with GLIPH2 and genome-wide antigen screening', *Nat Biotechnol*, 38: 1194-202.

Huang, Y. S., H. D. Chern, W. J. Su, J. C. Wu, S. L. Lai, S. Y. Yang, F. Y. Chang, and S. D. Lee. 2002. 'Polymorphism of the N-acetyltransferase 2 gene as a susceptibility risk factor for antituberculosis drug-induced hepatitis', *Hepatology*, 35: 883-9.

Hung, Shuen-Iu, Wen-Hung Chung, Lieh-Bang Liou, Chen-Chung Chu, Marie Lin, Hsien-Ping Huang, Yen-Ling Lin, Joung-Liang Lan, Li-Cheng Yang, Hong-Shang Hong, Ming-Jing Chen, Ping-Chin Lai, Mai-Szu Wu, Chia-Yu Chu, Kuo-Hsien Wang, Chien-Hsiun Chen, Cathy S. J. Fann, Jer-Yuarn Wu, and Yuan-Tsong Chen. 2005. 'HLA-B*5801 allele as a genetic marker for severe cutaneous adverse reactions caused by allopurinol', *Proceedings of the National Academy of Sciences of the United States of America*, 102: 4134.

Illing, P. T., J. P. Vivian, N. L. Dudek, L. Kostenko, Z. Chen, M. Bharadwaj, J. J. Miles, L. Kjer-Nielsen, S. Gras, N. A. Williamson, S. R. Burrows, A. W. Purcell, J. Rossjohn, and J. McCluskey. 2012. 'Immune self-reactivity triggered by drug-modified HLA-peptide repertoire', *Nature*, 486: 554-8.

Ishida, T., Y. Kano, Y. Mizukawa, and T. Shiohara. 2014. 'The dynamics of herpesvirus reactivations during and after severe drug eruptions: their relation to the clinical phenotype and therapeutic outcome', *Allergy*, 69: 798-805.

Janetzki, S., L. Price, H. Schroeder, C. M. Britten, M. J. Welters, and A. Hoos. 2015. 'Guidelines for the automated evaluation of Elispot assays', *Nat Protoc*, 10: 1098-115.

Jeong, Jiung, Ji Eun Yu, Yoo Duk Choi, Seul Kee Kim, Woong Yoon, and Young-Il Koh. 2019. 'Differentiation of angioimmunoblastic T-cell lymphoma from DRESS syndrome', *The Journal of Allergy and Clinical Immunology: In Practice*, 7: 1684-86. e1.

Jevtic, D., I. Dumic, T. Nordin, A. Singh, N. Sulovic, M. Radovanovic, M. Jecmenica, and T. Milovanovic. 2021. 'Less Known Gastrointestinal Manifestations of Drug Reaction with Eosinophilia and Systemic Symptoms (DRESS) Syndrome: A Systematic Review of the Literature', *J Clin Med*, 10.

Jin, H.J, D.Y Kang, Y. H Nam, Y. M. Ye, Y Il Koh, G. Y. Hur, S.H Kim, M. S Yang, S Kim, Y. Y Jeong, M. H Kim, J. H Choi, H. R Kang, E. J Jo, H. K Park, and Consortium Korean Severe Cutaneous Adverse Reactions. 2021. 'Severe Cutaneous Adverse Reactions to Anti-tuberculosis Drugs in Korean Patients', *Allergy, asthma & immunology research*, 13: 245-55.

Joint Tuberculosis Commitee of the British Thoracic Society. 1998. "Chemotherapy and management of tuberculosis in the United Kingdom: recommendations 1998. Joint Tuberculosis Committee of the British Thoracic Society." In *Thorax*, 536-48.

Kabashima, R., K. Sugita, Y. Sawada, R. Hino, M. Nakamura, and Y. Tokura. 2011. 'Increased circulating Th17 frequencies and serum IL-22 levels in patients with acute generalized exanthematous pustulosis', *J Eur Acad Dermatol Venereol*, 25: 485-8.

Kakande, B, and R.J Lehloenya. 2015. 'Drug reactions associated with anti-tuberculosis drugs: review article', *Current Allergy & Clinical Immunology*, 28: 264-68.

Kang, M. G., K. H. Sohn, D. Y. Kang, H. K. Park, M. S. Yang, J. Y. Lee, and H. R. Kang. 2019. 'Analysis of Individual Case Safety Reports of Severe Cutaneous Adverse Reactions in Korea', *Yonsei Med J*, 60: 208-15.

Kano, Y., K. Hiraharas, K. Sakuma, and T. Shiohara. 2006. 'Several herpesviruses can reactivate in a severe drug-induced multiorgan reaction in the same sequential order as in graft-versus-host disease', *Br J Dermatol*, 155: 301-6.

Kano, Yoko, Yukiko Ushigome, Chiho Horie, Yoshiko Mizukawa, and Tetsuo Shiohara. 2014. 'Immune reconstitution inflammatory syndrome observed in the setting of drug-induced hypersensitivity syndrome/drug reaction with eosinophilia and systemic symptoms (DIHS/DRESS)', *Clinical and Translational Allergy*, 4: 1-1.

Kardaun, S. H., M Mockenhaupt, and J. C. Roujeau. 2014. 'Comments on: DRESS syndrome', *J Am Acad Dermatol*, 71: 1000-00 e2.

Kardaun, S. H., P. Sekula, L. Valeyrie-Allanore, Y. Liss, C. Y. Chu, D. Creamer, A. Sidoroff, L. Naldi, M. Mockenhaupt, and J. C. Roujeau. 2013. 'Drug reaction with eosinophilia and systemic symptoms (DRESS): an original multisystem adverse drug reaction. Results from the prospective RegiSCAR study', *Br J Dermatol*, 169: 1071-80.

Kardaun, S. H., A. Sidoroff, L. Valeyrie-Allanore, S. Halevy, B. B. Davidovici, M. Mockenhaupt, and J. C. Roujeau. 2007. 'Variability in the clinical pattern of cutaneous side-effects of drugs with systemic symptoms: does a DRESS syndrome really exist?', *Br J Dermatol*, 156: 609-11.

Kato, K., A. Kawase, H. Azukizawa, T. Hanafusa, Y. Nakagawa, H. Murota, S. Sakaguchi, H. Asada, and I. Katayama. 2017. 'Novel interferon-gamma enzyme-linked immunoSpot assay using activated cells for identifying hypersensitivity-inducing drug culprits', *J Dermatol Sci*, 86: 222-29.

Kazer, S. W., T. P. Aicher, D. M. Muema, S. L. Carroll, J. Ordovas-Montanes, V. N. Miao, A. A. Tu, C. G. K. Ziegler, S. K. Nyquist, E. B. Wong, N. Ismail, M. Dong, A. Moodley, B. Berger, J. C. Love, K. L. Dong, A. Leslie, Z. M. Ndhlovu, T. Ndung'u, B. D. Walker, and A. K. Shalek. 2020. 'Integrated single-cell analysis of multicellular immune dynamics during hyperacute HIV-1 infection', *Nat Med*, 26: 511-18.

Keane, N. M, S. G Roberts, C. M Almeida, T Krishnan, A Chopra, E Demaine, R Laird, M Tschochner, J. M Carlson, S Mallal, D Heckerman, I James, and M John. 2012. 'High-avidity, high-IFNγ-producing CD8 T-cell responses following immune selection during HIV-1 infection', *Immunology and cell biology*, 90: 224-34.

Keane, N. M., R. K. Pavlos, E. McKinnon, A. Lucas, C. Rive, C. C. Blyth, D. Dunn, M. Lucas, S. Mallal, and E. Phillips. 2014. 'HLA Class I restricted CD8+ and Class II restricted CD4+ T cells are implicated in the pathogenesis of nevirapine hypersensitivity', *AIDS*, 28: 1891-901.

Keller, M., Z. Spanou, P. Schaerli, M. Britschgi, N. Yawalkar, M. Seitz, P. M. Villiger, and W. J. Pichler. 2005. 'T cell-regulated neutrophilic inflammation in autoinflammatory diseases', *J Immunol*, 175: 7678-86.

Kennedy, A. E., U. Ozbek, and M. T. Dorak. 2017. 'What has GWAS done for HLA and disease associations?', *Int J Immunogenet*, 44: 195-211.

Khan, D. A., and R. Solensky. 2010. 'Drug allergy', *J Allergy Clin Immunol*, 125: S126-37.

Khodadoust, Michael S, Niclas Olsson, Lisa E Wagar, Ole AW Haabeth, Binbin Chen, Kavya Swaminathan, Keith Rawson, Chih Long Liu, David Steiner, and Peder Lund. 2017. 'Antigen presentation profiling reveals recognition of lymphoma immunoglobulin neoantigens', *Nature*, 543: 723-27.

Kim, D., T. Kobayashi, B. Voisin, J. H. Jo, K. Sakamoto, S. P. Jin, M. Kelly, H. B. Pasieka, J. L. Naff, J. H. Meyerle, I. D. Ikpeama, G. A. Fahle, F. P. Davis, S. D. Rosenzweig, J. C. Alejo, S. Pittaluga, H. H. Kong, A. F. Freeman, and K. Nagao. 2020. 'Targeted therapy guided by single-cell transcriptomic analysis in drug-induced hypersensitivity syndrome: a case report', *Nat Med*, 26: 236-43.

King, D., S. Tomkins, A. Waters, P. J. Easterbrook, L. M. Thurmond, D. E. Thorborn, F. Raffi, D. M. Kemeny, and A. Vyakarnam. 2005. 'Intracellular cytokines may model immunoregulation of abacavir hypersensitivity in HIV-infected subjects', *J Allergy Clin Immunol*, 115: 1081-7.

Klaewsongkram, J., S. Buranapraditkun, P. Thantiworasit, P. Rerknimitr, P. Tuchinda, L. Chularojanamontri, T. Rerkpattanapipat, K. Chanprapaph, W. Disphanurat, P. Chakkavittumrong, N. Tovanabutra, C. Srisuttiyakorn, Y. Srinoulprasert, C. Sukasem, and Y. Chongpison. 2021. 'The Role of In Vitro Detection of Drug-Specific Mediator-Releasing Cells to Diagnose Different Phenotypes of Severe Cutaneous Adverse Reactions', *Allergy Asthma Immunol Res*, 13: 896-907.

Kleinewietfeld, M., F. Puentes, G. Borsellino, L. Battistini, O. Rötzschke, and K. Falk. 2005. 'CCR6 expression defines regulatory effector/memory-like cells within the CD25(+)CD4+ T-cell subset', *Blood*, 105: 2877-86.

Knight, L. K., R. J Lehloenya, E Sinanovic, and A. Pooran. 2019. 'Cost of managing severe cutaneous adverse drug reactions to first-line tuberculosis therapy in South Africa', *Trop Med Int Health*, 24: 994-1002.

Knight, L., G. Todd, R. Muloiwa, M. Matjila, and R. J. Lehloenya. 2015. 'Stevens Johnson Syndrome and Toxic Epidermal Necrolysis: Maternal and Foetal Outcomes in Twenty-Two Consecutive Pregnant HIV Infected Women', *PLoS One*, 10: e0135501.

Ko, T. M., W. H. Chung, C. Y. Wei, H. Y. Shih, J. K. Chen, C. H. Lin, Y. T. Chen, and S. I. Hung. 2011. 'Shared and restricted T-cell receptor use is crucial for carbamazepine-induced Stevens-Johnson syndrome', *J Allergy Clin Immunol*, 128: 1266-76.e11.

Konvinse, K. C., J. A. Trubiano, R. Pavlos, I. James, C. M. Shaffer, C. A. Bejan, R. J. Schutte, D. A. Ostrov, M. A. Pilkinton, M. Rosenbach, J. P. Zwerner, K. B. Williams, J. Bourke, P. Martinez, F. Rwandamuriye, A. Chopra, M. Watson, A. J. Redwood, K. D. White, S. A. Mallal, and E. J. Phillips. 2019. 'HLA-A*32:01 is strongly associated with vancomycin-induced drug reaction with eosinophilia and systemic symptoms', *J Allergy Clin Immunol*, 144: 183-92.

Kouotou, E. A., J. R. Nansseu, V. N. Ngono, S. A. Tatah, A. C. Zoung-Kanyi Bissek, and E. C. Ndjitoyap Ndam. 2017. 'Prevalence and Clinical Profile of Drug Eruptions among Antiretroviral Therapy-Exposed HIV Infected People in Yaoundé, Cameroon', *Dermatol Res Pract*, 2017: 6216193.

Kupper, T. S., and R. C. Fuhlbrigge. 2004. 'Immune surveillance in the skin: mechanisms and clinical consequences', *Nat Rev Immunol*, 4: 211-22.

LaHood, Nicole, and Kristin Sokol. 2017. 'DRESS syndrome associated with splenic thrombosis', *Annals of Allergy, Asthma & Immunology*, 119: 463-64.

Landovitz, R. J., S. Li, B. Grinsztejn, H. Dawood, A. Y. Liu, M. Magnus, M. C. Hosseinipour, R. Panchia, L. Cottle, G. Chau, P. Richardson, M. A. Marzinke, C. W. Hendrix, S. H. Eshleman, Y. Zhang, E. Tolley, J. Sugarman, R. Kofron, A. Adeyeye, D. Burns, A. R. Rinehart, D. Margolis, W. R. Spreen, M. S. Cohen, M. McCauley, and J. J. Eron. 2018. 'Safety, tolerability, and pharmacokinetics of long-acting injectable cabotegravir in low-risk HIV-uninfected individuals: HPTN 077, a phase 2a randomized controlled trial', *PLoS Med*, 15: e1002690.

Lanier, Lewis L. 1998. 'NK CELL RECEPTORS', *Annual Review of Immunology*, 16: 359-93.

Lastrucci, Claire, Alan Bénard, Luciana Balboa, Karine Pingris, Shanti Souriant, Renaud Poincloux, Talal Al Saati, Voahangy Rasolofo, Pablo González-Montaner, Sandra Inwentarz, Eduardo Jose Moraña, Ivanela Kondova, Frank A. W. Verreck, Maria del Carmen Sasiain, Olivier Neyrolles, Isabelle Maridonneau-Parini, Geanncarlo Lugo-Villarino, and Céline Cougoule. 2015. 'Tuberculosis is associated with expansion of a motile, permissive and immunomodulatory CD16+ monocyte population via the IL-10/STAT3 axis', *Cell Research*, 25: 1333-51.

Lavergne, S. N., H. Wang, H. E. Callan, B. K. Park, and D. J. Naisbitt. 2009. '"Danger" conditions increase sulfamethoxazole-protein adduct formation in human antigen-presenting cells', *J Pharmacol Exp Ther*, 331: 372-81.

Lebedeva, Tatiana V., Marina Ohashi, Georgia Zannelli, Rebecca Cullen, and Neng Yu. 2007. 'Comprehensive approach to high-resolution KIR typing', *Human Immunology*, 68: 789-96.

Lehloenya, R. J, T Isaacs, T Nyika, A Dhana, L Knight, S Veenstra, and J Peter. 2021a. 'Early high-dose intravenous corticosteroids rapidly arrest Stevens Johnson syndrome and drug reaction with eosinophilia and systemic symptoms recurrence on drug re-exposure', *The journal of allergy and clinical immunology. In practice*, 9: 582-84.e1.

Lehloenya, R. J, J. G Peter, A Copascu, J. A Trubiano, and E. J. Phillips. 2020a. 'Delabeling Delayed Drug Hypersensitivity: How Far Can You Safely Go?', *The journal of allergy and clinical immunology. In practice*, 8: 2878-95.e6.

Lehloenya, R. J, G Todd, L Mogotlane, N Gantsho, C Hlela, and K. Dheda. 2012. 'Lichenoid drug reaction to antituberculosis drugs treated through with topical steroids and phototherapy', *J Antimicrob Chemother*, 67: 2535-7.

Lehloenya, R. J, G. Todd, M Badri, and K. Dheda. 2011. 'Outcomes of reintroducing anti-tuberculosis drugs following cutaneous adverse drug reactions', *Int J Tuberc Lung Dis*, 15: 1649-57.

Lehloenya, R. J. 2022. 'Disease severity and status in Stevens-Johnson syndrome and toxic epidermal necrolysis: Key knowledge gaps and research needs', *Front Med (Lausanne)*, 9: 901401.

Lehloenya, R. J., and K. Dheda. 2012. 'Cutaneous adverse drug reactions to anti-tuberculosis drugs: state of the art and into the future', *Expert Rev Anti Infect Ther*, 10: 475-86.

Lehloenya, R. J., S. Dlamini, R. Muloiwa, B. Kakande, M. R. Ngwanya, G. Todd, and K. Dheda. 2016. 'Therapeutic Trial of Rifabutin After Rifampicin-Associated DRESS Syndrome in Tuberculosis-Human Immunodeficiency Virus Coinfected Patients', *Open Forum Infect Dis*, 3: ofw130.

Lehloenya, R. J., T. Isaacs, T. Nyika, A. Dhana, L. Knight, S. Veenstra, and J. Peter. 2021b. 'Early high-dose intravenous corticosteroids rapidly arrest Stevens Johnson syndrome and drug reaction with eosinophilia and systemic symptoms recurrence on drug re-exposure', *J Allergy Clin Immunol Pract*, 9: 582-84.e1.

Lehloenya, R. J., G. Todd, J. Wallace, M. R. Ngwanya, R. Muloiwa, and K. Dheda. 2016. 'Diagnostic patch testing following tuberculosis-associated cutaneous adverse drug reactions induces systemic reactions in HIV-infected persons', *Br J Dermatol*, 175: 150-6.

Lehloenya, R. J., J. Wallace, G. Todd, and K. Dheda. 2012. 'Multiple drug hypersensitivity reactions to anti-tuberculosis drugs: five cases in HIV-infected patients', *Int J Tuberc Lung Dis*, 16: 1260-4.

Lehloenya, Rannakoe J, Jonny G Peter, Ana Copascu, Jason A Trubiano, and Elizabeth J Phillips. 2020b. 'Delabeling delayed drug hypersensitivity: how far can you safely go?', *The Journal of Allergy and Clinical Immunology: In Practice*, 8: 2878-95. e6.

Li, Chuanyin, Yaheng Li, Zhiling Yan, Shuying Dai, Shuyuan Liu, Xia Wang, Jun Wang, Xinwen Zhang, Li Shi, and Yufeng Yao. 2020. 'Polymorphisms in endoplasmic reticulum aminopeptidase genes are associated with cervical cancer risk in a Chinese Han population', *BMC cancer*, 20: 1-11.

Li, L. F., and C. Ma. 2006. 'Epidemiological study of severe cutaneous adverse drug reactions in a city district of China', *Clin Exp Dermatol*, 31: 642-7.

Lockhart, S. M., R. C. Rathbun, J. R. Stephens, D. L. Baker, D. A. Drevets, R. A. Greenfield, M. R. Salvaggio, and S. Vincent. 2007. 'Cutaneous reactions with tenofovir disoproxil fumarate: a report of nine cases', *AIDS*, 21: 1370-3.

Loo, C. H., W. C. Tan, Y. H. Khor, and L. C. Chan. 2018. 'A 10-years retrospective study on Severe Cutaneous Adverse Reactions (SCARs) in a tertiary hospital in Penang, Malaysia', *Med J Malaysia*, 73: 73-77.

Lopez Angel, Cesar J., Edward A. Pham, Huixun Du, Francesco Vallania, Benjamin J. Fram, Kevin Perez, Thai Nguyen, Yael Rosenberg-Hasson, Aijaz Ahmed, Cornelia L. Dekker, Philip M. Grant, Purvesh Khatri, Holden T. Maecker, Jeffrey S. Glenn, Mark M. Davis, and David Furman. 2021. 'Signatures of immune dysfunction in HIV and HCV infection share features with chronic inflammation in aging and persist after viral reduction or elimination', *Proceedings of the National Academy of Sciences*, 118: e2022928118.

Loubser, S., M. Paximadis, N. L. Gentle, A. Puren, and C. T. Tiemessen. 2020. 'Human leukocyte antigen class I (A, B, C) and class II (DPB1, DQB1, DRB1) allele and haplotype variation in Black South African individuals', *Hum Immunol*, 81: 6-7.

Loubser, S., M. Paximadis, and C. T. Tiemessen. 2017. 'Human leukocyte antigen class I (A, B and C) allele and haplotype variation in a South African Mixed ancestry population', *Hum Immunol*, 78: 399-400.

Lund, O., M. Nielsen, C. Kesmir, A. G. Petersen, C. Lundegaard, P. Worning, C. Sylvester-Hvid, K. Lamberth, G. Røder, S. Justesen, S. Buus, and S. Brunak. 2004. 'Definition of supertypes for HLA molecules using clustering of specificity matrices', *Immunogenetics*, 55: 797-810.

Ma, Joseph D., Kelly C. Lee, and Grace M. Kuo. 2010. 'HLA-B*5701 testing to predict abacavir hypersensitivity', *PLoS currents*, 2: RRN1203-RRN03.

Madden, D. R. 1995. 'The three-dimensional structure of peptide-MHC complexes', *Annu Rev Immunol*, 13: 587-622.

Maecker, H. T., J. P. McCoy, and R. Nussenblatt. 2012. 'Standardizing immunophenotyping for the Human Immunology Project', *Nat Rev Immunol*, 12: 191-200.

Maecker, Holden T., Jeffrey Hassler, Janice K. Payne, Amanda Summers, Karrie Comatas, Manar Ghanayem, Michael A. Morse, Timothy M. Clay, Herbert K. Lyerly, Sonny Bhatia, Smita A. Ghanekar, Vernon C. Maino, Corazon delaRosa, and Mary L. Disis. 2008. 'Precision and linearity targets for validation of an IFNγ ELISPOT, cytokine flow cytometry, and tetramer assay using CMV peptides', *BMC Immunology*, 9: 9.

Mahnke, Y. D., T. M. Brodie, F. Sallusto, M. Roederer, and E. Lugli. 2013. 'The who's who of T-cell differentiation: human memory T-cell subsets', *Eur J Immunol*, 43: 2797-809.

Mallal, S., D. Nolan, C. Witt, G. Masel, A. M. Martin, C. Moore, D. Sayer, A. Castley, C. Mamotte, D. Maxwell, I. James, and F. T. Christiansen. 2002. 'Association between presence of HLA-

B*5701, HLA-DR7, and HLA-DQ3 and hypersensitivity to HIV-1 reverse-transcriptase inhibitor abacavir', *Lancet*, 359: 727-32.
Mallal, S., E. Phillips, G. Carosi, J. M. Molina, C. Workman, J. Tomazic, E. Jägel-Guedes, S. Rugina, O. Kozyrev, J. F. Cid, P. Hay, D. Nolan, S. Hughes, A. Hughes, S. Ryan, N. Fitch, D. Thorborn, and A. Benbow. 2008. 'HLA-B*5701 screening for hypersensitivity to abacavir', *N Engl J Med*, 358: 568-79.
Mallal, S., E. Phillips, G. Carosi, J. M. Molina, C. Workman, J. Tomazic, E. Jagel-Guedes, S. Rugina, O. Kozyrev, J. F. Cid, P. Hay, D. Nolan, S. Hughes, A. Hughes, S. Ryan, N. Fitch, D. Thorborn, A. Benbow, and Predict- Study Team. 2008. 'HLA-B*5701 screening for hypersensitivity to abacavir', *N Engl J Med*, 358: 568-79.
Manosuthi, W., S. Sungkanuparph, S. Tansuphaswadikul, Y. Inthong, W. Prasithsirikul, S. Chottanapund, W. Mankatitham, S. Chimsuntorn, C. Sittibusaya, V. Moolasart, N. Chumpathat, P. Termvises, and A. Chaovavanich. 2007. 'Incidence and risk factors of nevirapine-associated skin rashes among HIV-infected patients with CD4 cell counts <250 cells/microL', *Int J STD AIDS*, 18: 782-6.
Manosuthi, W., S. Thongyen, N. Chumpathat, K. Muangchana, and S. Sungkanuparph. 2006. 'Incidence and risk factors of rash associated with efavirenz in HIV-infected patients with preceding nevirapine-associated rash', *HIV Medicine*, 7: 378-82.
Manson, L. E. N., J. J. Swen, and H. J. Guchelaar. 2020. 'Diagnostic Test Criteria for HLA Genotyping to Prevent Drug Hypersensitivity Reactions: A Systematic Review of Actionable HLA Recommendations in CPIC and DPWG Guidelines', *Front Pharmacol*, 11: 567048.
Margolis, D. J., N. Mitra, O. J. Hoffstad, B. S. Kim, D. S. Monos, and E. J. Phillips. 2021. 'Association of KIR Genes and MHC Class I Ligands with Atopic Dermatitis', *J Immunol*, 207: 1522-29.
Margolis, David J., Nandita Mitra, Ole J. Hoffstad, Ronald Berna, Brian S. Kim, Abha Chopra, and Elizabeth J. Phillips. 2023. 'Association of KIR2DL5, KIR2DS5, and KIR2DS1 allelic variation and atopic dermatitis', *Scientific reports*, 13: 1730.
Marsh, Steven GE, Peter Parham, and Linda D Barber. 1999. *The HLA factsbook* (Elsevier).
Martin, Annalise M., Coral-Ann Almeida, Paul Cameron, Anthony W. Purcell, David Nolan, Ian James, James McCluskey, Elizabeth Phillips, Alan Landay, and Simon Mallal. 2007. 'Immune responses to abacavir in antigen-presenting cells from hypersensitive patients', *AIDS (London, England)*, 21: 1233-44.
Martin, M. D., and V. P. Badovinac. 2018. 'Defining Memory CD8 T Cell', *Front Immunol*, 9: 2692.
Martin, M. P., X. Gao, J. H. Lee, G. W. Nelson, R. Detels, J. J. Goedert, S. Buchbinder, K. Hoots, D. Vlahov, J. Trowsdale, M. Wilson, S. J. O'Brien, and M. Carrington. 2002. 'Epistatic interaction between KIR3DS1 and HLA-B delays the progression to AIDS', *Nat Genet*, 31: 429-34.
Martin-Carbonero, L., M. Nunez, J. Gonzalez-Lahoz, and V. Soriano. 2003. 'Incidence of liver injury after beginning antiretroviral therapy with efavirenz or nevirapine', *HIV Clin Trials*, 4: 115-20.
Martinez, E., J. Collazos, and J. Mayo. 1999. 'Hypersensitivity reactions to rifampin. Pathogenetic mechanisms, clinical manifestations, management strategies, and review of the anaphylactic-like reactions', *Medicine (Baltimore)*, 78: 361-9.
Matono, T., T. Nishijima, K. Teruya, E. Morino, J. Takasaki, H. Gatanaga, Y. Kikuchi, M. Kaku, and S. Oka. 2017. 'Substantially Higher and Earlier Occurrence of Anti-Tuberculosis Drug-Related Adverse Reactions in HIV Coinfected Tuberculosis Patients: A Matched-Cohort Study', *AIDS Patient Care STDS*, 31: 455-62.
McCormack, M., A. Alfirevic, S. Bourgeois, J. J. Farrell, D. Kasperavičiūtė, M. Carrington, G. J. Sills, T. Marson, X. Jia, P. I. de Bakker, K. Chinthapalli, M. Molokhia, M. R. Johnson, G. D. O'Connor, E. Chaila, S. Alhusaini, K. V. Shianna, R. A. Radtke, E. L. Heinzen, N. Walley, M. Pandolfo, W. Pichler, B. K. Park, C. Depondt, S. M. Sisodiya, D. B. Goldstein, P. Deloukas, N. Delanty, G. L. Cavalleri, and M. Pirmohamed. 2011. 'HLA-A*3101 and carbamazepine-induced hypersensitivity reactions in Europeans', *N Engl J Med*, 364: 1134-43.

McInnes, Leland, John Healy, and James Melville. 2018. 'Umap: Uniform manifold approximation and projection for dimension reduction', *arXiv preprint arXiv:1802.03426*.
McMichael, Andrew J., and Sarah L. Rowland-Jones. 2001. 'Cellular immune responses to HIV', *Nature*, 410: 980-87.
McNeil, Benjamin D., Priyanka Pundir, Sonya Meeker, Liang Han, Bradley J. Undem, Marianna Kulka, and Xinzhong Dong. 2015. 'Identification of a mast-cell-specific receptor crucial for pseudo-allergic drug reactions', *Nature*, 519: 237-41.
Mehta, U., and G. Maartens. 2007. 'Is it safe to switch between efavirenz and nevirapine in the event of toxicity?', *Lancet Infect Dis*, 7: 733-8.
Meintjes, G., J. C. M. Brust, J. Nuttall, and G. Maartens. 2019. 'Management of active tuberculosis in adults with HIV', *Lancet HIV*, 6: e463-e74.
Meintjes, Graeme, Cari Stek, Lisette Blumenthal, Friedrich Thienemann, Charlotte Schutz, Jozefien Buyze, Raffaella Ravinetto, Harry van Loen, Amy Nair, Amanda Jackson, Robert Colebunders, Gary Maartens, Robert J. Wilkinson, and Lutgarde Lynen. 2018. 'Prednisone for the Prevention of Paradoxical Tuberculosis-Associated IRIS', *New England Journal of Medicine*, 379: 1915-25.
Mendy, M, E Caboux, B. S Sylla, J Dillner, J Chinquee, and C. Wild. 2014. 'Infrastructure and facilities for human biobanking in low- and middle-income countries: a situation analysis', *Pathobiology*, 81: 252-60.
Mertes, P. M., M. Lambert, R. M. Guéant-Rodriguez, I. Aimone-Gastin, C. Mouton-Faivre, D. A. Moneret-Vautrin, J. L. Guéant, J. M. Malinovsky, and P. Demoly. 2009. 'Perioperative anaphylaxis', *Immunol Allergy Clin North Am*, 29: 429-51.
Metterle, Lauren, Leigh Hatch, and Lucia Seminario-Vidal. 2020. 'Pediatric drug reaction with eosinophilia and systemic symptoms: a systematic review of the literature', *Pediatric Dermatology*, 37: 124-29.
Michel, Fabrice, Jean-Christophe Navellou, Denis Ferraud, Eric Toussirot, and Daniel Wendling. 2005. 'DRESS syndrome in a patient on sulfasalazine for rheumatoid arthritis', *Joint Bone Spine*, 72: 82-85.
Mifsud, N. A., A. W. Purcell, W. Chen, R. Holdsworth, B. D. Tait, and J. McCluskey. 2008. 'Immunodominance hierarchies and gender bias in direct T(CD8)-cell alloreactivity', *Am J Transplant*, 8: 121-32.
Mockenhaupt, M. 2017. 'Epidemiology of cutaneous adverse drug reactions', *Allergol Select*, 1: 96-108.
Mockenhaupt, M., C. Viboud, A. Dunant, L. Naldi, S. Halevy, J. N. Bouwes Bavinck, A. Sidoroff, J. Schneck, J. C. Roujeau, and A. Flahault. 2008. 'Stevens-Johnson syndrome and toxic epidermal necrolysis: assessment of medication risks with emphasis on recently marketed drugs. The EuroSCAR-study', *J Invest Dermatol*, 128: 35-44.
Mockenhaupt, Maja. 2012. 'Epidemiology of cutaneous adverse drug reactions', *Adverse Cutaneous Drug Eruptions*, 97: 1-17.
Montessori, Valentina, Natasha Press, Marianne Harris, Linda Akagi, and Julio S. G. Montaner. 2004. 'Adverse effects of antiretroviral therapy for HIV infection', *CMAJ : Canadian Medical Association journal = journal de l'Association medicale canadienne*, 170: 229-38.
Murphy, R. A., H. Sunpath, D. R. Kuritzkes, F. Venter, and R. T. Gandhi. 2007. 'Antiretroviral therapy-associated toxicities in the resource-poor world: the challenge of a limited formulary', *J Infect Dis*, 196 Suppl 3: S449-56.
Musette, P., and B. Janela. 2017. 'New Insights into Drug Reaction with Eosinophilia and Systemic Symptoms Pathophysiology', *Front Med (Lausanne)*, 4: 179.
Musvosvi, M., H. Huang, C. Wang, Q. Xia, V. Rozot, A. Krishnan, P. Acs, A. Cheruku, G. Obermoser, A. Leslie, S. M. Behar, W. A. Hanekom, N. Bilek, M. Fisher, S. H. E. Kaufmann, G. Walzl, M. Hatherill, M. M. Davis, and T. J. Scriba. 2023. 'T cell receptor repertoires associated with control and disease progression following Mycobacterium tuberculosis infection', *Nat Med*, 29: 258-69.
Naegele, D., P. Sekula, M. Paulmann, and M. Mockenhaupt. 2020. 'Incidence of Epidermal Necrolysis: Results of the German Registry', *J Invest Dermatol*, 140: 2525-27.

Nagarajan, S., and P. Whitaker. 2018. 'Management of adverse reactions to first-line tuberculosis antibiotics', *Curr Opin Allergy Clin Immunol*, 18: 333-41.

Nair, R. P., P. E. Stuart, I. Nistor, R. Hiremagalore, N. V. C. Chia, S. Jenisch, M. Weichenthal, G. R. Abecasis, H. W. Lim, E. Christophers, J. J. Voorhees, and J. T. Elder. 2006. 'Sequence and haplotype analysis supports HLA-C as the psoriasis susceptibility 1 gene', *Am J Hum Genet*, 78: 827-51.

Nakkam, Nontaya, Andrew Gibson, Effie Mouhtouris, Katherine C Konvinse, Natasha E Holmes, Kyra Y Chua, Pooja Deshpande, Danmeng Li, David A Ostrov, and Jason Trubiano. 2021. 'Cross-reactivity between vancomycin, teicoplanin, and telavancin in patients with HLA-A∗ 32: 01–positive vancomycin-induced DRESS sharing an HLA class II haplotype', *Journal of Allergy and Clinical Immunology*, 147: 403-05.

Nalitye Haitembu, B. N, M. N Porter, W Basera, R Hickmann, S. K Dlamini, C. W Spearman, J. G Peter, and R. J Lehloenya. 2021. 'Pattern and impact of drug-induced liver injury in South African patients with Stevens-Johnson syndrome/toxic epidermal necrolysis and a high burden of HIV', *The Journal of Allergy and Clinical Immunology: In Practice*.

Naranjo, C. A., U. Busto, E. M. Sellers, P. Sandor, I. Ruiz, E. A. Roberts, E. Janecek, C. Domecq, and D. J. Greenblatt. 1981. 'A method for estimating the probability of adverse drug reactions', *Clin Pharmacol Ther*, 30: 239-45.

Nassif, A., A. Bensussan, L. Boumsell, A. Deniaud, H. Moslehi, P. Wolkenstein, M. Bagot, and J. C. Roujeau. 2004. 'Toxic epidermal necrolysis: effector cells are drug-specific cytotoxic T cells', *J Allergy Clin Immunol*, 114: 1209-15.

Nassif, A., A. Bensussan, G. Dorothée, F. Mami-Chouaib, N. Bachot, M. Bagot, L. Boumsell, and J. C. Roujeau. 2002. 'Drug specific cytotoxic T-cells in the skin lesions of a patient with toxic epidermal necrolysis', *J Invest Dermatol*, 118: 728-33.

Ndhlovu, Z. M., P. Kamya, N. Mewalal, H. N. Kløverpris, T. Nkosi, K. Pretorius, F. Laher, F. Ogunshola, D. Chopera, K. Shekhar, M. Ghebremichael, N. Ismail, A. Moodley, A. Malik, A. Leslie, P. J. Goulder, S. Buus, A. Chakraborty, K. Dong, T. Ndung'u, and B. D. Walker. 2015. 'Magnitude and Kinetics of CD8+ T Cell Activation during Hyperacute HIV Infection Impact Viral Set Point', *Immunity*, 43: 591-604.

Nguyen, T. T., S. C. Chang, I. Evnouchidou, I. A. York, C. Zikos, K. L. Rock, A. L. Goldberg, E. Stratikos, and L. J. Stern. 2011. 'Structural basis for antigenic peptide precursor processing by the endoplasmic reticulum aminopeptidase ERAP1', *Nat Struct Mol Biol*, 18: 604-13.

Nishimura, Yoshiaki, Charles R Brown, Joseph J Mattapallil, Tatsuhiko Igarashi, Alicia Buckler-White, Bernard AP Lafont, Vanessa M Hirsch, Mario Roederer, and Malcolm A Martin. 2005. 'Resting naive CD4+ T cells are massively infected and eliminated by X4-tropic simian–human immunodeficiency viruses in macaques', *Proceedings of the National Academy of Sciences*, 102: 8000-05.

Norman, P. J., J. A. Hollenbach, N. Nemat-Gorgani, L. A. Guethlein, H. G. Hilton, M. J. Pando, K. A. Koram, E. M. Riley, L. Abi-Rached, and P. Parham. 2013. 'Co-evolution of human leukocyte antigen (HLA) class I ligands with killer-cell immunoglobulin-like receptors (KIR) in a genetically diverse population of sub-Saharan Africans', *PLoS Genet*, 9: e1003938.

Nunn, P., D. Kibuga, S. Gathua, R. Brindle, A. Imalingat, K. Wasunna, S. Lucas, C. Gilks, M. Omwega, J. Were, and et al. 1991. 'Cutaneous hypersensitivity reactions due to thiacetazone in HIV-1 seropositive patients treated for tuberculosis', *Lancet*, 337: 627-30.

Nyaku, A. N., L. Zheng, R. M. Gulick, M. Olefsky, B. Berzins, C. L. Wallis, C. Godfrey, P. E. Sax, E. P. Acosta, D. W. Haas, K. Y. Smith, B. E. Sha, C. N. Van Dam, and B. O. Taiwo. 2019. 'Dolutegravir plus lamivudine for initial treatment of HIV-1-infected participants with HIV-1 RNA <500 000 copies/mL: week 48 outcomes from ACTG 5353', *J Antimicrob Chemother*.

Ogawa, K., H. Morito, A. Hasegawa, F. Miyagawa, N. Kobayashi, H. Watanabe, H. Sueki, M. Tohyama, K. Hashimoto, Y. Kano, T. Shiohara, K. Ito, H. Fujita, M. Aihara, and H. Asada. 2014. 'Elevated serum thymus and activation-regulated chemokine (TARC/CCL17) relates to reactivation of human herpesvirus 6 in drug reaction with eosinophilia and systemic symptoms (DRESS)/drug-induced hypersensitivity syndrome (DIHS)', *Br J Dermatol*, 171: 425-7.

Ombrello, M. J., D. L. Kastner, and E. F. Remmers. 2015. 'Endoplasmic reticulum-associated amino-peptidase 1 and rheumatic disease: Genetics', *Current Opinion in Rheumatology*, 27: 349-56.
Ostrov, D. A., B. J. Grant, Y. A. Pompeu, J. Sidney, M. Harndahl, S. Southwood, C. Oseroff, S. Lu, J. Jakoncic, C. A. de Oliveira, L. Yang, H. Mei, L. Shi, J. Shabanowitz, A. M. English, A. Wriston, A. Lucas, E. Phillips, S. Mallal, H. M. Grey, A. Sette, D. F. Hunt, S. Buus, and B. Peters. 2012. 'Drug hypersensitivity caused by alteration of the MHC-presented self-peptide repertoire', *Proc Natl Acad Sci U S A*, 109: 9959-64.
Padovan, E., D. Mauri-Hellweg, W. J. Pichler, and H. U. Weltzien. 1996. 'T cell recognition of penicillin G: structural features determining antigenic specificity', *Eur J Immunol*, 26: 42-8.
Palomino, J. C., and A. Martin. 2014. 'Drug Resistance Mechanisms in Mycobacterium tuberculosis', *Antibiotics (Basel)*, 3: 317-40.
Pan, Ren-You, Mu-Tzu Chu, Chuang-Wei Wang, Yun-Shien Lee, Francois Lemonnier, Aaron W. Michels, Ryan Schutte, David A. Ostrov, Chun-Bing Chen, Elizabeth Jane Phillips, Simon Alexander Mallal, Maja Mockenhaupt, Teresa Bellón, Wichittra Tassaneeyakul, Katie D. White, Jean-Claude Roujeau, Wen-Hung Chung, and Shuen-Iu Hung. 2019. 'Identification of drug-specific public TCR driving severe cutaneous adverse reactions', *Nature Communications*, 10: 3569.
Paquet, P., and G. E. Piérard. 1998. 'Soluble fractions of tumor necrosis factor-alpha, interleukin-6 and of their receptors in toxic epidermal necrolysis: a comparison with second-degree burns', *Int J Mol Med*, 1: 459-62.
Para, M. F., D. Finkelstein, S. Becker, M. Dohn, A. Walawander, and J. R. Black. 2000. 'Reduced toxicity with gradual initiation of trimethoprim-sulfamethoxazole as primary prophylaxis for Pneumocystis carinii pneumonia: AIDS Clinical Trials Group 268', *J Acquir Immune Defic Syndr*, 24: 337-43.
Pavlos, R., P. Deshpande, A. Chopra, S. Leary, K. Strautins, D. Nolan, D. Thorborn, M. Shaefer, A. Rauch, D. Dunn, J. Montaner, A. Rachlis, C. A. Almeida, L. Choo, I. James, A. J. Redwood, Y. Li, S. Gaudieri, S. A. Mallal, and E. J. Phillips. 2020. 'New genetic predictors for abacavir tolerance in HLA-B*57:01 positive individuals', *Hum Immunol*, 81: 300-04.
Pavlos, R., S. Mallal, D. Ostrov, S. Buus, I. Metushi, B. Peters, and E. Phillips. 2015. 'T cell-mediated hypersensitivity reactions to drugs', *Annu Rev Med*, 66: 439-54.
Pavlos, R., S. Mallal, D. Ostrov, Y. Pompeu, and E. Phillips. 2014. 'Fever, rash, and systemic symptoms: understanding the role of virus and HLA in severe cutaneous drug allergy', *J Allergy Clin Immunol Pract*, 2: 21-33.
Pavlos, R., E. J. McKinnon, D. A. Ostrov, B. Peters, S. Buus, D. Koelle, A. Chopra, R. Schutte, C. Rive, A. Redwood, S. Restrepo, A. Bracey, T. Kaever, P. Myers, E. Speers, S. A. Malaker, J. Shabanowitz, Y. Jing, S. Gaudieri, D. F. Hunt, M. Carrington, D. W. Haas, S. Mallal, and E. J. Phillips. 2017. 'Shared peptide binding of HLA Class I and II alleles associate with cutaneous nevirapine hypersensitivity and identify novel risk alleles', *Sci Rep*, 7: 8653.
Pegram, P. S., Jr., J. D. Mountz, and P. R. O'Bar. 1981. 'Ethambutol-induced toxic epidermal necrolysis', *Arch Intern Med*, 141: 1677-8.
Peiser, M, A Becht, and R Wanner. 2007. 'Antibody blocking of MHC II on human activated regulatory T cells abrogates their suppressive potential', *Allergy*, 62: 773-80.
Pende, Daniela, Michela Falco, Massimo Vitale, Claudia Cantoni, Chiara Vitale, Enrico Munari, Alice Bertaina, Francesca Moretta, Genny Del Zotto, Gabriella Pietra, Maria Cristina Mingari, Franco Locatelli, and Lorenzo Moretta. 2019. 'Killer Ig-Like Receptors (KIRs): Their Role in NK Cell Modulation and Developments Leading to Their Clinical Exploitation', *Frontiers in Immunology*, 10.
Penn, Dustin, and Petteri Ilmonen. 2005. 'Major Histocompatibility Complex: Human.' in.
Peter, J. G., R. Lehloenya, S. Dlamini, K. Risma, K. D. White, K. C. Konvinse, and E. J. Phillips. 2017. 'Severe Delayed Cutaneous and Systemic Reactions to Drugs: A Global Perspective on the Science and Art of Current Practice', *J Allergy Clin Immunol Pract*, 5: 547-63.
Peter, Jonny, Phuti Choshi, and Rannakoe J. Lehloenya. 2019. 'Drug hypersensitivity in HIV infection', *Current opinion in allergy and clinical immunology*, 19: 272-82.
Phanuphak, N., T. Apornpong, S. Teeratakulpisarn, S. Chaithongwongwatthana, C. Taweepolcharoen, S. Mangclaviraj, S. Limpongsanurak, T. Jadwattanakul, P. Eiamapichart, W. Luesomboon, A.

Apisarnthanarak, A. Kamudhamas, A. Tangsathapornpong, C. Vitavasiri, N. Singhakowinta, V. Attakornwattana, R. Kriengsinyot, P. Methajittiphun, K. Chunloy, W. Preetiyathorn, T. Aumchantr, P. Toro, E. J. Abrams, W. El-Sadr, and P. Phanuphak. 2007. 'Nevirapine-associated toxicity in HIV-infected Thai men and women, including pregnant women', *HIV Med*, 8: 357-66.

Phillips, E., and S. Mallal. 2007. 'Drug hypersensitivity in HIV', *Curr Opin Allergy Clin Immunol*, 7: 324-30.

Phillips, Elizabeth J., Paul Bigliardi, Andreas J. Bircher, Ana Broyles, Yoon-Seok Chang, Wen-Hung Chung, Rannakoe Lehloenya, Maja Mockenhaupt, Jonny Peter, Munir Pirmohamed, Jean-Claude Roujeau, Neil H. Shear, Luciana Kase Tanno, Jason Trubiano, Rocco Valluzzi, and Annick Barbaud. 2019. 'Controversies in drug allergy: Testing for delayed reactions', *Journal of Allergy and Clinical Immunology*, 143: 66-73.

Picard, D., B. Janela, V. Descamps, M. D'Incan, P. Courville, S. Jacquot, S. Rogez, L. Mardivirin, H. Moins-Teisserenc, A. Toubert, J. Benichou, P. Joly, and P. Musette. 2010. 'Drug reaction with eosinophilia and systemic symptoms (DRESS): a multiorgan antiviral T cell response', *Sci Transl Med*, 2: 46ra62.

Pichler, W. J. 2003. 'Delayed drug hypersensitivity reactions', *Ann Intern Med*, 139: 683-93.

Pichler, W. J., J. Adam, S. Watkins, N. Wuillemin, J. Yun, and D. Yerly. 2015. 'Drug Hypersensitivity: How Drugs Stimulate T Cells via Pharmacological Interaction with Immune Receptors', *Int Arch Allergy Immunol*, 168: 13-24.

Pichler, W. J., D. J. Naisbitt, and B. K. Park. 2011. 'Immune pathomechanism of drug hypersensitivity reactions', *J Allergy Clin Immunol*, 127: S74-81.

Pinti, M., V. Appay, J. Campisi, D. Frasca, T. Fülöp, D. Sauce, A. Larbi, B. Weinberger, and A. Cossarizza. 2016. 'Aging of the immune system: Focus on inflammation and vaccination', *Eur J Immunol*, 46: 2286-301.

Polak, M. E., G. Belgi, C. McGuire, C. Pickard, E. Healy, P. S. Friedmann, and M. R. Ardern-Jones. 2013. 'In vitro diagnostic assays are effective during the acute phase of delayed-type drug hypersensitivity reactions', *Br J Dermatol*, 168: 539-49.

Pollard, R. B., P. Robinson, and K. Dransfield. 1998. 'Safety profile of nevirapine, a nonnucleoside reverse transcriptase inhibitor for the treatment of human immunodeficiency virus infection', *Clin Ther*, 20: 1071-92.

Pollock, N. R., G. F. Harrison, and P. J. Norman. 2022. 'Immunogenomics of Killer Cell Immunoglobulin-Like Receptor (KIR) and HLA Class I: Coevolution and Consequences for Human Health', *J Allergy Clin Immunol Pract*, 10: 1763-75.

Porebski, G., T. Pecaric-Petkovic, M. Groux-Keller, M. Bosak, T. T. Kawabata, and W. J. Pichler. 2013. 'In vitro drug causality assessment in Stevens-Johnson syndrome - alternatives for lymphocyte transformation test', *Clin Exp Allergy*, 43: 1027-37.

Porter, Mireille, Phuti Choshi, Sarah Pedretti, Tafadzwa Chimbetete, Rhodine Smith, Graeme Meintjes, Elizabeth Phillips, Rannakoe Lehloenya, and Jonny Peter. 2022. 'IFN-γ ELISpot in Severe Cutaneous Adverse Reactions to First-line Anti-tuberculosis Drugs in an HIV Endemic Setting', *Journal of Investigative Dermatology*.

Rajaratnam, R., C. Mann, P. Balasubramaniam, J. R. Marsden, S. M. Taibjee, F. Shah, R. Lim, R. Papini, N. Moiemen, and H. Lewis. 2010. 'Toxic epidermal necrolysis: retrospective analysis of 21 consecutive cases managed at a tertiary centre', *Clin Exp Dermatol*, 35: 853-62.

Ramírez, E., N. Medrano-Casique, H. Y. Tong, T. Bellón, R. Cabañas, A. Fiandor, J. González-Ramos, P. Herranz, E. Trigo, M. Muñoz, A. M. Borobia, A. J. Carcas, and J. Frías. 2017. 'Eosinophilic drug reactions detected by a prospective pharmacovigilance programme in a tertiary hospital', *Br J Clin Pharmacol*, 83: 400-15.

Rasmussen, Michael, Mikkel Harndahl, Anette Stryhn, Rachid Boucherma, Lise Lotte Nielsen, François A. Lemonnier, Morten Nielsen, and Søren Buus. 2014. 'Uncovering the peptide-binding specificities of HLA-C: a general strategy to determine the specificity of any MHC class I molecule', *Journal of immunology (Baltimore, Md. : 1950)*, 193: 4790-802.

Reeves, E., A. Colebatch-Bourn, T. Elliott, C. J. Edwards, and E. James. 2014. 'Functionally distinct ERAP1 allotype combinations distinguish individuals with Ankylosing Spondylitis', *Proc Natl Acad Sci U S A*, 111: 17594-9.

Reeves, E., C. J. Edwards, T. Elliott, and E. James. 2013. 'Naturally occurring ERAP1 haplotypes encode functionally distinct alleles with fine substrate specificity', *J Immunol*, 191: 35-43.
Rizvi, S. M., N. Salam, J. Geng, Y. Qi, J. H. Bream, P. Duggal, S. K. Hussain, J. Martinson, S. M. Wolinsky, M. Carrington, and M. Raghavan. 2014. 'Distinct assembly profiles of HLA-B molecules', *J Immunol*, 192: 4967-76.
Rockwood, N., F. Sirgel, E. Streicher, R. Warren, G. Meintjes, and R. J. Wilkinson. 2017. 'Low Frequency of Acquired Isoniazid and Rifampicin Resistance in Rifampicin-Susceptible Pulmonary Tuberculosis in a Setting of High HIV-1 Infection and Tuberculosis Coprevalence', *J Infect Dis*, 216: 632-40.
Rodriguez-Pena, R., S. Lopez, C. Mayorga, C. Antunez, T. D. Fernandez, M. J. Torres, and M. Blanca. 2006. 'Potential involvement of dendritic cells in delayed-type hypersensitivity reactions to beta-lactams', *J Allergy Clin Immunol*, 118: 949-56.
Romano, Antonino, M Blanca, MJ Torres, A Bircher, W Aberer, K Brockow, WJ Pichler, P Demoly, ENDA, and the EAACI interest group on drug hypersensitivity. 2004. 'Diagnosis of nonimmediate reactions to β-lactam antibiotics', *Allergy*, 59: 1153-60.
Rossjohn, Jamie, Stephanie Gras, John J. Miles, Stephen J. Turner, Dale I. Godfrey, and James McCluskey. 2015. 'T Cell Antigen Receptor Recognition of Antigen-Presenting Molecules', *Annual Review of Immunology*, 33: 169-200.
Roujeau, J. C. 2006. 'Immune mechanisms in drug allergy', *Allergol Int*, 55: 27-33.
Roujeau, J. C., J. P. Kelly, L. Naldi, B. Rzany, R. S. Stern, T. Anderson, A. Auquier, S. Bastuji-Garin, O. Correia, F. Locati, and et al. 1995. 'Medication use and the risk of Stevens-Johnson syndrome or toxic epidermal necrolysis', *N Engl J Med*, 333: 1600-7.
Rozieres, A, A Hennino, K Rodet, M. C Gutowski, N Gunera-Saad, F Berard, G Cozon, J Bienvenu, and J. F. Nicolas. 2009. 'Detection and quantification of drug-specific T cells in penicillin allergy', *Allergy*, 64: 534-42.
Rozieres, A., M. Vocanson, B. B. Said, A. Nosbaum, and J. F. Nicolas. 2009. 'Role of T cells in nonimmediate allergic drug reactions', *Curr Opin Allergy Clin Immunol*, 9: 305-10.
Sánchez-Borges, Mario, Bernard Thong, Miguel Blanca, Luis Felipe Chiaverini Ensina, Sandra González-Díaz, Paul A. Greenberger, Edgardo Jares, Young-Koo Jee, Luciana Kase-Tanno, David Khan, Jung-Won Park, Werner Pichler, Antonino Romano, and Maria José Torres Jaén. 2013. 'Hypersensitivity reactions to non beta-lactam antimicrobial agents, a statement of the WAO special committee on drug allergy', *World Allergy Organization Journal*, 6: 1-23.
Sarfo, F. S., M. A. Sarfo, B. Norman, R. Phillips, and D. Chadwick. 2014. 'Incidence and determinants of nevirapine and efavirenz-related skin rashes in West Africans: nevirapine's epitaph?', *PLoS One*, 9: e94854.
Sassolas, B., C. Haddad, M. Mockenhaupt, A. Dunant, Y. Liss, K. Bork, U. F. Haustein, D. Vieluf, J. C. Roujeau, and H. Le Louet. 2010. 'ALDEN, an algorithm for assessment of drug causality in Stevens-Johnson Syndrome and toxic epidermal necrolysis: comparison with case-control analysis', *Clin Pharmacol Ther*, 88: 60-8.
Saulle, I., C. Vicentini, M. Clerici, and M. Biasin. 2020. 'An Overview on ERAP Roles in Infectious Diseases', *Cells*, 9.
Schaberg, T, K Rebhan, and H Lode. 1996. 'Risk factors for side-effects of isoniazid, rifampin and pyrazinamide in patients hospitalized for pulmonary tuberculosis', *European Respiratory Journal*, 9: 2026-30.
Schäbitz, A., C. Hillig, M. Mubarak, M. Jargosch, A. Farnoud, E. Scala, N. Kurzen, A. C. Pilz, N. Bhalla, J. Thomas, M. Stahle, T. Biedermann, C. B. Schmidt-Weber, F. Theis, N. Garzorz-Stark, K. Eyerich, M. P. Menden, and S. Eyerich. 2022. 'Spatial transcriptomics landscape of lesions from non-communicable inflammatory skin diseases', *Nat Commun*, 13: 7729.
Schatz, Stephanie N., and R. Weber. 2018. 'Adverse drug reactions', *British Medical Journal*, 363.
Schietinger, Andrea, and Philip D Greenberg. 2014. 'Tolerance and exhaustion: defining mechanisms of T cell dysfunction', *Trends in immunology*, 35: 51-60.
Schlapbach, C., A. Zawodniak, N. Irla, J. Adam, R. E. Hunger, D. Yerly, W. J. Pichler, and N. Yawalkar. 2011. 'NKp46+ cells express granulysin in multiple cutaneous adverse drug reactions', *Allergy*, 66: 1469-76.

Seitz, C. S., P. Pfeuffer, P. Raith, E. B. Bröcker, and A. Trautmann. 2006. 'Anticonvulsant hypersensitivity syndrome: cross-reactivity with tricyclic antidepressant agents', *Ann Allergy Asthma Immunol*, 97: 698-702.

Sekula, Peggy, Ariane Dunant, Maja Mockenhaupt, Luigi Naldi, Jan Nico Bouwes Bavinck, Sima Halevy, Sylvia Kardaun, Alexis Sidoroff, Yvonne Liss, Martin Schumacher, and Jean-Claude Roujeau. 2013. 'Comprehensive Survival Analysis of a Cohort of Patients with Stevens–Johnson Syndrome and Toxic Epidermal Necrolysis', *Journal of Investigative Dermatology*, 133: 1197-204.

Serçinoğlu, O., and P. Ozbek. 2020. 'Sequence-structure-function relationships in class I MHC: A local frustration perspective', *PLoS One*, 15: e0232849.

Serwold, Thomas, Stephanie Gaw, and Nilabh Shastri. 2001. 'ER aminopeptidases generate a unique pool of peptides for MHC class I molecules', *Nature Immunology*, 2: 644-51.

Shah, Kinjal, Amr Al-Haidari, Jianmin Sun, and Julhash U. Kazi. 2021. 'T cell receptor (TCR) signaling in health and disease', *Signal Transduction and Targeted Therapy*, 6: 412.

Sharma, S. K., A. Balamurugan, P. K. Saha, R. M. Pandey, and N. K. Mehra. 2002. 'Evaluation of clinical and immunogenetic risk factors for the development of hepatotoxicity during antituberculosis treatment', *Am J Respir Crit Care Med*, 166: 916-9.

Shi, C., and E. G. Pamer. 2011. 'Monocyte recruitment during infection and inflammation', *Nat Rev Immunol*, 11: 762-74.

Shiohara, T., M. Inaoka, and Y. Kano. 2006. 'Drug-induced hypersensitivity syndrome (DIHS): a reaction induced by a complex interplay among herpesviruses and antiviral and antidrug immune responses', *Allergol Int*, 55: 1-8.

Shiohara, T., and Y. Mizukawa. 2019. 'Drug-induced hypersensitivity syndrome (DiHS)/drug reaction with eosinophilia and systemic symptoms (DRESS): An update in 2019', *Allergol Int*, 68: 301-08.

Sidney, John, Bjoern Peters, Nicole Frahm, Christian Brander, and Alessandro Sette. 2008. 'HLA class I supertypes: a revised and updated classification', *BMC Immunology*, 9: 1.

Sisay, Mekonnen, Dida Bute, Dumessa Edessa, Getnet Mengistu, Firehiwot Amare, Tigist Gashaw, and Temesgen Bihonegn. 2018. 'Appropriateness of Cotrimoxazole Prophylactic Therapy Among HIV/AIDS Patients in Public Hospitals in Eastern Ethiopia: A Retrospective Evaluation of Clinical Practice', *Frontiers in Pharmacology*, 9.

Smith, L. K., G. M. Boukhaled, S. A. Condotta, S. Mazouz, J. J. Guthmiller, R. Vijay, N. S. Butler, J. Bruneau, N. H. Shoukry, C. M. Krawczyk, and M. J. Richer. 2018. 'Interleukin-10 Directly Inhibits CD8(+) T Cell Function by Enhancing N-Glycan Branching to Decrease Antigen Sensitivity', *Immunity*, 48: 299-312.e5.

Soriano, V., C. Dona, P. Barreiro, and J. Gonzalez-Lahoz. 2000. 'Is there cross-toxicity between nevirapine and efavirenz in subjects developing rash?', *AIDS*, 14: 1672-3.

Stainsby, C. M., T. M. Perger, V. Vannappagari, K. C. Mounzer, R. K. Hsu, C. E. Henegar, J. Oyee, R. Urbaityte, C. E. Lane, L. M. Carter, G. E. Pakes, and M. S. Shaefer. 2019. 'Abacavir Hypersensitivity Reaction Reporting Rates During a Decade of HLA-B*5701 Screening as a Risk-Mitigation Measure', *Pharmacotherapy*, 39: 40-54.

Stewart, A., R. Lehloenya, A. Boulle, R. de Waal, G. Maartens, and K. Cohen. 2016. 'Severe antiretroviral-associated skin reactions in South African patients: a case series and case-control analysis', *Pharmacoepidemiol Drug Saf*, 25: 1313-19.

Stoeckius, Marlon, Christoph Hafemeister, William Stephenson, Brian Houck-Loomis, Pratip K. Chattopadhyay, Harold Swerdlow, Rahul Satija, and Peter Smibert. 2017. 'Simultaneous epitope and transcriptome measurement in single cells', *Nature Methods*, 14: 865-68.

Strange, A., F. Capon, C. C. Spencer, J. Knight, M. E. Weale, M. H. Allen, A. Barton, G. Band, C. Bellenguez, J. G. Bergboer, J. M. Blackwell, E. Bramon, S. J. Bumpstead, J. P. Casas, M. J. Cork, A. Corvin, P. Deloukas, A. Dilthey, A. Duncanson, S. Edkins, X. Estivill, O. Fitzgerald, C. Freeman, E. Giardina, E. Gray, A. Hofer, U. Hüffmeier, S. E. Hunt, A. D. Irvine, J. Jankowski, B. Kirby, C. Langford, J. Lascorz, J. Leman, S. Leslie, L. Mallbris, H. S. Markus, C. G. Mathew, W. H. McLean, R. McManus, R. Mössner, L. Moutsianas, A. T. Naluai, F. O. Nestle, G. Novelli, A. Onoufriadis, C. N. Palmer, C. Perricone, M. Pirinen, R. Plomin, S. C. Potter, R. M. Pujol, A. Rautanen, E. Riveira-Munoz, A. W. Ryan, W. Salmhofer, L.

Samuelsson, S. J. Sawcer, J. Schalkwijk, C. H. Smith, M. Ståhle, Z. Su, R. Tazi-Ahnini, H. Traupe, A. C. Viswanathan, R. B. Warren, W. Weger, K. Wolk, N. Wood, J. Worthington, H. S. Young, P. L. Zeeuwen, A. Hayday, A. D. Burden, C. E. Griffiths, J. Kere, A. Reis, G. McVean, D. M. Evans, M. A. Brown, J. N. Barker, L. Peltonen, P. Donnelly, and R. C. Trembath. 2010. 'A genome-wide association study identifies new psoriasis susceptibility loci and an interaction between HLA-C and ERAP1', *Nat Genet*, 42: 985-90.

Streeck, H, N Frahm, and B. D. Walker. 2009. 'The role of IFN-gamma Elispot assay in HIV vaccine research', *Nat Protoc*, 4: 461-9.

Su, S. C., M. Mockenhaupt, P. Wolkenstein, A. Dunant, S. Le Gouvello, C. B. Chen, O. Chosidow, L. Valeyrie-Allanore, T. Bellon, P. Sekula, C. W. Wang, M. Schumacher, S. H. Kardaun, S. I. Hung, J. C. Roujeau, and W. H. Chung. 2017. 'Interleukin-15 Is Associated with Severity and Mortality in Stevens-Johnson Syndrome/Toxic Epidermal Necrolysis', *J Invest Dermatol*, 137: 1065-73.

Suarez-Lorenzo, I., R. Castillo-Sainz, M. A. Carden-Santana, and T. Carrillo-Diaz. 2016. 'Severe reaction to emtricitabine and lamiduvine: evidence of cross-reactivity', *Contact Dermatitis*, 74: 253-4.

Subramanian Vignesh, K., and G. S. Deepe, Jr. 2017. 'Metallothioneins: Emerging Modulators in Immunity and Infection', *Int J Mol Sci*, 18.

Sulkowski, M. S., D. L. Thomas, S. H. Mehta, R. E. Chaisson, and R. D. Moore. 2002. 'Hepatotoxicity associated with nevirapine or efavirenz-containing antiretroviral therapy: role of hepatitis C and B infections', *Hepatology*, 35: 182-9.

Surjapranata, F. J., and N. N. Rahaju. 1979. 'A case of Stevens-Johnson's syndrome caused by ethambutol', *Paediatr Indones*, 19: 195-201.

Sutterwala, F. S., S. Haasken, and S. L. Cassel. 2014. 'Mechanism of NLRP3 inflammasome activation', *Ann N Y Acad Sci*, 1319: 82-95.

Svensson, C. K., E. W. Cowen, and A. A. Gaspari. 2001. 'Cutaneous drug reactions', *Pharmacol Rev*, 53: 357-79.

Swanson, Bradley J., Masaaki Murakami, Thomas C. Mitchell, John Kappler, and Philippa Marrack. 2002. 'RANTES Production by Memory Phenotype T Cells Is Controlled by a Posttranscriptional, TCR-Dependent Process', *Immunity*, 17: 605-15.

Taiwo, B. O., L. Zheng, A. Stefanescu, A. Nyaku, B. Bezins, C. L. Wallis, C. Godfrey, P. E. Sax, E. Acosta, D. Haas, K. Y. Smith, B. Sha, C. Van Dam, and R. M. Gulick. 2018. 'ACTG A5353: A Pilot Study of Dolutegravir Plus Lamivudine for Initial Treatment of Human Immunodeficiency Virus-1 (HIV-1)-infected Participants With HIV-1 RNA <500000 Copies/mL', *Clin Infect Dis*, 66: 1689-97.

Takahashi, Ryo, Yoko Kano, Yoshimi Yamazaki, Momoko Kimishima, Yoshiko Mizukawa, and Tetsuo Shiohara. 2009. 'Defective Regulatory T Cells In Patients with Severe Drug Eruptions: Timing of the Dysfunction Is Associated with the Pathological Phenotype and Outcome', *The Journal of Immunology*, 182: 8071.

Takahashi, Ryo, Yoshiko Mizukawa, Yoshimi Yamazaki, Kazuhito Hayakawa, Jun Hayakawa, Akihiko Kudo, and Tetsuo Shiohara. 2003. 'In vitro differentiation from naive to mature E-selectin binding CD4 T cells: acquisition of skin-homing properties occurs independently of cutaneous lymphocyte antigen expression', *The Journal of Immunology*, 171: 5769-77.

Tan, W. C., C. K. Ong, S. C. Kang, and M. A. Razak. 2007. 'Two years review of cutaneous adverse drug reaction from first line anti-tuberculous drugs', *Med J Malaysia*, 62: 143-6.

Tapia, B., A. Padial, E. Sánchez-Sabaté, J. Alvarez-Ferreira, E. Morel, M. Blanca, and T. Bellón. 2004. 'Involvement of CCL27-CCR10 interactions in drug-induced cutaneous reactions', *J Allergy Clin Immunol*, 114: 335-40.

Taranta, Anna, Alessandra Gianviti, Alessia Palma, Veronica De Luca, Liliana Mannucci, Maria Antonietta Procaccino, Gian Marco Ghiggeri, Gianluca Caridi, Doriana Fruci, and Silvia Ferracuti. 2009. 'Genetic risk factors in typical haemolytic uraemic syndrome', *Nephrology Dialysis Transplantation*, 24: 1851-57.

Tassaneeyakul, W., T. Jantararoungtong, P. Chen, P. Y. Lin, S. Tiamkao, U. Khunarkornsiri, P. Chucherd, P. Konyoung, S. Vannaprasaht, C. Choonhakarn, P. Pisuttimarn, A. Sangviroon, and W. Tassaneeyakul. 2009. 'Strong association between HLA-B*5801 and allopurinol-

induced Stevens-Johnson syndrome and toxic epidermal necrolysis in a Thai population', *Pharmacogenet Genomics*, 19: 704-9.
Teraki, Y., and T. Fukuda. 2017. 'Skin-Homing IL-13-Producing T Cells Expand in the Circulation of Patients with Drug Rash with Eosinophilia and Systemic Symptoms', *Dermatology*, 233: 242-49.
Teraki, Y., H. Murota, and S. Izaki. 2008. 'Toxic epidermal necrolysis due to zonisamide associated with reactivation of human herpesvirus 6', *Arch Dermatol*, 144: 232-5.
Thananchai, Hathairat, Geraldine Gillespie, Maureen P Martin, Arman Bashirova, Nobuyo Yawata, Makoto Yawata, Philippa Easterbrook, Daniel W McVicar, Katsumi Maenaka, and Peter Parham. 2007. 'Cutting Edge: Allele-specific and peptide-dependent interactions between KIR3DL1 and HLA-A and HLA-B', *The Journal of Immunology*, 178: 33-37.
Thomas, M., C. Hopkins, E. Duffy, D. Lee, P. Loulergue, D. Ripamonti, D. A. Ostrov, and E. Phillips. 2017. 'Association of the HLA-B*53:01 Allele With Drug Reaction With Eosinophilia and Systemic Symptoms (DRESS) Syndrome During Treatment of HIV Infection With Raltegravir', *Clin Infect Dis*, 64: 1198-203.
Thomsen, Martin, Claus Lundegaard, Søren Buus, Ole Lund, and Morten Nielsen. 2013. 'MHCcluster, a method for functional clustering of MHC molecules', *Immunogenetics*, 65: 655-65.
Tian, Yuan, Mariana Babor, Jerome Lane, Veronique Schulten, Veena S. Patil, Grégory Seumois, Sandy L. Rosales, Zheng Fu, Gaelle Picarda, Julie Burel, Jose Zapardiel-Gonzalo, Rashika N. Tennekoon, Aruna D. De Silva, Sunil Premawansa, Gayani Premawansa, Ananda Wijewickrama, Jason A. Greenbaum, Pandurangan Vijayanand, Daniela Weiskopf, Alessandro Sette, and Bjoern Peters. 2017. 'Unique phenotypes and clonal expansions of human CD4 effector memory T cells re-expressing CD45RA', *Nature Communications*, 8: 1473.
Tohyama, M., H. Watanabe, S. Murakami, Y. Shirakata, K. Sayama, M. Iijima, and K. Hashimoto. 2012. 'Possible involvement of CD14+ CD16+ monocyte lineage cells in the epidermal damage of Stevens-Johnson syndrome and toxic epidermal necrolysis', *Br J Dermatol*, 166: 322-30.
Torres, Maria J, M Blanca, J Fernandez, A Romano, A De Weck, W Aberer, K Brockow, Werner J Pichler, Pascal Demoly, and ENDA. 2003. 'Diagnosis of immediate allergic reactions to beta-lactam antibiotics', *Allergy*, 58: 961-72.
Trubiano, Jason A., Kaija Strautins, Alec J. Redwood, Rebecca Pavlos, Katherine C. Konvinse, Ar Kar Aung, Monica A. Slavin, Karin A. Thursky, M. Lindsay Grayson, and Elizabeth J. Phillips. 2018. 'The Combined Utility of Ex Vivo IFN-γ Release Enzyme-Linked ImmunoSpot Assay and In Vivo Skin Testing in Patients with Antibiotic-Associated Severe Cutaneous Adverse Reactions', *The Journal of Allergy and Clinical Immunology: In Practice*, 6: 1287-96.e1.
Tsai, Y. G., J. H. Liou, S. I. Hung, C. B. Chen, T. M. Chiu, C. W. Wang, and W. H. Chung. 2019. 'Increased Type 2 Innate Lymphoid Cells in Patients with Drug Reaction with Eosinophilia and Systemic Symptoms Syndrome', *J Invest Dermatol*, 139: 1722-31.
Usui, T., and D. J. Naisbitt. 2017. 'Human leukocyte antigen and idiosyncratic adverse drug reactions', *Drug Metab Pharmacokinet*, 32: 21-30.
van der Merwe, P. Anton, and Omer Dushek. 2011. 'Mechanisms for T cell receptor triggering', *Nature Reviews Immunology*, 11: 47-55.
van Deutekom, H. W., and C. Keşmir. 2015. 'Zooming into the binding groove of HLA molecules: which positions and which substitutions change peptide binding most?', *Immunogenetics*, 67: 425-36.
Van Gassen, S., B. Callebaut, M. J. Van Helden, B. N. Lambrecht, P. Demeester, T. Dhaene, and Y. Saeys. 2015. 'FlowSOM: Using self-organizing maps for visualization and interpretation of cytometry data', *Cytometry A*, 87: 636-45.
Verma, R., B. Vasudevan, and V. Pragasam. 2013. 'Severe cutaneous adverse drug reactions', *Med J Armed Forces India*, 69: 375-83.
Verma, R., B. Vasudevan, S. Shankar, V. Pragasam, B. Suwal, and R. Venugopal. 2012. 'First reported case of tenofovir-induced photoallergic reaction', *Indian J Pharmacol*, 44: 651-3.

Viard-Leveugle, I., O. Gaide, D. Jankovic, L. Feldmeyer, K. Kerl, C. Pickard, S. Roques, P. S. Friedmann, E. Contassot, and L. E. French. 2013. 'TNF-alpha and IFN-gamma are potential inducers of Fas-mediated keratinocyte apoptosis through activation of inducible nitric oxide synthase in toxic epidermal necrolysis', *J Invest Dermatol*, 133: 489-98.

Vignali, D. A., L. W. Collison, and C. J. Workman. 2008. 'How regulatory T cells work', *Nat Rev Immunol*, 8: 523-32.

Vinod, Kolar Vishwanath, Karyampudi Arun, and Tarun Kumar Dutta. 2013. 'Dapsone hypersensitivity syndrome: A rare life threatening complication of dapsone therapy', *Journal of pharmacology & pharmacotherapeutics*, 4: 158-60.

Walker, J. A., and A. N. J. McKenzie. 2018. 'TH2 cell development and function', *Nat Rev Immunol*, 18: 121-33.

Walmsley, S. L., A. Antela, N. Clumeck, D. Duiculescu, A. Eberhard, F. Gutierrez, L. Hocqueloux, F. Maggiolo, U. Sandkovsky, C. Granier, K. Pappa, B. Wynne, S. Min, and G. Nichols. 2013. 'Dolutegravir plus abacavir-lamivudine for the treatment of HIV-1 infection', *N Engl J Med*, 369: 1807-18.

Walmsley, S. L., A. Antela, N. Clumeck, D. Duiculescu, A. Eberhard, F. Gutierrez, L. Hocqueloux, F. Maggiolo, U. Sandkovsky, C. Granier, K. Pappa, B. Wynne, S. Min, G. Nichols, and Single Investigators. 2013. 'Dolutegravir plus abacavir-lamivudine for the treatment of HIV-1 infection', *N Engl J Med*, 369: 1807-18.

Wang, B., L. Abbott, K. Childs, C. Taylor, K. Agarwal, I. Cormack, R. Miquel, and A. Suddle. 2018. 'Dolutegravir-induced liver injury leading to sub-acute liver failure requiring transplantation: a case report and review of literature', *Int J STD AIDS*, 29: 414-17.

Wang, Jann-Yuan, Chien-Hong Chou, Li-Na Lee, Hsiao-Leng Hsu, I. Shiow Jan, Po-Ren Hsueh, Pan-Chyr Yang, and Kwen-Tay Luh. 2007. 'Diagnosis of tuberculosis by an enzyme-linked immunospot assay for interferon-gamma', *Emerging infectious diseases*, 13: 553-58.

Warren, K. J., D. E. Boxwell, N. Y. Kim, and B. A. Drolet. 1998. 'Nevirapine-associated Stevens-Johnson syndrome', *Lancet*, 351: 567.

Watanabe, H., Y. Watanabe, Y. Tashiro, T. Mushiroda, T. Ozeki, H. Hashizume, H. Sueki, T. Yamamoto, N. Utsunomiya-Tate, H. Gouda, and Y. Kusakabe. 2017. 'A docking model of dapsone bound to HLA-B*13:01 explains the risk of dapsone hypersensitivity syndrome', *J Dermatol Sci*, 88: 320-29.

Wei, Chun-Yu, Wen-Hung Chung, Hsiao-Wen Huang, Yuan-Tsong Chen, and Shuen-Iu Hung. 2012. 'Direct interaction between HLA-B and carbamazepine activates T cells in patients with Stevens-Johnson syndrome', *Journal of Allergy and Clinical Immunology*, 129: 1562-69.e5.

Wherry, E. J., and M. Kurachi. 2015. 'Molecular and cellular insights into T cell exhaustion', *Nat Rev Immunol*, 15: 486-99.

White, K. D., W. H. Chung, S. I. Hung, S. Mallal, and E. J. Phillips. 2015. 'Evolving models of the immunopathogenesis of T cell-mediated drug allergy: The role of host, pathogens, and drug response', *J Allergy Clin Immunol*, 136: 219-34; quiz 35.

Wong, P. C., W. W. Yew, C. F. Wong, and H. Y. Choi. 1995. 'Ethambutol-induced pulmonary infiltrates with eosinophilia and skin involvement', *Eur Respir J*, 8: 866-8.

Woolley, I. J., A. J. Veitch, C. S. Harangozo, M. Moyle, and T. M. Korman. 2004. 'Lichenoid drug eruption to tenofovir in an HIV/hepatitis B virus co-infected patient', *AIDS*, 18: 1857-8.

Wu, P. Y., C. Y. Cheng, C. E. Liu, Y. C. Lee, C. J. Yang, M. S. Tsai, S. H. Cheng, S. P. Lin, D. Y. Lin, N. C. Wang, Y. C. Lee, H. Y. Sun, H. J. Tang, and C. C. Hung. 2017. 'Multicenter study of skin rashes and hepatotoxicity in antiretroviral-naive HIV-positive patients receiving non-nucleoside reverse-transcriptase inhibitor plus nucleoside reverse-transcriptase inhibitors in Taiwan', *PLoS One*, 12: e0171596.

Wu, T. S., J. M. Lee, Y. G. Lai, J. C. Hsu, C. Y. Tsai, Y. H. Lee, and N. S. Liao. 2002. 'Reduced expression of Bcl-2 in CD8+ T cells deficient in the IL-15 receptor alpha-chain', *J Immunol*, 168: 705-12.

Yamada, Yoshiji, Fujiko Ando, and Hiroshi Shimokata. 2007. 'Association of candidate gene polymorphisms with bone mineral density in community-dwelling Japanese women and men', *International journal of molecular medicine*, 19: 791-801.

Yamamoto, Nao, Junko Nakayama, Kimiko Yamakawa-Kobayashi, Hideo Hamaguchi, Ryunosuke Miyazaki, and Tadao Arinami. 2002. 'Identification of 33 polymorphisms in the adipocyte-derived leucine aminopeptidase (ALAP) gene and possible association with hypertension', *Human mutation*, 19: 251-57.

Yang, C., A. Mosam, A. Mankahla, N. Dlova, and A. Saavedra. 2014. 'HIV infection predisposes skin to toxic epidermal necrolysis via depletion of skin-directed CD4(+) T cells', *J Am Acad Dermatol*, 70: 1096-102.

Yang, Min-Suk, Jin Yong Lee, Jayeun Kim, Gun-Woo Kim, Byung-Keun Kim, Ju-Young Kim, Heung-Woo Park, Sang-Heon Cho, Kyung-Up Min, and Hye-Ryun Kang. 2016. 'Incidence of Stevens-Johnson Syndrome and Toxic Epidermal Necrolysis: A Nationwide Population-Based Study Using National Health Insurance Database in Korea', *PLoS One*, 11: e0165933.

Ye, Y. M., G. Y. Hur, S. H. Kim, G. Y. Ban, Y. K. Jee, D. J. Naisbitt, H. S. Park, and S. H. Kim. 2017. 'Drug-specific CD4(+) T-cell immune responses are responsible for antituberculosis drug-induced maculopapular exanthema and drug reaction with eosinophilia and systemic symptoms syndrome', *Br J Dermatol*, 176: 378-86.

Yindom, L. M., R. Forbes, P. Aka, O. Janha, D. Jeffries, M. Jallow, D. J. Conway, and M. Walther. 2012. 'Killer-cell immunoglobulin-like receptors and malaria caused by Plasmodium falciparum in The Gambia', *Tissue Antigens*, 79: 104-13.

Yu, Guangchuang, Li-Gen Wang, Yanyan Han, and Qing-Yu He. 2012. 'clusterProfiler: an R package for comparing biological themes among gene clusters', *Omics: a journal of integrative biology*, 16: 284-87.

Yunihastuti, E., A. Widhani, and T. H. Karjadi. 2014. 'Drug hypersensitivity in human immunodeficiency virus-infected patient: challenging diagnosis and management', *Asia Pac Allergy*, 4: 54-67.

Yunna, C., H. Mengru, W. Lei, and C. Weidong. 2020. 'Macrophage M1/M2 polarization', *Eur J Pharmacol*, 877: 173090.

Zaccai, Nathan, Lucy Bird, and E. Jones. 1999. 'HLA-B27 and disease pathogenesis: New structural and functional insights', *Expert reviews in molecular medicine*, 1999: 1-10.

Zheng, Y., A. Chaudhry, A. Kas, P. deRoos, J. M. Kim, T. T. Chu, L. Corcoran, P. Treuting, U. Klein, and A. Y. Rudensky. 2009. 'Regulatory T-cell suppressor program co-opts transcription factor IRF4 to control T(H)2 responses', *Nature*, 458: 351-6.

Zitha, E., B. Chiliza, R. Muloiwa, and R. Lehloenya. 2014. 'Incidence of anxiety and depression in a predominantly HIV-infected population with severe adverse drug reactions', *Clin Transl Allergy*, 4: P95.

Zvyagin, I. V., I. Z. Mamedov, O. V. Britanova, D. B. Staroverov, E. L. Nasonov, A. G. Bochkova, A. V. Chkalina, A. A. Kotlobay, D. O. Korostin, D. V. Rebrikov, S. Lukyanov, Y. B. Lebedev, and D. M. Chudakov. 2010. 'Contribution of functional KIR3DL1 to ankylosing spondylitis', *Cell Mol Immunol*, 7: 471-6.

Appendix

1.1. Naranjo scaling

Naranjo Adverse Drug Reaction Probability Scale				
Question	Yes	No	Do Not Know	Score
1. Are there previous *conclusive* reports on this reaction?	+1	0	0	
2. Did the adverse event appear after the suspected drug was administered?	+2	-1	0	
3. Did the adverse reaction improve when the drug was discontinued or a *specific* antagonist was administered?	+1	0	0	
4. Did the adverse event reappear when the drug was re-administered?	+2	-1	0	
5. Are there alternative causes (other than the drug) that could on their own have caused the reaction?	-1	+2	0	
6. Did the reaction reappear when a placebo was given?	-1	+1	0	
7. Was the drug detected in blood (or other fluids) in concentrations known to be toxic?	+1	0	0	
8. Was the reaction more severe when the dose was increased or less severe when the dose was decreased?	+1	0	0	
9. Did the patient have a similar reaction to the same or similar drugs in *any* previous exposure?	+1	0	0	
10. Was the adverse event confirmed by any objective evidence?	+1	0	0	
TOTAL SCORE:				

Modified from: Naranjo CA et al. A method for estimating the probability of adverse drug reactions. Clin Pharmacol Ther 1981; 30: 239-245.

1.2. ALDEN algorithm

Table 5 Details of the algorithm of drug causality for epidermal necrolysis (ALDEN)

Criterion	Values	Rules to apply	
Delay from initial drug component intake to onset of reaction (index day)	Suggestive +3	From 5 to 28 days	−3 to 3
	Compatible +2	From 29 to 56 days	
	Likely +1	From 1 to 4 days	
	Unlikely −1	>56 Days	
	Excluded −3	Drug started on or after the index day	
		In case of previous reaction to the same drug, only changes for: Suggestive: +3: from 1 to 4 days Likely: +1: from 5 to 56 days	
Drug present in the body on index day	Definite 0	Drug continued up to index day or stopped at a time point less than five times the elimination half-life[a] before the index day	−3 to 0
	Doubtful −1	Drug stopped at a time point prior to the index day by more than five times the elimination half-life[a] but liver or kidney function alterations or suspected drug interactions[b] are present	
	Excluded −3	Drug stopped at a time point prior to the index day by more than five times the elimination half-life[a], without liver or kidney function alterations or suspected drug interactions[b]	
Prechallenge/rechallenge	Positive specific for disease and drug: 4	SJS/TEN after use of same drug	−2 to 4
	Positive specific for disease or drug: 2	SJS/TEN after use of similar[c] drug or other reaction with same drug	
	Positive unspecific: 1	Other reaction after use of similar[c] drug	
	Not done/unknown: 0	No known previous exposure to this drug	
	Negative −2	Exposure to this drug without any reaction (before or after reaction)	
Dechallenge	Neutral 0	Drug stopped (or unknown)	−2 or 0
	Negative −2	Drug continued without harm	
Type of drug (notoriety)	Strongly associated 3	Drug of the "high-risk" list according to previous case–control studies[d]	−1 to 3
	Associated 2	Drug with definite but lower risk according to previous case–control studies[d]	
	Suspected 1	Several previous reports, ambiguous epidemiology results (drug "under surveillance")	
	Unknown 0	All other drugs including newly released ones	
	Not suspected −1	No evidence of association from previous epidemiology study[d] with sufficient number of exposed controls[c]	
		Intermediate score = total of all previous criteria	−11 to 10
Other cause	Possible −1	Rank all drugs from highest to lowest intermediate score	−1
		If at least one has an intermediate score >3, subtract 1 point from the score of each of the other drugs taken by the patient (another cause is more likely)	
Final score −12 to 10			

<0, Very unlikely; 0–1, unlikely; 2–3, possible; 4–5, probable; ≥6, very probable.

ATC, anatomical therapeutic chemical; SJS, Stevens–Johnson syndrome; TEN, toxic epidermal necrolysis.

[a]Drug (or active metabolite) elimination half-life from serum and/or tissues (according to pharmacology textbooks, tentative list available in complementary table), taking into account kidney function for drugs predominantly cleared by kidney and liver function for those with high hepatic clearance. [b]Suspected interaction was considered when more than five drugs were present in a patient's body at the same time. [c]Similar drug = same ATC code up to the fourth level (chemical subgroups), see Methods. [d]See definitions for "high risk," "lower risk," and "no evidence of association" in Methods, ref. 15 (detailed list available in complementary table).

2.1. Drugs working solutions preparation

Rifampicin (0.1g powder in 2mL methanol) **(desired stock 50mg/mL)**

- Reconstitute 100mg in 2mL methanol – 50mg/mL = 50 000ug/mL
- Then put 0.5mL vials and store
- Then put 0.5mL in 4.5mL R10 to give 10 000ug/mL (starting stock concentration) – total 5 mL

			C1	V1 = 100 ul V2 = 200 ul (= 100+100 ul)		**C2**
	Stock drug concentration (ug/mL)	Dilution starting stock	Working drug concentration (ug/mL)	Volume working drug added to plate (ul)	Volume cells/media added to plate (ul)	**Final drug concentration (ug/mL)**
1	10 000	1:2	5000	100	100	**2500**
2	10 000	1:20	500	100	100	**250**
3	10 000	1:200	50	100	100	**25**

Pyrazinamide 0.5g powder (desired stock 50mg/mL)

Reconstitute 0.5g in 10mL DMSO – 50mg/mL = 50,000ug/mL

Then put 1mL vials and store

Then put 1mL in 1.5mL R10 to give 20 000ug/mL (starting stock concentration) – total 2.5mL

			C1	V1 = 100 ul V2 = 200 ul (= 100+100 ul)		**C2**
	Stock drug concentration (ug/mL)	Dilution starting stock	Working drug concentration (ug/mL)	Volume working drug added to plate (ul)	Volume cells/media added to plate (ul)	**Final drug concentration (ug/mL)**
1	20 000	1:2	10 000	100	100	**5000**
2	20 000	1:20	1000	100	100	**500**
3	20 000	1:200	100	100	100	**50**

Isoniazid 0.5g powder – (desired stock 50mg/mL)

- Reconstitute0.5g in 10mL water – 50mg/mL = 50,000ug/mL
- Then put 1mL in 1.5mL R10 to give 20 000ug/mL (starting stock concentration)

			C1	V1 = 100 ul V2 = 200 ul (= 100+100 ul)		**C2**
	Stock drug concentration (ug/mL)	Dilution starting stock	Working drug concentration (ug/mL)	Volume working drug added to plate (ul)	Volume cells/media added to plate (ul)	**Final drug concentration (ug/mL)**
	20 000	1:2	10 000	100	100	**5000**
1	20 000	1:20	1000	100	100	**500**
2	20 000	1:200	100	100	100	**50**

Ethambutol 0.5g powder – (desired stock 50mg/mL)

- Reconstitute 0.5g in 10mL water – 50mg/mL = 50,000ug/mL
- Then put 1mL in 1.5mL R10 to give 20 000ug/mL (starting stock concentration)

			C1	V1 = 100 ul V2 = 200 ul (= 100+100 ul)		**C2**
	Stock drug concentration (ug/mL)	Dilution starting stock	Working drug concentration (ug/mL)	Volume working drug added to plate (ul)	Volume cells/media added to plate (ul)	**Final drug concentration (ug/mL)**
1	20 000	1:2	10 000	100	100	**5000**
2	20 000	1:20	1000	100	100	**500**
3	20 000	1:200	100	100	100	**50**

2.2. Plate layout

Sample ID	**116**			**156**			**157**			**160**		
	1	**2**	**3**	**4**	**5**	**6**	**7**	**8**	**9**	**10**	**11**	**12**
A	aCD3	aCD3	aCD3	aCD3	aCD3	aCD3	aCD3	aCD3	aCD3	aCD3	aCD3	aCD3
B	EMB 50	EMB 50	EMB 50	EMB 50	EMB 50	EMB 50	EMB 50	EMB 50	EMB 50	EMB 50	EMB 50	EMB 50
C	INH 50	INH 50	INH 50	INH 50	INH 50	INH 50	INH 50	INH 50	INH 50	INH 50	INH 50	INH 50
D	PZA 50	PZA 50	PZA 50	PZA 50	PZA 50	PZA 50	PZA 50	PZA 50	PZA 50	PZA 50	PZA 50	PZA 50
E	RIF 25	RIF 25	RIF 25	RIF 25	RIF 25	RIF 25	RIF 25	RIF 25	RIF 25	RIF 25	RIF 25	RIF 25
F	TMP-SMX 50/250	TMP-SMX 50/250	TMP-SMX 50/250	TMP-SMX 50/250	TMP-SMX 50/250	TMP-SMX 50/250	TMP-SMX 50/250	TMP-SMX 50/250	TMP-SMX 50/250	TMP-SMX 50/250	TMP-SMX 50/250	TMP-SMX 50/250
G												
H	media	media	media	media	media	media	media	media	media	media	media	media

2.3. Flow cytometry gating strategy

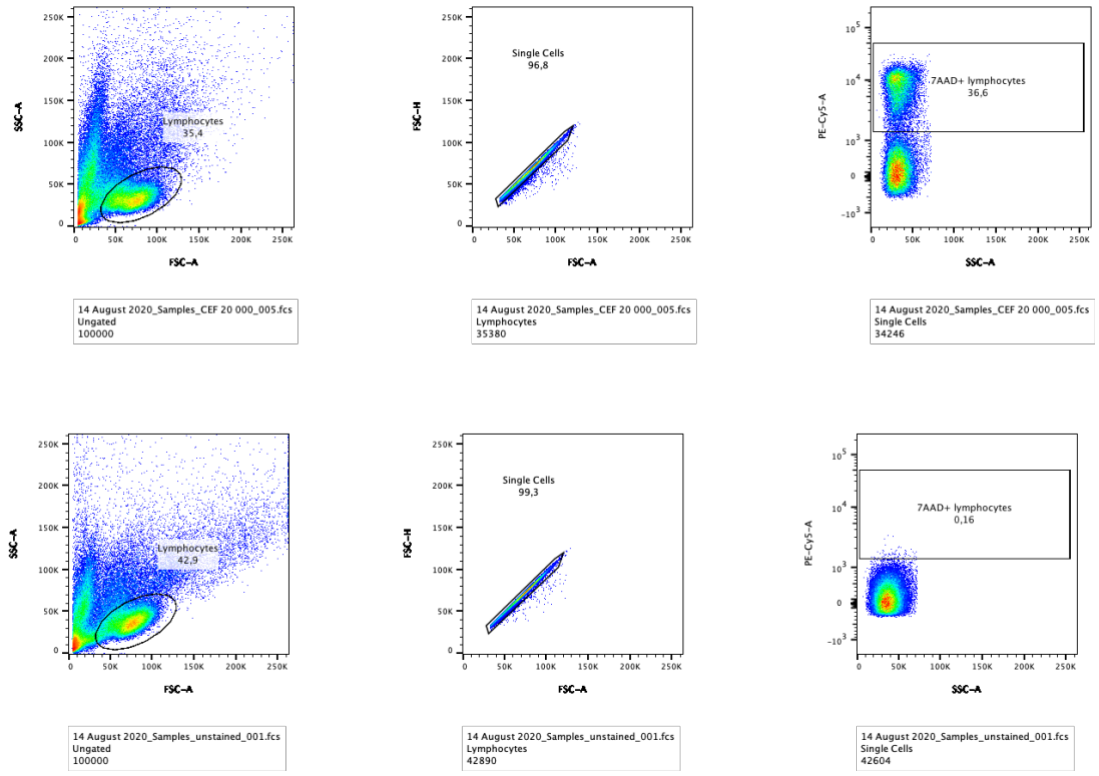

3.1. Distinct assembly profiles of HLA-B molecules

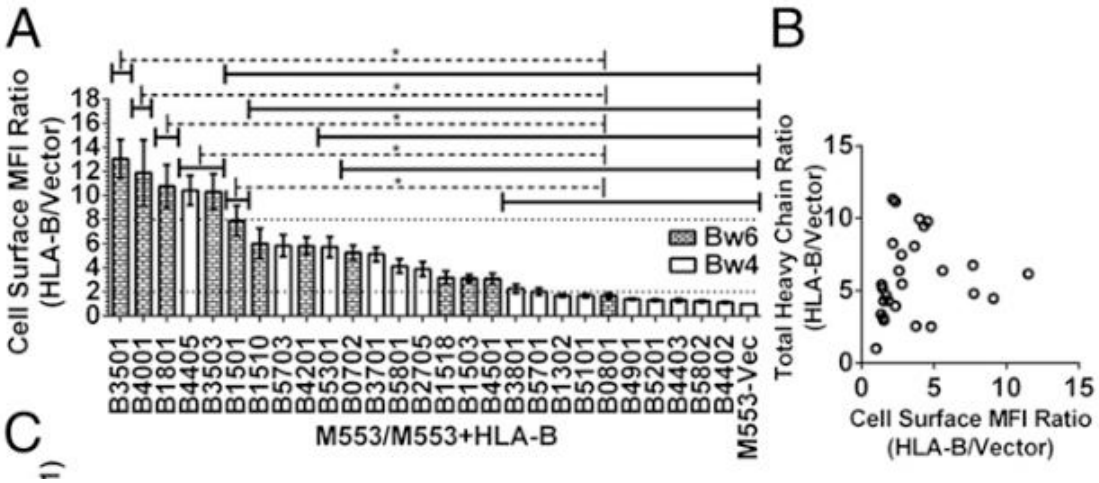

Adapted from (Rizvi et al. 2014)

3.2. Identity of ERAP1 haplotypes

		SNP	rs2287987	rs30187	rs150860	rs17482078	rs27044
		NT change	**T-C**	**T-C**	**C-T**	**C-T**	**G-C**
			A-G	**A-G**	**G-A**	**G-A**	**C-G**
	Activity	AA change	**(M349V)**	**(K528R)**	**(D575N)**	**(R725Q)**	**(Q730E)**
1	WT	WT	M	K	D	R	Q
2	WT	349V/575N/725Q	V	K	N	Q	Q
3	WT	349V	V	K	D	R	Q
10	WT	730E	M	K	D	R	E
8	Over	528R/725Q	M	R	D	Q	Q
9	Over	725Q/730E	M	K	D	Q	E
4	Under	5SNP	V	R	N	Q	E
5	Under	528R/730E	M	R	D	R	E
6	Under	528R	M	R	D	R	Q
7	Under	349V/528R	V	R	D	R	Q
11	Under	VRNQE	V	R	D	Q	E
13	Under	VRNRE	V	R	N	R	E
12	Under	VRNRQ	V	R	N	R	Q

4.1. CyTOF extracellular markers and concentrations

	Probe	Marker	Clone	Titration
1	155Gd	CD279 (PD-1)	EH12.2H7	2
2	154Sm	TIGIT	MBSA43	1
3	173Yb	HLA-DR	L243	1
4	150Nd	CD134 (OX40)	ACT35	1
5	209Bi	CD16	3G8	1
6	141Pr	CD196 (CCR6)	G034E3	0.85
7	145Nd	CD4	RPA-T4	0.8
8	152Sm	TCRgd	11F2	0.8
9	153Eu	CD194/CCR4	L291H4	0.8
10	160Gd	CD28	CD28.2	0.8
11	170Er	CD3	UCHT1	0.75
12	161Dy	CD26	BA5b	0.75
13	168Er	CD127 (IL-7Ra)	A019D5	0.75
14	159Tb	CD161	HP-3G10	0.7
15	171Yb	CD185/CXCR5	RF8B2	0.7
16	146Nd	CD8a	RPA-T8	0.5
17	156Gd	CD183 (CXCR3)	G025H7	0.5
18	167Er	CD27	O323/L128	0.5
19	172Yb	CD57	HCD57	0.5
20	176Yb	CLA	HECA-452	0.5
21	142Nd	CD19	HIB19	0.5
22	143Nd	CD45RA	HI100	0.5
23	144Nd	CD69	FN50	0.5
24	147Sm	CD11c	Bu15	0.5
25	151Eu	CD14	M5E2	0.5
26	149Sm	CD56 (NCAM)	NCAM16.2	0.5
27	169Tm	CD25 (IL-2R)	2A3	0.25

4.2. CyTOF intracellular markers and concentrations

	Probe	Marker	Clone	Titration
1	148Nd	IL-17A	BL168	1
2	175Lu	Perforin	B-D48	0.8
3	158Gd	IL-2	MQ1-17H12	0.5
4	165Ho	IFNg	B27	0.5
5	174Yb	TNFa	Mab11	0.5
6	163Dy	TGFbeta	TW4-6H10	0.1

4.3. CyTOF gating strategy

062514-Study 17-18-2013-all.jo LAYOUT-1

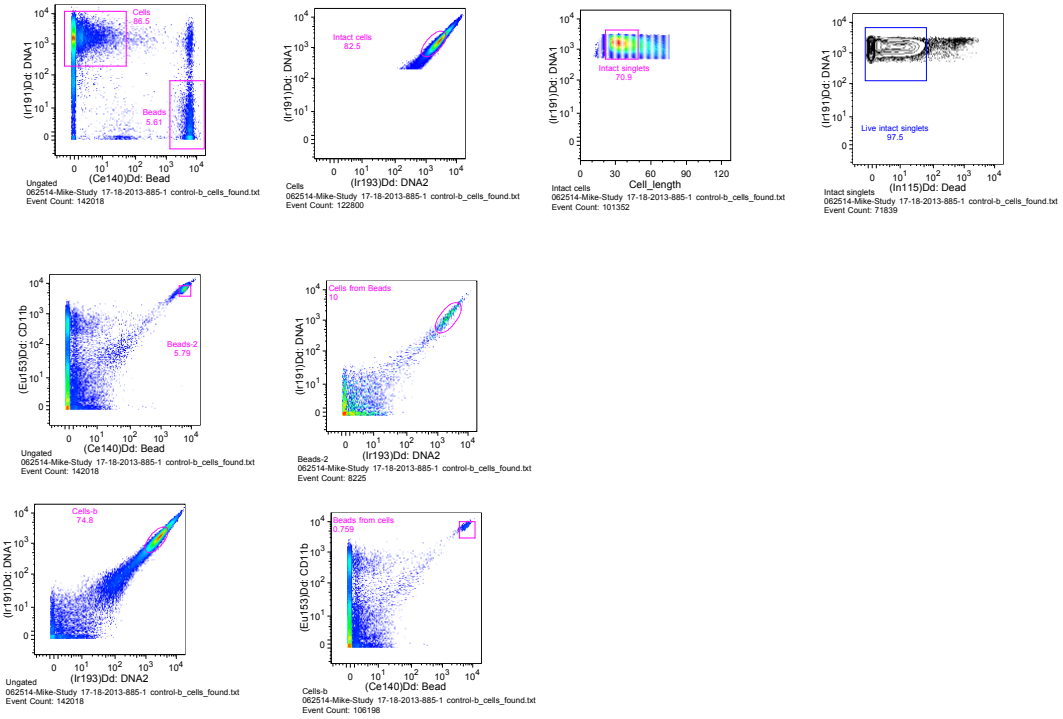

9/9/14 1:42 PM Page 1 of 1 (FlowJo v9.7.6)

Adapted from 062514-Study.

4.4. Mass cytometry antibody panel titration results

Titration Plan

- Healthy control, thawed and rested PBMCs for 2+ hours
- Stimulation – 10ug/ml PHA and unstimulated (R10) – stimulated for 18 hours. Added Monensin/Brefeldin an hour after incubation
- Titration concentrations tested – 0.125, 0.25, 0.5, 1 and FMO (fluorescence minus one)
- FMO has just the lineage markers
- Tested concentrations tubes (4 for each group, stim and Unstim) has lineage markers and antibodies being titrated

Antibodies Titrated			
142Nd	CD19	150Nd	CD134 (OX40)
143Nd	CD45RA	151Eu	CD14
144Nd	CD69	161Dy	CD26
146Nd	CD8a	163Dy	TGFbeta
147Sm	CD11c	168Er	CD127 (IL-7Ra)
148Nd	IL-17A	174Yb	TNFa
149Sm	CD56 (NCAM)	209Bi	CD16

Lineage markers to identify cell populations		
170Er	CD3	0.75
145Nd	CD4	0.8
172Yb	CD57	0.5
169Tm	CD25	0.25

1

Gating - FlowJo

- Gating strategy – BEADS> Live/Dead> DNA> CD3+/CD3-
- Used stimulated and unstimulated FMOs to set negative and postive gates
- Concatenated all CD3+ (concat2020) together and then CD3- (concat2019)
- Made layout edits for each marker, each concentration in stim and unstim to look at the separation of the neg from the pos.
- Added statistic to calculate neg and pos median for each marker
- Stimulation index calculation $SI = \frac{Med_{pos}-Med_{neg}}{[84\%_{neg}-Med_{neg})/0.995]}$
- Titration Curve example

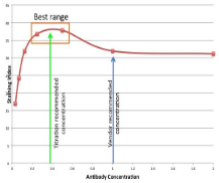

https://bitesizebio.com/22374/importance-of-antibody-titration-in-flow-cytometry/

2

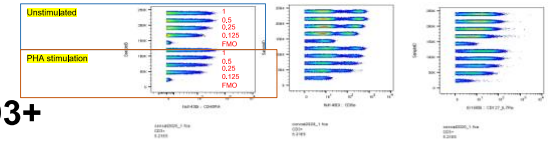

CD3+

- CD45RA
- CD8a
- CD127
- CD26
- CD134_OX40
- CD69
- TGFbeta
- IL-17A
- TNFa

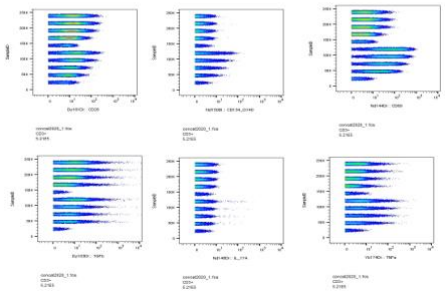

3

CD3-

- CD56
- CD19
- CD11c
- CD16
- CD14

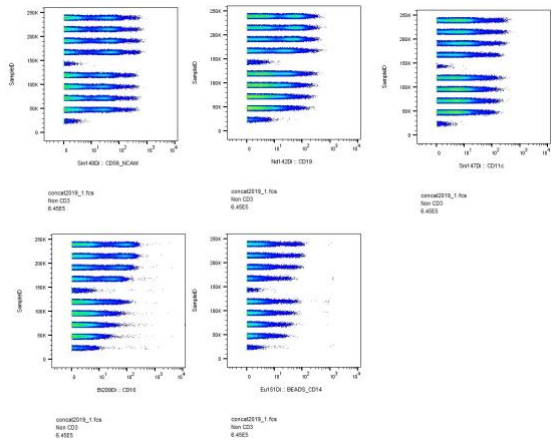

4

4.5. Cite-seq antibodies

DNA_ID	Description	Clone	Barcode
C0006	anti-human CD86	IT2.2	GTCTTTGTCAGTGCA
C0007	anti-human CD274 (B7-H1, PD-L1)	29E.2A3	GTTGTCCGACAATAC
C0020	anti-human CD270 (HVEM, TR2)	122	TGATAGAAACAGACC
C0023	anti-human CD155 (PVR)	SKII.4	ATCACATCGTTGCCA
C0024	anti-human CD112 (Nectin-2)	TX31	AACCTTCCGTCTAAG
C0026	anti-human CD47	CC2C6	GCATTCTGTCACCTA
C0029	anti-human CD48	BJ40	CTACGACGTAGAAGA
C0031	anti-human CD40	5C3	CTCAGATGGAGTATG
C0032	anti-human CD154	24-31	GCTAGATAGATGCAA
C0033	anti-human CD52	HI186	CTTTGTACGAGCAAA
C0034	anti-human CD3	UCHT1	CTCATTGTAACTCCT
C0046	anti-human CD8	SK1	GCGCAACTTGATGAT
C0047	anti-human CD56	5.1H11	TCCTTTCCTGATAGG
C0050	anti-human CD19	HIB19	CTGGGCAATTACTCG
C0052	anti-human CD33	P67.6	TAACTCAGGGCCTAT
C0053	anti-human CD11c	S-HCL-3	TACGCCTATAACTTG
C0058	anti-human HLA-A,B,C	W6/32	TATGCGAGGCTTATC
C0063	anti-human CD45RA	HI100	TCAATCCTTCCGCTT
C0064	anti-human CD123	6H6	CTTCACTCTGTCAGG
C0066	anti-human CD7	CD7-6B7	TGGATTCCCGGACTT
C0068	anti-human CD105	43A3	ATCGTCGAGAGCTAG
C0070	anti-human/mouse CD49f	GoH3	TTCCGAGGATGATCT
C0071	anti-human CD194 (CCR4)	L291H4	AGCTTACCTGCACGA
C0072	anti-human CD4	RPA-T4	TGTTCCCGCTCAACT
C0073	anti-mouse/human CD44	IM7	TGGCTTCAGGTCCTA
C0081	anti-human CD14	M5E2	TCTCAGACCTCCGTA
C0083	anti-human CD16	3G8	AAGTTCACTCTTTGC
C0085	anti-human CD25	BC96	TTTGTCCTGTACGCC
C0087	anti-human CD45RO	UCHL1	CTCCGAATCATGTTG
C0088	anti-human CD279	EH12.2H7	ACAGCGCCGTATTTA
C0089	anti-human TIGIT (VSTM3)	A15153G	TTGCTTACCGCCAGA
C0090	Mouse IgG1, κ isotype Ctrl	MOPC-21	GCCGGACGACATTAA
C0091	Mouse IgG2a, κ isotype Ctrl	MOPC-173	CTCCTACCTAAACTG
C0092	Mouse IgG2b, κ isotype Ctrl	MPC-11	ATATGTATCACGCGA
C0095	Rat IgG2b, κ Isotype Ctrl	RTK4530	GATTCTTGACGACCT
C0100	anti-human CD20	2H7	TTCTGGGTCCCTAGA
C0101	anti-human CD335 (NKp46)	9E2	ACAATTTGAACAGCG
C0124	anti-human CD31	WM59	ACCTTTATGCCACGG
C0134	anti-human CD146	P1H12	CCTTGGATAACATCA
C0136	anti-human IgM	MHM-88	TAGCGAGCCCGTATA
C0138	anti-human CD5	UCHT2	CATTAACGGGATGCC
C0140	anti-human CD183 (CXCR3)	G025H7	GCGATGGTAGATTAT

C0141	anti-human CD195 (CCR5)	J418F1	CCAAAGTAAGAGCCA
C0142	anti-human CD32	FUN-2	GCTTCCGAATTACCG
C0143	anti-human CD196 (CCR6)	G034E3	GATCCCTTTGTCACT
C0144	anti-human CD185 (CXCR5)	J252D4	AATTCAACCGTCGCC
C0145	anti-human CD103 (Integrin αE)	Ber-ACT8	GACCTCATTGTGAAT
C0146	anti-human CD69	FN50	GTCTCTTGGCTTAAA
C0147	anti-human CD62L	DREG-56	GTCCCTGCAACTTGA
C0149	anti-human CD161	HP-3G10	GTACGCAGTCCTTCT
C0151	anti-human CD152 (CTLA-4)	BNI3	ATGGTTCACGTAATC
C0152	anti-human CD223 (LAG-3)	11C3C65	CATTTGTCTGCCGGT
C0153	anti-human KLRG1 (MAFA)	SA231A2	CTTATTTCCTGCCCT
C0154	anti-human CD27	O323	GCACTCCTGCATGTA
C0155	anti-human CD107a (LAMP-1)	H4A3	CAGCCCACTGCAATA
C0156	anti-human CD95 (Fas)	DX2	CCAGCTCATTAGAGC
C0158	anti-human CD134 (OX40)	Ber-ACT35 (ACT35)	AACCCACCGTTGTTA
C0159	anti-human HLA-DR	L243	AATAGCGAGCAAGTA
C0160	anti-human CD1c	L161	GAGCTACTTCACTCG
C0161	anti-human CD11b	ICRF44	GACAAGTGATCTGCA
C0162	anti-human CD64	10.1	AAGTATGCCCTACGA
C0163	anti-human CD141 (Thrombomodulin)	M80	GGATAACCGCGCTTT
C0164	anti-human CD1d	51.1	TCGAGTCGCTTATCA
C0165	anti-human CD314 (NKG2D)	1D11	CGTGTTTGTTCCTCA
C0167	anti-human CD35	E11	ACTTCCGTCGATCTT
C0168	anti-human CD57 Recombinant	QA17A04	AACTCCCTATGGAGG
C0170	anti-human CD272 (BTLA)	MIH26	GTTATTGGACTAAGG
C0171	anti-human/mouse/rat CD278 (ICOS)	C398.4A	CGCGCACCCATTAAA
C0174	anti-human CD58 (LFA-3)	TS2/9	GTTCCTATGGACGAC
C0176	anti-human CD39	A1	TTACCTGGTATCCGT
C0179	anti-human CX3CR1	K0124E1	AGTATCGTCTCTGGG
C0180	anti-human CD24	ML5	AGATTCCTTCGTGTT
C0181	anti-human CD21	Bu32	AACCTAGTAGTTCGG
C0185	anti-human CD11a	TS2/4	TATATCCTTGTGAGC
C0187	anti-human CD79b (Igβ)	CB3-1	ATTCTTCAACCGAAG
C0189	anti-human CD244 (2B4)	C1.7	TCGCTTGGATGGTAG
C0206	anti-human CD169 (Sialoadhesin, Siglec-1)	7-239	TACTCAGCGTGTTTG
C0214	anti-human/mouse integrin β7	FIB504	TCCTTGGATGTACCG
C0215	anti-human CD268 (BAFF-R)	11C1	CGAAGTCGATCCGTA
C0216	anti-human CD42b	HIP1	TCCTAGTACCGAAGT
C0217	anti-human CD54	HA58	CTGATAGACTTGAGT
C0218	anti-human CD62P (P-Selectin)	AK4	CCTTCCGTATCCCTT
C0219	anti-human CD119 (IFN-γ R α chain)	GIR-208	TGTGTATTCCCTTGT
C0224	anti-human TCR α/β	IP26	CGTAACGTAGAGCGA
C0236	Rat IgG1, κ isotype Ctrl	RTK2071	ATCAGATGCCCTCAT
C0238	Rat IgG2a, κ Isotype Ctrl	RTK2758	AAGTCAGGTTCGTTT
C0241	Armenian Hamster IgG Isotype Ctrl	HTK888	CCTGTCATTAAGACT

C0246	anti-human CD122 (IL-2Rβ)	TU27	TCATTTCCTCCGATT
C0247	anti-human CD267 (TACI)	1A1	AGTGATGGAGCGAAC
C0352	anti-human FcεRIα	AER-37 (CRA-1)	CTCGTTTCCGTATCG
C0353	anti-human CD41	HIP8	ACGTTGTGGCCTTGT
C0355	anti-human CD137 (4-1BB)	4B4-1	CAGTAAGTTCGGGAC
C0358	anti-human CD163	GHI/61	GCTTCTCCTTCCTTA
C0359	anti-human CD83	HB15e	CCACTCATTTCCGGT
C0363	anti-human CD124 (IL-4Rα)	G077F6	CCGTCCTGATAGATG
C0364	anti-human CD13	WM15	TTTCAACGCCCTTTC
C0367	anti-human CD2	TS1/8	TACGATTTGTCAGGG
C0368	anti-human CD226 (DNAM-1)	11A8	TCTCAGTGTTTGTGG
C0369	anti-human CD29	TS2/16	GTATTCCCTCAGTCA
C0370	anti-human CD303 (BDCA-2)	201A	GAGATGTCCGAATTT
C0371	anti-human CD49b	P1E6-C5	GCTTTCTTCAGTATG
C0373	anti-human CD81 (TAPA-1)	5A6	GTATCCTTCCTTGGC
C0384	anti-human IgD	IA6-2	CAGTCTCCGTAGAGT
C0385	anti-human CD18	TS1/18	TATTGGGACACTTCT
C0386	anti-human CD28	CD28.2	TGAGAACGACCCTAA
C0389	anti-human CD38	HIT2	TGTACCCGCTTGTGA
C0390	anti-human CD127 (IL-7Rα)	A019D5	GTGTGTTGTCCTATG
C0391	anti-human CD45	HI30	TGCAATTACCCGGAT
C0393	anti-human CD22	S-HCL-1	GGGTTGTTGTCTTTG
C0394	anti-human CD71	CY1G4	CCGTGTTCCTCATTA
C0396	anti-human CD26	BA5b	GGTGGCTAGATAATG
C0407	anti-human CD36	5-271	TTCTTTGCCTTGCCA
C0420	anti-human CD158 (KIR2DL1/S1/S3/S5)	HP-MA4	TATCAACCAACGCTT
C0575	anti-human CD49a	TS2/7	ACTGATGGACTCAGA
C0576	anti-human CD49d	9F10	CCATTCAACTTCCGG
C0577	anti-human CD73 (Ecto-5'-nucleotidase)	AD2	CAGTTCCTCAGTTCG
C0581	anti-human TCR Vα7.2	3C10	TACGAGCAGTATTCA
C0582	anti-human TCR Vδ2	B6	TCAGTCAGATGGTAT
C0591	anti-human LOX-1	15C4	ACCCTTTACCGAATA
C0592	anti-human CD158b (KIR2DL2/L3, NKAT2)	DX27	GACCCGTAGTTTGAT
C0599	anti-human CD158e1 (KIR3DL1, NKB1)	DX9	GGACGCTTTCCTTGA
C0830	anti-human CD319 (CRACC)	162.1	AGTATGCCATGTCTT
C0845	anti-human CD99	3B2/TA8	ACCCGTCCCTAAGAA
C0853	anti-human CLEC12A	50C1	CATTAGAGTCTGCCA
C0864	anti-human CD352 (NTB-A)	NT-7	AGTTTCCACTCAGGC
C0867	anti-human CD94	DX22	CTTTCCGGTCCTACA
C0894	anti-human Ig light chain κ	MHK-49	AGCTCAGCCAGTATG
C0896	anti-human CD85j (ILT2)	GHI/75	CCTTGTGAGGCTATG
C0897	anti-human CD23	EBVCS-5	TCTGTATAACCGTCT
C0898	anti-human Ig light chain λ	MHL-38	CAGCCAGTAAGTCAC
C0902	anti-human CD328 (Siglec-7)	6-434	CTTAGCATTTCACTG
C0912	anti-human GPR56	CG4	GCCTAGTTTCCGTTT

C0918	anti-human HLA-E	3D12	GAGTCGAGAAATCAT
C0920	anti-human CD82	ASL-24	TCCCACTTCCGCTTT
C0944	anti-human CD101 (BB27)	BB27	CTACTTCCCTGTCAA
C1046	anti-human CD88 (C5aR)	S5/1	GCCGCATGAGAAACA
C1052	anti-human CD224	KF29	CTGATGAGATGTCAG

5.1. Patient 10085 post-SDC rifampicin reaction histology report

CLINICAL HISTORY:
41 year old female. RVD positive and CD4 count 39 (not on ARV's). PTB - 19/09/19, GXP positive and RIF (S). Now: presenting with erythematous/pruritic papular rash for 1 month. 3 Days off ... with TB therapy - no associated facial swelling and no fever. On exam: indurated, erythematous papules and plaques with epidermal necrosis. Palmar and plantar involvement and no eyes ... Differential diagnosis: DRESS secondary to rifafour versus SJS/TEN secondary to Rifafour.

MACROSCOPY:
Specimen consists of a punch biopsy measuring 4mm across x 6mm deep.

MICROSCOPY:
Sections of the punch biopsy show skin with basketweave hyperkeratosis and the epidermis showing an intact granular layer with spongiosis, follicular plugging and a distinct interface dermatitis of the hydropic/vacuolar degeneration type with numerous colloid bodies / dyskeratosis. The superficial dermis shows an interstitial and perivascular lymphohistiocytic dermatitis with pigmentary incontinence, oedema with no eosinophils. There is also periadnexal involvement.

COMMENT:
The differential diagnosis to this interface/ erythema multiforme - like dermatitis of the vacuolar degeneration type include lupus erythematosus, dermatomyositis and PLEVA with drug induced, least likely due to absence of eosinophils.

PATHOLOGICAL DIAGNOSIS:
Skin, punch biopsy:
- Interface, erythema multiforme-like dermatitis of the vacuolar degeneration type.

Reported by: Dr DJ Maartens